



# Concentrating Solar Power Impact on Grid Reliability

Nicholas W. Miller and Slobodan Pajic  
*GE Energy Consulting*

Kara Clark  
*National Renewable Energy Laboratory*

**NREL is a national laboratory of the U.S. Department of Energy  
Office of Energy Efficiency & Renewable Energy  
Operated by the Alliance for Sustainable Energy, LLC**

This report is available at no cost from the National Renewable Energy Laboratory (NREL) at [www.nrel.gov/publications](http://www.nrel.gov/publications).

**Technical Report**  
NREL/TP-5D00-70781  
August 2018

Contract No. DE-AC36-08GO28308



# Concentrating Solar Power Impact on Grid Reliability

Nicholas W. Miller and Slobodan Pajic  
*GE Energy Consulting*

Kara Clark  
*National Renewable Energy Laboratory*

Prepared under Task No. SETP.10304.23.01.10

**NREL is a national laboratory of the U.S. Department of Energy  
Office of Energy Efficiency & Renewable Energy  
Operated by the Alliance for Sustainable Energy, LLC**

This report is available at no cost from the National Renewable Energy Laboratory (NREL) at [www.nrel.gov/publications](http://www.nrel.gov/publications).

National Renewable Energy Laboratory  
15013 Denver West Parkway  
Golden, CO 80401  
303-275-3000 • [www.nrel.gov](http://www.nrel.gov)

**Technical Report**  
NREL/TP-5D00-70781  
August 2018

Contract No. DE-AC36-08GO28308

## NOTICE

This work was authored in part by the National Renewable Energy Laboratory, operated by Alliance for Sustainable Energy, LLC, for the U.S. Department of Energy (DOE) under Contract No. DE-AC36-08GO28308. Funding provided by the U.S. Department of Energy Office of Energy Efficiency and Renewable Energy Solar Energy Technologies Office. The views expressed in the article do not necessarily represent the views of the DOE or the U.S. Government. The U.S. Government retains and the publisher, by accepting the article for publication, acknowledges that the U.S. Government retains a nonexclusive, paid-up, irrevocable, worldwide license to publish or reproduce the published form of this work, or allow others to do so, for U.S. Government purposes.

This report is available at no cost from the National Renewable Energy Laboratory (NREL) at [www.nrel.gov/publications](http://www.nrel.gov/publications).

U.S. Department of Energy (DOE) reports produced after 1991 and a growing number of pre-1991 documents are available free via [www.OSTI.gov](http://www.OSTI.gov).

*Cover Photos by Dennis Schroeder: (left to right) NREL 26173, NREL 18302, NREL 19758, NREL 29642, NREL 19795.*

NREL prints on paper that contains recycled content.

## Acknowledgments

This work was authored in part by the National Renewable Energy Laboratory, operated by Alliance for Sustainable Energy, LLC, for the U.S. Department of Energy (DOE) under Contract No. DE-AC36-08GO28308. Funding provided by the U.S. Department of Energy Office of Energy Efficiency and Renewable Energy Solar Energy Technologies Office. The views expressed in the article do not necessarily represent the views of the DOE or the U.S. Government. The National Renewable Energy Laboratory and General Electric also thank the members of the technical review committee for their insightful comments and assistance. Participation in the committee does not imply agreement with the project findings. The committee included:

- Mark Ahlstrom, WindLogics
- Bradley Albert, APS
- William Anderson, Xcel Energy
- Jamie Austin, PacifiCorp
- Ron Belval, Tucson Electric Power
- Ray Byrne, Sandia National Laboratories
- Thomas Carr, Western Governors' Association
- Kemal Celik, U.S. Department of Energy
- Malati Chaudhary, Public Service Company of New Mexico
- Bob Cummings, North American Electric Reliability Corporation
- Donald Davies, Western Electricity Coordinating Council
- Joe Desmond, BrightSource
- Charles Diep, SolarReserve
- Tom Duane, Public Service Company of New Mexico
- Bob Easton, WAPA
- Sara Eftekharnjad, Tucson Electric Power
- Erik Ela, Electric Power Research Institute
- Tassos Golnas, U.S. Department of Energy
- Irena Green, California Independent System Operator
- Rebecca Johnson, Western Area Power Administration
- Debra Lew, General Electric
- Eddy Lim, Federal Energy Regulatory Commission
- Clyde Loutan, California Independent System Operator
- Kate Maracas, Western Grid Group
- Mark O'Malley, University College Dublin
- Brian Parsons, Independent consultant
- Henry Price, Independent consultant
- Vikas Singhvi, Electric Power Research Institute
- Charlie Smith, Utility Variable Generation Integration Group
- Guohui Yuan, U.S. Department of Energy

The National Renewable Energy Laboratory regrets any inadvertent omission of project participants and contributors.

## Executive Summary

This study examines the impact of concentrating solar power (CSP) on grid reliability by investigating the dynamic behavior of the Western Interconnection under conditions of high solar and wind generation. *Reliability* in this case refers to the somewhat narrow context of stability: transient stability and frequency response; and control stability, especially that associated with weak grids.

The objectives of this study were to identify renewable energy penetration levels and mixes, severe disturbances, and load conditions where grid performance and reliability could be enhanced with CSP plants. Instantaneous penetrations of wind and solar—both photovoltaics (PV) and CSP—up to approximately 60% were considered. The focus is on situations in the Western Interconnection bulk power system during which variable renewable generation has displaced other (non-CSP) synchronous thermal generation under highly stressed, weak system conditions. Particular attention was given to impacts of frequency-responsive controls and synchronous generation characteristics.

This is relatively new ground for the industry, and this investigation is not a substitute for detailed planning, but the risks illustrated can be analyzed and mitigated. Tools, data, and the current state-of-the-art interconnection and bulk power system stability studies, if used following good system engineering practices as systems are built out, will ensure continued reliability of power systems.

## Key Findings

### ***Grid Build-Out to Support Added Solar and Wind Changes Transient Stability***

Transmission added in solar-rich areas to avoid thermal and voltage violations, plus changes in dispatch and commitment (Section 2), have some effect on transient stability. The impacts are mixed, with some improvements and decreases (Section 5.2). No stability violations—noncompliance with Western Electricity Coordinating Council (WECC) criteria—were found for the primary fault-clearing cases tested (Section 5.2 and Section 10.2). As noted, good planning practice needs to be observed.

WECC-wide system inertia dropped up to 27%–32% from earlier light load planning cases. The earlier cases had less wind and solar generation and included synchronous generation, which was retired in the final study cases (Section 4.1). The lower system inertia did not present any significant stability or frequency response challenges.

We did not observe systemic issues related to frequency and transient stability resulting from the solar and wind build-out. That is, the overall behavior was similar in character to the present system. The system seems to better tolerate non design-basis north-south separation with the grid additions (Section 6.6).

For the conditions studied, a simultaneous nonsynchronous penetration (SNSP) of approximately 70% (Section 4.3) did not have an adverse impact on system-wide transient stability (Section 5.2). Transient stability issues seemed to be rather localized (Section 10.2).

## ***Primary Frequency Response from Concentrating Solar Power Helps Meet Frequency Response Obligation***

Because CSP uses a conventional synchronous steam turbine generator system to produce electricity, it always contributes inertia when running. Further, depending on the design and operation of the plant, it can provide primary frequency response (PFR) via governor action. It is by no means ensured that CSP plants will necessarily provide this service. Steam systems and turbines must be designed with this capability in mind for best economy. This report provides some discussion and concepts for possibly squeezing additional frequency response out of steam systems (Section 8.1). The discussion includes the concept of a triggered, open-loop control based on the accepted practice of fast-valving special protective systems (Section 8.3).

PFR from CSP benefits frequency response, improves the system nadir, and helps the system (and regions thereof, such as California) meet their frequency response obligations (FRO) (Section 9.3). The contribution of synchronous inertia is observable, but it not very important for the conditions and cases examined.

Tripping two of the Palo Verde Nuclear Generating Station units, for a loss of approximately 2,750 MW, is the design basis frequency event for WECC (Section 6.1.2). We have continued to use that event extensively in this study. Figure ES-1 shows three cases for that event run on the lighter load case (60% instantaneous wind and solar penetration for the U.S. WECC) that illustrate two separate points. The red trace shows the reference lighter load case. The CSP units are online contributing inertia, but there is no governor response. The blue trace shows the impact of enabling the governors on the CSP plants (per the model discussion in Section 3.2). As expected, both the frequency nadir and the settling frequency improve. The green trace shows the impact of replacing CSP with PV (so difference between this and the red case is the inertia of 10 GW of CSP machines). This case has the same 60% instantaneous penetration, but the SNSP is 70% because of the increased levels of inverter resources (Section 4.3). As expected, the CSP-to-PV case with less inertia shows a faster frequency drop, and the nadir occurs sooner and is approximately 1-mHz deeper. For this design basis case, the PFR is much more important than the inertia contribution (Section 6.3).

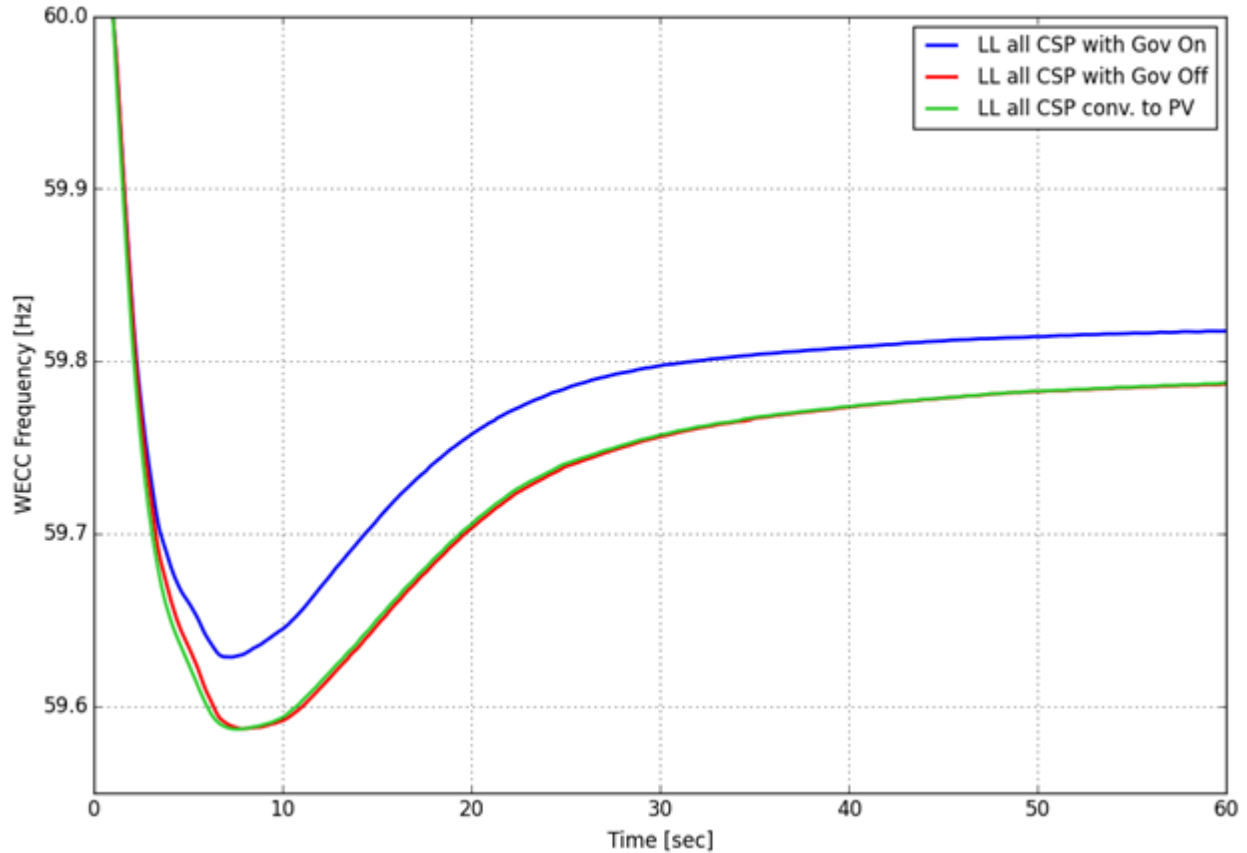


**Figure ES-1. Contribution of concentrating solar power governors and inertia to frequency response**

***Fast Frequency Response from Solar Photovoltaics or Energy Storage Improves Frequency Nadir and Adds Margin Against Underfrequency Load-Shedding***

The provision of fast frequency response (FFR) by utility-scale, transmission-connected PV or other inverter-based resources, such as energy storage devices, can improve the system frequency nadir and add margin against underfrequency load-shedding. FFR is the rapid injection of arresting power to the grid during the time immediately following a disturbance that unbalances the grid and causes the frequency to drop (Section 7.1). FFR slows the decline and helps make the minimum frequency better.

PV can be designed with FFR capability. This is particularly true for utility-scale PV. In the main report (Section 7.2), we include a detailed discussion of the fundamental concepts that allow PV to provide FFR. In brief, new controls, adaptive use of rating differences between PV inverters and panels, and possible transient overload of inverters can allow utility-scale PV to provide FFR.

Considerable effort was applied toward improving understanding of the timing and location considerations for FFR (Section 7.3 and Section 7.4). This study found that responding quickly after the disturbance produces improved performance (in terms of improved nadir), but responding within 1–2 seconds produces most of the of benefit. Faster response produces only marginally better performance and introduces robustness concerns.

Figure ES-2 shows the total results of a sequence of tests and the impact on the nadir as a function of timing. Higher nadir is better. The blue trace shows the base case without CSP governors enabled. The efficacy of the FFR is almost the same for approximately the first 3 seconds of the event, then the efficacy of the FFR drops to zero by the time of the nadir, indicated by the vertical red line. This is an important result that means that there is little systemic benefit in applying FFR with undue haste. Waiting for good information with which to make the decision to “trigger” the FFR has a small performance penalty and might produce significant robustness benefits.

The green trace presents the results in the case with CSP governors enabled. The impact of FFR timing on change in nadir is similar to the case without CSP governors enabled. The overall curve is better (higher) because of the CSP governor contribution, but otherwise the impact is very similar. This is another significant result. It shows that for a given operating condition, the beneficial contributions of multiple mitigations (in this case CSP governors *plus* FFR) are complementary and quite linear (they add up). This is not to say that the impacts are linear or uniform across very different operating conditions.

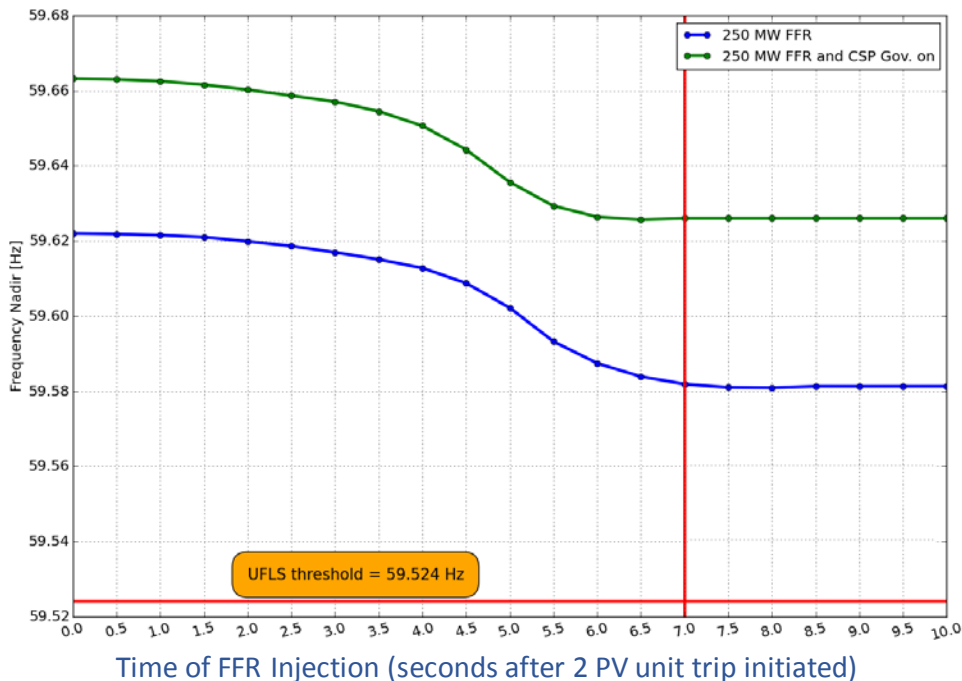


**Figure ES-2. Impact of fast frequency response timing on frequency nadir**

Further similar investigation showed that for energy-limited FFR (e.g., synthetic inertia from wind), the best efficacy is for FFR a few seconds into the event.

Figure ES-3 shows regional frequency measurements for two similarly sized events that are initiated at very different points in the system (Section 6.4). The blue trace (labeled 2PV) shows the trip of two Palo Verde Nuclear Generating Station units in Arizona, and the red trace shows an event in the middle of the Pacific Northwest. The location aspects dominate for approximately 2 seconds. Note, for example, how different the two events appear in the Northwest and

Southwest. Even though these events are approximately the same magnitude from a frequency perspective, they look very different during the first 2 seconds. This represents an acute challenge for triggering control actions that are sensitive to initial frequency drop or rate of change of frequency (ROCOF). Specifically, local differences in frequency during disturbances suggest that triggering FFR should be no faster than 0.5 seconds. This is an important observation relative to the results of Figure ES-2 because those results show little benefit from faster triggering for these system-wide events.

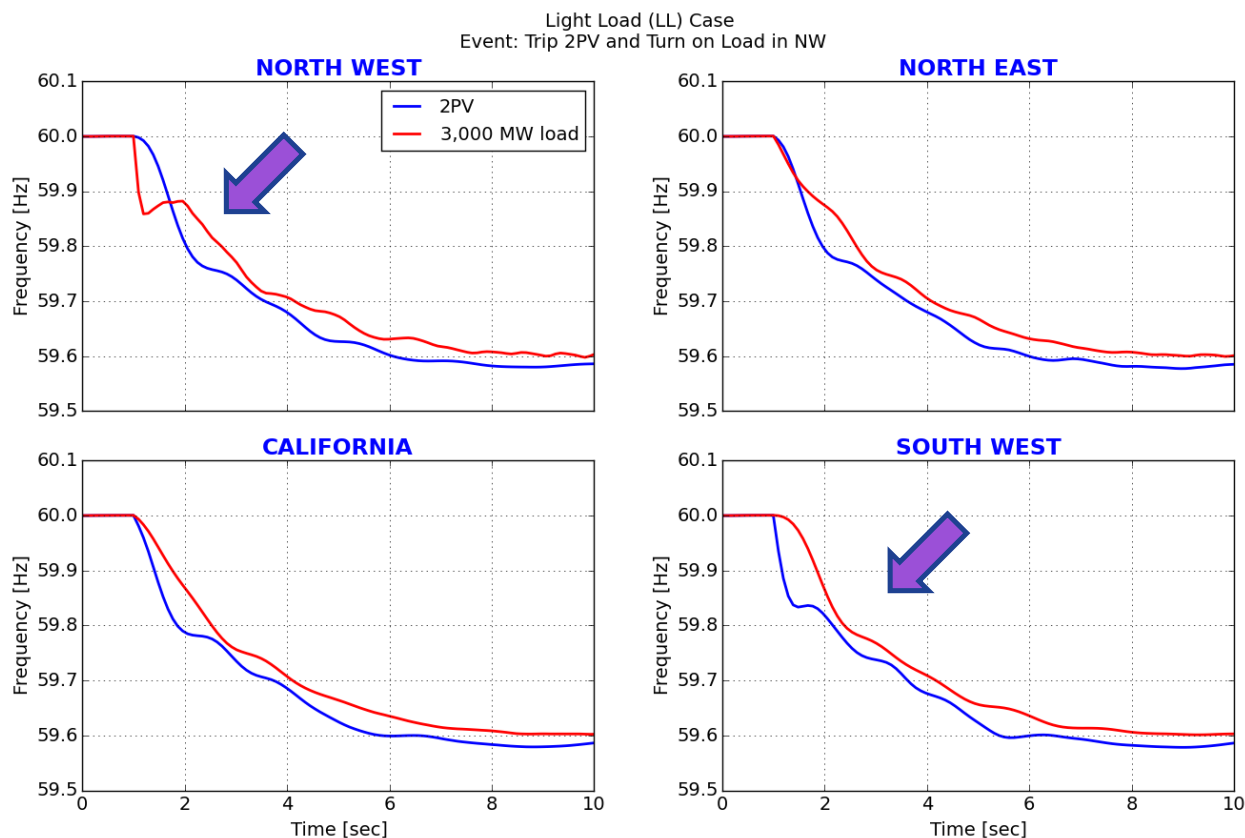


**Figure ES-3. The location of the event strongly affects the measured frequency during the first seconds.**

Investigation of the amount of FFR required to improve the frequency showed that the impact is relatively linear for small amounts. As the amount of FFR increases, the marginal benefit decreases. For the event and condition tested, FFR has good impact up to approximately 250 MW. The relative improvement declines for more FFR capacity; and for FFR greater than 500 MW, it immediately reverses the frequency decline, creating an inflection. The nadir is at the time of injection, and it does not change with increased FFR power. In the narrow context of arresting frequency and improving nadir, the contribution of the FFR is saturated and any FFR greater than 500 MW is wasted. This gives an interesting perspective: the event is approximately 2,750 MW, but more than 500 MW of FFR produces no additional benefit for this specific operating condition (Figure 65 in Section 7.4). The FFR works—*as always*—with the PFR from the committed generation that has active governors and headroom to act. The FFR does not impact the system in isolation, and the combination of the FFR and the amount and speed of PFR

dictates the megawatt-level of this saturation point. For systemic events, the location of the FFR resources is not very important.

Note that as (1) system inertia drops, (2) PFR becomes slower or scarcer, and (3) ROCOF increases, this inflection point becomes a larger fraction of the size (in MW) of the event. The authors have observed this in smaller systems with relatively low inertia. In the limit, as for example when a system approaches no inertia, the break point becomes equal to the size of the disturbance. That is, the FFR must fully, exactly, and quickly match the size of the disturbance to meet frequency performance objectives. The WECC system under consideration in this study is far from that point.

### ***Frequency Response from Concentrating Solar Power Can Substitute for Fast Frequency Response from Photovoltaics or Batteries***

Both CSP PFR and FFR from PV improve performance. These can be quantitatively compared (Section 8.2). In these cases, the benefit of frequency response from CSP is approximately equivalent to 3% of FFR from inverter/switched resources. That means, for example, that for each 100MW of CSP providing PFR, the equivalent of 3 MW of FFR is provided at that time. In this system, with approximately 10 GW of CSP, PFR on all the units would provide the same benefit for FRO as 300 MW of inverter-based FFR. Batteries or utility-scale PV, as discussed in Section 7.2, have potential to provide FFR. Obtaining FFR from these inverter-based resources will have accompanying costs, which might include costs of curtailment. The timing of available PFR or FFR will vary by resource. Both the amount (i.e., the number of hours per year that the service is available) and the timing (i.e., what hours the service is available) will be different by resource. Consequently, the overall (or annualized) economic value of the various alternatives derive from overall operational impact (i.e., over the full 8,760 hours of a year).

Figure ES-4 shows an example “equivalence” between the CSP governor and FFR. The reference case (black trace) is without FFR or CSP governor contribution. The blue trace shows the CSP governors enabled with no FFR, and the green trace shows 250 MW of FFR without CSP governors. The CSP governors produce a somewhat better frequency nadir than the 250 MW of FFR, giving an improvement equal to approximately 300 MW of FFR. The red trace is for both, showing that the impacts are additive.

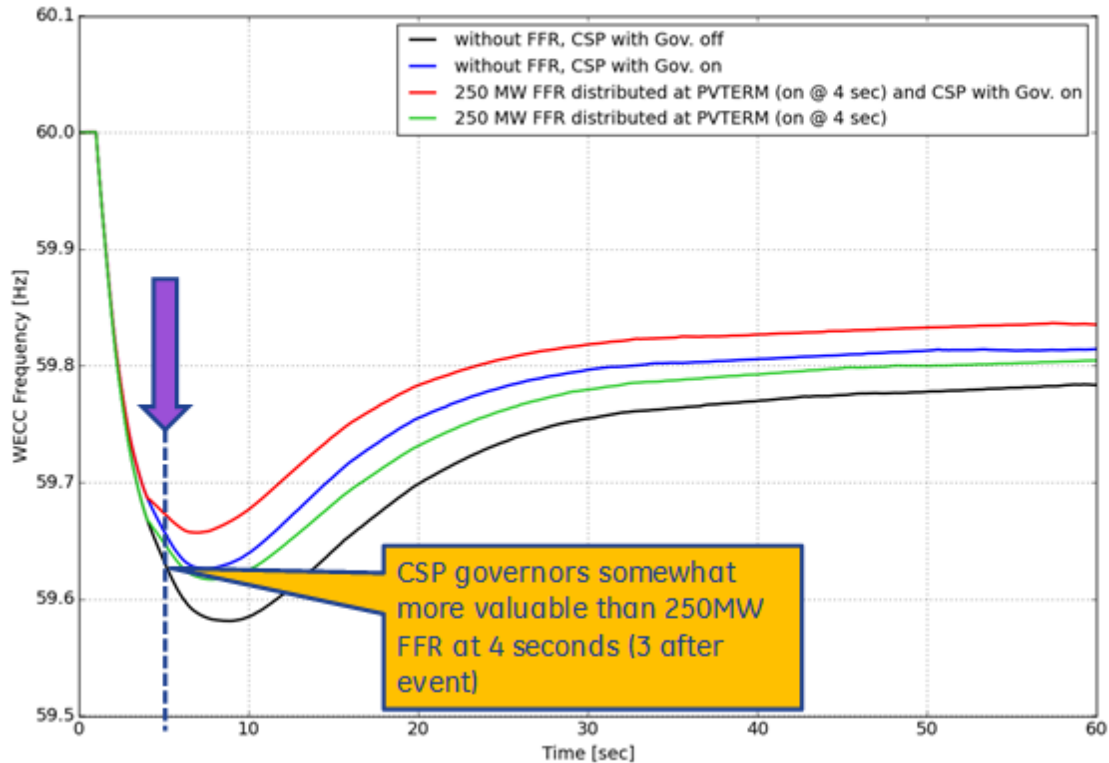


**Figure ES-4. Relative benefit of concentrating solar power governors compared to fast frequency response**

Tests on the use of fast-valving, open-loop controls on CSP showed that they might increase this benefit to approximately 4.5% (Section 8.3). Concepts were presented in the work for such controls, which would need further engineering design to ensure feasibility (Section 8.1).

Thermal storage should help the sustainability of PFR, and it might help the speed of response (Section 9.4). Again, more detailed design is required.

***The Benefits of Frequency Response from Concentrating Solar Power During Sunset Can Be Substantial and Might Represent Valuable Options During the Neck of the Duck Curve***

One challenge that has surfaced for systems with high levels of solar is managing the system as the sun sets and there is a drop in solar generation. As the solar power drops, there are potential issues with exhausting other resources. Thus, this concern is not about high instantaneous penetration but rather what might happen shortly afterward, as the sun sets. We looked closely at California for insight, but the issues are more general, and the findings apply to other parts of WECC and to other systems around the world that have or might have high levels of solar generation (Section 9.1).

The lighter load case is a reasonable proxy for operation during the low net load condition that precedes the start of sunset. During the time frames that are the focus of this study, one of the most pressing concerns that accompany sunset from high solar, light load conditions is frequency response (Section 9.2). During sunset, the system needs to meet the rise of net load by (1)

dispatching committed generation that has headroom and (2) committing (starting) additional resources.

Exercises aimed at improving understanding of the relationship between this net load following and the depletion of generation headroom that accompanies the upward dispatch were pursued. To that end, the work took the extreme case of looking at what happens if all the loss of solar generation is followed by resources that are already committed in California. Two sets of initial conditions were considered: (1) the lighter load case and (2) a sensitivity case in which more solar, less wind, and less initial synchronous resources were available (Section 9.3).

In the sequence, the utility solar generation production across WECC, both PV and CSP (if deployed without storage), is ramped down uniformly to reflect the drop in insolation that accompanies sunset. At each step along sunset, WECC, California, and other frequency response performance was tested with the Palo Verde Nuclear Generating Station trip events. The committed gas-fired thermal generation, including combined-cycle steam, in California is dispatched upward. This continues until these units are effectively out of headroom and cannot further increase output. At that point, the California hydro with headroom is dispatched upward. The distinction might be important because when modeling hydro we assume that there is sufficient water (and headroom) to allow this upward dispatch. A much closer look at the hydrology would be needed to confirm this. As noted in this work and in earlier WWSIS work, the contribution of California hydro to meeting the California Independent System Operator FRO is significant under these study conditions. Closer inspection of the actual capability and performance of these hydro plants is warranted

One set of results is shown in Figure ES-5. The figure shows California's frequency response (as mandated by the North American Electric Reliability Corporation) in units of MW/0.1 Hz<sup>1</sup> compared to the amount of solar generation lost in WECC because of sunset. For the sequence for the sensitivity case (Low Load, Low Frequency Response), California was initially out of compliance. This means that the potential value from adding CSP governors is high. A comparison set of cases on the low frequency response sensitivity was run with all CSP governors enabled (the purple trace). The benefit to California is substantial, initially adding 150 MW/0.1 Hz of frequency response to California. California can meet its frequency response for up to 1,500 MW of sunset (blue arrow). A linear extrapolation (orange dotted line and arrow) suggests that enabling the governors on all new CSP in this case is "worth" an approximate 2,500-MW reduction in utility-scale solar generation due to the sun setting.

---

<sup>1</sup> Meaning MW of response per 0.1 Hz change in frequency

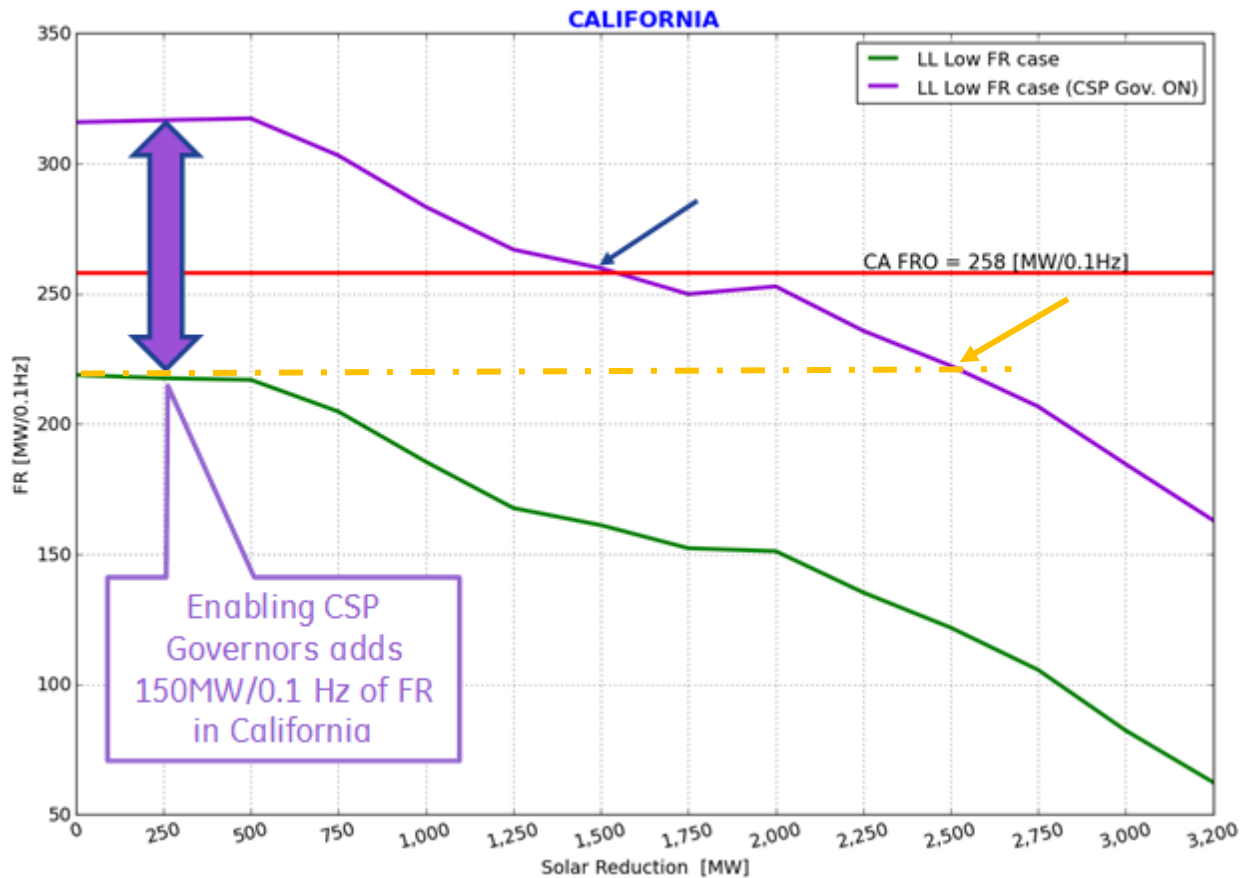


**Figure ES-5. California’s frequency response declines during sunset if headroom is depleted.**

Better dynamic response is also similar to effectively postponing sunset because it provides a frequency response benefit, such as retaining headroom. In this construct, the possible fast valving discussed in Section 8.3 is “worth” approximately 1,700 MW of sunset above and in addition to the approximately 2500MW benefit shown in Figure ES-5. This is a nontrivial contribution to California’s “duck curve.” But whether such capability is possible hinges on whether control and/or thermal storage can be used to extract better, i.e., faster and more sustained frequency, response from CSP.

Although these specific results are based on one sequence in California, directionally the results are applicable to any solar-heavy system facing declining frequency response during sunset. Further discussion is provided in Section 9.

**Available Dynamic Models Are Good, But They Have Some Limitations**

Validation of the dynamic stability models for the CSP thermal plant showed good correlation to field tests. CSP models lack modeling detail needed for testing the dynamic impacts of thermal energy storage (Section 8.1). Approximations showed significant promise, but more detailed modeling efforts are required for definitive quantitative results (Section 8.2 and Section 8.3).

Utility-scale PV models might be optimistic for weak grid conditions. In particular, generic models might not accurately capture fast voltage and fast regulator stability concerns under short-circuit conditions below equipment specifications. Generic models might show good

performance when the application behaves poorly in low short-circuit ratio (SCR) situations. The minimum system strength specified by the converter supplier can provide guidance for when different models and tools are required (Section 10.2).

Displacement of fossil-fueled generation by renewables increases dependence on hydro and makes modeling fidelity for hydro plants more important (Section 9.3).

### ***Stability Implications of Concentrating Solar Power Compared to Photovoltaics Are Mixed, But They Are Not Decisive for the Conditions Studied***

Short-circuit strength is one proxy widely used to screen for location-specific weak grid stability concerns. Further, SNSP is an emerging metric of systemic concerns about stability with high levels of inverter-based resources. A range of tests and screening for both metrics were pursued. One important finding was that short-circuit levels in the solar-rich areas tended to increase because of added transmission necessary to connect the new solar power plants without violating local voltage and thermal constraints. The added transmission tends to offset effects of decommitting synchronous generation. The only concerns identified tended to be very localized. These were sensitive to the fact that system strength declines as PV is substituted for CSP (Section 4.2).

Because SCR is a key metric for concern about inverter-based generation instability, a deliberately challenging test was devised in which the grid was degraded by removing one of the 230-kV lines providing egress for the power from the solar power plants. In this case, the SCR before the fault is 2. Figure ES-6 shows a comparison of two cases with the system degraded. The voltages in the upper set of axes show the CSP in blue and the utility-scale PV in red. The power swings of the local solar power plants are shown in the next two sets, with the CSP synchronous machines swings in the middle and the PV power on the bottom. The swing of the synchronous CSP machines is somewhat greater. Both cases meet WECC criteria (Section 10.2.2).

As the fault becomes longer, voltage recovery will degrade. Eventually, voltage recovery will violate criteria, or synchronous CSP machines will lose synchronism. Inverter-based generation, including PV, will tend to tolerate longer faults (discussion in Section 10.2.1).

The lowest grid strength here (i.e., SCR of approximately 2) is where inverters for stiffer grids might misbehave. Stress tests in simulations, where PV inverters were provided with control setting characteristics of very stiff (high short-circuit strength) systems, showed instability like that observed in the field; however, this class of instabilities is outside of the accuracy of positive sequence simulation (transient stability) tools. More sophisticated analysis is required for evaluation and mitigation (Section 10.3).

Solar-exporting areas generally showed better transient stability, i.e., reduced swings and better post-fault voltage recovery, with PV compared to CSP. No transient stability issues that resulted in violation of WECC criteria were observed for primary cleared faults regardless of the type of solar generation (Section 10.2).

Light Load (LL) Retirement Case  
 Fault: Eagleye 230 kV 3ph fault (line-out case)

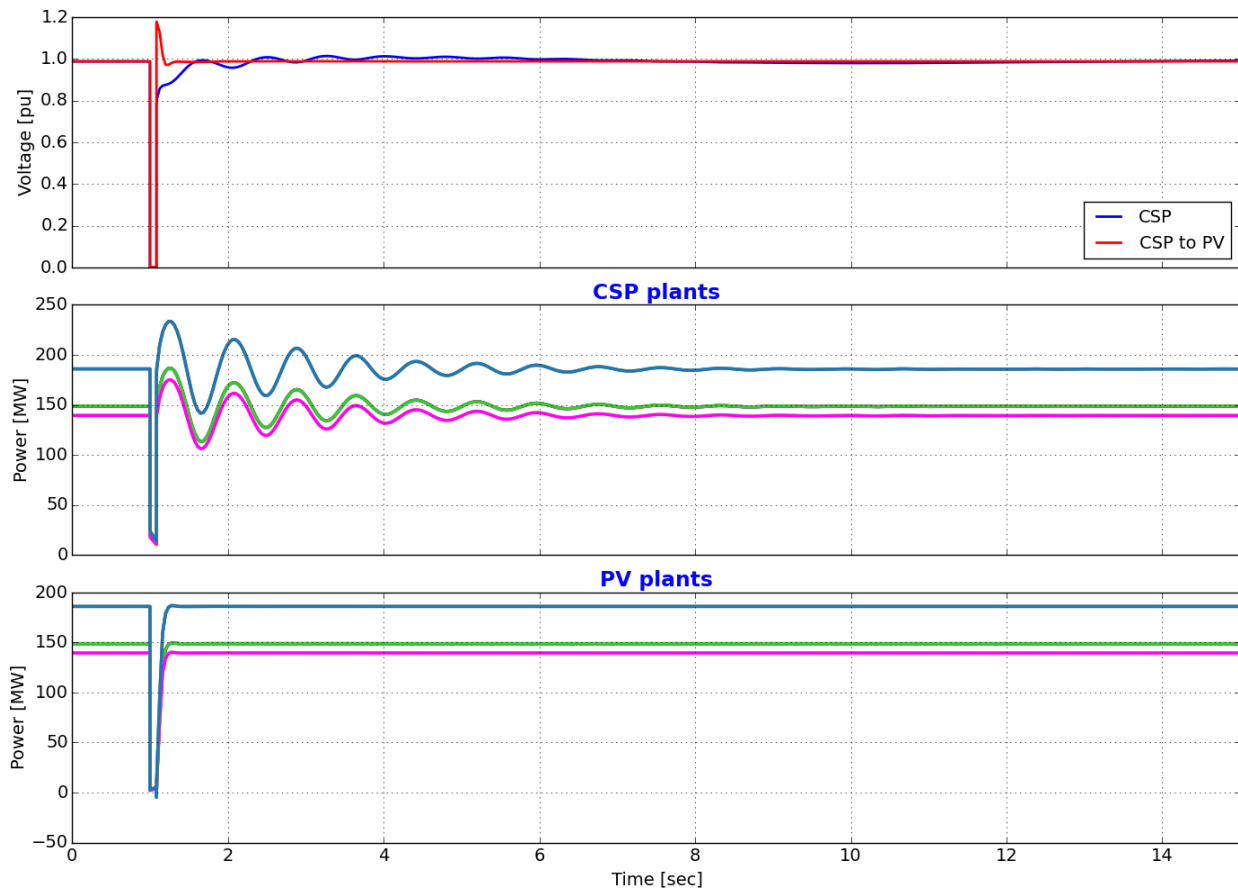


**Figure ES-6. Transient stability of CSP compared to PV in a low-grid-strength location**

The range of tests performed here did not show evidence of any widespread concerns about a weak grid, high SNSP, or low short-circuit levels for the predominantly utility-scale PV case. These cases do not provide observable motivation to prefer synchronous CSP instead of inverter PV regarding system transient and voltage stability.

## Executive Summary Closure

This investigation shows that integrating large amounts of solar power in the WECC system for the conditions studied does not present any obviously intractable challenges. We find that frequency response can be aided significantly by frequency-sensitive controls on CSP and PV solar. Stability problems, including those anticipated around weak grid issues, were not substantial.

## List of Acronyms

CAISO	California Independent System Operator
COI	California-Oregon Interface
CSP	Concentrating solar thermal power plant
DG	distributed generation, embedded PV
FFR	Fast frequency response
FRO	Frequency response obligation
GW	gigawatt
HVDC	high-voltage direct current
Hz	Hertz
mHz	millihertz
MVA	Megavolt ampere
MW	megawatt
NERC	North American Electric Reliability Corporation
PDCI	Pacific Direct Current Intertie
PFR	Primary frequency response
PV	Photovoltaic
ROCOF	Rate of change of frequency
SCE	Southern California Edison
SCR	Short-circuit ratio
SNSP	Simultaneous nonsynchronous penetration
WECC	Western Electricity Coordinating Council
WWSIS	Western Wind and Solar Integration Study

# Table of Contents

<b>Executive Summary</b> .....	<b>iv</b>
Key Findings .....	iv
Grid Build-Out to Support Added Solar and Wind Changes Transient Stability .....	iv
Primary Frequency Response from Concentrating Solar Power Helps Meet Frequency Response Obligation.....	v
Fast Frequency Response from Solar Photovoltaics or Energy Storage Improves Frequency Nadir and Adds Margin Against Underfrequency Load-Shedding .....	vi
Frequency Response from Concentrating Solar Power Can Substitute for Fast Frequency Response from Photovoltaics or Batteries.....	ix
Available Dynamic Models Are Good, But They Have Some Limitations .....	xii
Stability Implications of Concentrating Solar Power Compared to Photovoltaics Are Mixed, But They Are Not Decisive for the Conditions Studied .....	xiii
Executive Summary Closure .....	xiv
<b>1 Introduction</b> .....	<b>1</b>
1.1 Project Structure.....	1
1.1.1 Year 1 .....	1
1.1.2 Year 2 .....	2
1.2 Background and Related Work .....	2
1.2.1 Western Wind and Solar Integration Study: Phase 1 .....	2
1.2.2 Western Wind and Solar Integration Study: Phase 2 .....	3
1.2.3 Western Wind and Solar Integration Study: Phase 3 .....	3
1.2.4 Western Wind and Solar Integration Study: Phase 3A .....	3
1.3 Planning Context .....	3
<b>2 Database Refinement</b> .....	<b>4</b>
2.1 Case Evolution/Summary .....	4
2.2 Case Summaries .....	5
2.3 Western Interconnection Power Plant Retirements .....	7
2.4 Study Regions .....	9
2.5 Concentrating Solar Power Plants .....	9
2.6 Lighter Load .....	10
2.6.1 Lighter Load Analysis .....	11
2.6.2 Redispatch for Increased Solar and Lighter Load .....	12
2.7 Transmission Improvements .....	14
2.7.1 Pacific DC Intertie Upgrade .....	14
2.7.2 Improvements to Accommodate Increased Solar Production .....	15
2.8 Heavy Summer Retirement Case .....	17
2.9 Replacement of CSP with PV (CSP-to-PV) Sensitivity Case .....	19
<b>3 CSP Model Validation</b> .....	<b>20</b>
3.1 Exciter Model Validation Testing .....	20
3.2 Governor Model Validation Testing .....	22
3.3 Load Model Validation .....	24
<b>4 System Characterization</b> .....	<b>27</b>
4.1 System Inertia.....	27
4.2 Short-Circuit Strength .....	29
4.3 Simultaneous Nonsynchronous Penetration: General Discussion.....	32
4.3.1 Simultaneous Nonsynchronous Penetration: Effect of CSP to PV Conversion on Lighter Load Results.....	35
<b>5 System Transient Stability Performance</b> .....	<b>39</b>
5.1 Overview .....	39

5.1.1	Transient Stability Visualization .....	39
5.1.2	Previous Transient Stability Work: Western Wind Solar Integration Study: Phase 3 and Phase 3A.....	40
5.2	Regional Transient Stability Impacts of Required Transmission Changes .....	41
5.2.1	Heavy Summer Pacific DC Intertie Event Case: Initial Investigation .....	41
5.2.2	Investigation of Transmission Additions Impact on Transient Stability for Pacific DC Intertie Event.....	43
5.2.3	California-Oregon Interface Event.....	45
5.2.4	Overall Observations on Transient Stability Impact of Transmission Additions.....	46
<b>6</b>	<b>Frequency Performance .....</b>	<b>47</b>
6.1	Frequency Response Overview .....	47
6.1.1	Frequency Response Visualization .....	47
6.1.2	Frequency Response Obligation.....	50
6.1.3	Palo Verde Reference Event .....	51
6.2	Impacts of CSP and Load Condition on Dispatch.....	51
6.3	CSP Governor and Inertia Contributions .....	54
6.3.1	Lighter Load.....	54
6.3.2	Inertia impact on Rate of Change of Frequency.....	55
6.4	Locational Aspects of Inertia and Frequency Response.....	56
6.4.1	Locational Aspects of Primary Frequency Response.....	58
6.5	Heavy Summer.....	62
6.5.1	Impact of Retirements and DC Upgrade .....	62
6.5.2	Heavy Summer Impact of CSP Governors.....	63
6.5.3	Localized Damping Concerns .....	64
6.6	North-South Separation Disturbance.....	65
6.6.1	Heavy Summer North-South Separation.....	66
6.6.2	Impact of PV Compared to CSP on Separation Dynamics .....	69
6.6.3	Spring Lighter Load North-South Separation .....	70
<b>7</b>	<b>Fast Frequency Response and Enhanced PV Response.....</b>	<b>72</b>
7.1	Fast Frequency Response Discussion.....	72
7.2	Concepts for Transient Fast Frequency Response from PV.....	72
7.2.1	Solar PV Components and Fast Frequency Response.....	72
7.2.2	Curtailment, Overload, and Fast Frequency Response .....	74
7.2.3	Inverter and Panel Rating.....	77
7.2.4	Fast Frequency Response Control.....	79
7.3	Generalized Fast Frequency Response: Energy Impulse .....	80
7.4	Generalized Fast Frequency Response: Sustained Response.....	84
7.4.1	Linearity of Fast Frequency Response Impacts .....	87
7.4.2	Locational Aspects of Fast Frequency Response.....	88
7.4.3	Temporal Relationship Between Fast Frequency Response and Rate of Change of Frequency.....	90
<b>8</b>	<b>Enhanced Frequency Response from CSP .....</b>	<b>92</b>
8.1	Concepts for Enhanced Frequency Response from CSP.....	92
8.2	CSP Governor Response Compared to Inverter-Based Fast Frequency Response .....	94
8.3	Fast Valving and Enhanced CSP Response Results.....	97
8.3.1	Frequency Response Comparison of CSP Fast Valving to Fast Frequency Response from PV.....	99
<b>9</b>	<b>Sunset Net Load Ramp and Frequency Response .....</b>	<b>101</b>
9.1	Discussion: California Duck Curve.....	101
9.2	Depletion of Headroom.....	102
9.3	Lighter Load Low Frequency Response Sunset Sensitivity Investigation.....	106

9.3.1	Effect of Enabling CSP Governors During Sunset .....	112
9.3.2	Governor: Headroom, Frequency Response, and Storage.....	119
9.4	Implications for CSP Thermal Storage .....	120
9.5	Synopsis of Sunset Investigation.....	121
<b>10</b>	<b>Local Weak Grid and Regional High Simultaneous Nonsynchronous Penetration .....</b>	<b>123</b>
10.1	Introduction .....	123
10.1.1	Weak Grid Visualization.....	123
10.1.2	Investigation of Short-Circuit Strength on Weak and High-Change Buses .....	123
10.2	Investigation of Low Short-Circuit Strength at Solar Power Plants.....	124
10.2.1	Gila Bend .....	124
10.2.2	Eagle Eye .....	126
10.2.3	Discussion of Mechanisms of Weak Grid Inverter Instability .....	128
10.2.4	Experiments with Deliberately Induced PV Regulator Instability .....	130
10.3	Key Observations on Low Levels of Synchronous Generation .....	131
<b>11</b>	<b>Key Findings and Conclusions .....</b>	<b>133</b>
11.1	Key Findings .....	133
11.1.1	Changes in Frequency and Transient Stability Resulting from Solar and Wind Build-Out.....	133
11.1.2	Primary Frequency Response from CSP.....	133
11.1.3	Fast Frequency Response.....	134
11.1.4	Dynamic Models .....	134
11.1.5	Stability Implications of CSP Compared to PV .....	135
11.1.6	Economic Implications of CSP Compared to PV .....	135
11.2	Future Work .....	136
11.2.1	Western Interconnection Analysis .....	136
11.2.2	Protection and Relaying Investigation .....	136
11.2.3	Load Modeling .....	136
<b>12</b>	<b>References .....</b>	<b>137</b>

## List of Figures

Figure ES-1. Contribution of concentrating solar power governors and inertia to frequency response .....	vi
Figure ES-2. Impact of fast frequency response timing on frequency nadir.....	vii
Figure ES-3. The location of the event strongly affects the measured frequency during the first seconds. .....	viii
Figure ES-4. Relative benefit of concentrating solar power governors compared to fast frequency response.....	x
Figure ES-5. California’s frequency response declines during sunset if headroom is depleted. ....	xii
Figure ES-6. Transient stability of CSP compared to PV in a low-grid-strength location .....	xiv
Figure 1. Definition of regions.....	9
Figure 2. Geographic distribution of added CSP units .....	10
Figure 3. Lighter load duration analysis curves .....	11
Figure 4. Lighter load final commitment and dispatch.....	12
Figure 5. Lighter load final dispatch with imports.....	13
Figure 6. Lighter load wind and solar (PV plus CSP) penetration.....	14
Figure 7. Final commitment and dispatch for heavy summary retirement case .....	18
Figure 8. Final dispatch with imports for heavy summer retirement case .....	18
Figure 9. Excitation test of Genesis CSP plant .....	21
Figure 10. Simulation validation of exciter model(s) .....	22
Figure 11. Governor test of Genesis CSP plant .....	23
Figure 12. Simulation validation of governor models .....	23
Figure 13. Load data March 30, 2012, 10–11 a.m. ....	24
Figure 14. Composite load model with embedded PV .....	25
Figure 15. Dynamic behavior of composite load model for a selected bus .....	26
Figure 16. Spring: Western Interconnection system inertia.....	28
Figure 17. Spring: regional impact on inertia .....	29
Figure 18. Spring: impact on short-circuit strength .....	30
Figure 19. Short-circuit strength detail in SCE Zone.....	31
Figure 20. Changes in short-circuit strength from lighter load to lighter load PV-to-CSP case.....	32
Figure 21. Lighter load simultaneous nonsynchronous penetration for system based on generation (dispatch).....	33
Figure 22. Lighter load regional simultaneous nonsynchronous penetration based on generation (dispatch) .....	34
Figure 23. Lighter load simultaneous nonsynchronous penetration based on capacity (generator rating) .	35
Figure 24. Contribution of CSP to reducing simultaneous nonsynchronous penetration .....	36
Figure 25. Simultaneous nonsynchronous penetration for CSP-to-PV sensitivity .....	37
Figure 26. Lighter load CSP-to-PV case distribution of inverter-based resources .....	38
Figure 27. Lighter load CSP-to PV case changes in resources in the Southwest .....	38
Figure 28. Visualization of transient stability with synchronous generators and wind power plants.....	40
Figure 29. Frequency Pacific DC Intertie result .....	42
Figure 30. California-Oregon Interface Pacific DC Intertie event: key path flows .....	43
Figure 31. Pacific DC Intertie disturbance performance degraded by transmission additions .....	44
Figure 32. Path flow comparisons for PDCI disturbance showing performance degraded by transmission additions.....	45
Figure 33. California-Oregon Intertie event stability test details.....	46
Figure 34. Balance analogy for frequency stability .....	48
Figure 35. Electricity demand exceeds electricity generation and frequency drops.....	48
Figure 36. System frequency in response to a large generation trip .....	49
Figure 37. Light spring compared to lighter load frequency (no contribution from CSP).....	52

Figure 38. Light spring compared to lighter load regional primary frequency response (no contribution from CSP) .....	53
Figure 39. Light spring compared to lighter load regional primary frequency response in areas with significant CSP capacity (no contribution from CSP) .....	54
Figure 40. Impact of CSP governors and inertia on frequency for Lighter Load case .....	55
Figure 41. Inertia impact on initial rate of change of frequency .....	56
Figure 42. Locational aspects of rate of change of frequency impacts .....	57
Figure 43. Comparison: loss of two Palo Verde units (approximately 2,750 MW) compared to 3,000 MW load increase in the Northwest .....	59
Figure 44. Primary frequency response: loss of two Palo Verde units compared to 3,000 MW load increase in the Northwest .....	60
Figure 45. Voltage: loss of two Palo Verde units compared to 3,000 MW load increase in the Northwest .....	61
Figure 46. Initial regional frequency decline: loss of two Palo Verde units compared to 3,000 MW load increase in the Northwest .....	62
Figure 47. Heavy summer: impact of retirements and DC upgrade .....	63
Figure 48. Heavy summer retirement case: impact of CSP governors .....	64
Figure 49. Illustration of local damping risk with CSP on long radial interconnection .....	65
Figure 50. Illustrative North-South separation .....	66
Figure 51. Heavy summer: regional frequencies for North-South system separation .....	67
Figure 52. Heavy summer retirement case: North-South separation—key path flows.....	68
Figure 53. Heavy summer retirement case: North-South separation—selected bus voltages.....	69
Figure 54. CSP compared to PV separation dynamics .....	70
Figure 55. Lighter load spring case: North-South separation .....	71
Figure 56. Illustration of DC power impact of tracking.....	74
Figure 57. Inverter rating concept.....	75
Figure 58. PV current phasor for normal operation .....	76
Figure 59. Normal operation at steady-state current limits .....	77
Figure 60. DC power (different trackers) compared to AC inverter rating.....	78
Figure 61. Fast frequency response capability for reduced-rating PV inverters .....	79
Figure 62. Generic fast frequency response calibration simulations .....	81
Figure 63. Sweep of fast frequency response impulses .....	82
Figure 64. Nadir improvement compared to timing of arresting power injection .....	83
Figure 65. Sustained fast frequency response: two different amplitudes.....	85
Figure 66. A 250-MW fast frequency response at Vincent 500 kV: varied trigger timing .....	86
Figure 67. Timing and efficacy of 250-MW sustained fast frequency response .....	87
Figure 68. Impact of sustained fast frequency response magnitude .....	88
Figure 69. Distributed (at utility-scale PV plants) compared to single node fast frequency response .....	89
Figure 70. Fast frequency response impact on rate of change of frequency .....	91
Figure 71. CSP frequency control and steam balance.....	93
Figure 72. CSP governor compared to fast frequency response: impact on frequency .....	94
Figure 73. CSP governor compared to fast frequency response: power response .....	95
Figure 74. Synchronous units with governor .....	96
Figure 75. Delta of governor response.....	96
Figure 76. Frequency with CSP fast valving .....	98
Figure 77. All CSP response with fast valving .....	98
Figure 78. Fast valving on a single CSP unit.....	99
Figure 79. CAISO duck curve .....	102
Figure 80. California headroom - before and after reduction of 4,000 MW of utility-scale solar generation due to sunset.....	103
Figure 81. Frequency response to Palo Verde event during sunset .....	104

Figure 82. California frequency response during sunset.....	105
Figure 83. System-wide frequency response during sunset .....	106
Figure 84. Lighter load compared to California low frequency response case: commitment and dispatch .....	107
Figure 85. Lighter load low frequency response: dispatch at beginning and “end” of sunset .....	109
Figure 86. Lighter load low frequency response CSP sunset scenario .....	109
Figure 87. Sunset impact on California frequency response: low frequency response case.....	110
Figure 88. Sunset impact on WECC frequency response: low frequency response case .....	111
Figure 89. Sunset impact on frequency nadir: low frequency response case.....	112
Figure 90. Lighter load low frequency response during sunset with CSP governors on .....	113
Figure 91. Nadirs with enabled CSP governors .....	114
Figure 92. CSP governor response with headroom increase.....	115
Figure 93. Details of one CSP governor response as sun sets .....	116
Figure 94. Sunset with CSP governors plus fast valving .....	117
Figure 95. Fast valving during sunset .....	118
Figure 96. CSP fast-valving benefit during sunset.....	119
Figure 97. Thermal dispatch during sunset.....	120
Figure 98. Fast frequency response and storage impact on frequency response during sunset .....	121
Figure 99. Small wind power plant relative to the electric grid.....	123
Figure 100. Large wind power plant relative to the electric grid.....	123
Figure 101. Gila Bend disturbance: CSP compared to PV dynamics .....	125
Figure 102. Gila Bend disturbance: CSP compared to PV stuck breaker case .....	126
Figure 103. Eagle Eye fault: CSP compared to utility-scale PV.....	127
Figure 104. Eagle Eye fault: with initially lower short-circuit ratio .....	128
Figure 105. Measured utility-scale PV inverter instability .....	130
Figure 106. PV voltage regulator induced instability .....	131

## List of Tables

Table 1. Case Summary Synopsis.....	6
Table 2. Generation Retirements .....	8
Table 3. Once-Through Cooling Unit Retirements.....	8
Table 4. Transmission Additions .....	16
Table 5. Transformer Additions.....	17
Table 6. Capacitor Additions .....	17
Table 7. Heavy Summer Synchronous Condenser Additions.....	17
Table 8. Dispatch of CSP-to-PV Sensitivity Case .....	19
Table 9. Western Interconnection Frequency Response Obligation and Approximate Regional and Area Frequency Response Obligations.....	50
Table 10. Lighter Load Initial Rate of Change of Frequency .....	58
Table 11. Frequency Response: CSP Fast Valving Compared to Fast Frequency Response from PV .....	99
Table 12. Lighter Load Low Frequency Response CSP Scenario .....	108

# 1 Introduction

The stability of the North American electric power grids under conditions of high penetrations of wind and solar is a significant concern and possible impediment to reaching renewable energy goals. The 33% wind and solar annual energy penetration considered in this study results in substantial changes to the characteristics of the bulk power system. This includes different power flow patterns, different commitment and dispatch of existing synchronous generation, and different dynamic behavior from wind and solar generation.

The investigation reported in this document builds on the foundation of the different phases of the Western Wind and Solar Integration Study (WWSIS) described later. The specific focus of this work is on the frequency response, and the accompanying transient stability, of systems with substantial generation from concentrating solar power (CSP), wind, and solar photovoltaics (PV) (both transmission-connected utility-scale and distributed). The focus is on conditions in the Western Interconnection bulk power system during which variable renewable generation has displaced non-CSP synchronous thermal generation under highly stressed, weak system conditions.

This work focuses on “traditional” fundamental frequency stability issues, such as maintaining synchronism, frequency, and voltage. This work does not explore nonfundamental frequency issues, such as subsynchronous phenomena, harmonics, unbalances, transients, and small-signal analysis.

The objectives of this study are to identify renewable energy penetration levels and mixes, severe disturbances, and load conditions where grid performance and reliability could be enhanced with frequency-responsive controls on CSP plants.

## 1.1 Project Structure

This 2-year project followed a sequence of tasks in the execution of the work. This report includes the results of the 2-year effort, but it does not exactly follow the task sequence. The project held regular meetings with a highly knowledgeable industry technical review committee. Participation and guidance from these industry representatives was critical to the success of the project. Acknowledgement to these contributors is provided in the acknowledgments section. A brief synopsis of the task structure and task objectives follows.

### 1.1.1 Year 1

Develop study scenarios and databases. Activities included reviewing and modifying existing databases, modeling and validating CSP plant and load models, and adding various levels and mixes of other renewable (i.e., inverter-based) generation.

Task 1.1: Develop study databases. The starting databases were those developed for the Western Wind and Solar Integration Study: Phase 3 (WWSIS-3) and the follow-up analysis focusing on low levels of synchronous generation. These were compared to the current Western Electricity Coordinating Council (WECC) outlook and updated. The databases were updated to accommodate CSP plants, including local transmission to enable interconnection, and to include appropriate future transmission projects and generation retirements. The work included an examination of load model performance and comparison of the load model to National

Renewable Energy Laboratory-provided measurements. The task also identified disturbances and developed scripts for simulation.

Task 1.2: Develop and validate CSP models. This task developed appropriate CSP plant-specific models for positive-sequence power flow and dynamic analysis. The models were tested and validated for performance against measured data from operational plants.

### **1.1.2 Year 2**

Year 2 included performing the bulk of the frequency response/transient stability simulation and analysis as well as preparing this final report. The work was specifically charged with examining the impact of CSP plants on frequency response and transient stability.

Task 2.1: Perform detailed analysis of CSP impact on grid performance. Building on the models and databases developed in Year 1, this task examined grid performance and reliability for the various study scenarios. Performance was measured against applicable North American Electric Reliability Corporation (NERC), regional, and local criteria. The project specifically set out to examine inverter-based generation that meets or exceeds 70% instantaneous penetration—i.e., 70% simultaneous nonsynchronous penetration (SNSP)—with the remaining 30% met by synchronous generation, including CSP.

Task 2.2: Pursue detailed analysis of mitigation strategies to address a variety of performance concerns and opportunities in response to large system disturbances. The work identified mitigation strategies and how they might change under the various study scenarios. The mitigation work had emphasis on frequency-responsive controls for CSP plants, but frequency response from transmission-connected utility-scale PV and other resources (such as energy storage) were also addressed.

Task 2.3: Prepare final report—this document.

## **1.2 Background and Related Work**

The WWSIS, sponsored by the U.S. Department of Energy, is one of the largest regional solar and wind integration study sequences to date. In multiple phases, it explored different aspects of the question: Can we integrate large amounts of wind and solar energy into the electric power system of the West? An overview of the WWSIS research program is provided next.

### **1.2.1 Western Wind and Solar Integration Study: Phase 1**

The first phase of WWSIS (GE Energy 2010a; GE Energy 2010b) investigated the benefits and challenges of integrating up to 35% wind and solar energy in the WestConnect subregion and, more broadly, the Western Interconnection in 2017. The study showed that it is operationally feasible to accommodate 30% wind and 5% solar energy *if* utilities substantially increase their coordination of operations throughout wider geographic areas and schedule their generation and interchanges on an intra-hour basis.

### **1.2.2 Western Wind and Solar Integration Study: Phase 2**

Phase 2 of WWSIS was initiated to determine the wear-and-tear costs and emissions impacts of cycling and to simulate grid operations to investigate the detailed impacts of wind and solar power on the fossil-fueled fleet in the West (Lew and Brinkman 2013; Lew et al. 2013).

### **1.2.3 Western Wind and Solar Integration Study: Phase 3**

Phase 3 of WWSIS delved into the dynamic performance of the grid in the fractions of a second to 1 minute following a large disturbance (e.g., loss of a large power plant or a major transmission line), which is critical to system reliability. This study examined the large-scale transient stability and frequency response of the Western Interconnection with high penetrations of wind and solar, and it identified means to mitigate any adverse performance impacts via transmission reinforcements, storage, advanced control capabilities, or other alternatives (Miller et al. 2014a; Miller et al. 2014b).

### **1.2.4 Western Wind and Solar Integration Study: Phase 3A**

Phase 3A of WWSIS delved further into the transient stability of the grid under weak grid conditions and very low levels of synchronous generation. The work focused on the challenges and characterization of the behavior of a portion of the Western Interconnection with very high levels of wind generation that exports power to the rest of the interconnection and that displaces the fossil-fueled synchronous generation for which the regional transmission system was originally designed (Miller, Leonardi, and D'Aquila 2015).

## **1.3 Planning Context**

This is not a planning study. The investigations are intended to provide insight into how the Western Interconnection, and more broadly how other real systems, behave dynamically with high levels of solar generation. The data sets, discussed in detail in the next chapter, include a high level of accurate detail about the Western Interconnection, but they are not official planning databases. A comprehensive planning study would start with different databases and evaluate more scenarios, more disturbances, more paths, and more types of analysis (e.g., steady-state contingency analysis).

## 2 Database Refinement

As noted in the introduction, this study relies heavily on the foundation of work of the preceding WWSIS. Building credible load flows and dynamic models for the investigation is key to creating meaningful results. The reports (listed in Section 1.2) from the earlier work provide details of the evolution of the data up to the beginning of this study.

### 2.1 Case Evolution/Summary

As with the preceding WWSIS, we kept two broad groups of models of the western system: a set of light spring load conditions and a set of heavy summer load conditions.

The overall evolution of the data sets for this study are presented here, and then in the next sections various details of the creation of the new cases are presented. In this study, we started with two pairs of databases:

1. Circa 2013 WECC “base” power flow cases: These cases were improved at the beginning of WWSIS-3.
  - A. Heavy summer 2023: Planning case with minor wind and solar expansion.
  - B. Light spring 2022: Planning case with moderate wind and solar (no distributed generation)
2. High-mix cases: These cases were developed for WWSIS-3 and improved further for WWSIS-3A.
  - A. Mix of 33% wind and solar annual energy, evenly split (annual energy)
  - B. Mix of CSP, utility PV, and distributed PV.

In this report, we include summary information about these cases, but the details of the creation of these cases are included in the respective WWSIS reports. This project did not have the option to start with completely new databases. Rather, the intent was to capture plant retirements and major transmission projects that are likely to impact the transient stability of the system, particularly in the focus area with high levels of solar generation. As such, focus was directed particularly at changes in the Southwest and California areas of the system. There was no intent to get exact topologies. From the high-mix cases, we created for this project:

1. New “retirement” and “lighter load” cases: These were intended to capture current expectations about aspects of the Western Interconnection that are germane to this study. Specifically, for both heavy summer and light spring, these new cases included:
  - A. Thermal plant retirements (mainly important for the Heavy Summer case)
  - B. Transmission improvements.

Further, for the light spring case, the system load was reduced, creating a lighter load case. The effect of retirements is minimal in the spring case, since most of the retired units were not committed anyway.

2. New “CSP-to-PV” sensitivity cases, with future CSP plants converted to utility-scale PV plants for the lighter load condition.

For context, note that the sequence of database improvements, starting with WWSIS-3 have focused on incremental improvements rather than on developing a substantially different wind and solar penetration level. The databases have undergone many changes from the original generation and topology found in the WECC 2022–2023 cases, including the latest inputs discussed in Section 2.3. The intent of this project is to gain insight into grid dynamics with high levels of solar generation, not to perform a system planning study.

For clarity, note that in this study we continued the practice adopted for all the WWSIS work of making a distinction between utility-scale PV and distributed PV or distributed generation. Throughout this work, *utility-scale* means PV projects large enough to be connected to transmission buses explicitly represented in Western Interconnection databases. These PV plants are all assumed to have, and are modeled with, dedicated plant transformers between the transmission bus and an explicitly represented lower voltage collector bus.

The selection of the initial condition for the stability analysis was a key consideration. During the WWSIS-3 process, lengthy discussions were held regarding which conditions should be examined. Some of that decision-making process is recorded in the study report, but it is useful to provide some context here. To evaluate the impact on transient stability and frequency response of high levels of wind and solar generation, it is useful to select conditions in which the penetration levels of these resources are high. Further, it is well known that light load conditions represent some of the more challenging conditions, especially for frequency response. The California Independent System Operator and others are particularly worried about light load in the spring, when there is a high level of hydropower production. Thus, light spring conditions with high levels of wind *and* solar are of particular interest. Because it must be daytime for there to be solar generation, such light load conditions (e.g., a sunny, windy weekend morning) are not the absolute minimum load condition. That is likely to happen in the early, presunrise hours of the morning. But there will be only wind generation then, so the maximum instantaneous penetration for this mix of variable renewable generation is expected to be lower. Although these cases were expected to be both challenging and illuminating for this investigation, there is no implication that these cases are necessarily the *most difficult* in all regards.

## 2.2 Case Summaries

A detailed summary of the critical metrics for all the study cases for this project is given in Table 1. Generation levels in the table are power production, not equipment ratings. Then, in the subsequent subsections of this section, details of the cases are provided. The table includes metrics for the lighter load low frequency response sensitivity case, discussed in Section 9.3.

**Table 1. Case Summary Synopsis**

	<b>LIGHT SPRING (LSP) BASE CASE</b>	<b>LIGHT SPRING (LSP) HIMIX CASE</b>	<b>LIGHTER LOAD (LL) CSP CASE</b>	<b>LIGHTER LOAD (LL) CSP TO PV CASE</b>	<b>HEAVY SUMMER (HS) BASE CASE</b>	<b>HEAVY SUMMER (HIMIX) CASE</b>	<b>HEAVY SUMMER RETIREMENT CASE</b>
<b>Load [GW]</b>	92.9	91	78	78	161	166	166
<b>Wind [GW production]</b>	19.2	25.5	25.5	25.5	4.6	13.3	13.3
<b>Utility PV [GW production]</b>	3.9	10.2	10.2	17.8	1.3	11.2	15.2
<b>CSP [GW production]</b>	0.9	8.5	8.5	0.86	0.4	6.6	10.6
<b>DG [GW production]</b>	0	6.8	5.65	5.65	0	9.6	9.6
<b>CSP to PV conversion</b>	No	No	No	Yes	No	No	No
<b>CSP governors</b>	NA	On/off	On/off	On/off	NA	On/off	On/off
<b>Instantaneous wind and solar penetration (% of WECC)</b>	25.1	53.9	60.1	60.1	3.5	23	28
<b>SNSP commitment (%)</b>	28.8	59	66	74	6.3	35	36
<b>Retirement</b>	No	No	Yes	Yes	No	No	Yes
<b>New transmission</b>	No	No	Yes	Yes	No	No	No
<b>Headroom [GW]</b>	16	17.4	13	13	19.2	22.8	21.61
<b>Inertia metric (MVA*H)</b>	534,746	462,417	394,176	358,615	1,013,500	861,401	833,499
<b>Inertia (H)</b>	3.68	3.77	3.8	3.81	3.89	3.75	3.74
<b>Inertia (MVA*H/LOAD)</b>	5.75	5.07	5.03	4.58	6.18	5.2	5.02
<b>PDCI [MW]</b>	2200	0	-2735	-2735	2604	3091	3800
<b>Path 66 (COI) [MW]</b>	2346	-269	418	418	3529	4779	4693
<b>Path 49 (EOR) [MW]</b>	3099	3599	5500	5500	3716	878	4775
<b>Path 46 (WOR) [MW]</b>	4204	7132	9622	9622	6684	3793	8094
<b>Path 26 (Northern-Southern California) [MW]</b>	1140	-2660	-2558	-2558	2704	1852	-1111

## 2.3 Western Interconnection Power Plant Retirements

Unit retirements, especially in California, will alter the system dynamics considerably. Further, it is part of California’s energy plan that renewable resources displace some of the existing fossil-fueled thermal plants. Retirements in the study database are made by decommitting the retired units and redispatching other resources upward to fill in the lost generation. Retirements are based on the California Independent System Operator (CAISO) 2016 unified planning assumptions document (CAISO 2016b). The retirements imposed in the study data sets fall into three categories:

- Nuclear units: All the remaining nuclear power plants in California—e.g., Diablo Canyon—are shut down.
- Scheduled retirements (listed in Table A3-1 of the planning appendix as “to be retired in planning horizon”): These are listed in Table 2, with the capacity of the units in Southern California Edison from the WECC heavy summer planning case for this study overwriting the rating from the table.
- Retirements resulting from the once-through cooling policy (listed as “Potential OTC<sup>2</sup> Generating Unit Early Retirement to Accommodate CPUC<sup>3</sup>-Approved Repowering Projects in planning horizon”): These are listed in Table 3, again with the unit ratings from the study database overwriting the table entry. The two synchronous condenser conversions are included in the study.

Overall, approximately 5,700 MW of generation dispatch is displaced with the removal of these units from the heavy summer case. These units were not committed in the light spring case.

To make up for the lost thermal generation, utility-scale PV and CSP solar are dispatched upward, reflecting a condition with higher insolation than the original case. The CSP plants, especially in California, are producing power at levels closer to their rating. That is, we have assumed that there is more solar insolation in the snapshot of time that is being studied. (This higher production is relevant throughout the study, especially in the sunset investigation of Section 9.)

---

<sup>2</sup> Once-through cooling

<sup>3</sup> California Public Utilities Commission

## Table 2. Generation Retirements

Table A3-1: Generation plants projected to be retired in planning horizon<sup>37</sup>

PTO AREA	PROJECT	CAPACITY	FIRST YEAR TO BE RETIRED
SCE	EL Segundo 3	325	2013
	Huntington Beach 3	0	2013
	Huntington Beach 4	0	2013
SDG&E	Kearny Peakers	135	2017
	Miramar GT1 and GT2	36	2017
	El Cajon GT	16	2017

## Table 3. Once-Through Cooling Unit Retirements

ALAMITOS	MW	RETIREMENT DATE
Alamitos Unit 1	165	12/31/19
Alamitos Unit 2	165	12/31/19
Alamitos Unit 3	310	12/31/20
Alamitos Unit 4	120	12/31/20
Alamitos Unit 5	470	12/31/19
Alamitos Unit 6	470	12/31/20

HUNTINGTON BEACH	MW	RETIREMENT DATE
Huntington Beach Unit 1	210	10/31/19
Huntington Beach Unit 2	210	10/31/20

REDONDO BEACH	MW	RETIREMENT DATE
Redondo Beach Unit 5	160	12/31/20
Redondo Beach Unit 6	140	12/31/20
Redondo Beach Unit 7	480	10/31/19
Redondo Beach Unit 8	480	12/31/20

SYNCHRONOUS CONDENSERS	MW	RETIREMENT DATE
Unit 3	145 MVA <sub>r</sub>	12/31/16
Unit 4	145 MVA <sub>r</sub>	12/31/17

## 2.4 Study Regions

One of the objectives of this study is to better understand the locational aspects of system stability and solar generation. The WECC model includes representation of 20 “areas” that are, for the most part, representative of the major balancing authority boundaries in the interconnection. The study also includes four U.S. regions, as shown in Figure 1. The boundaries of the regions have been modified from previous WWSIS studies to more closely align with those used in other WECC activities. Results presented throughout this report are for these four regions, which do not include non-U.S. contributions. When WECC-wide results are presented, the non-U.S. contributions are included, so the sum of the four regions does not always equal the WECC totals.

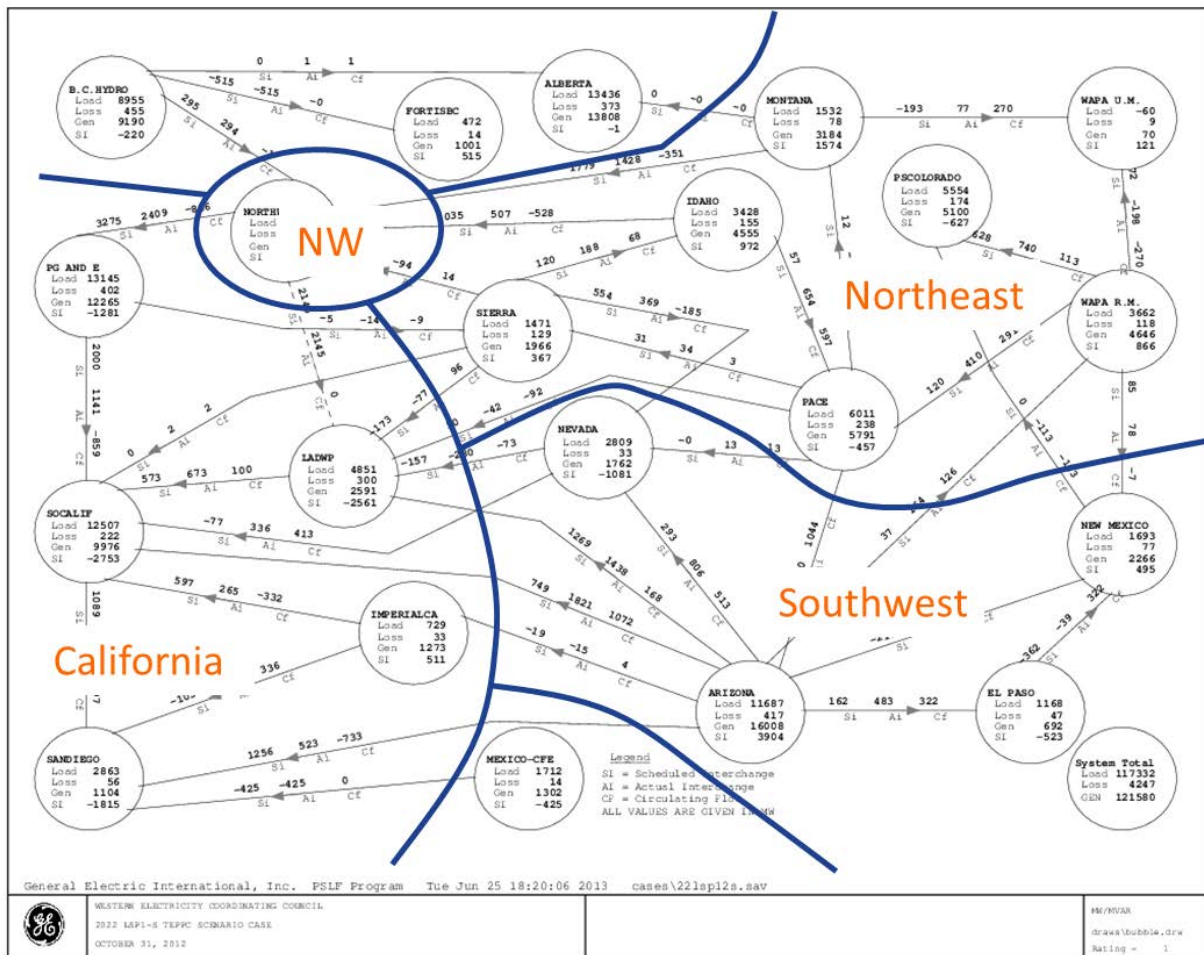


Figure 1. Definition of regions

## 2.5 Concentrating Solar Power Plants

CSP plants are a key element of this study. The Western Interconnection system model (i.e., the original WECC planning case) included 14 CSP plants. During the preceding WWSIS studies, 78 new CSP plants were sited and added to the system. Originally, these plants as well as the other PV and wind generation in the system had their dispatch (production) modeled based on a representative weather condition with good solar and wind. As noted, the CSP in the retirement

cases was dispatched farther upward to account for the displacement from the retired plants. The final commitment and dispatch for the heavy summer retirement cases are:

- Fourteen existing CSP plants with a total rating of 954 MW in the original planning cases at 860-MW dispatch/production
- Seventy-eight new CSP plants with a total rating of 10,211 MW added to the study cases at 7,589-MW dispatch/production.

The geographic distribution of the CSP plants is shown in Figure 2, with the plants concentrated in the sunny southern part of the West.

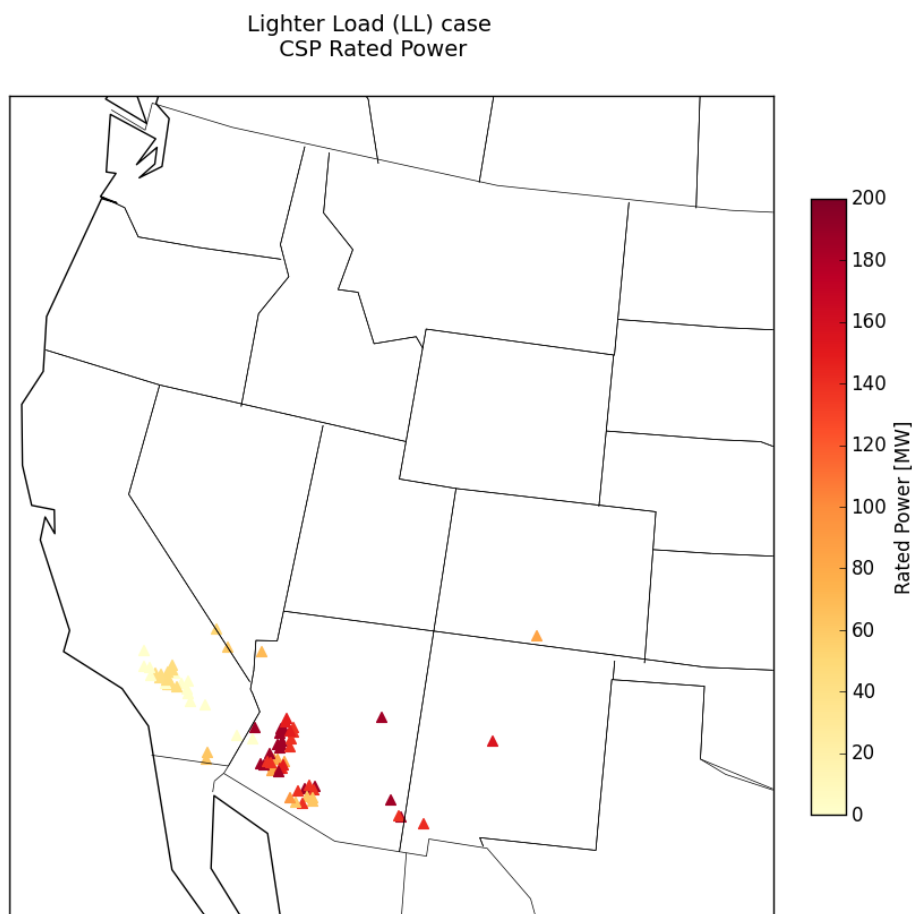


**Figure 2. Geographic distribution of added CSP units**

## 2.6 Lighter Load

The light spring cases used in the preceding WWSIS studies had operating conditions and system load selected by the WECC stakeholder process. The system load in the U.S. portion of WECC for those cases was 93 GW, and it was based on the consensus at the time. Concerns were raised that this load level is relatively high for a “light load” condition and that investigation of system dynamics at low load and high solar and wind might be more illuminating at lower load levels.

### 2.6.1 Lighter Load Analysis

Two data sources were used to check on both the historical spring load levels and forecasts for future spring load conditions.

Historical load analysis was performed for the U.S. WECC region. Only daytime hours (defined as the hours during which the average hourly PV output was more than 10% of the PV max for the year) were considered. We performed both an annual analysis and one for the spring season (defined here as March, April, and May).

Creating a forecast for the lighter load for the year 2023 was done using two methods:

- Linear regression
- Analysis of MAPS (i.e., from General Electric data) forecast.

The historical U.S. WECC daytime spring loads for the decade 2005–2014 were bucketed in deciles. The results are shown in Figure 3, with the load level of the original light spring case indicated by the left arrow. For the lighter load scenario, we opted to target loading in the lowest decile, as indicated by the arrow on the right. A linear regression of the 10<sup>th</sup> decile loads, extrapolated to 2023, resulted in a load level of 73.2 GW. General Electric data, used for other analysis outside of this study, gave a similar projection of 74.1 GW for 2023.

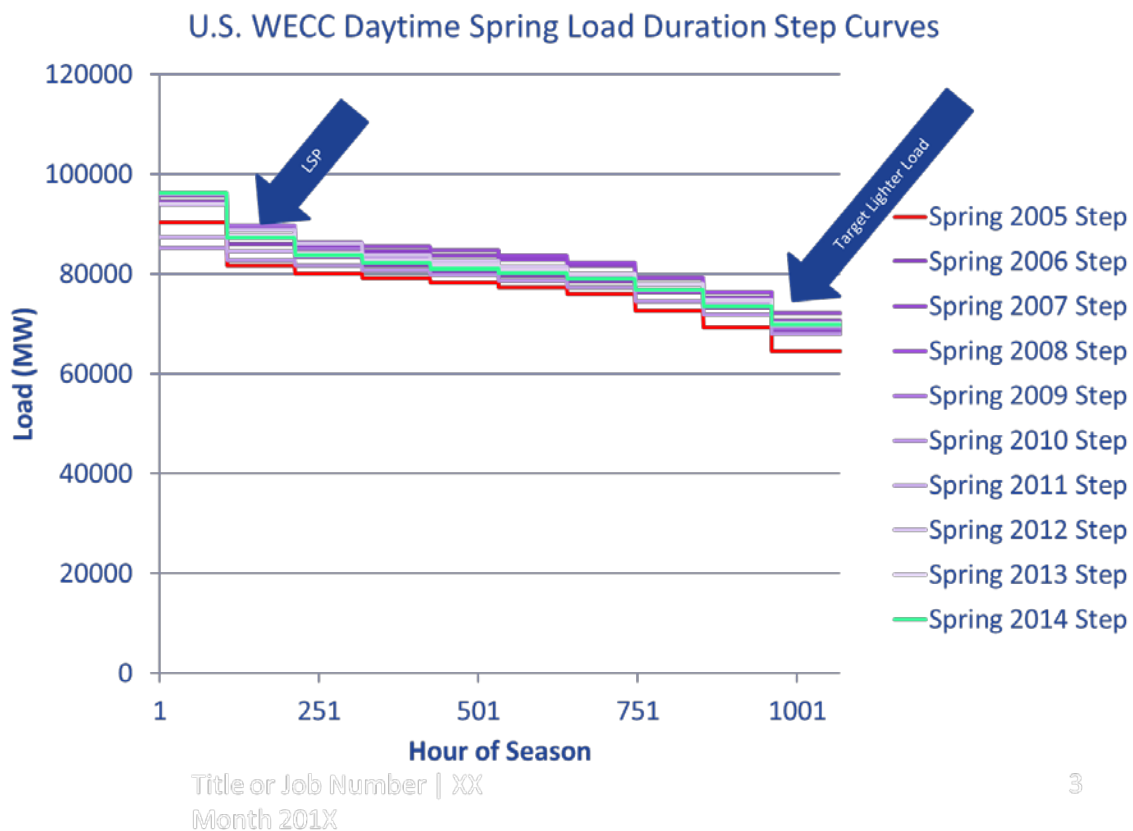


Figure 3. Lighter load duration analysis curves

## 2.6.2 Redispatch for Increased Solar and Lighter Load

The U.S. WECC load was reduced with uniform scaling of system loads to 73 GW. Because the high-mix, light-load case, even before this load reduction, had displaced most of the fossil-fueled generation available for redispatch or decommitment, most of the reduction in generation was accomplished by reducing the hydro generation in the Northwest. This resulted in significant south-to-north flows, a condition that today is relatively unusual in the West.

The commitment (operating MW rating) and dispatch (MW production) of renewable and other resources for the final lighter load case is shown in Figure 4. Nuclear units are included in “steam”.

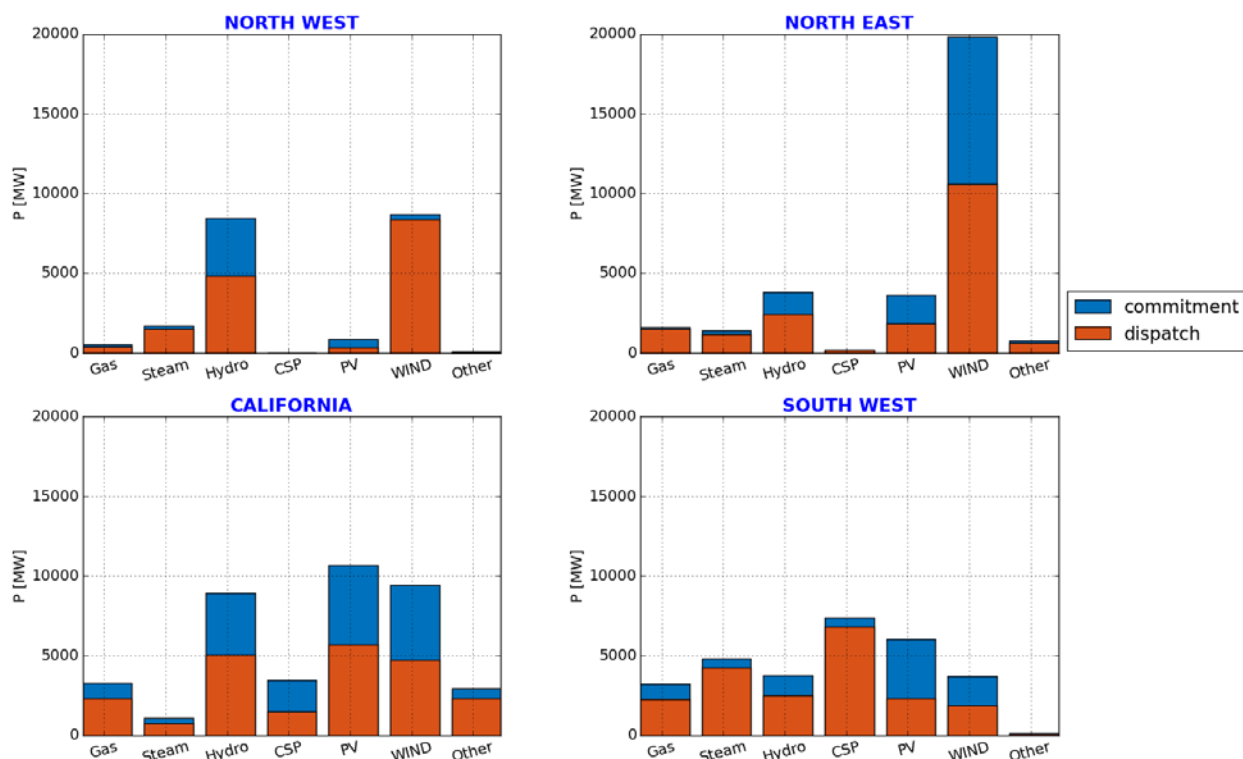
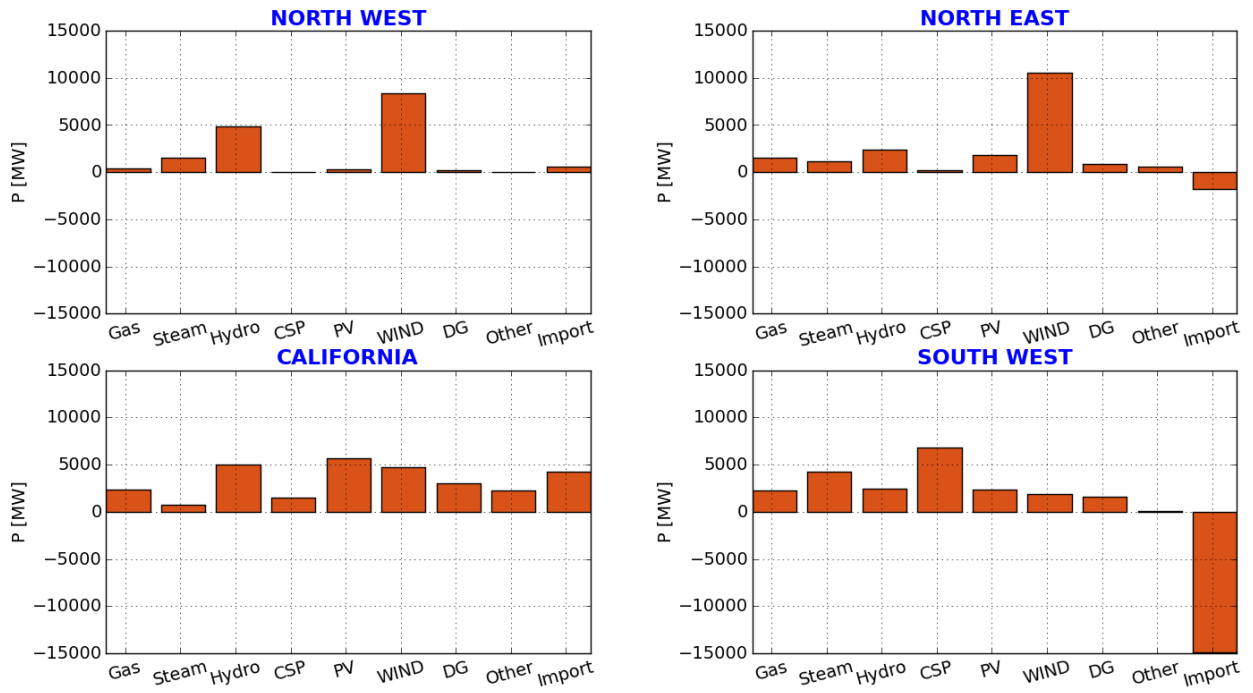


Figure 4. Lighter load final commitment and dispatch

Although power exchange among regions is a significant element in overall system stability, it is not the same thing as dispatch. To show the relative magnitude of the regional exchanges compared to dispatch, a second plot, which includes imports (negative being export) for this condition, is shown in Figure 5. Massive export from the Southwest and some import to the Northwest are consequences of the combination of high solar production in the South, high wind everywhere, and load in the lowest 10<sup>th</sup> decile for spring daytime conditions.

Light Load Case (CSP)



**Figure 5. Lighter load final dispatch with imports**

The regional penetration of solar and wind are shown in Figure 6 for the lighter load case.

Lighter Load Case (CSP)

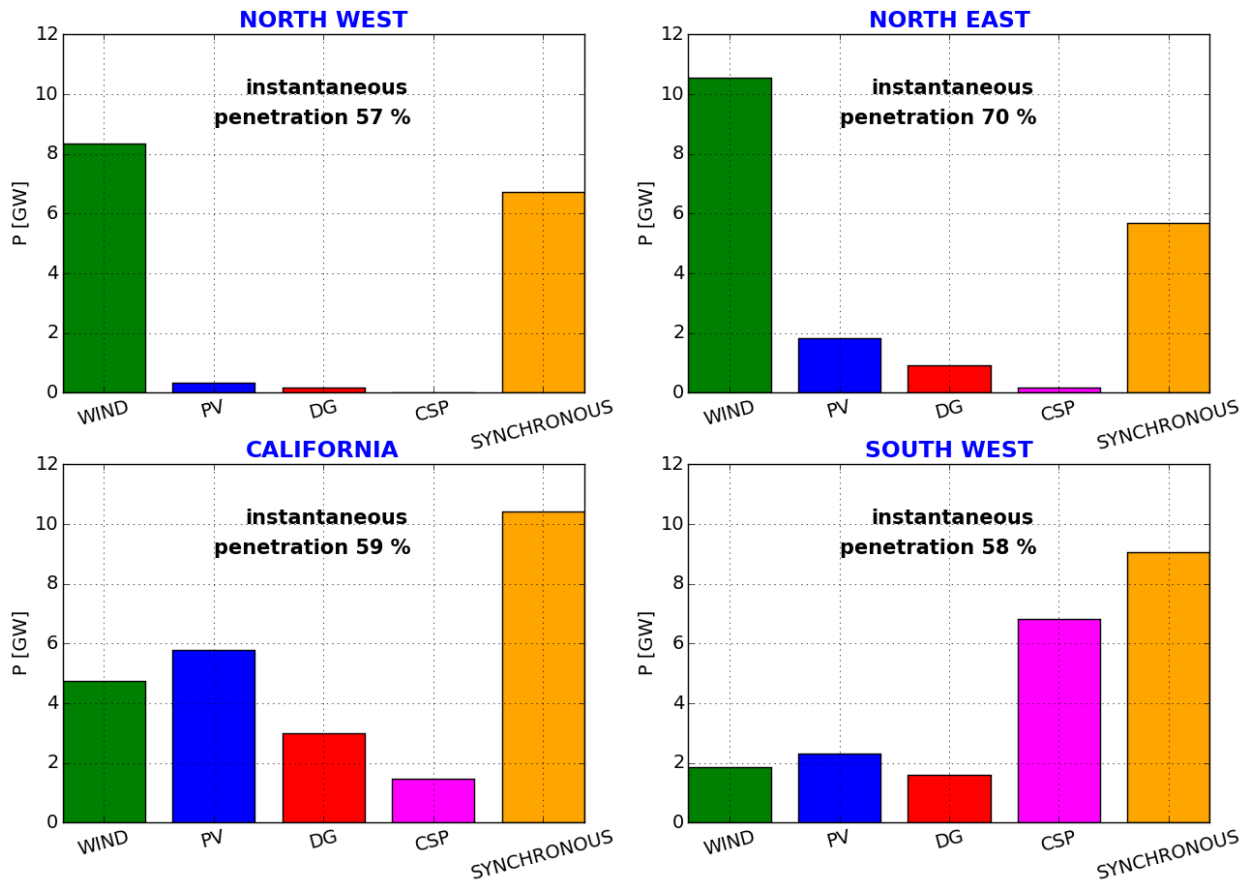


Figure 6. Lighter load wind and solar (PV plus CSP) penetration

## 2.7 Transmission Improvements

Several updates to the transmission topology were made to the two final retirement power flow cases.

### 2.7.1 Pacific DC Intertie Upgrade

The Pacific DC Intertie (PDCI) was upgraded at the Oregon end. This upgrade increases the line’s capability for north-to-south flow. The capability remains the same for south-to-north transfer, at 3,100 MW. The longer term plan is for the upgrade to raise the north-to-south limit to 3,800 MW. We used that limit in this work. At present, only a portion of the increase from 3,100 MW to 3,800 MW is allowed for operation.

For the heavy summer case, we increased transfer to this future 3,800-MW limit. For the lighter load case, the transfer is south-to-north. In both cases, we have not altered the HVDC dynamic model; instead, we added positive and negative loads at the rectifier and inverter, respectively, to capture the increased transfer. An estimate of the incremental losses is included (i.e., the incremental power coming out of the HVDC “addition” is less than that going in.)

### **2.7.2 Improvements to Accommodate Increased Solar Production**

Many other local reinforcements were carried forward from WWSIS-3 and WWSIS-3A. These were additions to the light spring base that allowed the two retirement cases for this study to avoid severe overloads or local voltage problems. To accommodate the higher level of solar generation, many 230-kV line and 230-/500-kV transformer additions were made.

These transmission improvements were made in the narrow context of relieving local thermal and voltage problems, and they were emphatically not the result of a larger transmission expansion planning exercise. Clearly, such detailed planning would be necessary as actual solar projects are proposed. Improvements included:

- Added segments of 230 kV, 345 kV, and 500 kV
- Added transformers of 230/500 kV
- Additional reactive compensation.

In all cases, new circuit elements were added in parallel with existing circuits (e.g., in several locations, single circuits have been converted to double circuits). No new routes were created, although wider rights-of-way might be required. The transmission additions are shown in Table 4. The two highlighted circuits were needed for the heavy summer cases (after the other lines were added for the lighter load case). New transformers are shown in Table 5. Reactive compensation additions are shown in Table 6 and Table 7. Note that these compensation additions are in the Nevada desert, where a considerable amount of solar was added. Realistically, the amount of solar added in that region would require a more comprehensive transmission expansion plan rather than the piecemeal stopgap approach used here. We made enough improvements to avoid creating localized stability problems that would compromise the larger picture results of the study.

**Table 4. Transmission Additions**

FROM BUS NUMBER	FROM BUS NAME	KV	TO BUS NUMBER	TO BUS NAME	KV	CIRCUIT ID
14209	EAGLEYE	230	19052	LIBERTY	230	2
14209	EAGLEYE	230	19052	LIBERTY	230	3
14225	SAGUARO	230	14229	TATMOMLI	230	2
14226	SNTAROSA	230	14229	TATMOMLI	230	2
14238	GILARIVR	230	14235	GILABEND	230	2
15090	HASSYAMP	500	22342	HDWSH	500	2
16109	WINCHSTR	345	16105	VAIL	345	2
16109	WINCHSTR	345	16112	WILLOW	345	2
19029	HOVRA5A6	230	19012	MEAD S	230	2
19042	PARKER	230	14209	EAGLEYE	230	2
19052	LIBERTY	230	15230	RUDD	230	3
60240	MIDPOINT	500	64668	MPRSSC 1	500	1
21076	RAMON	230	24806	MIRAGE	230	2
44911	MARENGO	230	44912	TALBOT	230	2
47830	KLONDSCH	230	40584	JOHN DAY	230	2
22342	HDWSH	500	22536	N.GILA	500	2
22536	N.GILA	500	22360	IMPRLVLY	500	2
24016	BARRE	230	25201	LEWIS	230	2
24025	CHINO	230	25656	MIRALOME	230	4
24092	MIRALOMA	500	24138	SERRANO	500	1
24155	VINCENT	230	24283	VI-WI 1	230	2
24155	VINCENT	230	25616	PEARBLSM	230	2
24283	VI-WI 1	230	24918	E-W-WILD	230	2
24601	VICTOR	230	24085	LUGO	230	3
24701	KRAMER	230	24085	LUGO	230	3
24701	KRAMER	230	24085	LUGO	230	4
24760	OXBOW B	230	24701	KRAMER	230	1
24918	E-W-WILD	230	24245	EASTWIND	230	2
25406	J.HINDS	230	24806	MIRAGE	230	2
29206	BUCK230	230	25406	J.HINDS	230	2
24375	REDBLUFF	230	21045	MIDWAY X	230	2

**Table 5. Transformer Additions**

FROM BUS NUMBER	FROM BUS NAME	KV	TO BUS NUMBER	TO BUS NAME	KV	CIRCUIT ID
<b>24374</b>	REDBLUFF	500	24375	REDBLUFF	230	tp
<b>24138</b>	SERRANO	500	24137	SERRANO	230	4
<b>14007</b>	GILARIVR	500	14238	GILARIVR	230	2

**Table 6. Capacitor Additions**

BUS NUMBER	BUS NAME	KV	MVAR
<b>62365</b>	MATL AB	230	100
<b>64069</b>	MACHACEK	230	150
<b>64045</b>	FRONTIER	230	70

**Table 7. Heavy Summer Synchronous Condenser Additions**

BUS NUMBER	BUS NAME	KV	AREA	AREA NAME	MVAR
<b>964125</b>	SC-964125	13.8	64	SIERA	100
<b>964127</b>	SC-964127	13.8	64	SIERA	100
<b>964037</b>	SC-964037	13.8	64	SIERA	100
<b>964400</b>	SC-964400	13.8	64	SIERA	100
<b>964045</b>	SC-964045	13.8	64	SIERA	300
<b>924760</b>	SC-924760	13.8	64	SIERA	200

Eleven CSP units and one combined-cycle plant (Blythe) needed to have power system stabilizers added to alleviate damping problems in the retirement cases as well.

## 2.8 Heavy Summer Retirement Case

The heavy summer case includes the PDCI upgrade, the transmission improvements, and the unit retirements. The regional commitment and dispatch are shown in Figure 7. The imports and dispatch are shown in Figure 8. Under these conditions, there is still substantial export from the Southwest. The Northwest is also exporting to California, a typical condition for heavy summer loads.

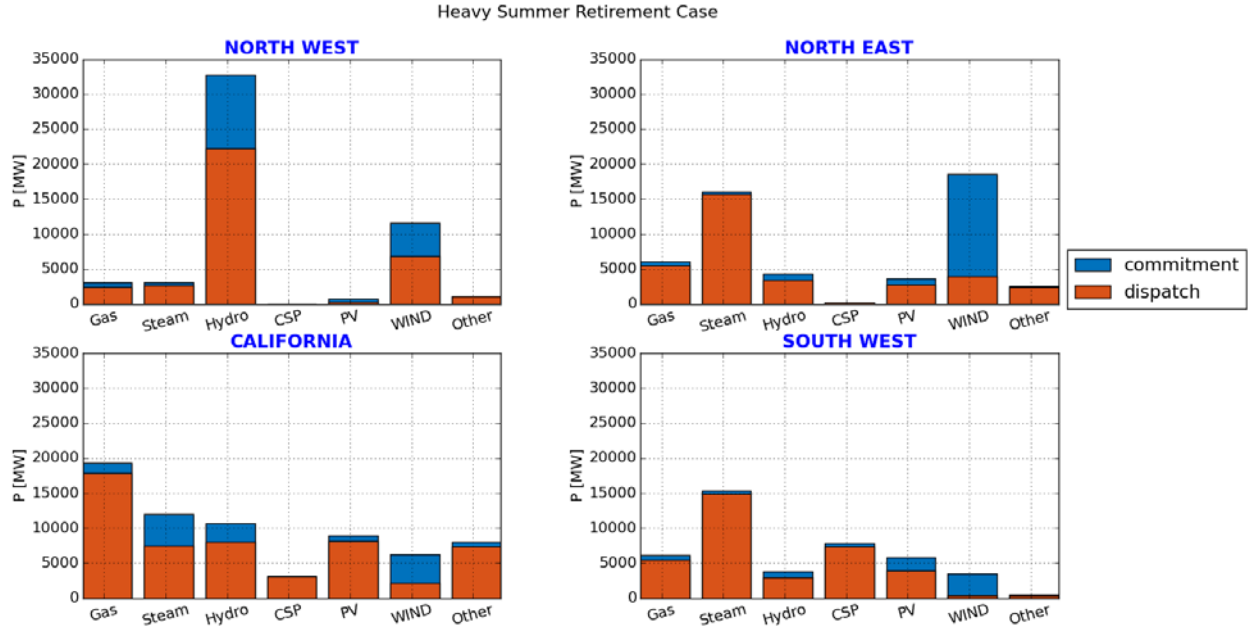


Figure 7. Final commitment and dispatch for heavy summary retirement case

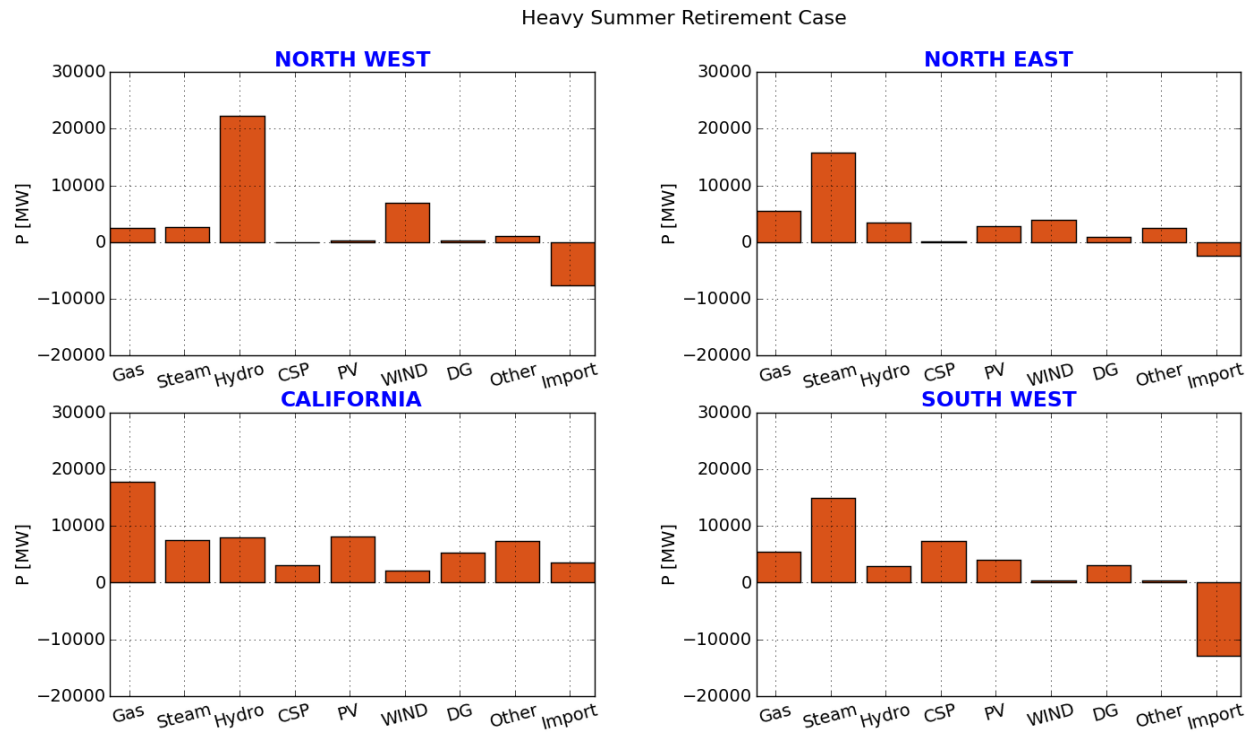


Figure 8. Final dispatch with imports for heavy summer retirement case

## 2.9 Replacement of CSP with PV (CSP-to-PV) Sensitivity Case

The light spring base case includes approximately 900 MW of CSP plants. The new lighter load case has approximately 10 GW; however, since the development of these cases, the market for CSP in the western United States has largely disappeared. Many proposed CSP projects have been canceled or converted to utility-scale PV projects. For this study, all the CSP plants in the original light spring case were retained. All other CSP plants were converted to utility-scale PV, with the plant MW rating retained in the conversion. The net result was that 78 plants totaling approximately 7.6 GW dispatch were converted from CSP to utility-scale PV, retaining the same power production.

**Table 8. Dispatch of CSP-to-PV Sensitivity Case**

	LIGHTER LOAD (LLC) CSP CASE	LIGHTER LOAD (LLC) CSP TO PV CASE
<b>Load [GW]</b>	78	78
<b>Wind [GW]</b>	25.5	25.5
<b>Utility PV [GW]</b>	10.2	17.8
<b>CSP [GW]</b>	8.5	0.86
<b>DG [GW]</b>	5.65	5.65
<b>CSP to PV conversion</b>	No	Yes

## 3 CSP Model Validation

The dynamic models of the CSP plants added for this investigation are based on the characteristics of actual CSP plants operating in the Western Interconnection. Validation of those models are presented here.

WECC/NERC rules dictate that the dynamic performance of stability models for operating power plants be periodically validated. The resulting validated models are documented and provided to WECC. The project team obtained field-test reports for two operating CSP plants in the Western Interconnection:

- Genesis Plant (by GE Energy Consulting)
- Mohave Plant (by Kestrel).

Both are in the Mohave Desert.

The approach used for model validation here was to implement the parameters from the field tests in a single plant model for all CSP plants in the study cases. The validation then repeated, as possible, the field tests used for the commercial reports.

Plant models have standard components for the generators, excitation systems, and the one turbine governor as follows:

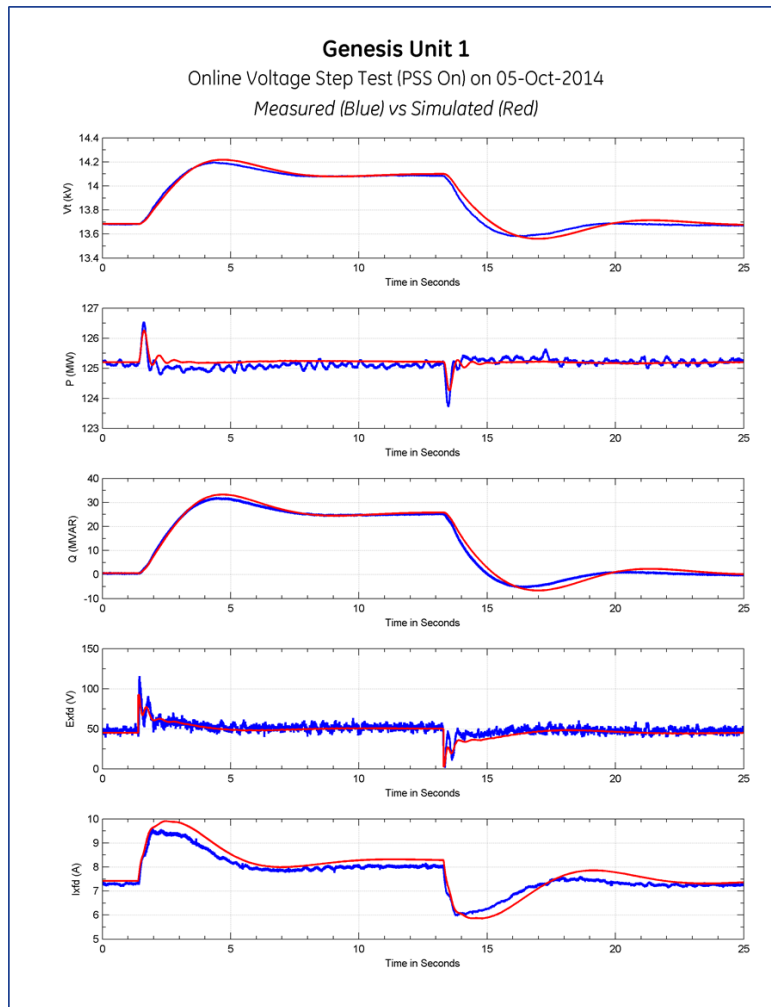
- NextEra Genesis 1 Plant
  - Genrou
  - Esac7b
  - Pss2b
  - Ieeeg1.
- Mojave Plant
  - Genrou
  - Esst4b
  - Pss2a.

The representation in these tests had some additional refinements. For example, the Genesis unit in the WECC model did not have the rating. This test model was updated to available data for the physical plant.

### 3.1 Exciter Model Validation Testing

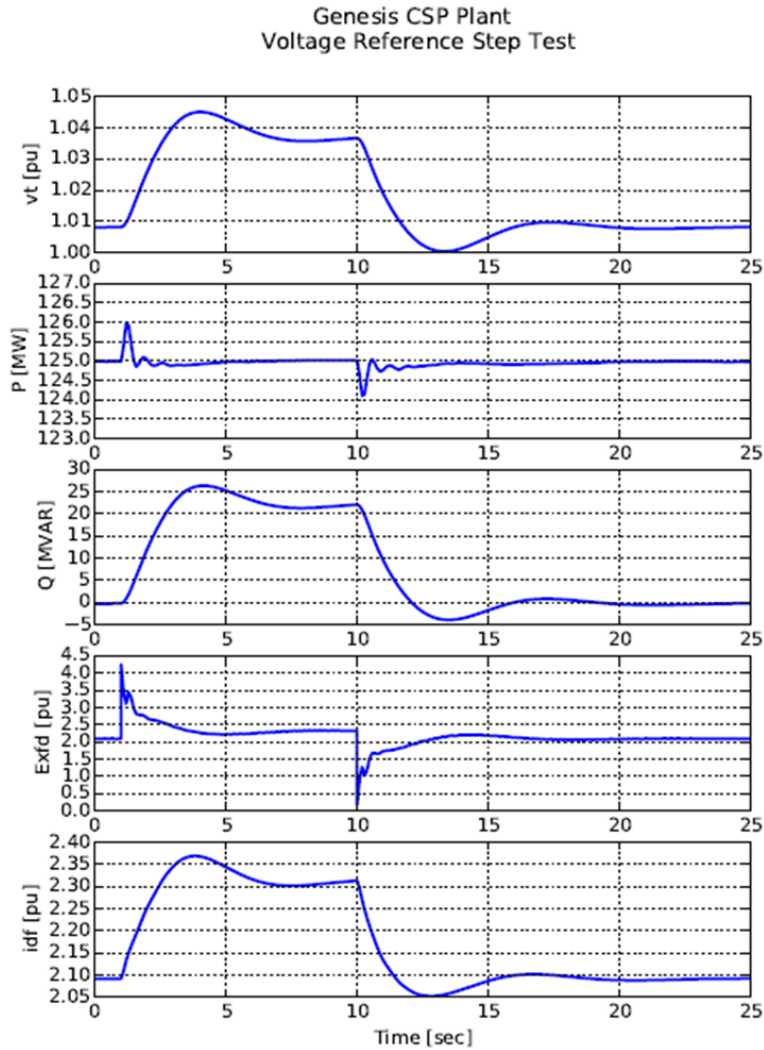
These tests gave the same stimulus, but there is no record of the condition or short-circuit strength of the Western grid when the tests were performed. So, for example, a voltage reference step test should exhibit the same general speed and dynamic performance, but the magnitude of the response will vary with grid operating condition. This difference was observed in these tests.

Figure 9 shows the field measurement and simulated response of the Genesis exciter and voltage regulator model. As required, the simulation model does a good but not perfect job of capturing the response to step tests.



**Figure 9. Excitation test of Genesis CSP plant**

In Figure 10, the same voltage reference step test is applied to the Genesis plant in a study database. The performances are very close, but the VAR swing is less in our test. The power bump is slightly smaller, too. The behavior is consistent with a weaker grid, which in turn is consistent with expectations of a future system with fewer synchronous machines and more inverter-based resources. This means that relatively fewer VARs are needed to move the voltage.



**Figure 10. Simulation validation of exciter model(s)**

The behavior of the Mohave plant was also checked, with similar results.

### 3.2 Governor Model Validation Testing

Figure 11 shows the governor test on the Genesis plant. Note that no governor tests were performed on the Mohave plant because the steam turbine is operated with steam valves wide open, and therefore it provides no governing behavior. This control, or lack thereof, is important for this study, and it is discussed at length later.

As with the exciter test, the governor model produced a good match to the physical field tests. For a 10-MW reference step, the speed of the turbine response was approximately 0.7 MW/second. The speed of response plays a key role in frequency control, and it is examined later.

The simulation model in the study database, shown in Figure 12, produced a good match, as expected.

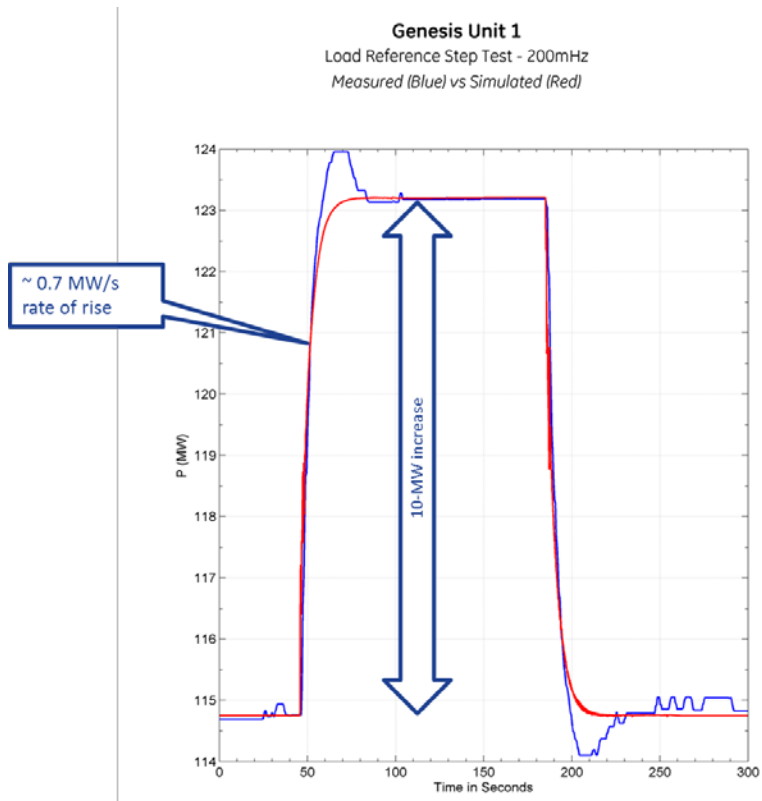


**Figure 11. Governor test of Genesis CSP plant**

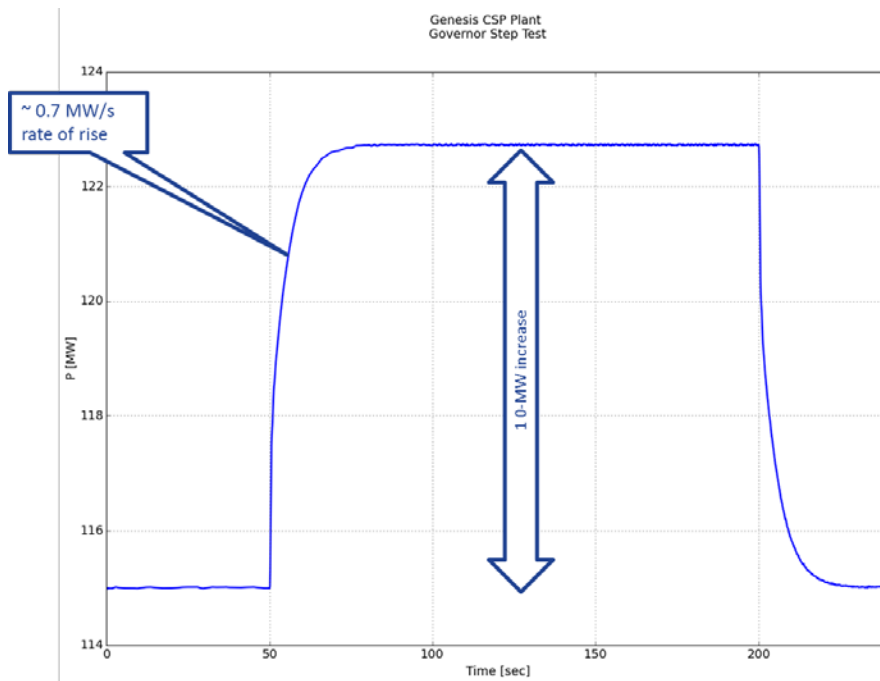


**Figure 12. Simulation validation of governor models**

In summary, the models from the commercial validation tests were implemented in the study models. The performance of these updated models is consistent with the field tests and model validation for the conditions in the study model.

The performance of the generic governor model used across the system representation for new plants is very similar to the one available from field tests for system-wide frequency events. The models used for the investigations of this study provide a good baseline of realizable, validated performance.

### 3.3 Load Model Validation

The dynamic behavior of loads, and now of load equivalents with lots of embedded solar photovoltaics, has been shown in our earlier Western Wind and Solar Integration study work to have a significant impact on bulk system performance. Since the behavior of the loads is known to have an important impact on stability simulation results under some conditions, having validation of the model behavior (compared to observed actual behavior) will contribute to confidence in the overall study findings. There is a relative paucity of field validation of the load models, so an effort to validate the dynamic behavior of the modeled load was made.

We obtained some high-resolution measurements of load behavior at a low-voltage load node in the system. Then we identified a few significant frequency events in the Western Interconnection that corresponded to times when we had data. It was our hope that we could show a comparison of a composite load with measured data for validation.

Figure 13 shows measured frequency for an actual event on the left and the active power at the measured load node on the right. The frequency signature is characteristic of events in the West, and it is of the variety specifically targeted by the NERC BAL-003-1 frequency response obligation (FRO). The active power signal for the same time shows no observable response to the frequency event. This is surprising and at odds with accepted wisdom about composite load dynamics. Another event shows similar insensitivity to frequency for this load node.

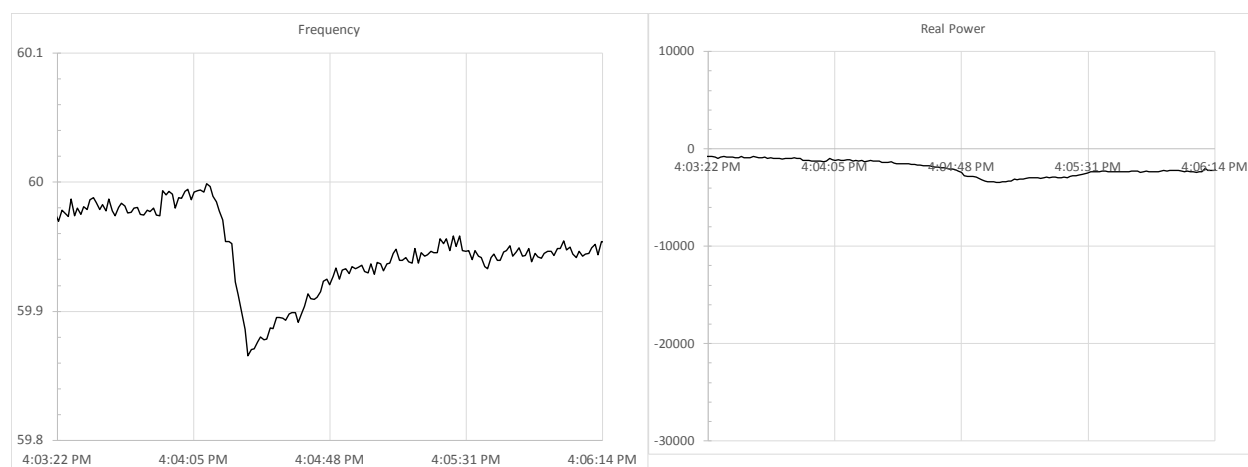


Figure 13. Load data March 30, 2012, 10–11 a.m.

A second look at the measured data was made to see if there was useful information in the low-amplitude, continuous variation in load and frequency at the bus. A linear regression of the data shows a very high sensitivity to frequency: on the order of 10 to 1, which is many times as great as conventional modeling assumes. Although the regression shows a steep slope, the scatter of the data makes the regression of questionable usefulness. A second set of data showed similar lack of observable dynamic response with frequency and questionable correlation of load and frequency.

In short, this exercise produced no meaningful insights into the load dynamic sensitivity to frequency. This is a small sample, so broad conclusions are not warranted. Nevertheless, this reinforces the need for the industry to give further attention to load modeling, including doing a better job of capturing the effects of short-term frequency excursions.

The study continued to use the present state-of-the-art WECC composite load model with embedded PV, as shown in Figure 14. The details of the behavior of the Western Interconnection node from this exercise are shown in Figure 15. The event has both voltage and frequency swings. The behavior of the load model shows a significant reduction in power during the swing, at least some of which is attributable to frequency.

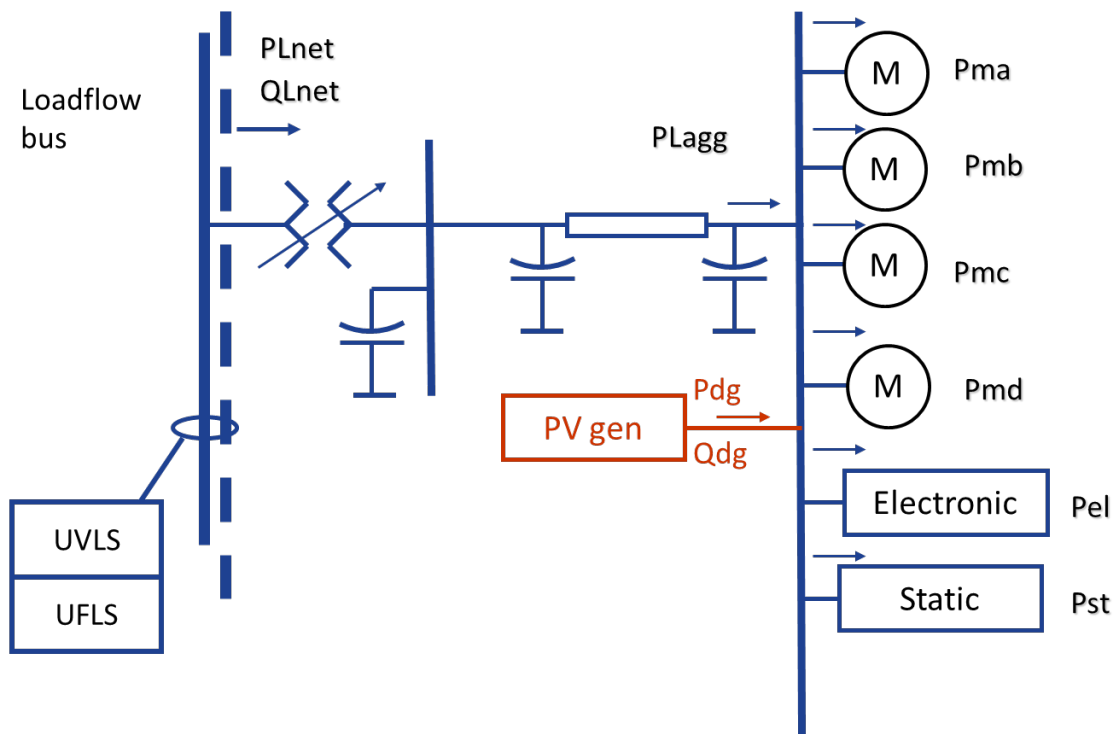
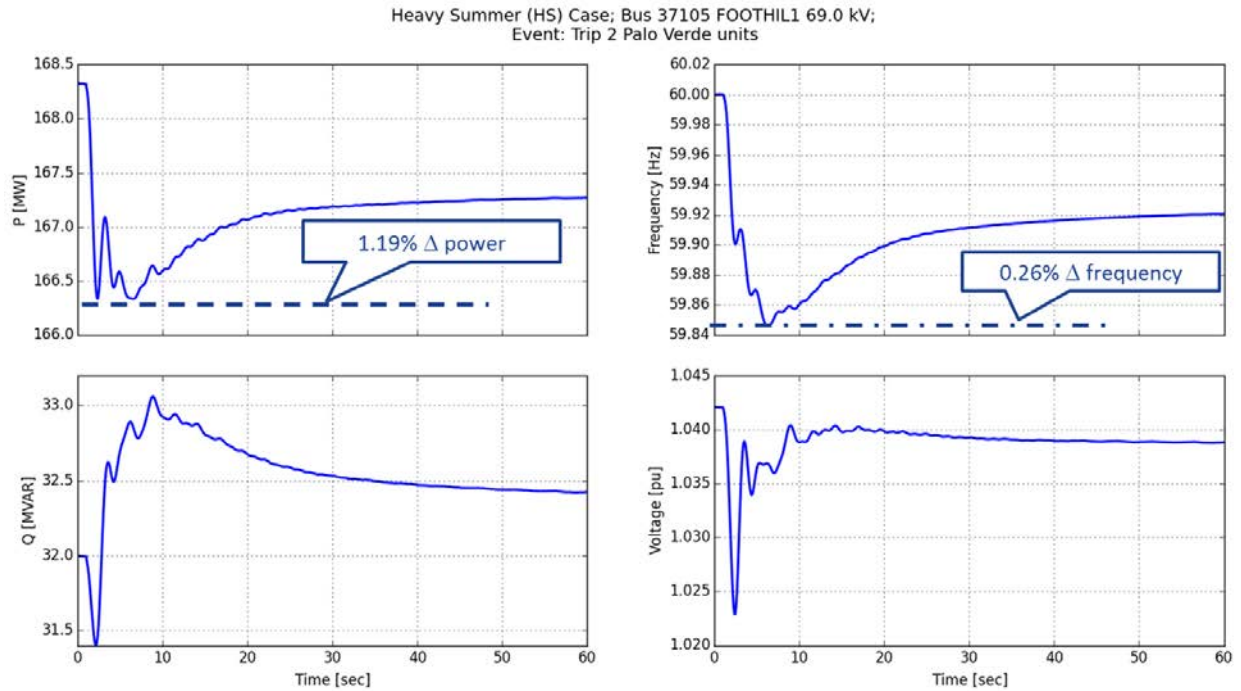


Figure 14. Composite load model with embedded PV



**Figure 15. Dynamic behavior of composite load model for a selected bus**

In summary, we regard the load mode validation exercise to be inconclusive, and we have proceeded with the best available load modeling using the WECC composite load model (WECC 2012).

## 4 System Characterization

In this section, several key elements of the various study databases are compared. The intent is to provide quantitative reference to how system characteristics change with the addition of large amounts of solar and wind generation.

In most of the results presented in these sections, the four lighter load conditions discussed above are used.

### 4.1 System Inertia

As wind and solar generation displace other, mostly thermal resources, the total inertia on the system tends to drop. As noted in earlier work (Miller et al. 2014a), this drop in inertia is often incorrectly used as a shorthand for a spectrum of frequency control problems that can accompany this displacement. Nevertheless, having the system get “lighter” does affect the dynamics of frequency.

Figure 16 presents the four related measures for the four spring cases (the original light spring base case; the light spring high-mix case; the new lighter load retirement case with new CSP; and the sensitivity case, in which most of the possible CSP comes in as utility-scale PV).

In the top left of the figure, the inertia of the system, given in units of MW-sec is provided. This is the megavolt ampere (MVA) rating times the H inertia constant of every synchronous machine that is committed. The purple arrow highlights the fact that from the original planning case to the PV sensitivity case, the system inertia declines by approximately one-third (32.9%). The trace on the top right is the total MVA of the synchronous generation running (committed). It drops a similar amount, which means that the average inertia constant, shown in the lower left, changes very little. That is, the “system” inertia constant stays approximately 3.7–3.8 MW-sec/MVA. This last observation means that the mix of synchronous generation that remains committed has approximately the same individual inertial characteristics as those being decommitted to make room for the solar. Finally, the trace on the lower right reflects the fact that the load has dropped from the earlier cases to the lighter load cases for this study. The amount of inertia per unit of load drops 20%, which in a sense normalizes the reduction in inertia resulting from the added inverter-based renewables. CSP is synchronous, so the change between the third and fourth cases in each plot is solely caused by the loss of inertia from converting new CSP to PV.

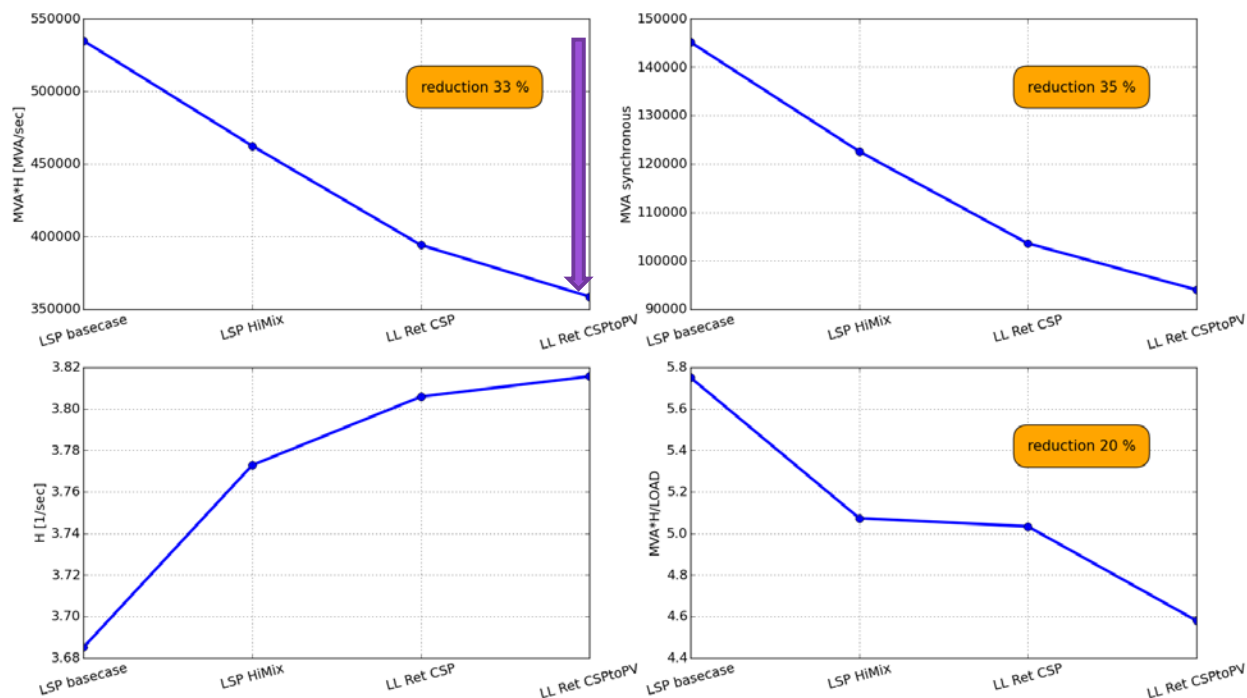


**Figure 16. Spring: Western Interconnection system inertia**

Figure 17 shows the change in inertia for the four regions. As wind and solar are added, from the spring base case to the high-mix case, the biggest change is in the Northeast, where the green arrow highlights the fact that coal was mostly on the margin and displaced by the added wind and solar. Then, as load dropped, relatively little fossil-fueled generation was left that could be dispatched down or decommitted; and hydro in the Northwest was substantially reduced, as highlighted by the red arrow. Finally, the CSP that changed to PV was mostly in the Southwest, highlighted by the purple arrow, with some in California as well.

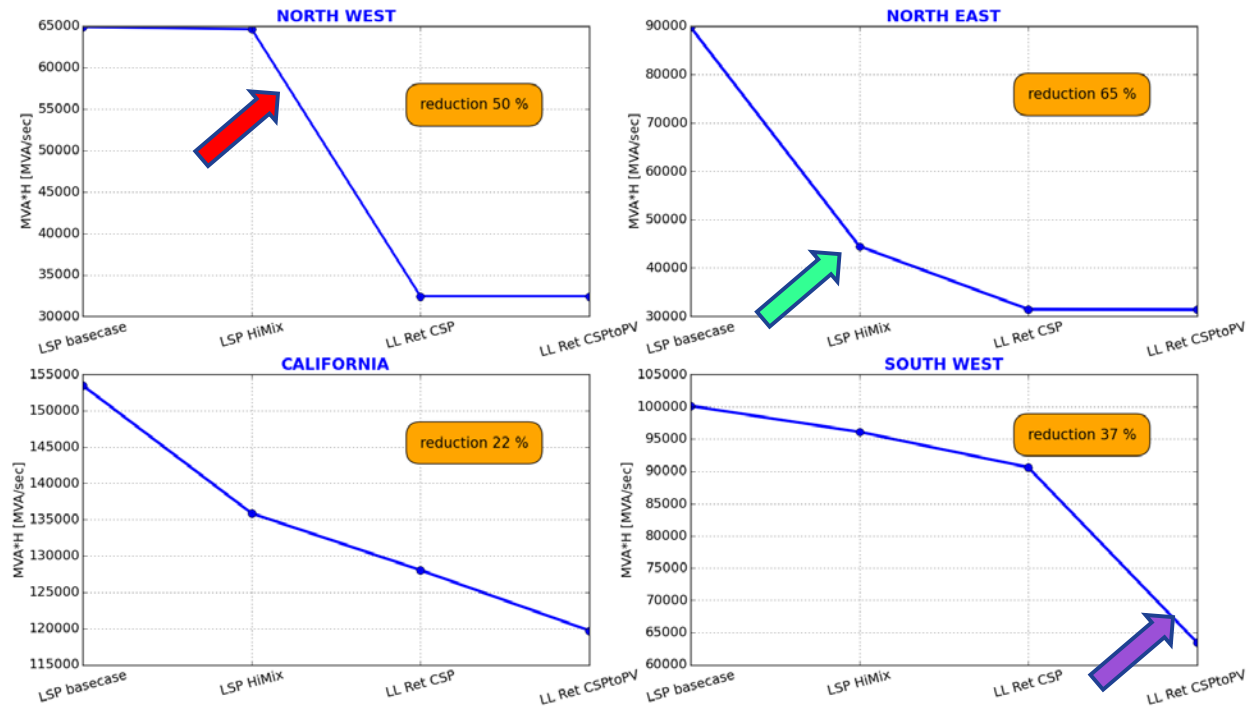


Figure 17. Spring: regional impact on inertia

## 4.2 Short-Circuit Strength

Grid strength is a concern with inverter-based variable renewables (CIGRE 2016.) The short-circuit strength of individual nodes is one metric of system strength. In this set of evaluations, we examine what is happening to short-circuit strength (measured in MVA) at every bus of 230 kV and more.

We are primarily concerned in this investigation with changes in short-circuit strength and with locations that are weak relative to the inverter-based generation that the node hosts. Three factors enter the picture:

1. The decommitment of synchronous generation displaced by wind and solar reduces short-circuit strength.
2. The addition of new transmission (as described mainly in Section 2.7.2) increases short-circuit strength.
3. The addition of CSP generation increases short-circuit strength.

In the following figures, we looked at short-circuit strength for each of the four lighter load cases. Further, we looked at changes using the lighter load case as a reference. For example, we:

1. Calculated short-circuit strength MVA for all buses 230 kV and more for the four lighter load cases
2. Plotted these quantities, sorting from high to low for the lighter load (labeled SC MVA LL) case

3. Calculated the change in short-circuit strength going from the lighter load (SC MVA LL) case to the other cases (and plotted from high to low for the PV sensitivity case)
4. Calculated the percentage change in short-circuit strength going from the lighter load case to the lighter load PV sensitivity case (using the following formula):

$$\Delta SC MVA[\%] = \frac{SC MVA_{CSP} - SC MVA_{CSPtoPV}}{SC MVA_{CSP}} \cdot 100$$

A total of 2,056 buses were considered. Figure 18 gives the absolute short-circuit strength for the four cases. The points are each for the same bus, with the lighter load case buses (in grey; difficult to see) sorted from highest to lowest short-circuit strength. Very few buses have very high strength, and many are in the range from 20,000 MVA to a few thousand. The relative change, which is shown in the other case by the colors above or below the curve and then again in the lower curve, only shows the change (delta) from the lighter load case. There are some interesting trends to observe. The lighter load case tends to be stiffer than the PV sensitivity case (grey lines in the lower plot). This is as expected because everything between the two cases is the same except for the inverter PV being substituted for synchronous CSP. The high-mix case tends to be stiffer (orange, below the line), but there are many exceptions (above the line) where added transmission or added CSP have stiffened the system even though the load and other generation has dropped.

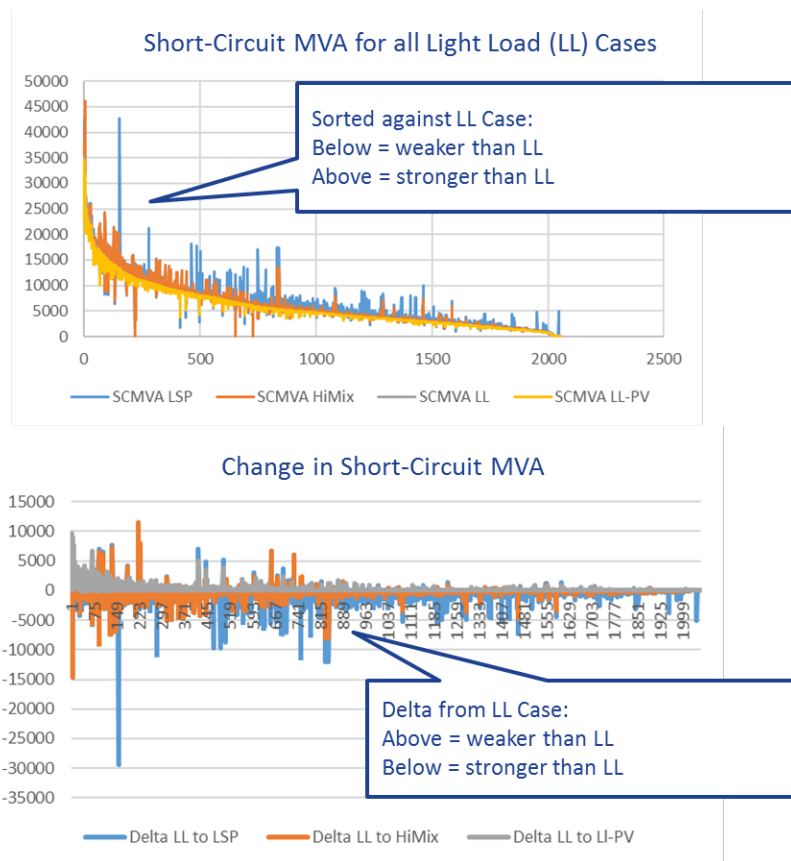


**Figure 18. Spring: impact on short-circuit strength**

These results are for the entire system. Much of the CSP of interest is in Southern California Edison (SCE) zone, so we looked more carefully at SCE buses. There is a lot of new solar, and we added a significant amount of 230kV transmission to accommodate it. Figure 19 plots the changes for the SCE buses of 230 kV and more. The balloons highlight some interesting points that are consistent with those raised earlier. The trends reinforce but do not point to specific buses to be studied. Short-circuit strength is a location-specific metric, and individual nodes become important. Many buses in Figure 18 have very small short-circuit MVA change. We are interested in locations that experience substantial change so that we can look for significant stability effects associated with the difference. Figure 20 shows the geographic distribution of buses that experience a substantial (more than 10%) drop in short-circuit strength when the CSP is converted to PV. Not surprisingly, a number of nodes show very large drops (the deeper colors).

The locations in this figure that are the weakest, which have the biggest difference between CSP and utility-scale PV and have relatively large amounts of new solar generation, are candidates for closer investigation. Results of this investigation are presented in Section 10.

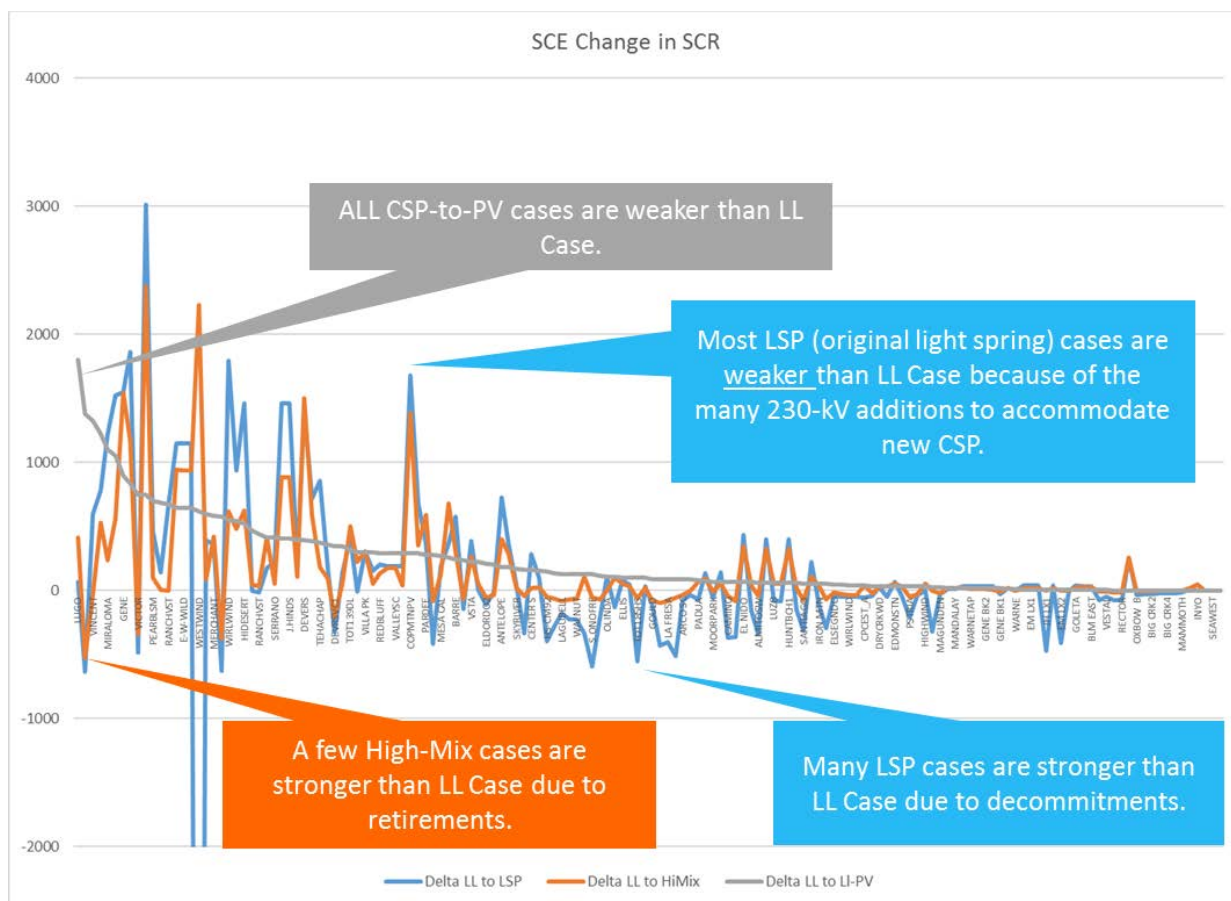


Figure 19. Short-circuit strength detail in SCE Zone

Lighter Load (LL) case with CSP and CSPToPV  
 Short Circuit Level change due to conversion of CSP to PV units

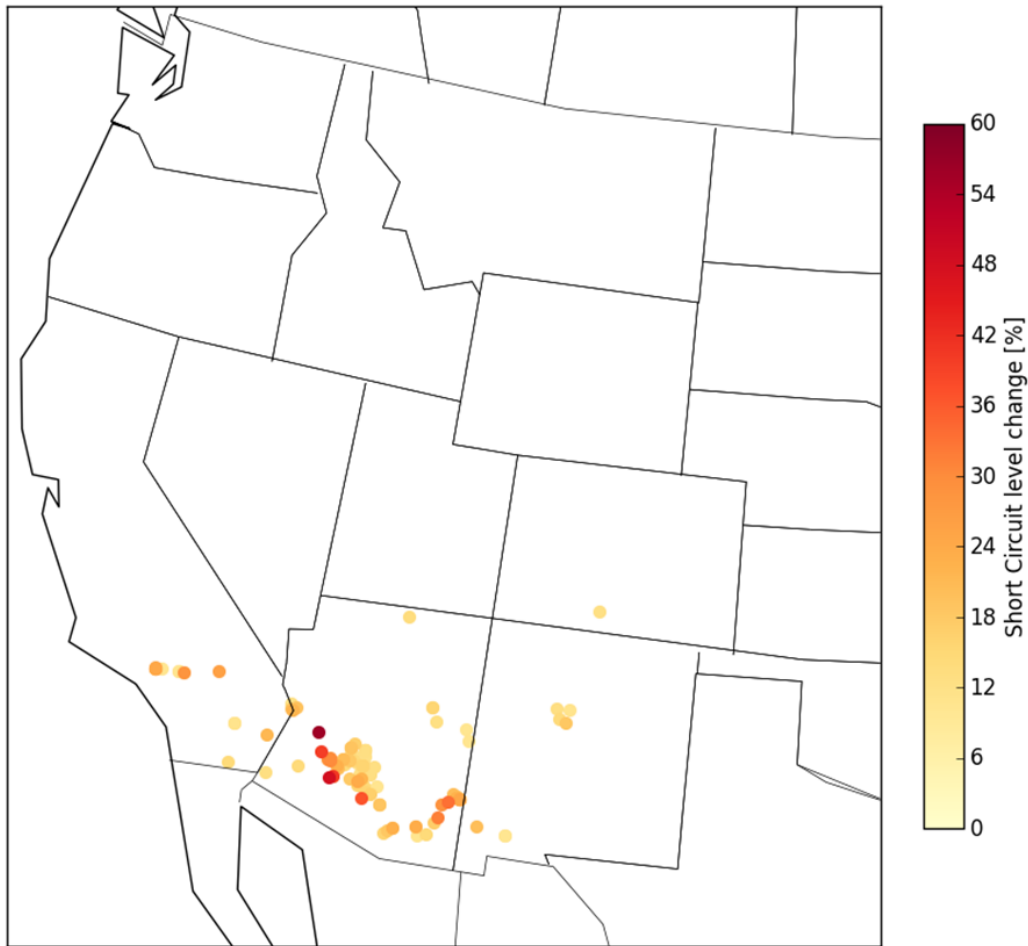


Figure 20. Changes in short-circuit strength from lighter load to lighter load PV-to-CSP case

### 4.3 Simultaneous Nonsynchronous Penetration: General Discussion

SNSP is a metric of the degree to which the grid depends on power that is delivered through inverters (and not synchronous machines).

It was originally introduced by EirGrid, the grid operator for Ireland (O’Sullivan, Rogers, and Kennedy 2011), and it is presently a key metric there in limiting the instantaneous penetration of inverter-based resources (i.e., wind plus HVDC). EirGrid calculates SNSP using the *dispatch* of resources. It is basically the total generation from wind and HVDC divided by the total generation from all resources. Today, EirGrid limits SNSP based on transient stability limitations. Having started with a limit of <50%, they have been meeting their objective of raising that limit by 5% per year, reaching a limit of 60% today. Today, wind power is curtailed to adhere to the limit. They have a goal of raising that limit to 75% by 2020 (EirGrid 2015). EirGrid’s long-term (2030) goal is to be able to accommodate 100% instantaneous penetration.

EirGrid pioneered the use of SNSP as metric of system behavior and a quantitative limitation on system operation. EirGrid limits system operation based on a maximum allowable SNSP, has been stepping up in 5% increments over the past few years towards the 75% target. SNSP is a piece of the puzzle in understanding system performance with high penetrations of inverter-based resources. It is a systemic metric for which we are trying to understand the implications for the Western Interconnection and other U.S. grids. The work reported here builds on the SNSP investigation of WWSIS-3. Figure 21 shows the SNSP and the contributing elements for the lighter load case. The SNSP is 58%, which puts it squarely in the range considered the present limit by EirGrid. The genesis of the EirGrid SNSP limit is primarily transient stability. Hence, use of actual generation levels, i.e., dispatch, is a rational metric.

EirGrid applies the SNSP metric at the systemic level (i.e., all of the Irish grid); however, the Western Interconnection is much larger, both geographically and in terms of total rating. Figure 22 shows the SNSP and contributing elements from the four regions (of Figure 1). The Northwest has an SNSP of 77% in the lighter load case because there are large amounts of wind generation in the region, and we have decommitted hydro (as discussed earlier) to rebalance the system at the lighter load condition.

Other concerns, particularly with respect to inverter stability, are arguably more tied to the ratings of equipment relative to the total system. Figure 23 shows the SNSP metric calculated based on the *rating* of the operating equipment rather than the dispatch (or production). The high level (84%) in the Northeast was examined in WWSIS-3.

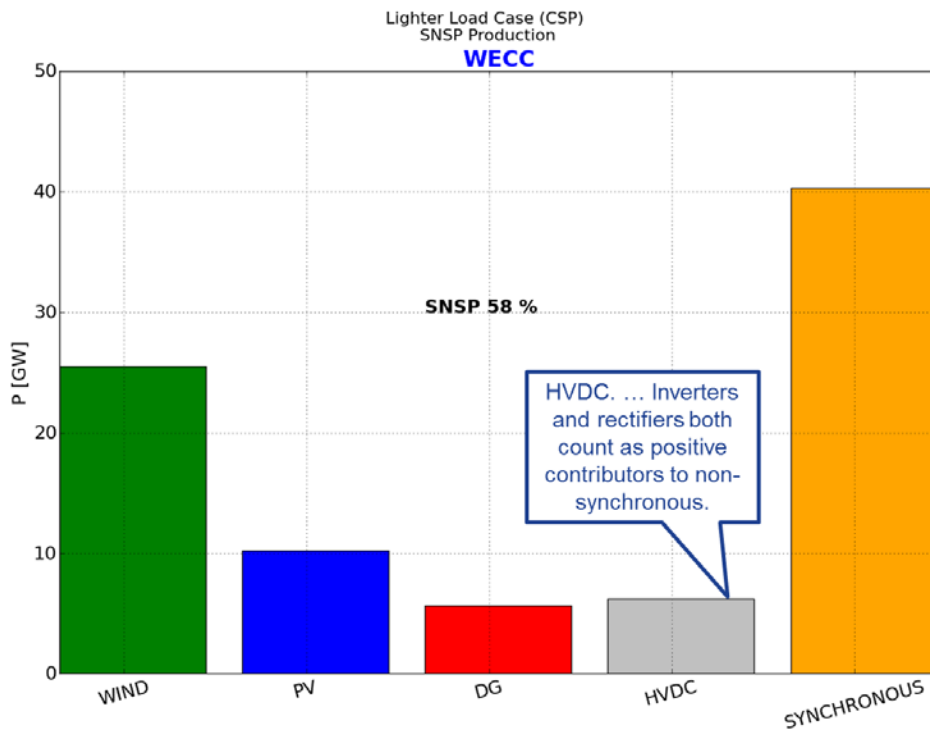


**Figure 21. Lighter load simultaneous nonsynchronous penetration for system based on generation (dispatch)**

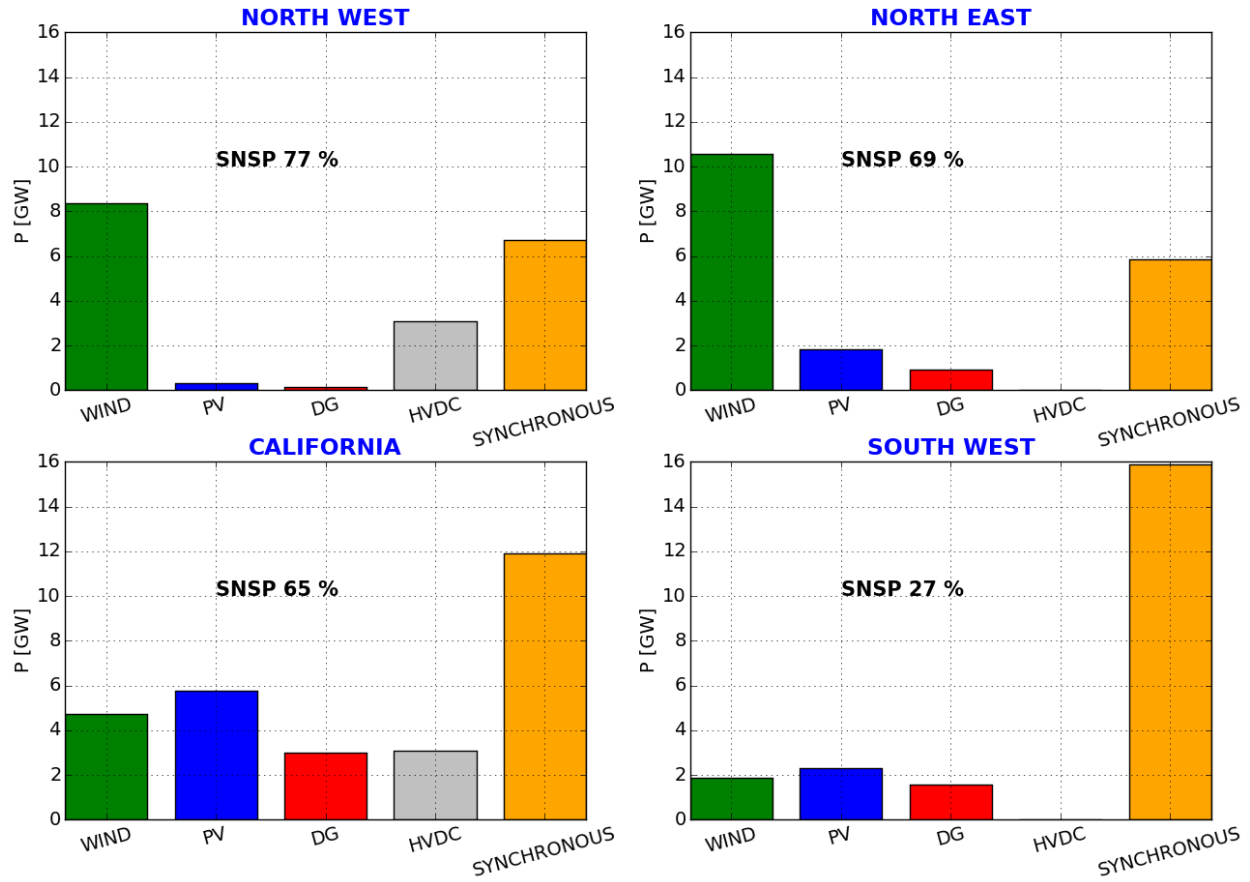


Figure 22. Lighter load regional simultaneous nonsynchronous penetration based on generation (dispatch)

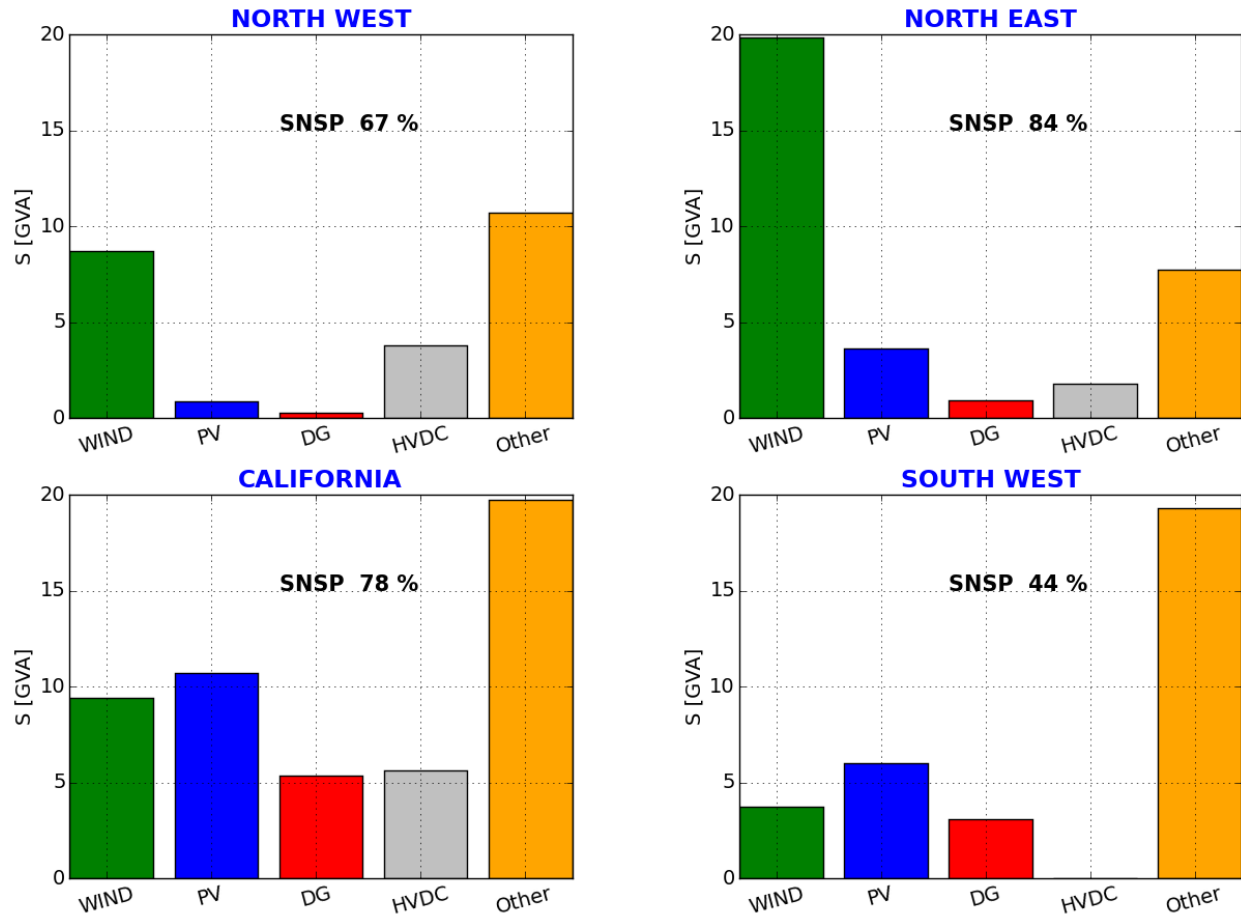
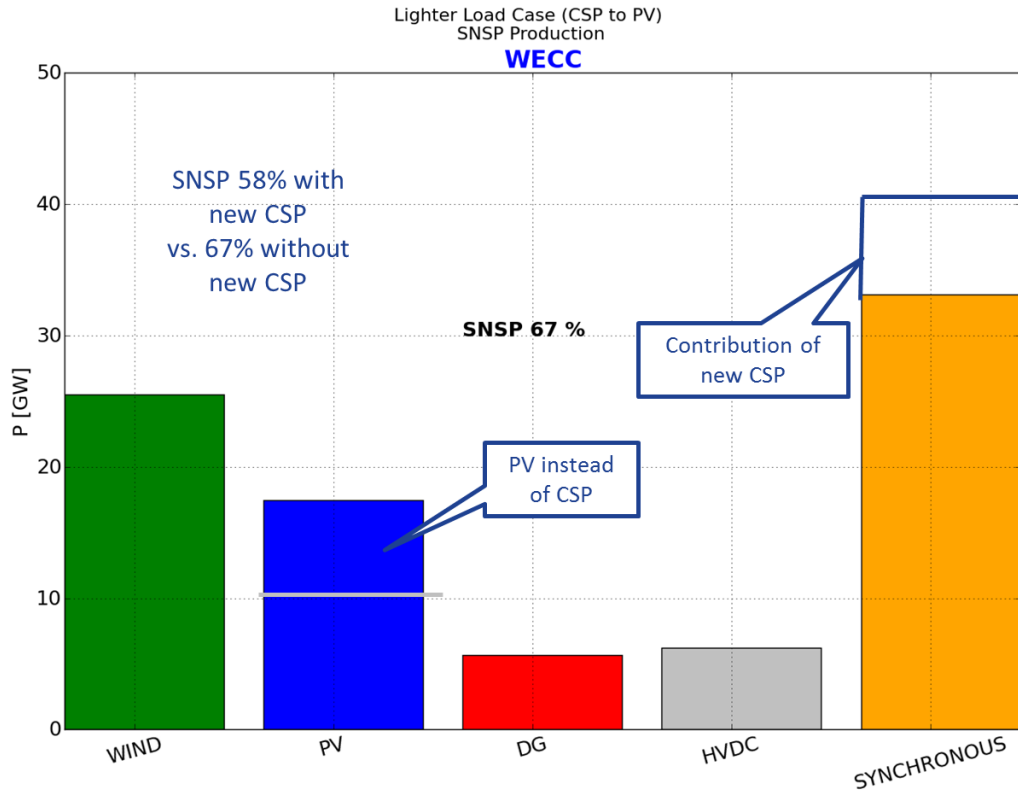


Figure 23. Lighter load simultaneous nonsynchronous penetration based on capacity (generator rating)

#### 4.3.1 Simultaneous Nonsynchronous Penetration: Effect of CSP to PV Conversion on Lighter Load Results

The sensitivity case in which new CSP is replaced with utility-scale PV has a substantial effect on the SNSP in the Southwest, particularly in Arizona. Figure 24 illustrates the impact on the entire system, with the approximate 10-GW conversion of CSP to PV causing the system-wide SNSP to rise from 58% to 67%.

The regional effect is more pronounced, as shown in Figure 25, where the SNSP in the Southwest rises from 28% (Figure 22) to 57%. The split between inverter and synchronous generators is shown in even finer granularity on Figure 26. Some of the smaller areas, such as New Mexico, have relatively high levels of inverters (red portion of bar). But as Figure 27 shows, the Southwest region is dominated by Arizona. The relative performance of Arizona between the two conditions is examined in some detail in Section 10.



**Figure 24. Contribution of CSP to reducing simultaneous nonsynchronous penetration**

Lighter Load Case (CSP to PV)  
SNSP Production

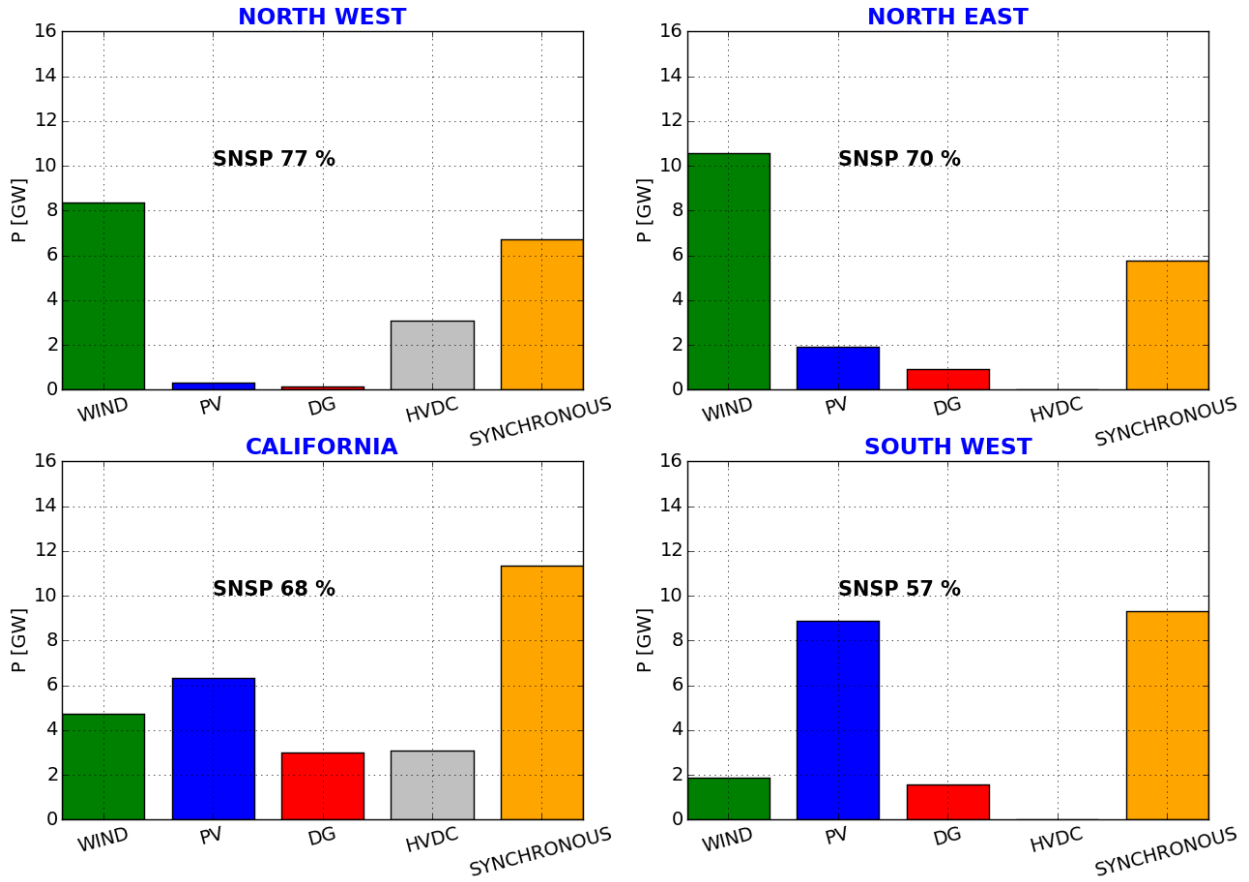


Figure 25. Simultaneous nonsynchronous penetration for CSP-to-PV sensitivity

Lighter Load (LL) Case (CSP to PV)

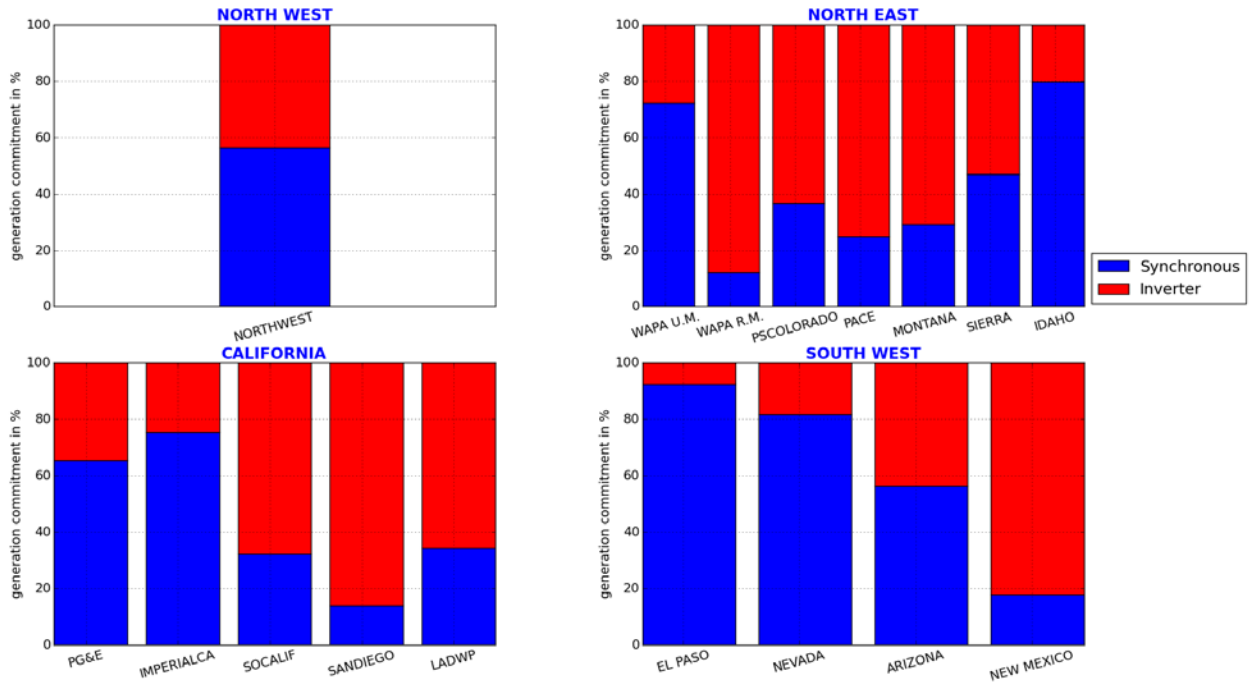


Figure 26. Lighter load CSP-to-PV case distribution of inverter-based resources

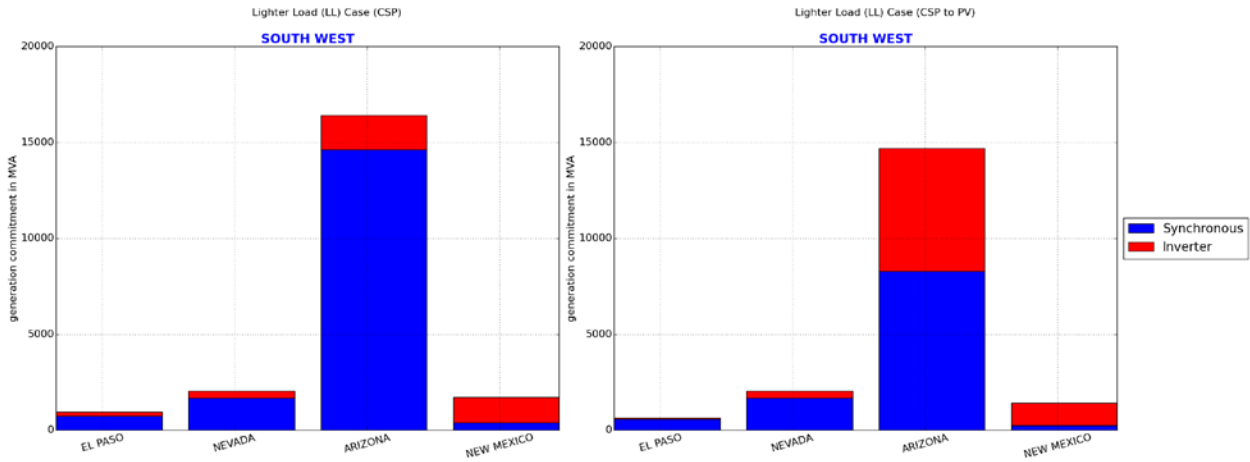


Figure 27. Lighter load CSP-to PV case changes in resources in the Southwest

## 5 System Transient Stability Performance

### 5.1 Overview

Transient stability is one of the limiting dynamic phenomena in the Western Interconnection. In preceding WWSIS, we provided background discussion of the technical basics of Transient Stability (Miller et al. 2014a, Section 1.1.3]

#### 5.1.1 Transient Stability Visualization

Here we present a simple visual model intended to help understand the basic problem of transient stability in interconnected systems, that we have used in previous Western Wind and Solar Integration studies (Miller et al 2014a).

In addition to maintaining the balance between electricity generation and electricity demand, power system operators must ensure that the grid can successfully transition from normal operation (e.g., all transmission lines and generating units are in service), through a disturbance (e.g., an abrupt outage of a major transmission line or large generator), and into a new stable operating condition in the 10–20 seconds immediately following a disturbance. The ability to make this successful transition is called transient stability.

Figure 28 shows an updated visualization of the problem originally presented in Elgerd (1971) to include wind and PV. The round masses (inertias) represent generators, with the tension on the various springy lines representing power transfer. The board at the top represents the simplified idea of an infinite bus—a real, finite power system is floating. The level at which it is floating is a proxy for frequency, which must stay close to 60 Hz. The hands represent wind and PV. They put tension (inject power) on the system, but they are all control and not weight. The mission of these devices, unless taught to do otherwise, is to pull uniformly, regardless of whether the node to which they are connected is moving or not.

The scissors represent a disturbance, which might cut a line or disconnect a generator. The rubbery mass-spring system bounces around. If the event is too severe or some of the lines are stretched too tight (too much loading), more lines will break. It is easy to imagine a cascading failure in which each successive break leads to another failure. A substantial part of system planning is aimed at avoiding such unacceptable consequences.

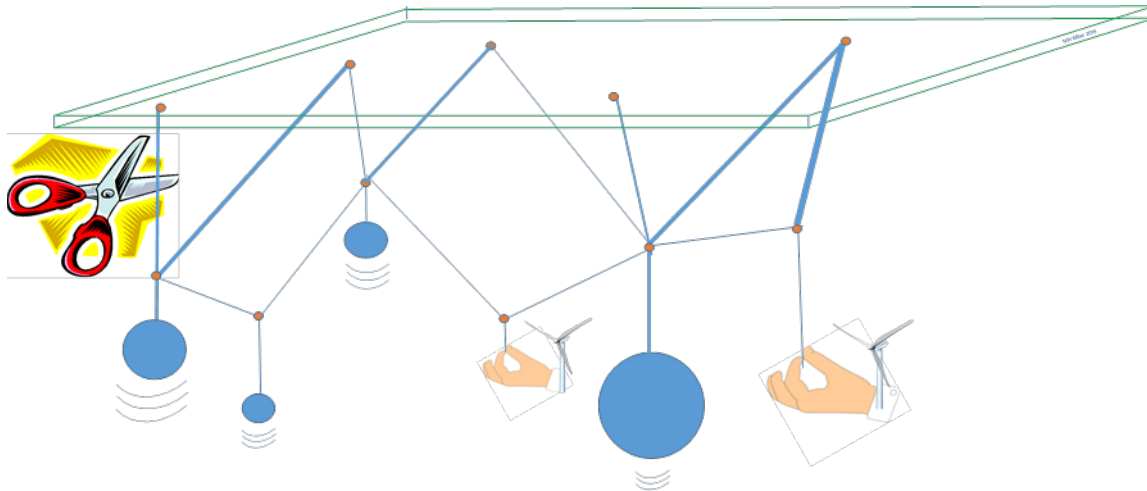


**Figure 28. Visualization of transient stability with synchronous generators and wind power plants**

U.S. interconnections have a long history of constraints because of transient stability limitations that vary depending on system characteristics such as electricity demand (e.g., peak summer load), the power flowing on the transmission system (e.g., heavy flows on critical paths), and the location of the generating plants in operation (e.g., remote from population centers). Transient stability can be both systemic and local. The primary performance criteria follow NERC and regional reliability entity standards.

### **5.1.2 Previous Transient Stability Work: Western Wind Solar Integration Study: Phase 3 and Phase 3A**

In WWSIS-3a, we conducted extensive experiments on the transient stability in eastern Wyoming, which has a very high level of *exported* power generated by inverter-based resources in the study cases. In that work, we found that the exporting system tended to have good stability limits and high levels of export were achievable, potentially higher than could be achieved with export from synchronous generation. We also found evidence that the system, when pushed to transient stability failure, tended to lose synchronism faster and with less warning (i.e., the system stability performance looks good until the system is very close to the limit).

In that investigation, more emphasis was placed on understanding the local behavior driving the stress and instability. After diving into the details of the characteristics of the system instability, the investigation turned to potential system adjustments and control features of wind turbine generators as means to reestablish stability.

Note that the current study is an investigation to increase understanding about how highly stressed systems with high levels of wind and solar generation and low levels of synchronous generation behave in the system nearer the bulk of the system load and with emphasis on solar generation rather than wind generation.

As noted earlier, the industry has limited experience with large, geographically diverse grids in which solar and wind generation have displaced most of the synchronous generation.

## 5.2 Regional Transient Stability Impacts of Required Transmission Changes

The addition of new transmission elements to accommodate the steady-state thermal and voltage requirements was described in Section 2.7. These transmission changes will alter the transient stability of the system as well. In this section, we present investigations of the impact of these transmission changes on the system transient stability.

### 5.2.1 Heavy Summer Pacific DC Intertie Event Case: Initial Investigation

The disruption of flow on the PDCI is a severe transient stability event. In past WWSIS studies, a simplified version of the event was run in which the HVDC terminal is blocked, but none of the other remedial action schemes are engaged. The intent was to examine the differences caused by the changes from the addition of solar and wind resources rather than to evaluate exactly whether the case is stable or not.

In this study, we continued that investigation. As noted, for this study we upgraded the PDCI capability to align with its planned future capability. Figure 29 shows the heavy summer high-mix case and the new heavy summer retirements case. As in earlier studies, the high-mix case is unstable without the remedial action scheme, with a loss of synchronism and system separation occurring at approximately 5 seconds. By comparison, the new heavy summer case with retirements and added transmission for the new solar power plants is stable. The key path flows for the successful new case are shown in Figure 30.

This result was something of a surprise because the transmission and generation additions were mostly rather remote from the California-Oregon Interface (COI) stress points mostly affected by the PDCI event. This surprising result led to into a more detailed investigation, which is reported next.

On a final note for this section, the PDCI event for the lighter load case is relatively uninteresting. As noted earlier, because there is substantial excess of generation in the southern half of the system, the PDCI is operating from south to north, exporting power from the Los Angeles basin. When the DC is blocked, the system tolerates the extra power in the South without major stress on the systems.

Heavy Summer HiMix (HS HiMix) and Heavy Summer Retirement (HS RET) Case  
Event: PDCI Trip

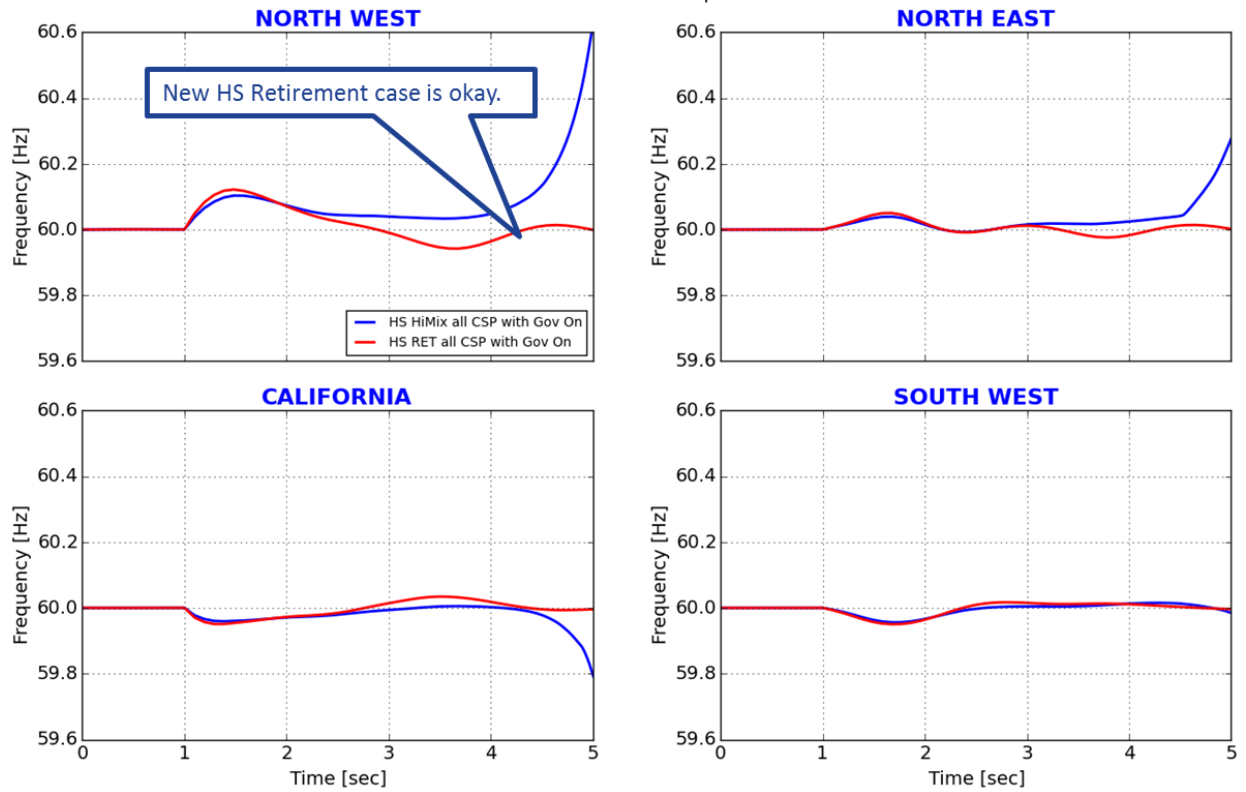


Figure 29. Frequency Pacific DC Intertie result

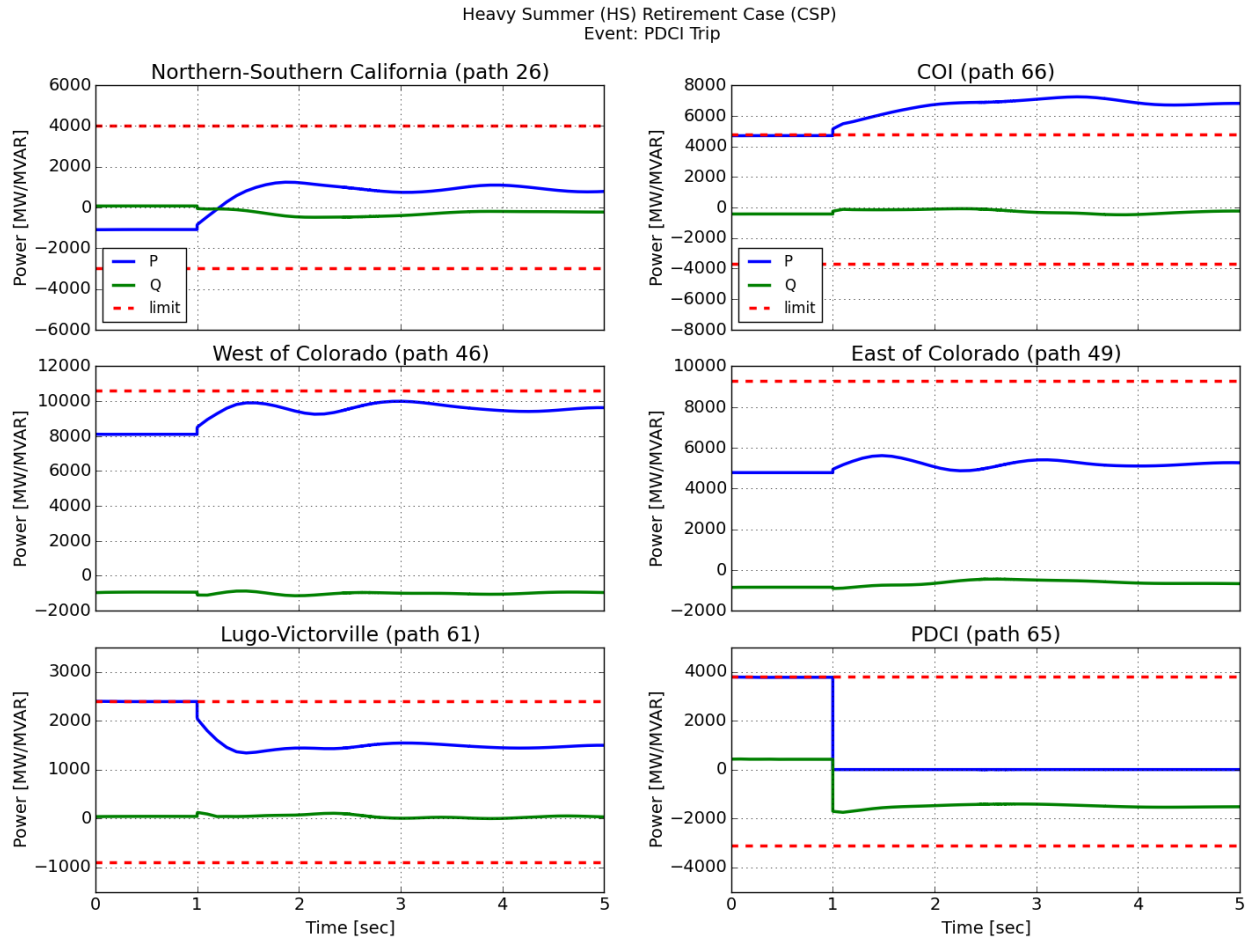
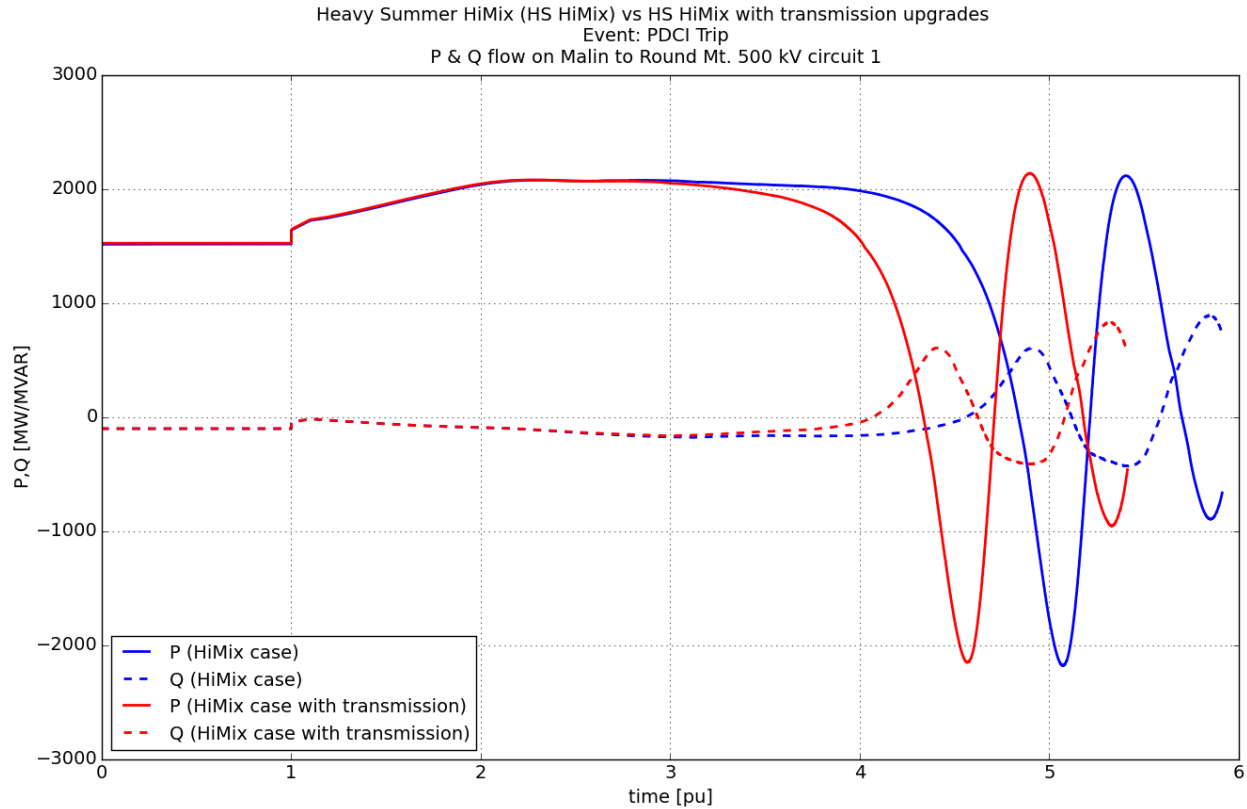


Figure 30. California-Oregon Interface Pacific DC Intertie event: key path flows

## 5.2.2 Investigation of Transmission Additions Impact on Transient Stability for Pacific DC Intertie Event

The first test performed to try to understand the change in stability for the new heavy summer case with increased solar was to check the impact of the PDCI upgrade on the heavy summer high-mix base case. The case with only higher PDCI power was, as expected, considerably less stable, since the disturbance is bigger and the transmission hadn't changed. We expected that the addition of the other transmission, which was needed for the new heavy summer case, would improve the performance of the original heavy summer high-mix case. Again, however, somewhat counter to our expectations, the case *with more transmission* is less stable, as shown in Figure 31. Note that both cases are unstable, but the added transmission (mostly in Southern California and Arizona) results in the system separating faster, i.e., it is less stable.



**Figure 31. Pacific DC Inertie disturbance performance degraded by transmission additions**

Closer investigation of the flows, reactive power balances, and voltage profiles throughout the system provided some insights. Some key path flows are shown in Figure 32. We also tested a long sequence of intermediate steps, adding pieces of the total transmission additions (from Table 4). Each successive stiffening of the system in the desert resulted in somewhat worse performance for this specific event. We concluded that strengthening the grid to the south, and in particular the Arizona and Southern California region, results in the swing stress on the COI and Northern California being slightly faster and more acute.

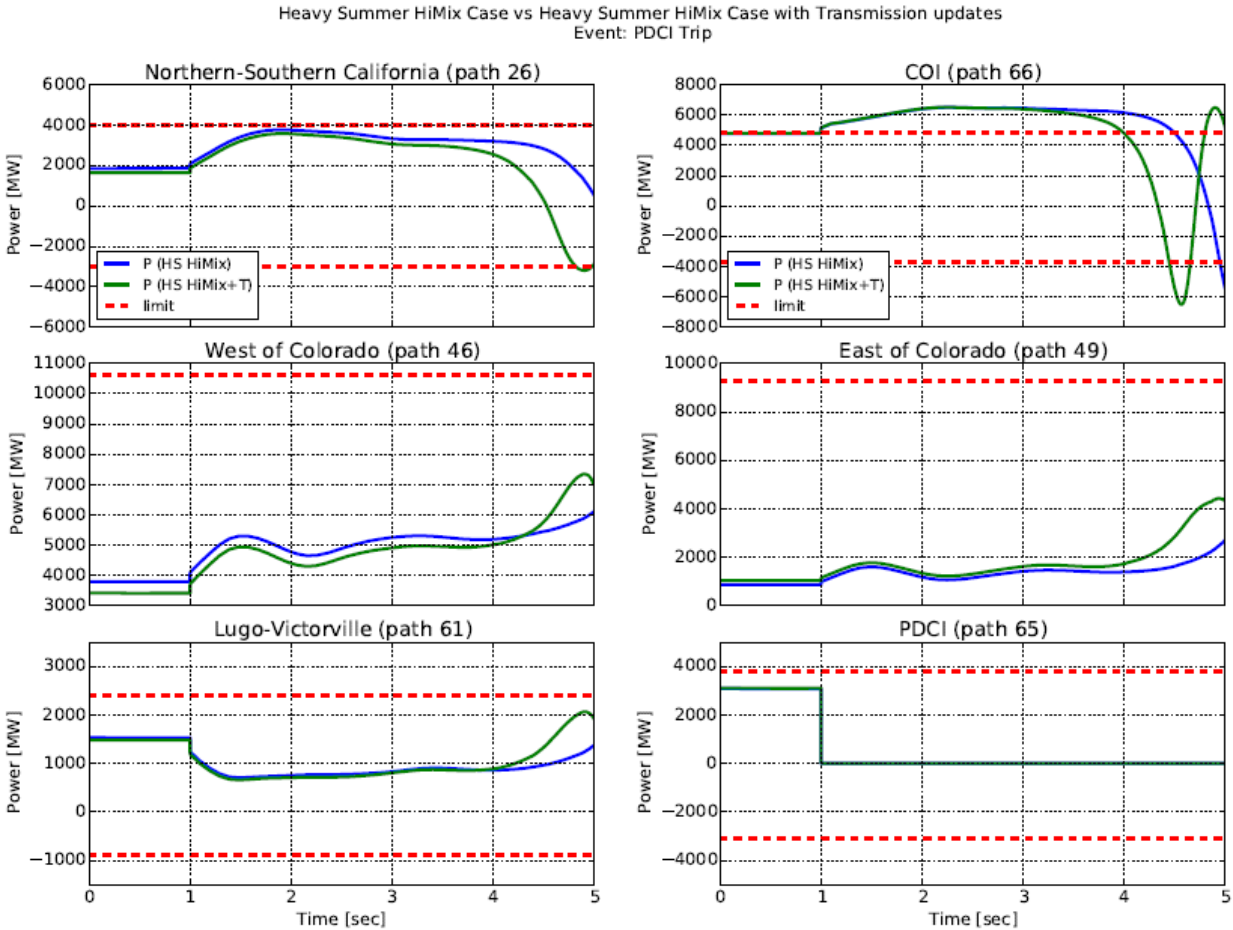


**Figure 32. Path flow comparisons for PDCI disturbance showing performance degraded by transmission additions**

### 5.2.3 California-Oregon Interface Event

For further investigation, we designed a test case that stresses the system electrically closer to the reinforcements. A COI event was created in which we trip all three 500 kV lines across the COI border. The case was created so that power from the Northwest that would have crossed into California on the COI needs to loop around toward the east and across the Colorado River interfaces to the south. The comparison of performance shown in Figure 33 is for the heavy summer high-mix condition with and without the new transmission added. Again, both cases fail, but the case with new transmission holds on longer. It is more stable. The separation occurs farther south for this event, nearer to reinforcements. This result is as expected because the reinforcements tend to support the part of California starved for power by the trip of the COI.

The overall observation for the COI event is that the added transmission in Southern California and the Mohave Desert improves performance for events that depend on that path.

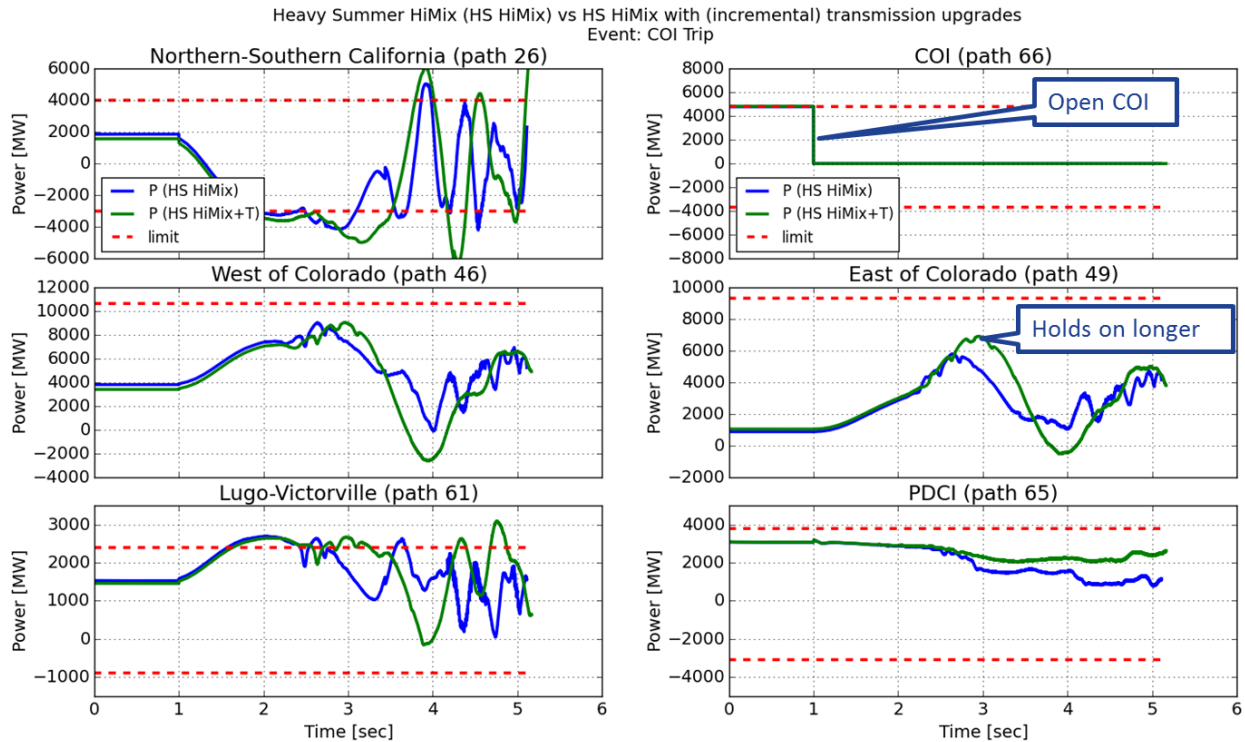


**Figure 33. California-Oregon Intertie event stability test details**

#### 5.2.4 Overall Observations on Transient Stability Impact of Transmission Additions

Additional transmission, necessary to avoid local voltage and thermal problems that accompany the significant build-out of solar in Arizona and California, impacts the transient stability of the bulk power system. The impacts might be positive or negative, depending on the event. The differences in performance are not dramatic; the most observable changes in the stability behavior tend to be variations in the timing of instability, advancing or retarding separations by a second or so.

Good but well-established system planning practice will need to accompany the build-out of transmission and the addition of solar power plants, as it would for any other major system changes. There is no obvious change in practice required based on this narrow investigation.

## 6 Frequency Performance

### 6.1 Frequency Response Overview

#### 6.1.1 Frequency Response Visualization

The need to manage grid frequency has been addressed in several of the studies that preceded this work. Here we present a brief tutorial and visualization of frequency response that is adapted from earlier reports.

To reliably operate a large interconnected electric grid, such as the Western Interconnection, requires a constant balancing of electricity generation with electricity demand. Electricity must be generated at the same instant it is used, so operating procedures have developed to forecast electricity demand, schedule electric generators to meet that demand, and ensure sufficient generating reserves are available to respond to forecast errors and system disturbances. The measure of success in this balancing act is frequency. In North America, that means maintaining system frequency at or very close to 60 Hz, as shown in Figure 34.

However, disturbances do occur, including large ones (e.g., abrupt outage of a large generator or a major transmission line) that affect overall system frequency. For example, a transmission line outage might disconnect a large industrial customer. As a result, the total electricity generation exceeds the total electricity demand and frequency rises. Because operators, in general, have more control over generation than demand, they can execute a generation reduction to regain the balance, and return system frequency to near 60 Hz.

A potentially more significant problem is the loss of a large generating plant. As a result of this type of disturbance, the total electricity demand exceeds the total electricity generated and frequency drops as shown in Figure 35. In general, an electric grid is designed and operated to withstand the loss of the single largest generator; however, the loss of multiple generators or plants might cause the frequency to drop significantly, such that protective devices act to disconnect customers to preserve the bulk of the system. It is a serious reliability failure when operators lose the ability to supply all the electricity needed to meet demand.

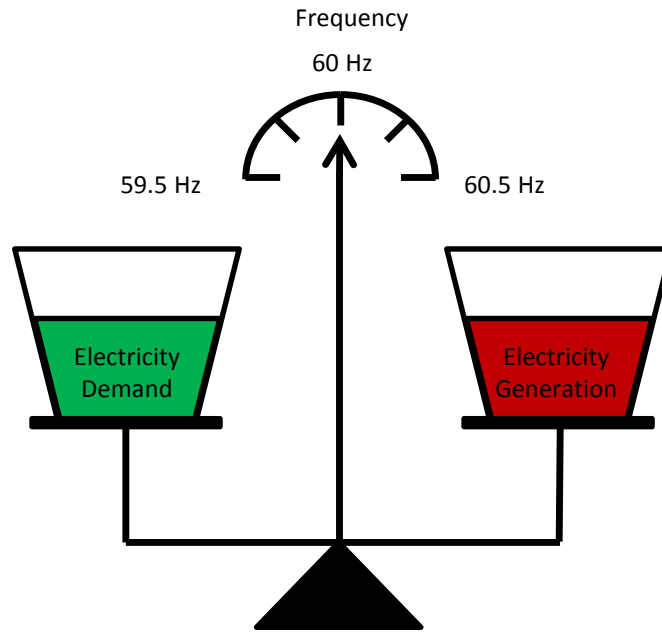


**Figure 34. Balance analogy for frequency stability**

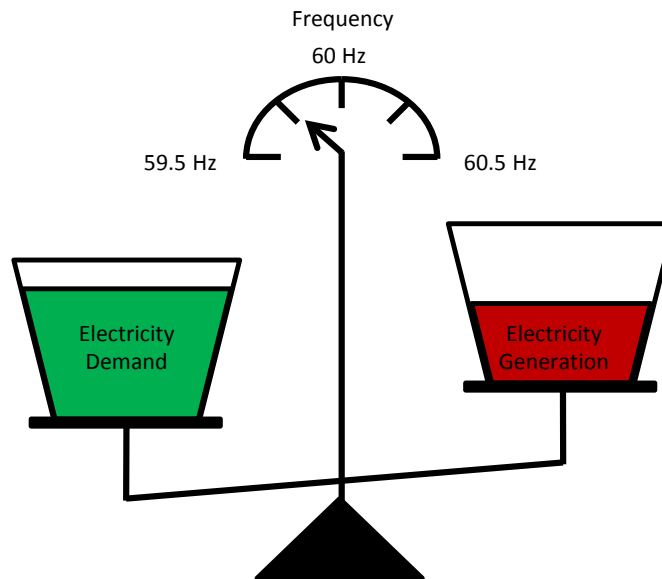


**Figure 35. Electricity demand exceeds electricity generation and frequency drops**

An example of system frequency in response to a large generation trip is shown in Figure 36. The system is operating normally, with a frequency of 60 Hz, up to 1 second. At that time, a large generating unit is abruptly lost. Load now exceeds generation, so the frequency drops. The speed of the initial decline is related to the number of conventional synchronous generators on the system. More generators mean more inertia, which retards the initial rate of frequency decline, the rate of change of frequency (ROCOF); however, the slowing and eventual reversal of the frequency decline is emphatically *not* caused by inertia but rather various resources providing *arresting power*. The resources that respond to the declining frequency by increasing generation or reducing load before the frequency nadir are the source of arresting power. They

“catch” the system on the way down. In this example, at approximately 10 seconds, the frequency nadir or minimum is reached. Only resources that have acted during the time before the nadir are relevant to this performance. Frequency nadir is one measure of a system’s frequency stability—it must be above the highest level of underfrequency load shedding. At that point in time, the generators with governor controls have begun to act to increase power output, and thus the system frequency begins to recover. By approximately 60 seconds, the system frequency has settled to somewhat below the normal operating frequency of 60 Hz. A metric of frequency stability is based on the change in frequency between the nadir and this settling frequency and the change in power in this interval. Measurements are averaged over a defined period following the nadir, as indicated with the brackets, and the ratio of change in power to change in frequency is calculated. This is called frequency response and is formally defined by NERC (2012a). After 60 seconds, even more generators begin to increase their power output, and the frequency returns to normal within approximately 10 minutes. This section of the report focuses on system frequency behavior in the first 60 seconds.

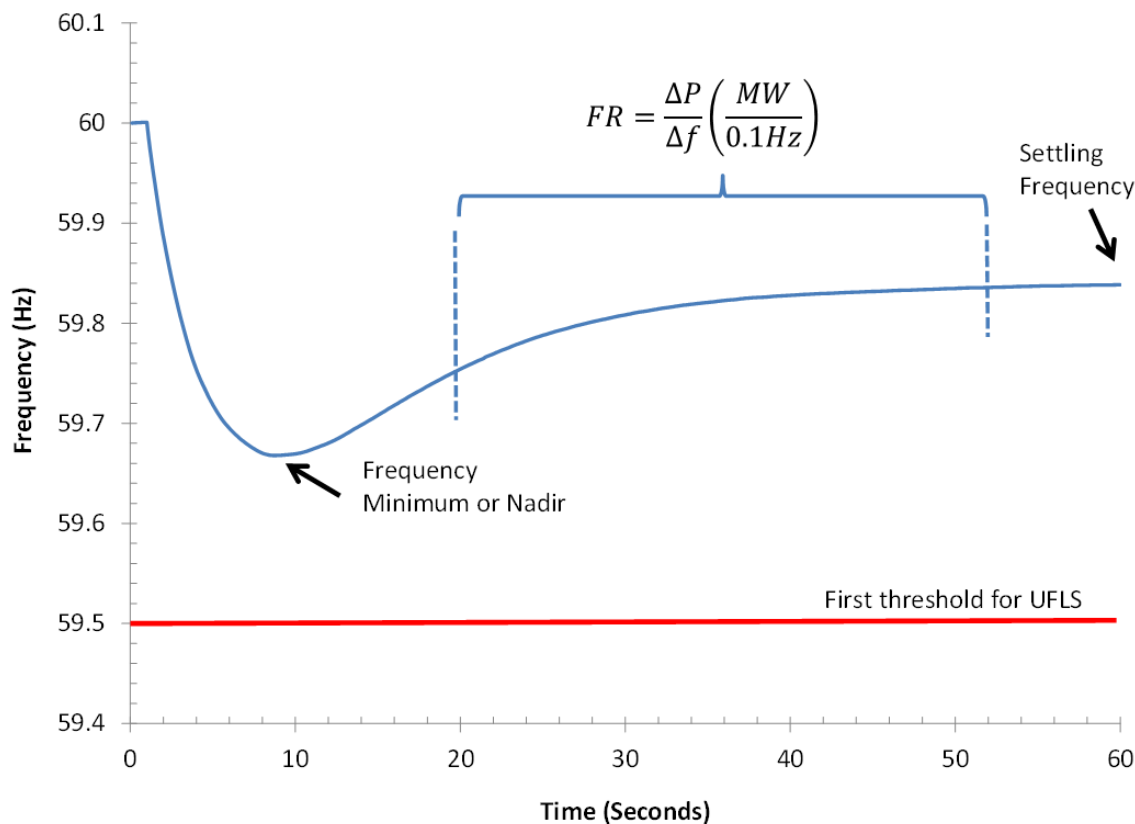


**Figure 36. System frequency in response to a large generation trip**

There is general concern regarding the degradation of frequency response in North America during the past two decades. The decline is caused by various factors, such as the withdrawal of primary or governor response shortly after an event, the lack of in-service governors on conventional generation, and the unknown and changing nature of load frequency characteristics. Large penetrations of inverter-based, or nonsynchronous, generation technologies further complicate this issue. Without special operation or controls, wind and solar power plants do not inherently participate in the regulation of grid frequency. By contrast, synchronous machines

always contribute to system inertia, and some fraction of the synchronous generation in operation at any point has governor controls enabled. When wind and solar (especially PV) generation displaces conventional synchronous generation, the mix of the remaining synchronous generators changes. All these factors have the potential to adversely impact overall frequency response.

Therefore, one of the primary objectives of this investigation is to evaluate and better understand the impact of high-penetration solar power on system-wide frequency response to large generator outages in the first minute after the outage occurs and to examine the differences in behavior between synchronous concentrating solar power plants and inverter-based utility-scale PV plants.

### 6.1.2 Frequency Response Obligation

The Western Interconnection FRO is given in Table 9 and throughout the report as 840 MW/0.1 Hz. Part of the NERC BAL-003-1 standard sets the obligation includes periodic update of the Western Interconnection FRO (NERC 2012b). Consequently, this is only a reference point, not a static and absolute statement of obligation. The other FROs in the table are estimates based on the heavy summer base case initial conditions using the generation and load from that condition as an approximation for the peak generation and load levels dictated by the standard. These figures are for reference only. FRO is assigned to each balancing authority in proportion its size relative to the entire interconnection. This calculation is only an approximation, and it should not be used to determine whether any balancing authority is in compliance.

Later, when the frequency response is calculated and compared to the FRO, the Western Interconnection totals always include the contribution of resources in Canada and Mexico. Only U.S. resources are included in the regional and area levels.

There is also a locational aspect of FRO. NERC standard BAL-003-1 does not stipulate that the balancing authorities need to meet their FRO with their own resources (NERC 2012b). A formal contractual arrangement is required. This is still relatively new ground for the industry. Throughout this report and investigation, the results are reported based on how regions and areas meet the estimated FROs. This is not a statement that balancing authorities need to do it all themselves; rather these are metrics on how much the regions and entities contribute.

**Table 9. Western Interconnection Frequency Response Obligation and Approximate Regional and Area Frequency Response Obligations**

ID	NAME	GENERATION (GW)	LOAD (GW)	FRO (MW/0.1 HZ)
1	Western Interconnection	204	185	840
<i>By Region</i>				
2	California	68.8	67.9	296
3	Southwest	53.9	47.8	220
4	Northeast	19.7	18.0	82
40	Northwest	33.3	27.2	131

The frequency response performances of the interconnection and the individual entities are given by the ratio of the change in power resulting from a disturbance-induced change in frequency. For this metric, the frequency change is assumed to be uniform across the interconnection. In the work presented here, the only power change measured and included in the calculations is that of

the turbine power of the responsive generation. Load response is not considered in the calculation of frequency response. This study focuses on system-wide frequency response. Measuring the frequency at a single node in the grid following a disturbance can be confusing and misleading. In the study, an MVA weighted sum of synchronous machine speeds is calculated and used as a composite frequency

### **6.1.3 Palo Verde Reference Event**

The design basis event in WECC for the NERC Western Interconnection FRO is the simultaneous trip of two Palo Verde Nuclear Generating Station units for a total loss of approximately 2,750 MW. That event is used throughout this investigation of frequency performance.

## **6.2 Impacts of CSP and Load Condition on Dispatch**

The changes from the light spring high-mix case to the new lighter load case are substantial: the system load is much lower; several plants have been retired; and several plants that provide primary frequency response (PFR), especially in the Northwest, have been decommitted.

The following figures show the impact on frequency response of those changes. With lower load and fewer responsive resources, the 2,750-MW event is relatively larger for the system. As expected, the system frequency excursion shown in Figure 37 is more severe for the new lighter load case (red trace) compared to the light spring high-mix case (blue). Figure 38 shows the reduction in contribution by generation in the Northwest in the top left trace. The added CSP shows up in the California and Southwest blocks because the CSP is included in these summations, but *for this comparison* the CSP units are not contributing to PFR (their governors are in baseload mode, reflecting their operation without underfrequency response). Figure 39 shows further details, including the five areas with most of the CSP. The primary frequency response (as shown by the change in mechanical power to the turbine-generators with active governors – P<sub>mech</sub>) in the lighter load case (red trace) for those areas is somewhat greater, reflecting the deeper frequency excursion and reduced contribution to frequency response from the Northwest. This provides a useful baseline for the next exercise, in which we enable the governors on the new CSP plants.

The main point of this comparison is to emphasize that having additional generation dispatch from solar in conjunction with lower load can push frequency-responsive generation out of the system commitment, resulting in degraded frequency response. The performance of both cases meets performance criteria. A further discussion of the frequency response relative to the FRO is provided in Section 9.

Light Spring (LSP) and Lighter Load (LL) Case  
Event: Trip 2 Palo Verde units

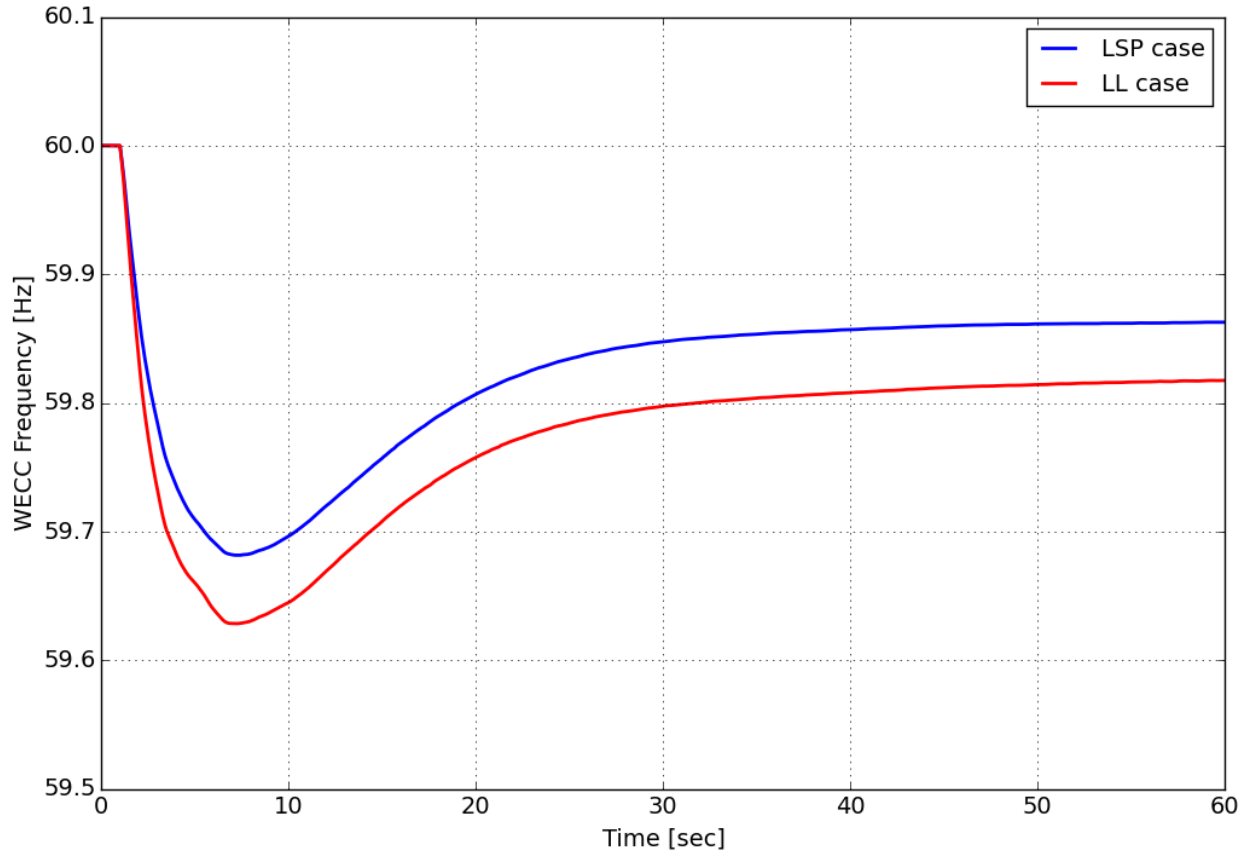
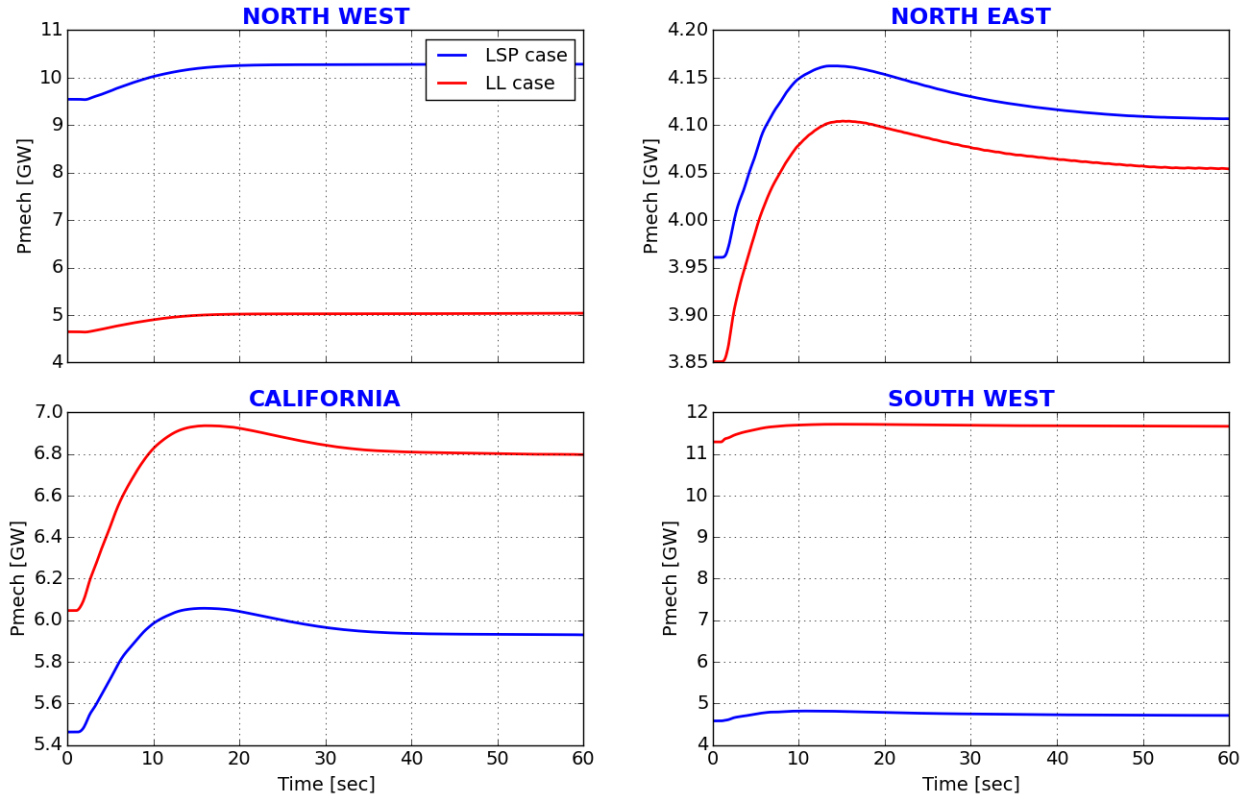
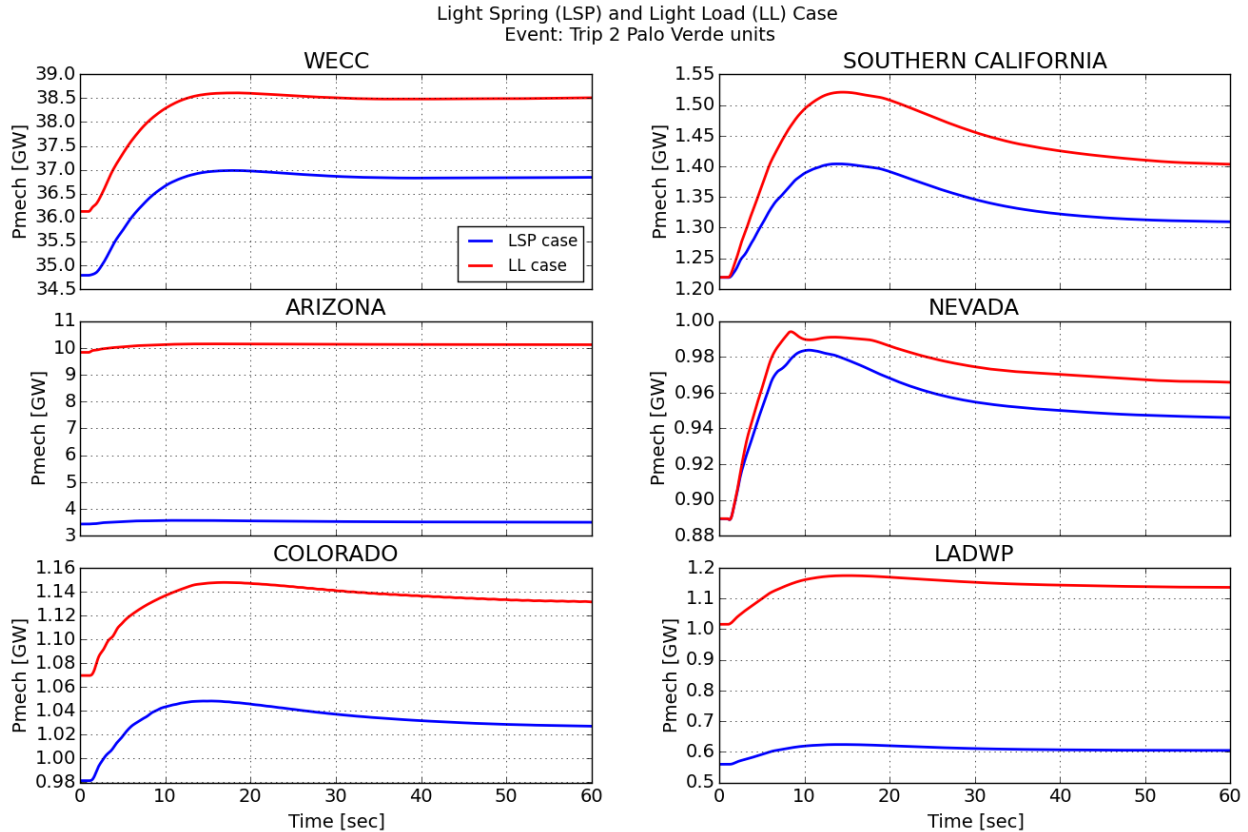


Figure 37. Light spring compared to lighter load frequency (no contribution from CSP)

Light Spring (LSP) and Lighter Load (LL) Case  
Event: Trip 2 Palo Verde units



**Figure 38. Light spring compared to lighter load regional primary frequency response (no contribution from CSP)**



**Figure 39. Light spring compared to lighter load regional primary frequency response in areas with significant CSP capacity (no contribution from CSP)**

### 6.3 CSP Governor and Inertia Contributions

The addition of synchronous CSP generation provides system inertia, and it can provide governor response. Again, the lighter load case is more interesting because the system has less inertia and less committed generation, but the event size remains the same.

#### 6.3.1 Lighter Load

Figure 40 shows three cases that illustrate two separate points. The red trace corresponds to the red in the lighter load case in the preceding three figures—that is, the CSP units are online contributing inertia, but there is no governor response. In the blue trace, we have enabled the governors (per the model discussion in Section 3.2). As expected, both the frequency nadir and the settling frequency improve. The green trace is for the CSP-to-PV sensitivity case. This is interesting because the only significant difference between this and the red case is the inertia of the CSP machines. As expected, the frequency drop is faster, and the nadir occurs sooner and is approximately 1 mHz deeper. We look more closely at this next.

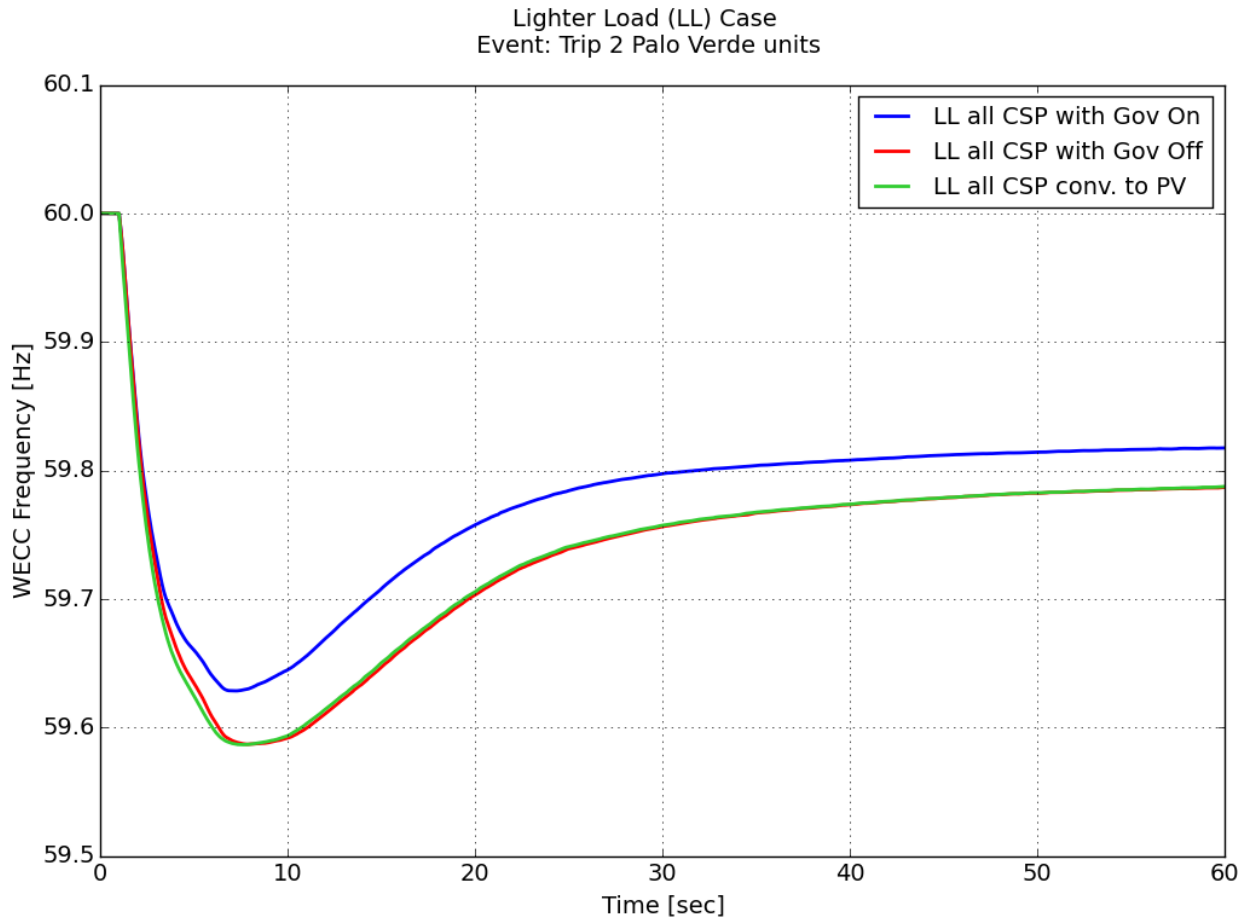


**Figure 40. Impact of CSP governors and inertia on frequency for Lighter Load case**

### 6.3.2 Inertia impact on Rate of Change of Frequency

Figure 41 shows the first 2.5 seconds of the system frequency decline. (This is the same information as that shown in Figure 40 but magnified.) The initial ROCOF with the CSP units not contributing to system inertia is greater, with the green trace dropping faster. As expected, the blue and red traces are initially coincident because the CSP governors (blue trace) have little to no impact during the first 0.5 second. The ROCOF numbers in the figure callouts are based on the change in the first 0.5 second.

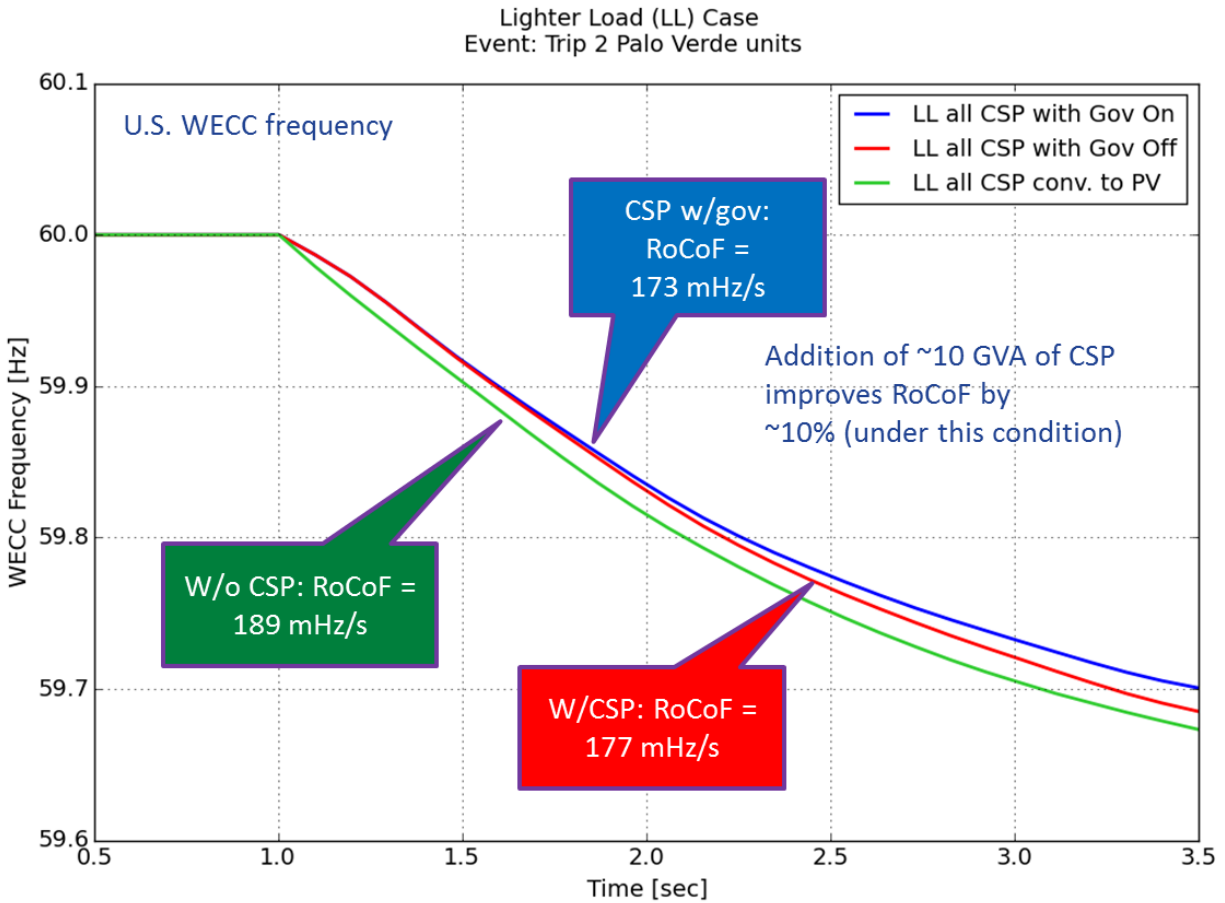


**Figure 41. Inertia impact on initial rate of change of frequency**

## 6.4 Locational Aspects of Inertia and Frequency Response

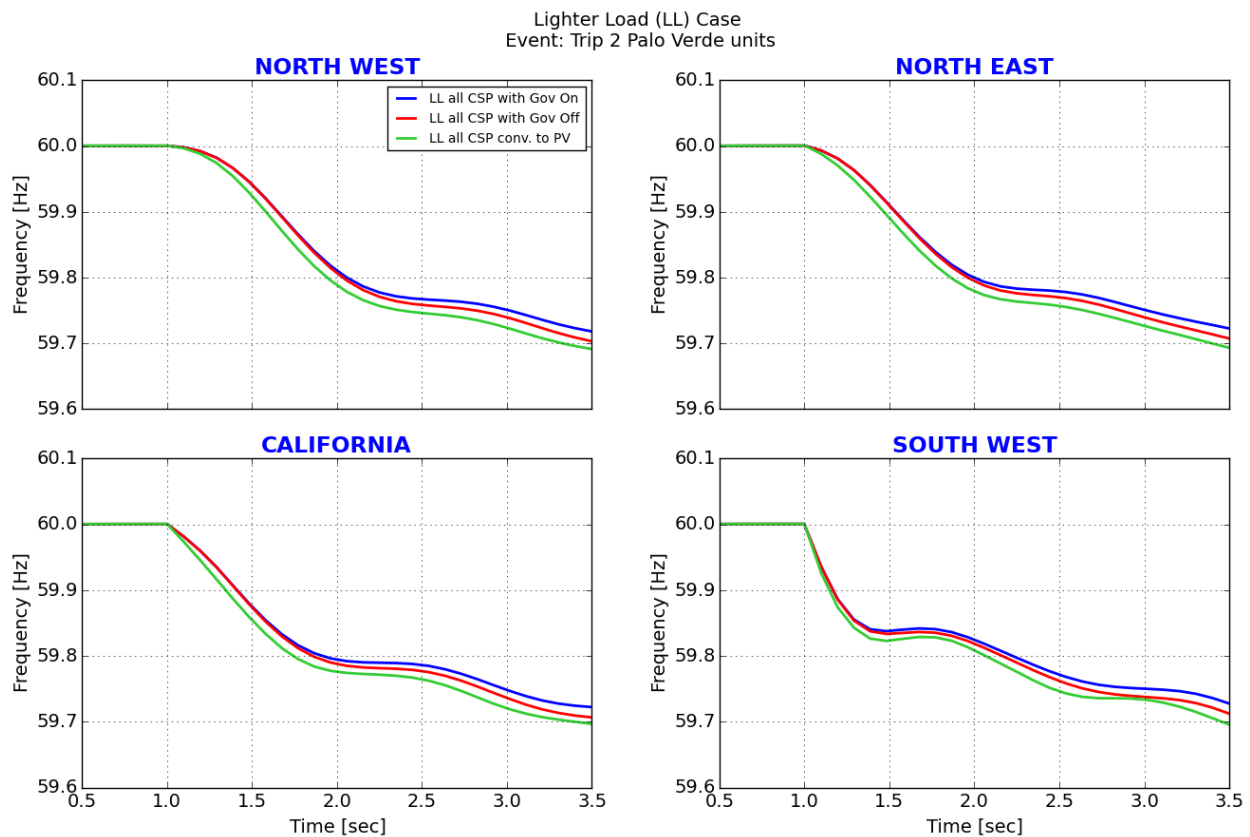
A locational aspect of the change in inertia occurs that impacts the frequency behavior between the CSP cases and the CSP converted to PV case. Figure 17 shows the changes in system inertia by region. Note that in that figure, the change between these two cases (lower right-hand side) is the most dramatic. The new CSP is in relatively close electrical proximity to the Palo Verde Nuclear Generating Station. That means that the added inertia “sees” the disturbance relatively quickly after the generation trips.

Figure 42 plots the frequencies of the four regions. This sheds some interesting light on the locational aspects of frequency. The ROCOF for all these traces, summarized in Table 10, is calculated as the change in frequency during two periods: for the first 0.1 second and then for 0.5 second of the event.

Because the disturbance occurs in the Southwest (where the Palo Verde Nuclear Generating Station is located), the initial frequency decline there occurs much sooner, and the ROCOF is approximately three times the system ROCOF. Further, the difference between the green trace (no CSP inertia) and the red trace in the Southwest is most noticeable. The aggregate frequency (and ROCOF) in Figure 41 rather masks this locational factor. It is also interesting to note that the more remote parts of the system respond later in the case. That means that the ROCOF

calculated during the first 0.1 second is actually lower for the more remote parts of the system compared to the ROCOF calculated during the first 0.5 second. For context, the Irish system is concerned with the system-wide ROCOF exceeding 2 Hz per second (Eirgrid 2015); the Electric Reliability Council of Texas might see system-wide ROCOF reaching as high as 0.5 Hz in the near future (ERCOT 2010).

This raises some interesting questions, mainly: Do we care that the ROCOF is higher? In these cases, the system frequency response is improved by the contribution of the CSP governors. The impact of inertia on frequency response and on the frequency nadir is quite small in this case. Those two metrics have the greatest reliability and economic impact. In later sections we examine the control and robustness implications of the locational aspects of frequency with attention to options to mitigate frequency problems.



**Figure 42. Locational aspects of rate of change of frequency impacts**

**Table 10. Lighter Load Initial Rate of Change of Frequency**

<b>ROCOF (HZ/S)–MEASURED DURING FIRST 0.1 SECOND</b>			
	<b>CSP GOV ON</b>	<b>CSP GOV OFF</b>	<b>CSP TO PV</b>
<b>WECC</b>	0.197	0.197	0.208
<b>Northeast</b>	0.074	0.074	0.127
<b>Northwest</b>	0.025	0.025	0.039
<b>California</b>	0.192	0.192	0.273
<b>Southwest</b>	0.656	0.656	0.752
<b>ROCOF (HZ/S)–MEASURED DURING FIRST 0.5 SECOND</b>			
	<b>CSP GOV ON</b>	<b>CSP GOV OFF</b>	<b>CSP TO PV</b>
<b>WECC</b>	0.173	0.177	0.189
<b>Northeast</b>	0.194	0.196	0.229
<b>Northwest</b>	0.137	0.138	0.172
<b>California</b>	0.252	0.256	0.288
<b>Southwest</b>	0.277	0.286	0.302

#### **6.4.1 Locational Aspects of Primary Frequency Response**

Results show that, as expected, the frequency tends to drop fastest in locations close to the point of the initiating unbalance. To look further into frequency response and dependence on location of the initiating event, a learning exercise with an event of similar size to the Palo Verde event was tried in the Northwest. The idea is to examine what difference the location of the event makes. This locational aspect is a potential concern, since if it were to be shown that the location of the initiating event has a substantial impact on primary frequency response, then operation and control strategies will need to take this impact into consideration.

The simulated event is a fiction created for this test. We did not identify a reasonable event that would cause an approximate 3,000-MW loss of generation in the Northwest. Instead, we added load in the Northwest that resulted in a similar settling frequency. A bit more load was added (3,000 MW) compared to the 2,750-MW loss with tripping the two Palo Verde units to get the same settling frequency, as shown in Figure 43.

Lighter Load (LL) Case  
Event: Trip 2PV and Turn on Load in North West

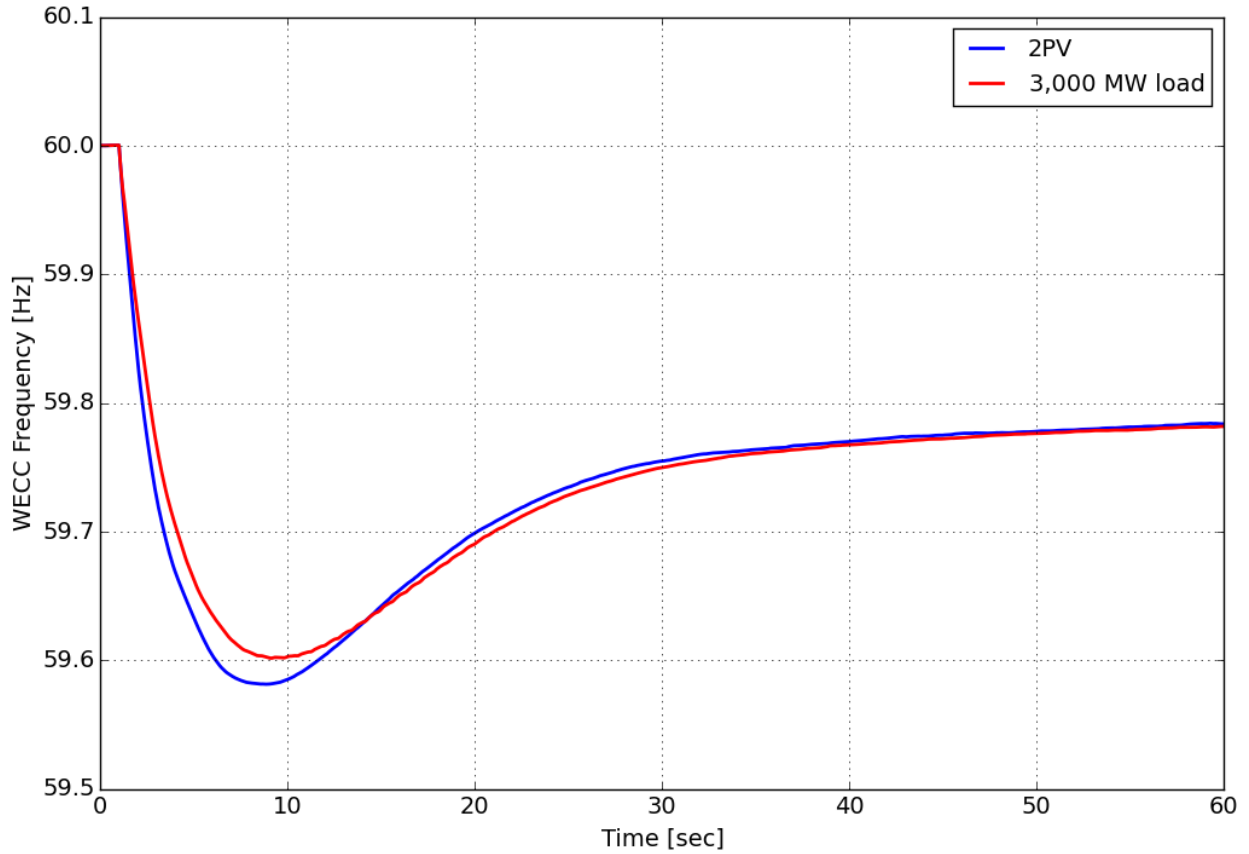


**Figure 43. Comparison: loss of two Palo Verde units (approximately 2,750 MW) compared to 3,000 MW load increase in the Northwest**

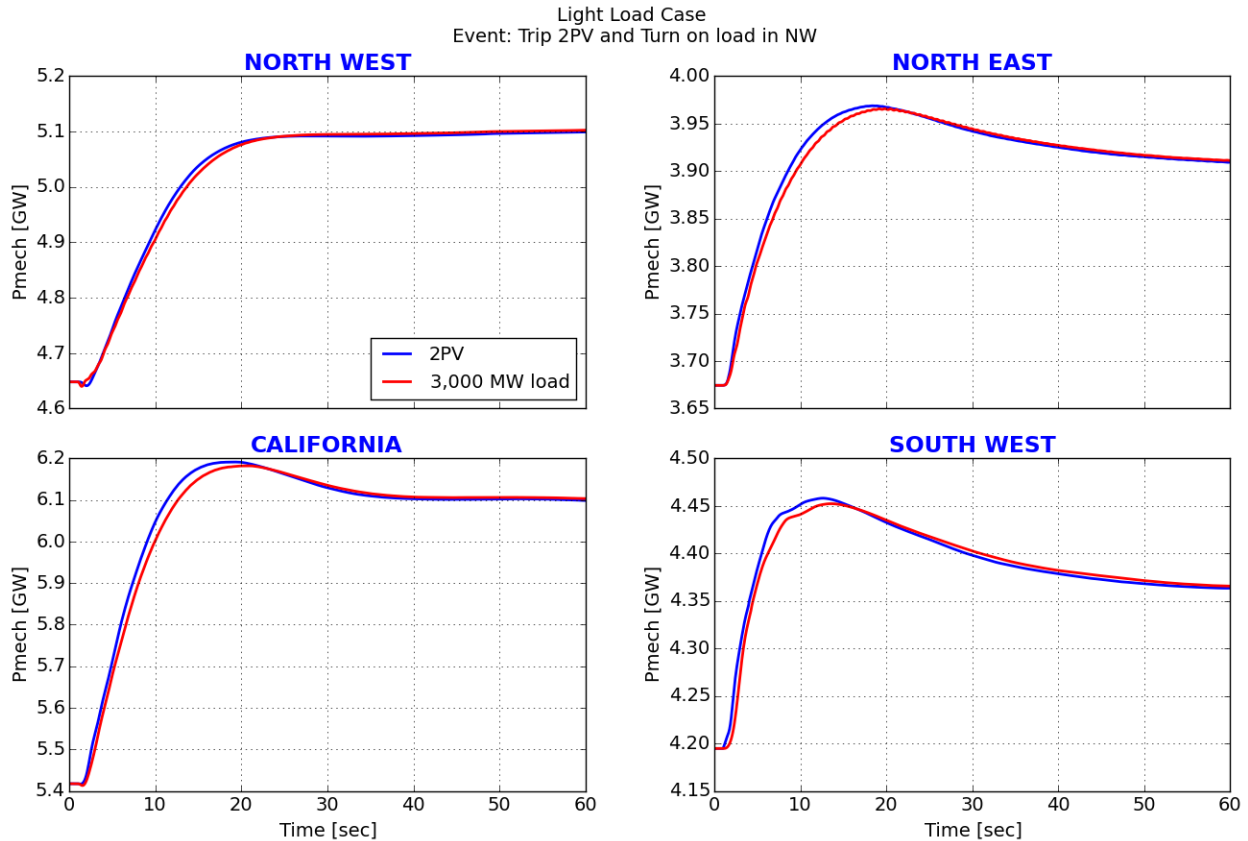


**Figure 44. Primary frequency response: loss of two Palo Verde units compared to 3,000 MW load increase in the Northwest**

Although the system-wide frequency response is broadly similar, the reasons why the Northwest required approximately 250 MW more load to get the same settling frequency as the Palo Verde generation loss in the Southwest are not immediately obvious. The aggregate regional governor responses between the two cases, shown in Figure 44, are similar and settle at almost the same level. This leaves loads and losses as the possible source of the difference.

The load model, described in Section 3.3, results in behavior that has a substantial dependence on voltage. The voltages in the Northwest are depressed by the Northwest event, as shown in Figure 45. The insert in the figure shows that the voltages for the Palo Verde event are largely unchanged. The depressed voltage results in load relief, making the event somewhat less severe for frequency response. This is consistent with other results shown from earlier WWSIS studies: the voltage impact on load is a significant consideration for frequency events, and it is often more important than the frequency sensitivity of the load model. Voltage response to big disturbances has a substantial locational dependence, and as such the location of an initiating frequency event will have some locational dependence from the load response.

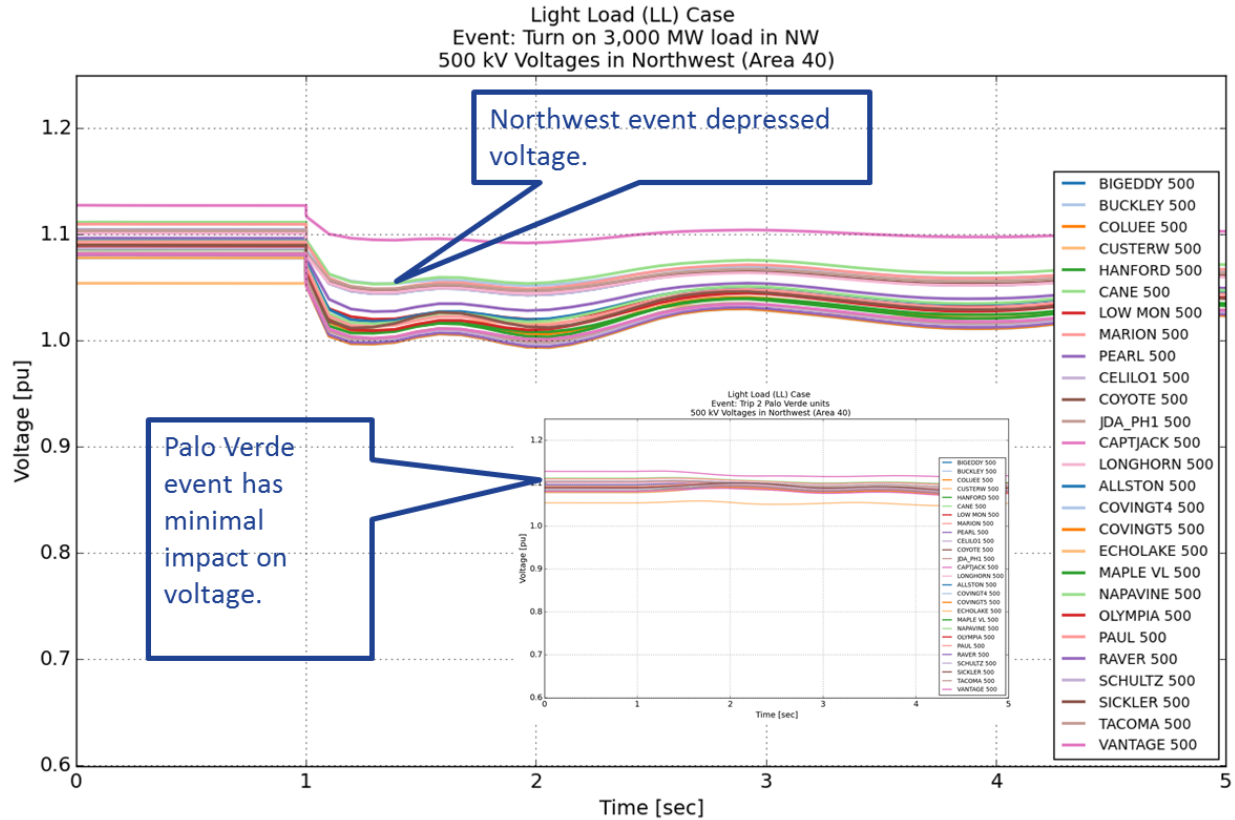


**Figure 45. Voltage: loss of two Palo Verde units compared to 3,000 MW load increase in the Northwest**

Another locational aspect is the ROCOF. As shown in Figure 42, proximity to the event is important. Figure 46 shows details of the regional frequencies for the two cases. The locational aspects dominate for approximately 2 seconds. Note, for example, how different the two events “look” in the Northwest and in the Southwest. Even though these are events of approximately the same magnitude, from a frequency perspective they look very different during the first 2 seconds. This represents an acute challenge for triggering control actions that are sensitive to initial frequency or ROCOF. This is an important point for system control and for frequency response design, which will be explored in more detail in Section 7.4.

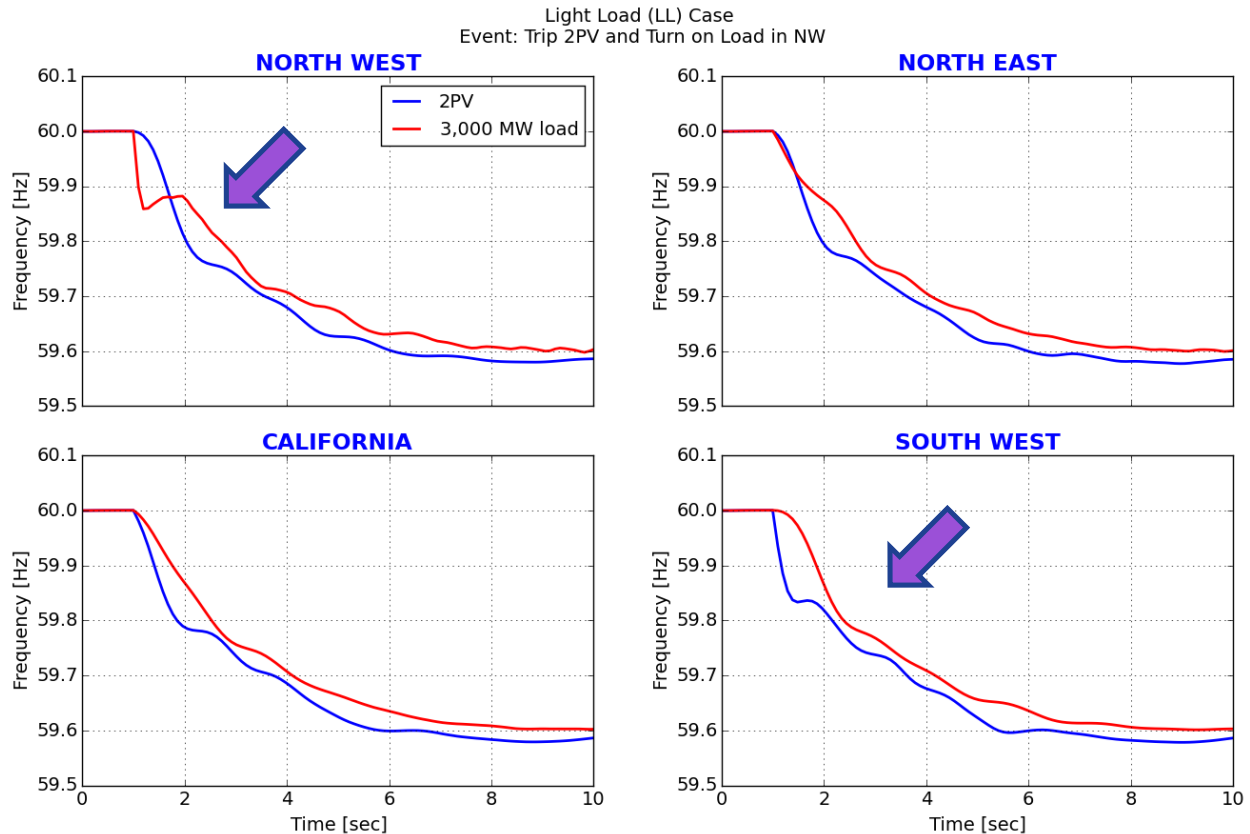


**Figure 46. Initial regional frequency decline: loss of two Palo Verde units compared to 3,000 MW load increase in the Northwest**

In summary of the locational aspects of frequency, in this section we have shown:

- Location has a significant impact on initial transient and measured frequency.
- Voltage impact on loads has a significant impact.
- Decisions based on local frequency to meet system-wide performance objectives should not be made too fast.

This last point will be examined further in Section 7.

## 6.5 Heavy Summer

### 6.5.1 Impact of Retirements and DC Upgrade

Figure 47 shows three traces. The blue trace is for the heavy summer high-mix case. The red trace shows the isolated impact of the PDCI upgrade on the high-mix case—the impact is minimal. The green trace is for the new heavy summer retirement case. The redispatch for this condition results in slightly better performance for the Palo Verde event, but the difference is small. Basically, the frequency response under heavy load conditions for this system is not very interesting. It might become so in a future with even higher levels of solar. For example, if solar continues to grow such that instantaneous solar penetration levels under high load levels are high, frequency response and some of the locational issues identified for the lighter load condition will likely be more challenging.

Heavy Summer (HS), Heavy Summer DC Upgrade (HS DCU) and Heavy Summer Retirement (HS RET) Case  
Event: Trip 2 Palo Verde units

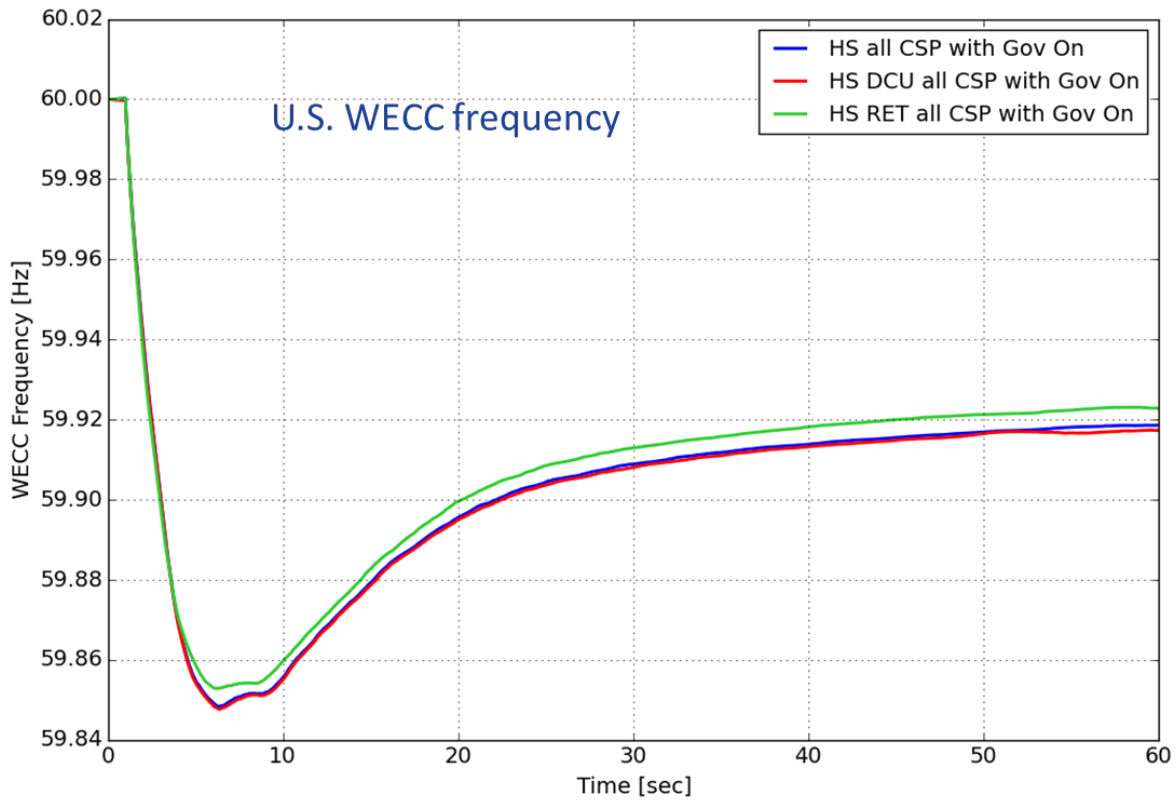
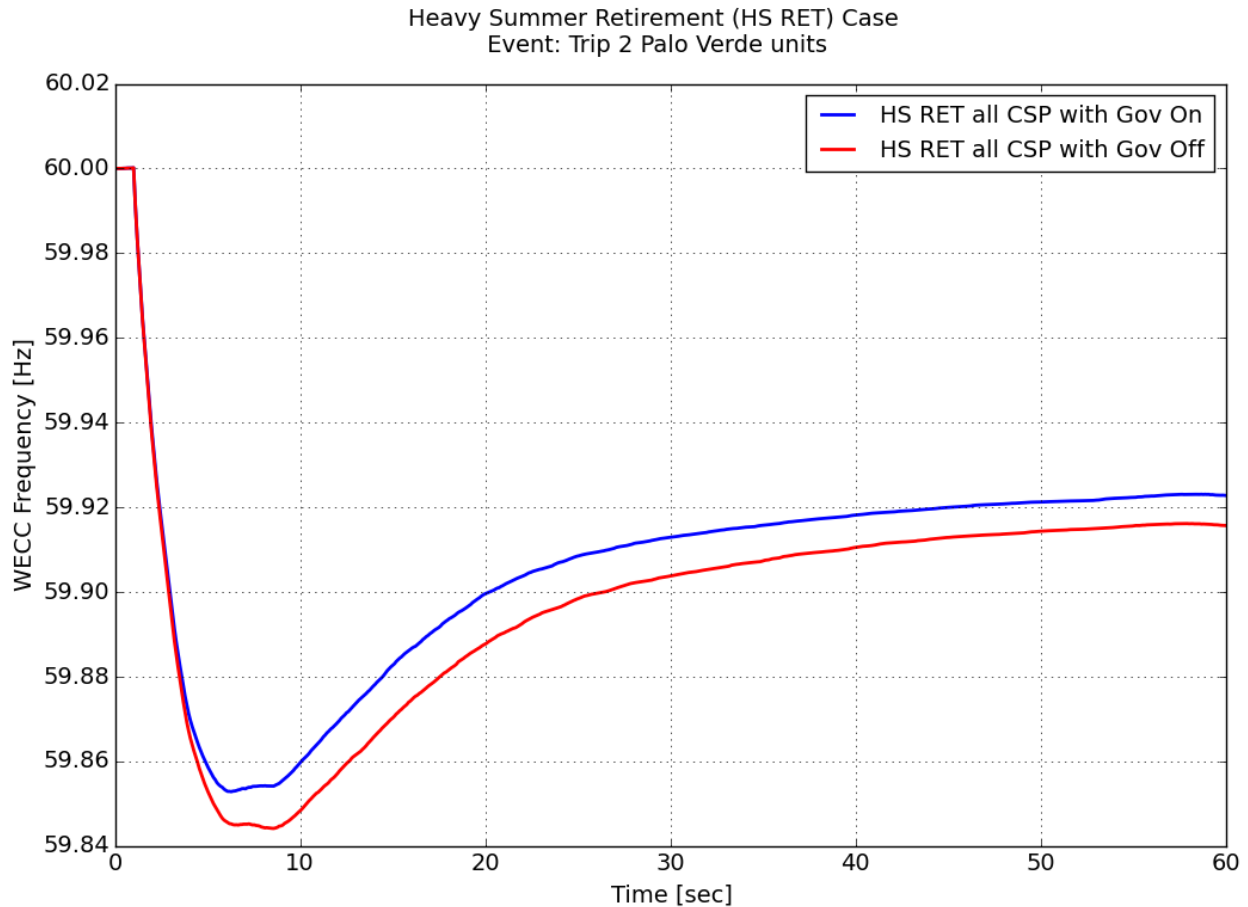


Figure 47. Heavy summer: impact of retirements and DC upgrade

### 6.5.2 Heavy Summer Impact of CSP Governors

The heavy summer cases have more generation committed to handle the higher loads. With more responsive units committed and higher inertia, the loss of Palo Verde is a relatively smaller event. The difference in performance when the CSP governors are turned on for the heavy summer retirement case is shown in Figure 48. Again, the CSP governors make a significant contribution to the system frequency response.



**Figure 48. Heavy summer retirement case: impact of CSP governors**

### 6.5.3 Localized Damping Concerns

During the development of the heavy summer retirement case, the dispatch of CSP generation was increased (per Table 1). Some locations in the desert areas are host to clusters of new CSP plants. One of the areas with several new plants in the study case is in western Nevada, with essentially radial transmission connection southward to the more fully developed grid to the north and east of Los Angeles. These plant sites were selected in WWSIS-2, based mainly on solar resource and location, and they are not individual proposed or actual plants. Nevertheless, they have realistic factors in their siting. The total dispatch from the multiple plants in the area identified in the right-hand side of Figure 49 was such that the plants in the area developed acute damping problems, as shown in the swings of the figure. This occurred even though the transmission had been strengthened sufficiently to avoid thermal problems in the study case. The poor damping was mitigated by the addition of power system stabilizers and reduction of exciter gains on the oscillating plants. Although these are not real plants, the incident is representative of a risk that is always present with radially connected synchronous plants. These damping problems can normally be remedied with appropriate control tuning, power system stabilizers, and other means. Because PV plants do not have moving parts, the risk of this type of instability is low with utility-scale PV.

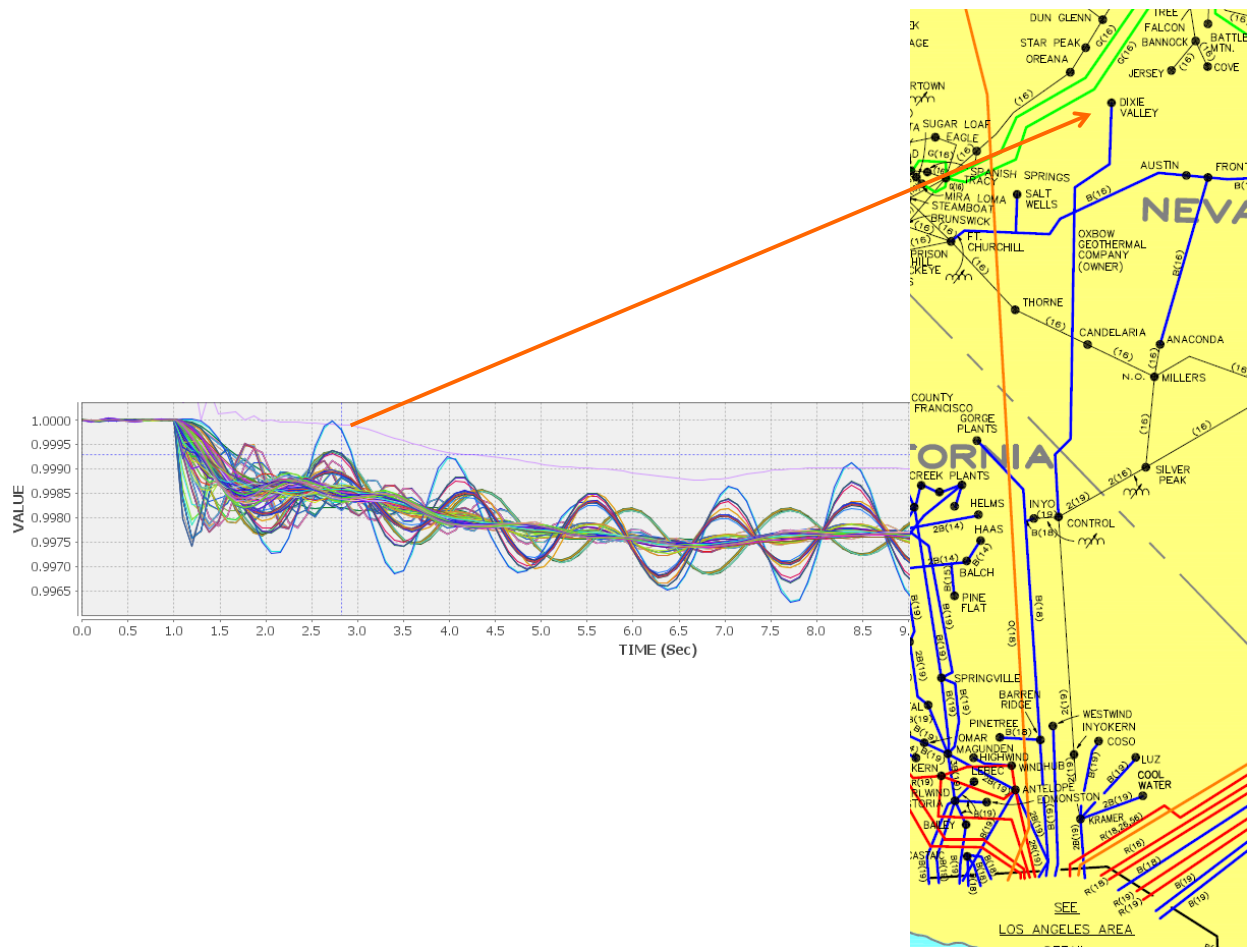


Figure 49. Illustration of local damping risk with CSP on long radial interconnection

## 6.6 North-South Separation Disturbance

Earlier work, particularly the frequency response investigation of WWSIS-3, showed that there is a tendency for a disproportionate amount of the system's frequency response to come from the Northwest under some high wind and solar dispatch conditions. That work did not identify any strong concerns about this shift in the location of responsive resources for the cases investigated.

All the cases in that work were limited to individual, usually design basis N-1, events. In this section, we examine a broader question of location. The Western Interconnection has on rare occasion separated, breaking into two or more parts (Aggarwal et al. 1997).

Historically, there have been separation remedial action schemes in the West that are designed to create a more orderly division between the North and South under extreme disturbance conditions. One of the intents of these schemes is to create large electrical islands that have a better chance of reaching a viable equilibrium post-disturbance. To look at the impact of the added variable renewables in this context, we created a North-South separation test event. In these cases, the system is split along the interface shown in Figure 50. The reader is cautioned that this is a simulation experiment, and it is not intended to replicate any specific, known separation or the actions of a specific remedial action scheme. Rather, we are interested in

examining the relative impact of having the location and amount of frequency response generation differ between scenarios.

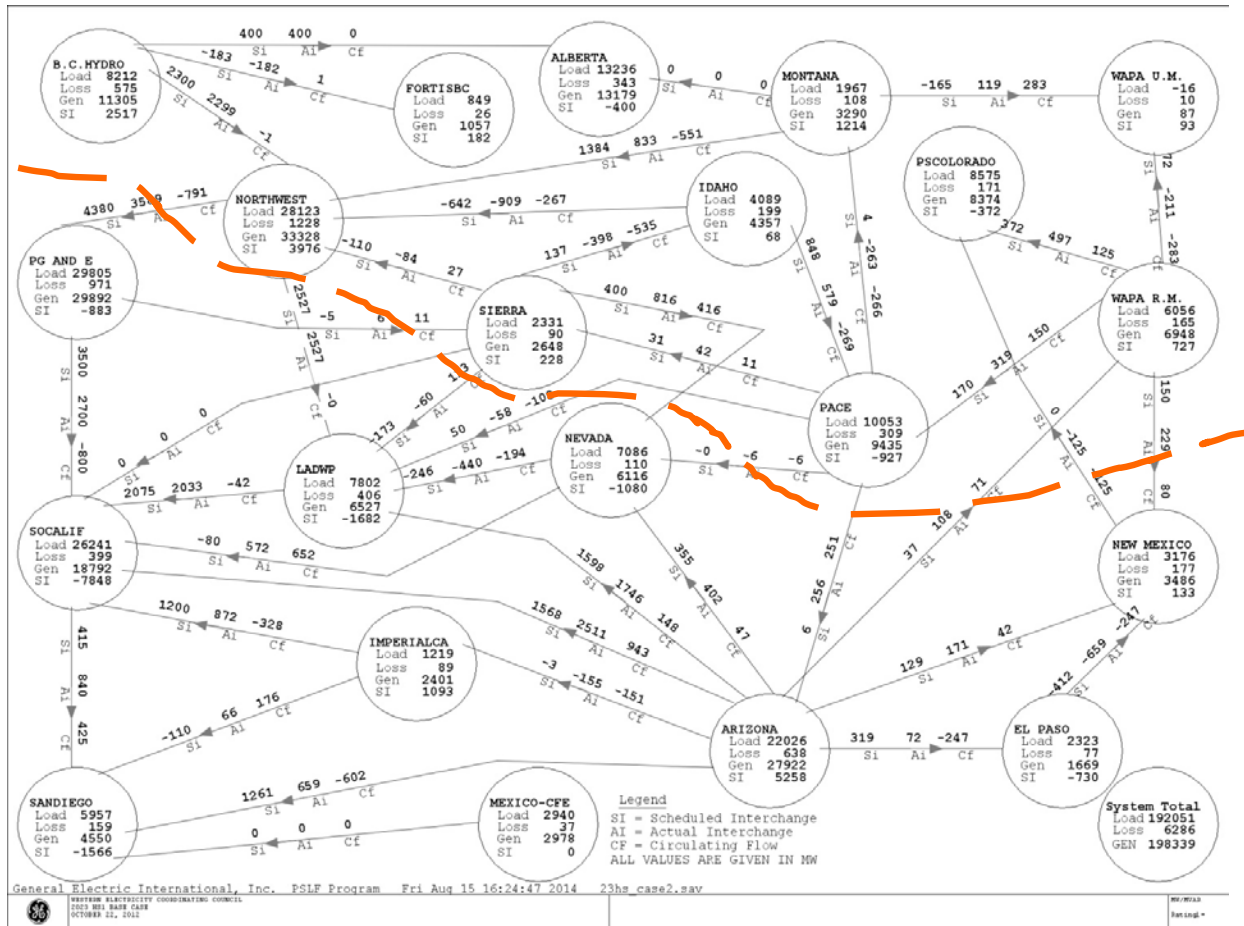


Figure 50. Illustrative North-South separation

### 6.6.1 Heavy Summer North-South Separation

The North-South separation disturbance under heavy summer load conditions, as modeled, is a severe event, resulting in system failure for all the cases tested. The difference in performance between the high-mix and the new retirement case is minimal. Figure 51 shows frequencies of the four regions. Note that, as expected, the two regions in the North, which are initially exporting to the South, experience a rise in frequency. The two regions in the South have a frequency drop. The two regions in the South remain connected as the frequency drops below 59.5 Hz approximately 1 second after the event starts. At this point, the simulation is not very meaningful because underfrequency load shedding, which is not modeled here, would begin to act. It is possible, although by no means ensured, that the southern island could reach a stable equilibrium. The system stress is such that the Southwest and California also exhibit voltage and flow dynamics that are indicative of separation. Flows on key lines are shown in Figure 52. The separation occurs approximately 0.8 second after the event (time 1.8 seconds in plots), with voltages in Southern California (shown in Figure 53) showing characteristics of separation. Note that relatively small differences in unit commitment can determine whether the system breaks up or not. Although the specific details of this simulation are not especially meaningful (e.g., we do

not have protective relaying modeled in sufficient detail to capture how the system would really unravel), the difference is notable. For this condition, the bulk system dynamics are highly sensitive to initial conditions, which can create a substantively different outcome.

From a planning perspective, this result suggests (and reinforces earlier results) that the performance of the remedial action scheme and other protective schemes needs to be carefully checked, and possibly updated, to address changes in system dynamics that are likely to occur with high levels of variable renewables in the West.

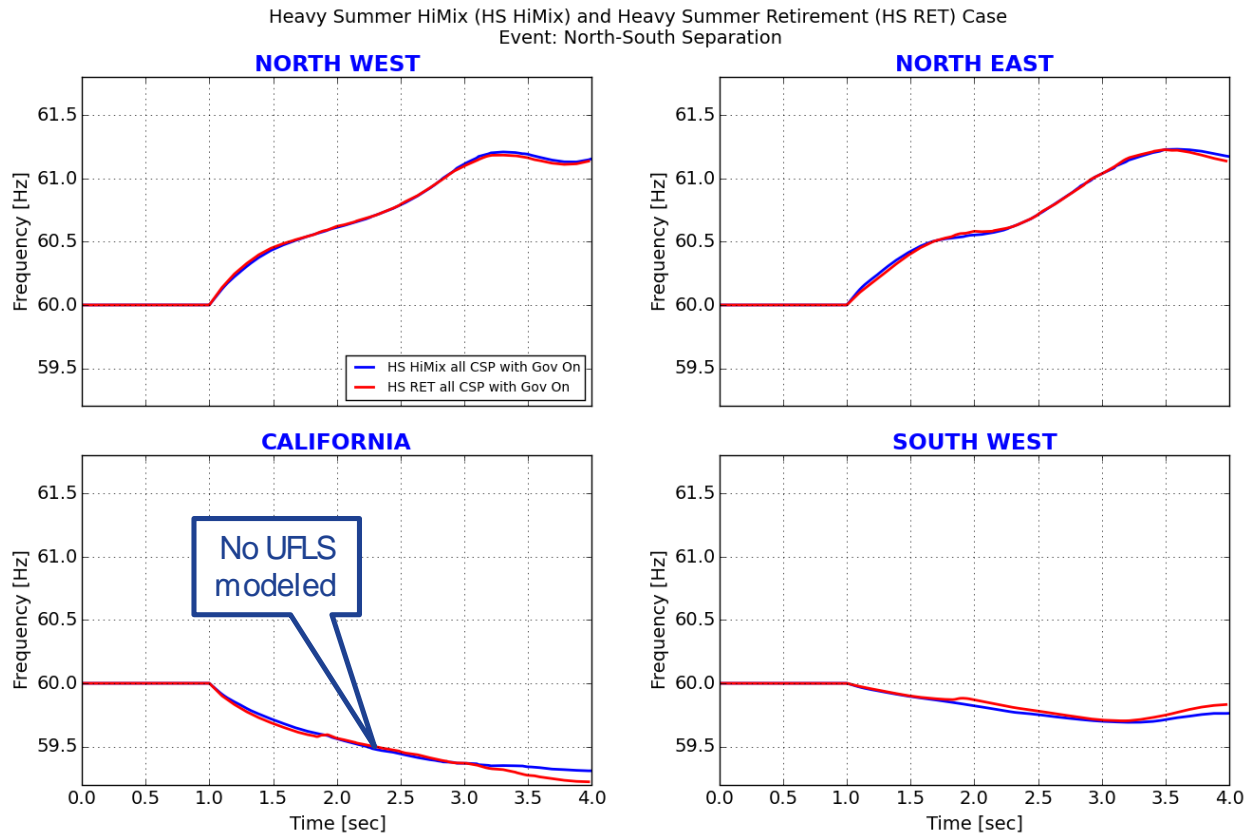


**Figure 51. Heavy summer: regional frequencies for North-South system separation**

Heavy Summer (HS) Retirement Case (CSP)  
Event: North-South Separation

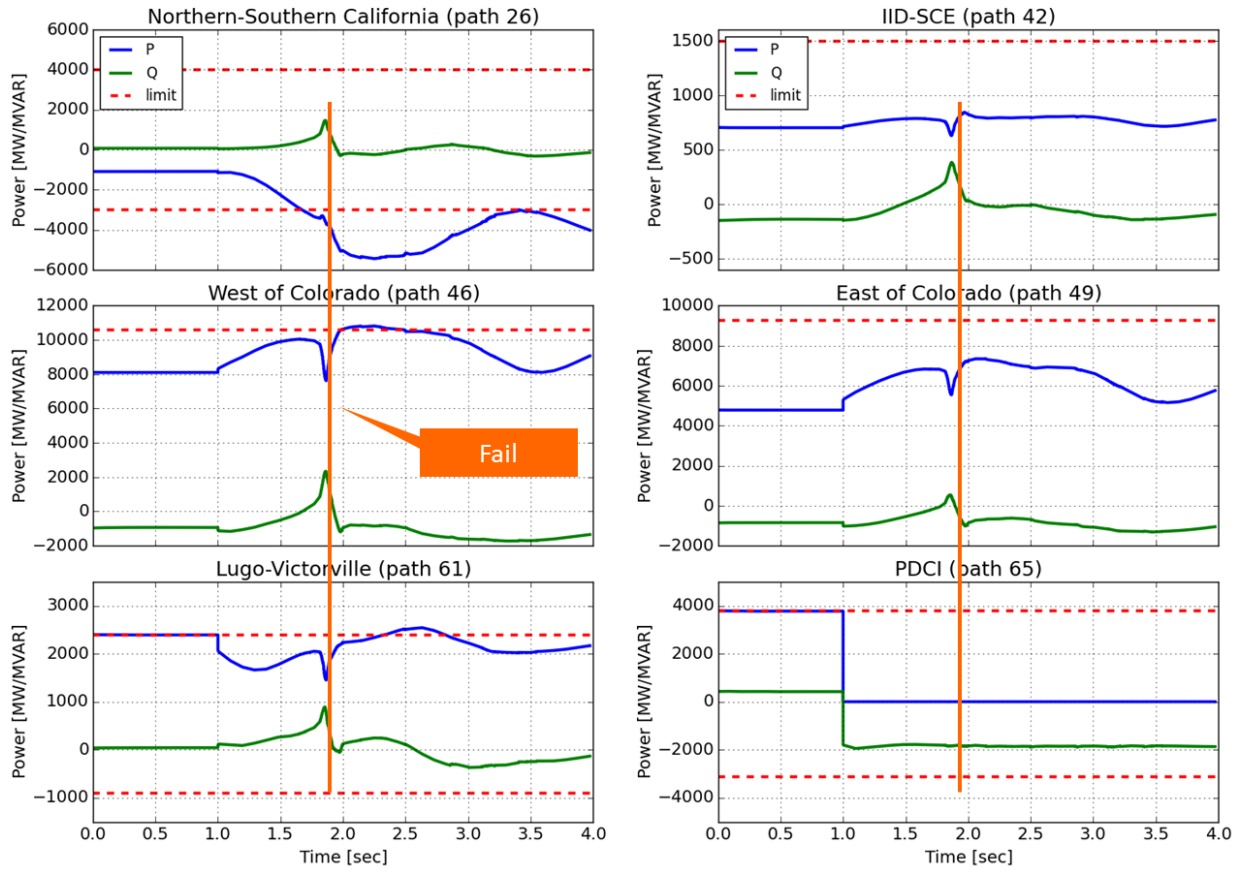
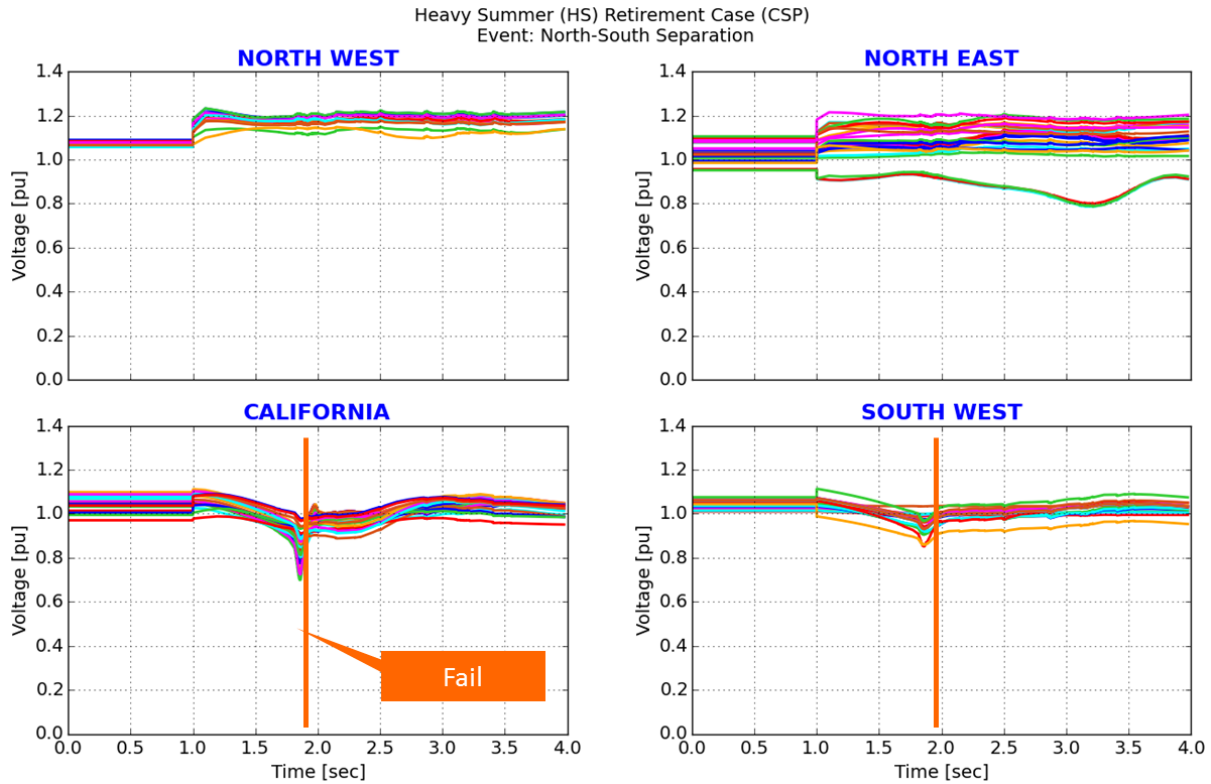


Figure 52. Heavy summer retirement case: North-South separation—key path flows



**Figure 53. Heavy summer retirement case: North-South separation—selected bus voltages**

### 6.6.2 Impact of PV Compared to CSP on Separation Dynamics

To test the effect of synchronous compared to inverter-based solar, we tried the CSP-to-PV sensitivity case for the heavy summer system as well. The system with PV also separated and failed in California. Note that the behavior was noticeably different. Figure 54 shows the reactive power output of the generators in the remaining southern half of the system. The case with PV fails a few hundred milliseconds later, and the reactive swings as the system separates look noticeably different.

The case reinforces that changes in generator technology will have some impact on the dynamics of the system under extreme conditions.

Heavy Summer (HS) Retirement Case  
Event: North-South Separation

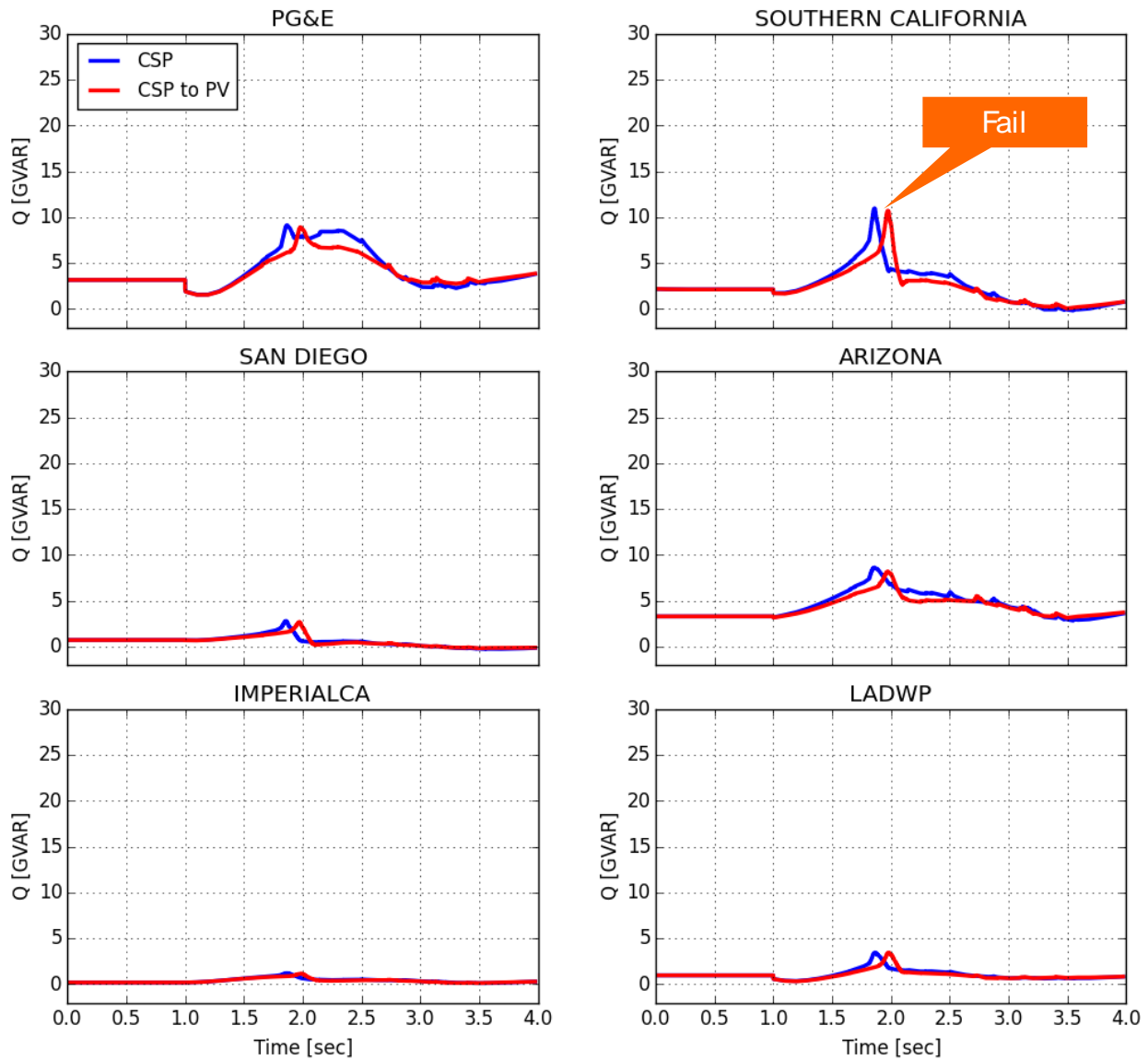
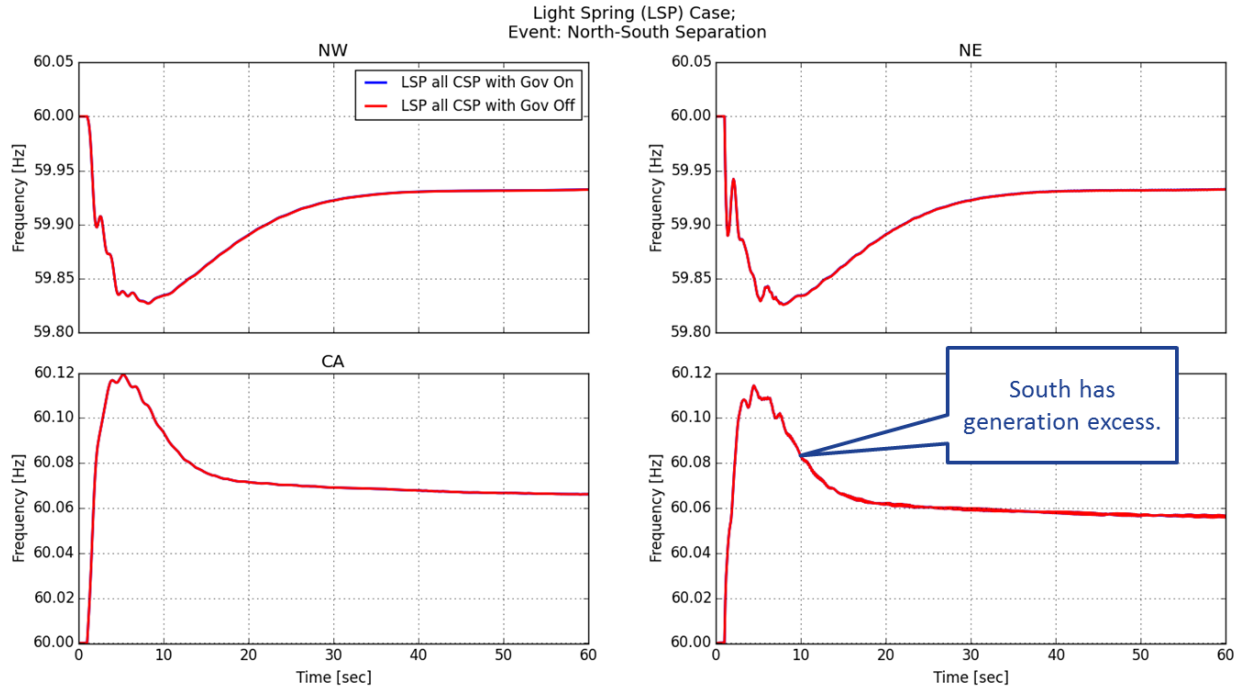


Figure 54. CSP compared to PV separation dynamics

### 6.6.3 Spring Lighter Load North-South Separation

In all the lighter load cases, the southern portion of the system exports excess generation to the North. This operating condition is radically different from the heavy summer case, and it has little resemblance to operating conditions observed in the West today.

Because the South has excess generation, the regional frequency swings following the North-South separation, as shown in Figure 55, are reversed. The frequency dip in the Northwest and Northeast is well handled by the responsive generation there, and the overfrequency in the South is also moderate. This suggests that, at least under conditions of high solar production, the separation of the Western Interconnection might be easier to tolerate.



**Figure 55. Lighter load spring case: North-South separation**

## 7 Fast Frequency Response and Enhanced PV Response

In this chapter, we examine new technology options for managing frequency, including those based on solar generation. Some aspects of the results are also applicable to a wider spectrum of inverter-based resources, particularly battery and other energy storage technologies.

### 7.1 Fast Frequency Response Discussion

Section 6.1 presented a discussion of frequency response and accompanying metrics of performance. It introduced the concept of *arresting power*. Historically, the early (pre-nadir) part of PFR from synchronous machine governors represented the vast majority of the arresting power.

Traditional systems relied on “spin,” of which a portion was fast enough to provide sufficient arresting power to avoid underfrequency load-shedding. As inertias have dropped, ROCOF has become steeper/greater, and the need for speed has increased (NERC 2012a). The traditional sources of PFR have become rarer, at least under some operating conditions with high penetrations of variable renewable generation.

These factors, combined with the possibility for fast-acting resources enabled by power electronics, creates an opportunity to reward the provision of arresting power by a new product: fast frequency response (FFR). In this construct, the sole benefit of FFR is to improve the frequency nadir—and avoid underfrequency load-shedding by delivering arresting power, i.e., injecting power in the time before the frequency nadir. Different technologies might provide other benefits beyond this narrow impact, but those aspects are not germane to this discussion.

The economic benefit of not depending solely on PFR can be significant, especially as ROCOF increases and inertia decreases. Generation that might be required solely to provide PFR and inertia might otherwise be economically decommitted. The options are increased, with success now being a function of three parameters: inertia, PFR, and FFR.

The Electric Reliability Council of Texas has led the industry in describing and quantifying the relationship between the three (Matevosyan 2015.). Many technologies have the potential to provide FFR (Miller et al. 2017).

### 7.2 Concepts for Transient Fast Frequency Response from PV

#### 7.2.1 Solar PV Components and Fast Frequency Response

PV has the potential for FFR capability to be designed into it. This is particularly true for utility-scale PV. In this section, we provide a detailed discussion of the fundamental concepts that allow PV to provide FFR.

The two most basic components of PV for the provision of AC power are common to all applications in power ratings ranging from a fraction of a watt to utility-scale projects approaching (or even exceeding) a gigawatt. The first component is a collection of photosensitive semiconductor cells that when subjected to photons of appropriate wavelength, produce energetic electrons that will flow, when allowed to do so—that is, they produce direct

voltage and current. The product of this DC voltage and current is power, which must be converted to 60-Hz AC power by the second component, the power inverters. PV installations consist of one or more of these modules, normally connected in parallel. For projects of utility-scale, AC collector systems resemble those of a wind power plant, with a supervisory control providing an intelligent interface between the grid and the plant.

For this discussion of possible FFR, a few physical elements of PV are critical:

1. DC power rating: Individual photocells typically have voltage ratings on the order of 2 V and current ratings very roughly proportional to the area of the cell. The details of voltage, rating, sensitive wavelength, temperature sensitivity, etc., vary with different cell designs and materials, and they are not particularly important here. The DC rating of the collection of cells (i.e., a “panel”) dedicated to a specific inverter is important. The DC rating (for this discussion) is the maximum DC power that can be produced under conditions of maximum insolation (sunlight energy intensity at the panel). DC rating is independent of the inverter.
2. AC power rating: The inverter serves the function of converting the DC power to AC. The cost of the inverter is dominated by the AC current rating, although the rating is typically given in kVA at nominal AC voltage. The key point is that there is no fundamental requirement that the rating of the inverter “match” the DC rating of the panel. In practice, this has significant implications for FFR, as will be discussed below.
3. Tracking: The orientation of the panel relative to the sun dictates how much of the available insolation energy is converted. In general, PV installations can be fixed, single-axis trackers, or dual-axis trackers. Tracking installations physically orient the panels so that they capture more energy during the course of a daily solar transit. For a given day and DC rating, the DC power available from the three types of tracking (for similar DC ratings) are conceptually shown in Figure 56.

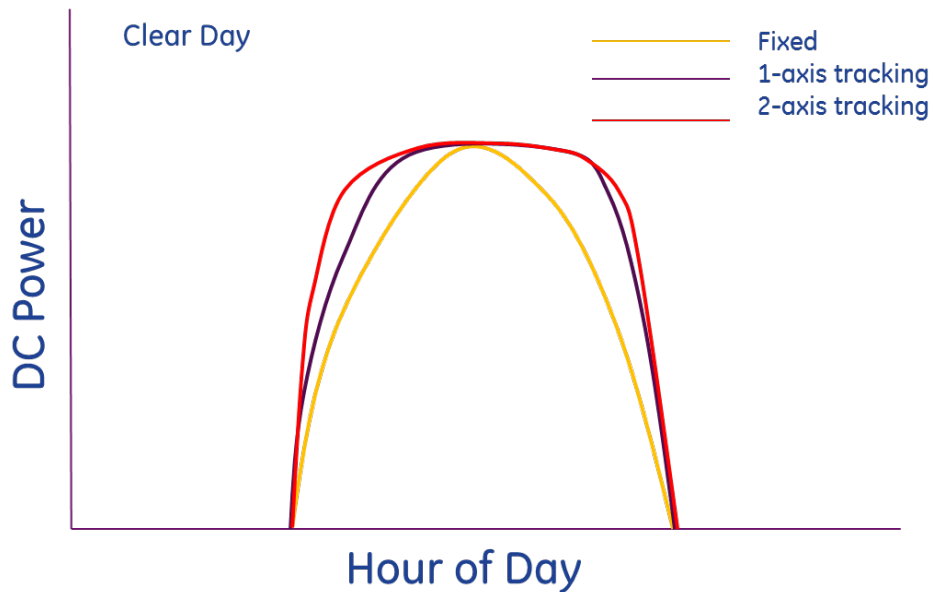


**Figure 56. Illustration of DC power impact of tracking**

4. Time of year: Shorter days and lower incidence angle affect the energy production. This seasonal variation has some importance, relative to the inverter rating, as will be discussed later.
5. Maximum power point tracking (MPPT) control: One of the functions of the inverter is to maintain the best DC voltage for the present condition by MPPT control. With MPPT the solar PV maintains the minimum of the maximum available DC power; maximum AC power, i.e., the inverter power limit; and power set point, i.e., a curtailment. The MPPT is normally a slower closed-loop control than the inverter current control loop and the supervisory voltage control loop. To maintain control stability between these controls, their speed of response is typically separated by an order of magnitude. Consequently, the MPPT control has a time constant on the order of a second.
6. Supervisory control: For utility-scale, transmission-connected PV installations (i.e., those that are most likely to be able to provide FFR), there is typically supervisory control that has many of the same functions as a wind power plant supervisory control. The supervisory control will accept curtailment (and other) instructions from the host utility and communicate them to the individual inverters for implementation. As in wind power plants, there are latencies in control and communications paths that limit how fast the supervisory control can transfer commands to the individual inverters. Again, similar to wind power plants, the industry has not yet been required to drive these latencies to very low levels.

### **7.2.2 Curtailment, Overload, and Fast Frequency Response**

Unlike wind, no inherent energy storage is available via kinetics (i.e., the rotating mass). Therefore, if a PV resource is to deliver any fast boost in power output, the inverter must be operating at an AC power transfer level that is *less than* the available DC power from the PV panel at that point in time (Kroposki et al. 2017). Under conditions when the AC inverter (and balance of plant) is not the limiting condition, this requires that the power production be curtailed

to a level less than the available power. This is a nearly perfect analog to the precurtailment of the wind power necessary to provide sustained FFR or PFR (Milligan et al. 2015).

The steady-state and short-term overload rating of the PV inverter can play an important role here. Although it is natural to think of the rating of the inverter in terms of kW, or kVA, the physical reality is that the rating is dominated by the current-carrying capability of the semiconductor valves. A simple illustration of the concept is shown in Figure 57. This figure is greatly simplified, but it captures the predominant character of the inverters not only for PV but also for Type 4 wind turbines and essentially all inverter-based energy storage devices. The figure is for a four-quadrant device: power can come in from the grid on the left hemisphere, which is only meaningful for energy storage and loads, and go out to the grid on the right; and it can provide reactive power to the grid (northern hemisphere) or consume it (southern hemisphere). A key point is that P (active power) and Q (reactive power) are controlled independently if the device is not at its limit. But when the combination of P and Q demand drives the operating point against the circle, the control must decide which takes priority. The issue is further complicated by the reality that these limits are actually current limits—the figure as labeled is meaningful for nominal terminal voltage. But when the voltage rises, the circles get bigger; and when it sags, the circles shrink. Finally, the outer circle, which represents overload capability, is a function of design and time. Depending on the inverter design, this overload capability might be very small and very short, i.e., a few percentage points of overload for fractions of seconds. But other designs might have more capability, either because of more robust design for other considerations or as a deliberate incremental capability for short-term overload.

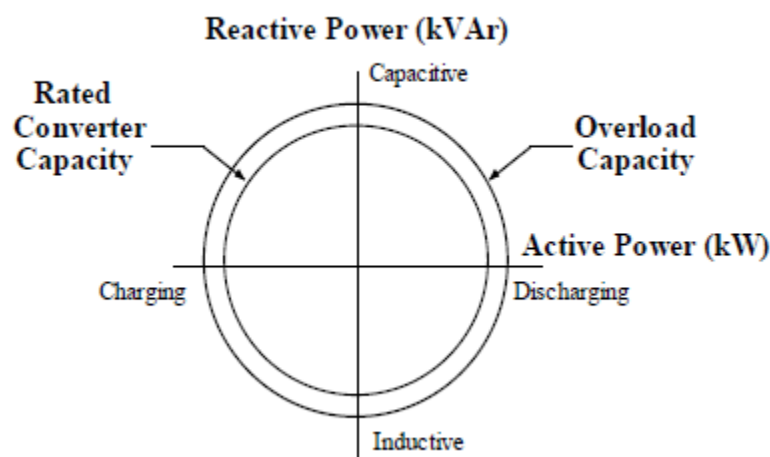


**Figure 57. Inverter rating concept**

Overall, this trade-off between active and reactive current capability and system voltage can be important for FFR. Two, not mutually exclusive, options exist:

1. Give active power priority over reactive power. This especially makes sense if the inverter is operating *underexcited* (i.e., consuming reactive power). It will raise the voltage, allowing more power to be delivered for a given current. Conversely, when the

inverter is supplying reactive power, reducing the VARs to make room for active power will decrease the voltage, increasing the current necessary to deliver the same active power. It will be systemically dependent, and it is possible that the voltage reduction will negate the benefit or create other systemic problems. These considerations are situational and will tend to be greater in weak grid situations.

2. Drive the inverter into the overload range. This must be done carefully and with knowledge of the design capability of the inverter. Considerations such as ambient temperature and predisturbance valve junction temperature might be important if squeezing out every bit of power is important.

These points only make sense if the inverter is limiting the delivery of active power. The inverter cannot cause the PV panel to make more power than the maximum allowed by the instantaneous insolation.

The interplay between these two options—the system requirements and the available DC power—can be rather confusing. Phasor diagrams help illuminate the relationships. Figure 58 shows the current for a normal operating condition (blue dot) in which the current limits of the inverter are not active. The blue phasor, shows active current ( $I_p$ ) being injected to the grid at a level of DC power (insolation), given by the vertical dotted blue line. The reactive current,  $I_q$ , in this quadrant is being injected into the grid to support voltage (presumably in response to required closed-loop voltage regulation). As long as the total current,  $I_{total}$ , is within the rating circle, the active and reactive injections are independently controllable.

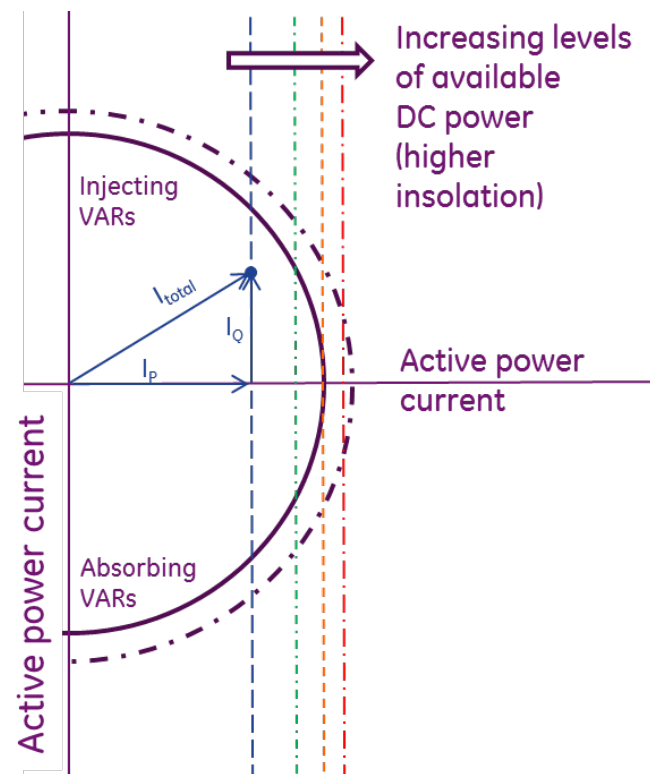
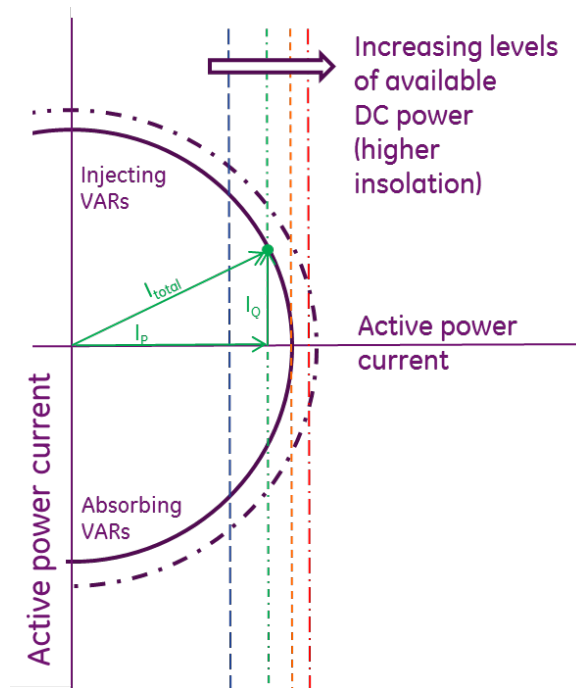


Figure 58. PV current phasor for normal operation

As available DC power increases, the operation moves toward the steady-state current limit. In Figure 59, the DC power is assumed to have increased to the green vertical dashed line, whereas the reactive current requirement remains the same. This new operating point, the green dot, represents operation at the steady-state current limits of the inverter. If the system reactive power demands (for  $I_Q$ ) and the available DC power ( $I_P$  at this voltage) together exceed the current rating, then the inverter must establish which function takes priority. If reactive support takes priority, which is typically the case up to the power factor required by interconnection requirements, then active power will be limited. Alternatively, reactive current can be reduced to make room for active current injection.



**Figure 59. Normal operation at steady-state current limits**

Giving priority to active power for high levels of insolation results in a reduction of reactive current injection. In the limit, the inverter could go to unity power factor without exceeding the steady-state current rating of the inverter.

Taking advantage of possible short-term overload rating of the inverter is illustrated by moving to the dashed circle in the phasor diagrams. The short-time overload rating circle can be time-, temperature-, and operating history-dependent. The two concepts, giving P priority and using short-term overload capability, can work together to provide control options for achieving FFR. Care is required in assigning these priorities. The stability work of WWSIS-3A showed that giving Q priority in weak exporting systems improves transient stability.

These current-rating and DC power relationships raise an interesting new option for FFR, as discussed in the next section.

### 7.2.3 Inverter and Panel Rating

Historically, the biggest cost component in PV systems was the semiconductor panel. Further, until recently, the overall cost of PV energy was considerably higher than from competing

generation resources. Consequently, the economics of PV design tended to strike a balance between using the absolute least-expensive components for the rest of the system (i.e., the balance-of-plant), including the inverter, and making sure that every unit of energy that the panels might produce would be delivered to the user (meter). Therefore, inverters were commonly rated to meet the maximum DC power of the panel. Further, the inverters were assumed to operate at unity power factor, thereby eliminating any extra current rating (and cost) associated with the delivery of reactive power.

Recently, two important changes have developed: the cost of panels has dropped precipitously, making the relative cost of inverters in the overall system much larger, and grid authorities are demanding (through grid codes, etc.) that PV provide voltage support and have reactive power capability (FERC 2005).

These factors drive different design decisions that are important for this discussion of FFR capability. Specifically, it is becoming common for the steady-state active power rating of the inverters to be less than the maximum DC power of the panels to which they are matched. The concept is illustrated in Figure 60. This concept presents an almost exact parallel to the “solar multiple” for CSP thermal plants (Jorgenson, Mehos, and Denholm 2014). That metric gives the ratio of the solar field rating to the power island rating.

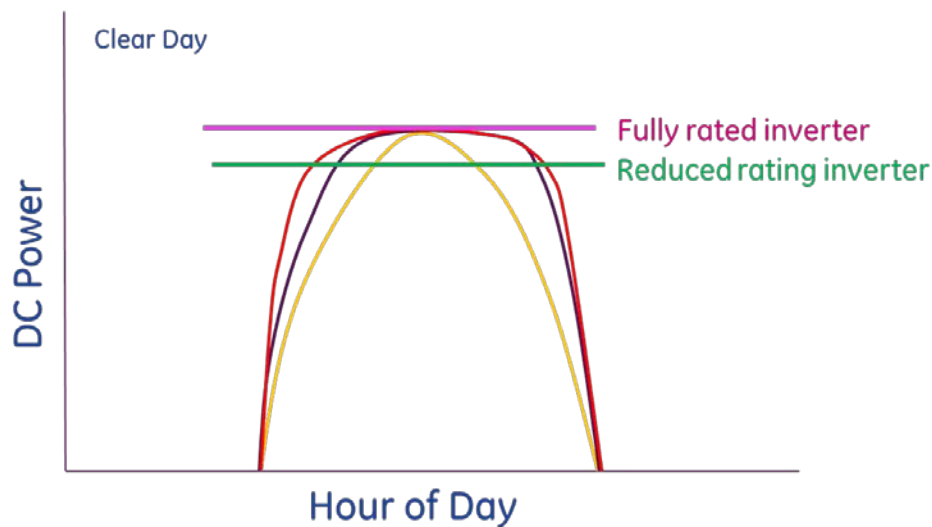


**Figure 60. DC power (different trackers) compared to AC inverter rating**

The implication of this rating difference for the provision of FFR is potentially profound. If the underrated inverter is designed to have a degree of short-term overload and/or the inverter is given active power priority over reactive power delivery, then there is extra active power available for delivery to the grid. The concept is illustrated in Figure 61.

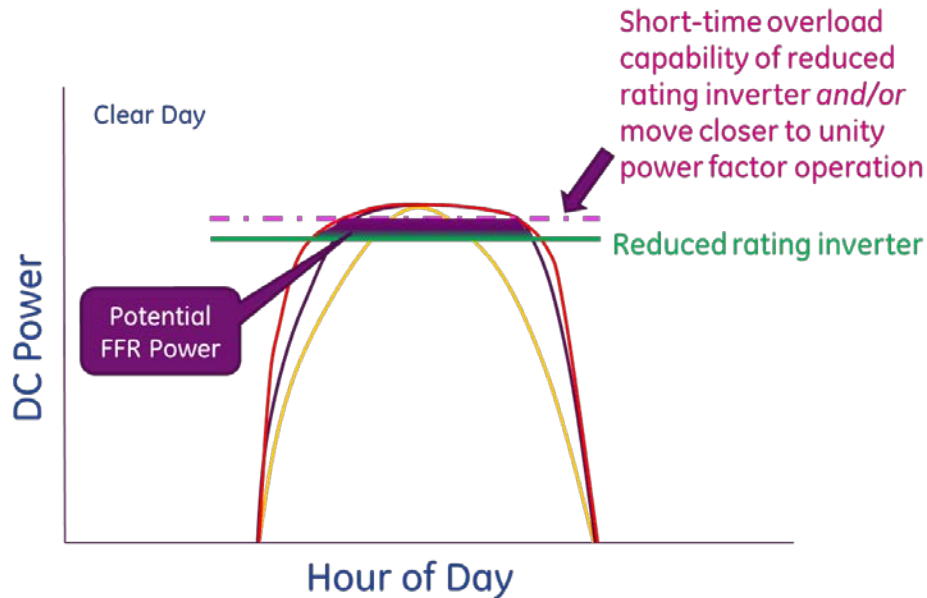


**Figure 61. Fast frequency response capability for reduced-rating PV inverters**

This means that during any period in which the insolation exceeds the steady-state capability of the inverter, there will be essentially zero opportunity cost to the PV plant to provide FFR up to the short-time limit of the inverter and the instantaneous insolation. The owner of the PV will incur capital costs to have this capability. Further, this is new ground. There is not, at this writing, industry precedence for this approach.

#### **7.2.4 Fast Frequency Response Control**

The use of FFR, in the form of devices that can deliver a burst of arresting energy to the grid, is relatively new ground for the power industry. There is little experience in designing control systems to take the best advantage of these new technologies. In broad terms, there are two classes of controls: closed-loop controls and open-loop “triggered” controls.

Closed-loop controls are based on continuous measurements, usually of bus frequency, that are processed through transfer functions, resulting in continuously varying output, i.e., varying incremental active power injection. Open-loop controls are one way in character. That is, once certain criteria are met, the device “triggers” and provides a preprogrammed injection of active power. This can be as simple as a step up to an equipment (and insolation) maximum in response to frequency dropping below a triggering set point. This is a simple and seemingly attractive option. But substantial care is needed to avoid misbehavior, especially false triggers, i.e., having FFR actuated when it is not needed or wanted. Measuring frequency is conceptually simple, but in practice good measurements require at least a few cycles of fundamental frequency. So reliable triggering faster than approximately 50 ms based solely on local frequency measurements is difficult. Further, the locational aspects examined in Section 6.4 make the decision to trigger based on local frequency measurements difficult, and potentially unrobust.

In the following sections, we investigate some fundamental concepts aimed at improving understanding of the relationships between the timing, amplitude, and location of FFR for the purpose of improving frequency nadir.

### **7.3 Generalized Fast Frequency Response: Energy Impulse**

In this section, we consider a generalized FFR in which a pulse of energy is injected into the system to help arrest the frequency decline. Why “generalized” FFR? The natural assumption is that “faster is better,” i.e., the sooner into a frequency event that arresting power can be injected into the system, the better the outcome. But there are penalties for acting too fast (e.g., inability to confidently trigger using local frequency measurements).

In the following two sections, we explore questions of “what behaviors produce the best outcomes?” and “how does one make a fair comparison in the reliability value of resources with very different behavior characteristics in their abilities to maintain system security?” The concepts and results present a broader framework for characterizing the quantitative impact on system security, particularly frequency nadir, for any resource that contributes arresting power. The intent is to allow an “apples-to-apples” comparison between resources, so that compensation, via markets or other means, can:

- Reward the behavior that best meets the reliability need.
- Allow the broadest participation by resources that can contribute.
- Ensure that the right amount of resources is procured.
- Pay fairly for the benefits delivered.

In the following sequence, we present a construct for the evaluation of FFR. A sequence of tests is conducted in which a 1,000-MW, 500-ms “block” of idealized FFR energy is injected at successive 0.5-second intervals (the total energy injected is therefore 500 MJ). The point of injection is in the middle of California at the Vincent 500-kV substation. The concept is illustrated on the heavy summer retirement case in Figure 62, with the baseline shown as the blue trace, and one perturbation. The baseline is our Western Interconnection case, subject to the design basis event (trip of the Palo Verde Nuclear Generating Station). The perturbation is the red trace, in which the energy pulse starts 3 seconds after the event starts and ends after another 0.5 second (500 ms).

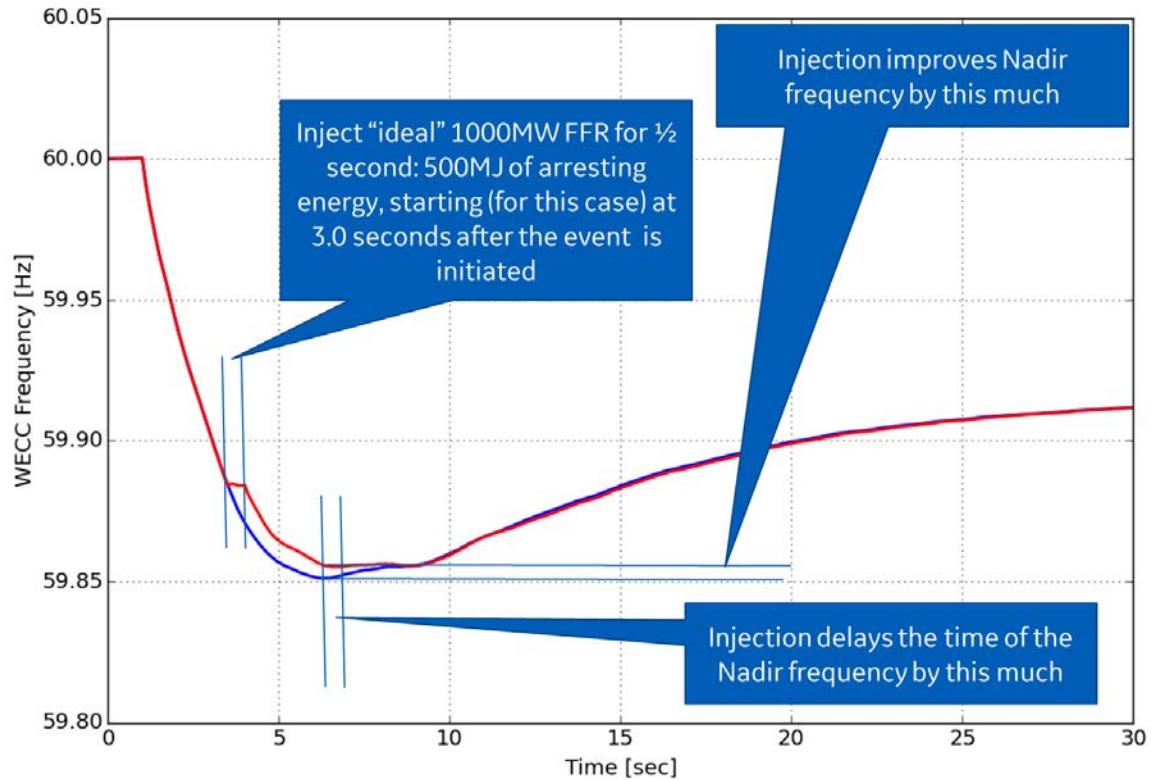


**Figure 62. Generic fast frequency response calibration simulations**

The added FFR arresting energy improves the frequency nadir and delays the time at which the nadir occurs. This occurs, to differing degrees, for each interval up to the time of the nadir. Obviously, FFR injections that occur after the nadir have no benefit. A composite of all the cases run in a sequence up to 10 seconds into the event is shown in Figure 63. The sequence of cases results in differing impact on the frequency nadir even though the arresting power and energy are the same for each perturbation.

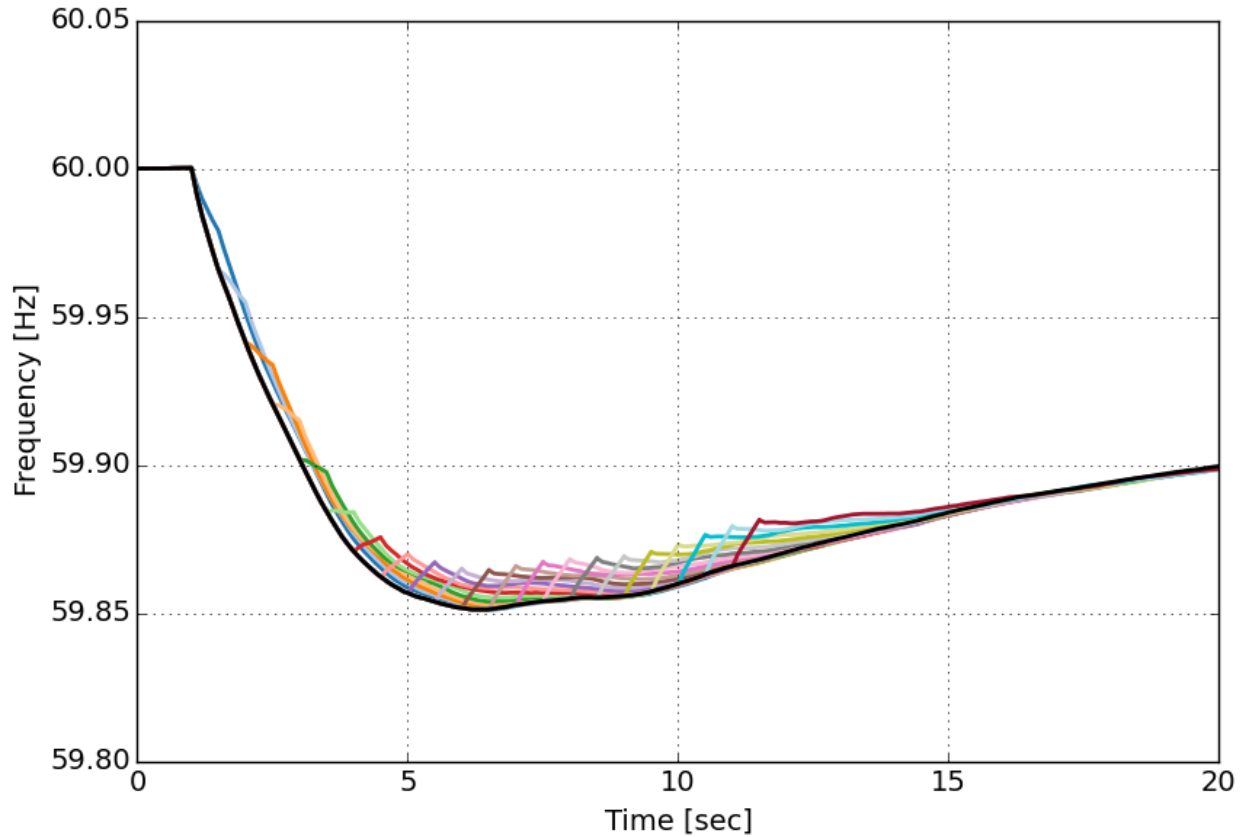


**Figure 63. Sweep of fast frequency response impulses**

The same exercise was done on the lighter load case, which is more limiting (i.e., has a lower frequency nadir). The results are qualitatively similar, which reinforces the generality of the approach. The change in nadir vs. the timing of the arresting energy pulse is shown in Figure 64.

Light Load Case with FFR of 1,000 MW at Vincent 500 kV (turn on/off)  
Event: Trip 2 Palo Verde units and FFR

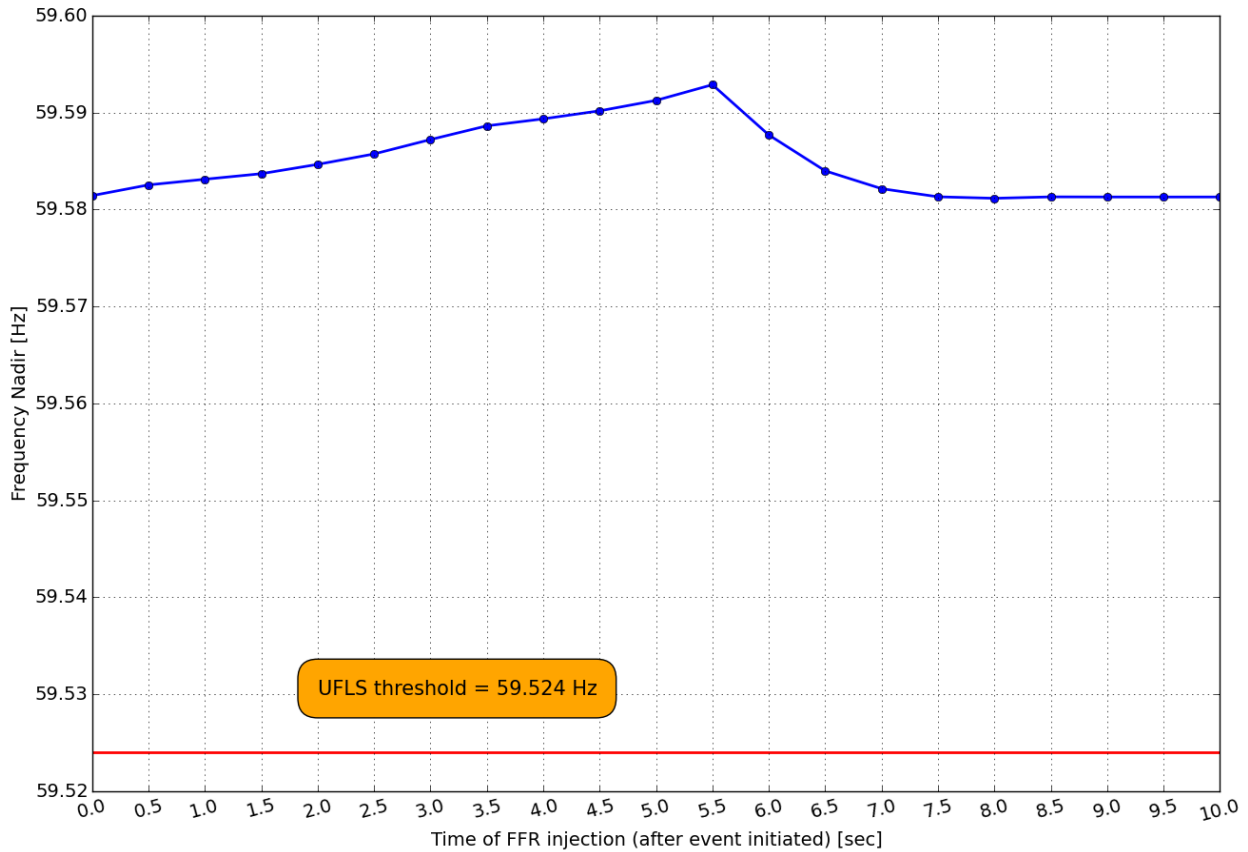


**Figure 64. Nadir improvement compared to timing of arresting power injection**

Note that injection of arresting energy later in the event has much higher efficacy at improving the nadir compared to injection that occurs immediately after the event starts. The efficacy reaches a relative maximum at about 5.5 seconds. This is because of the dynamic interaction of the FFR with the PFR. By allowing a more severe initial ROCOF, the PFR controls act more aggressively and produce better outcomes. The more aggressive response is because the speed governor, which is upstream in the control stream, sees a larger error sooner with higher ROCOF. The downstream turbine controls (e.g., the valve actuators on a steam turbine) “see” a larger signal sooner, and act—working through the relatively slower time constants of the turbines. In general, these “physical” time constants, those associated with moving valves, increase steam or fuel flow, are characteristics of the equipment and cannot be changed by simple control adjustments.

The efficacy tends to roll off as the nadir approaches partly because there is less scope for improvement as the frequency approaches the nadir. In this case, injections up to a few seconds before the nadir (at about 8.0 seconds) are more effective. The authors have tested this approach on other systems and have found this trend. Broadly, we have seen that systems with frequency nadirs occurring several seconds after the event have the best efficacy approximately 1 second

before the frequency nadir. The behavior for a system with very fast nadirs will have different quantitative results.

This might all seem rather convoluted, but the implications for most large systems are significant: very fast response is not necessary, and taking time to make good decisions about the deployment of FFR is not only desirable from a robustness perspective but also more effectively uses FFR resources with finite energy.

## **7.4 Generalized Fast Frequency Response: Sustained Response**

In this subsection, we look at the more common case of devices with sufficient rating to maintain power injection once initiated for the duration of the frequency event (i.e., at least until secondary frequency control kicks in).

Figure 65 shows the reference Palo Verde event (loss of approximately 2,750 MW) with two FFR injections. Both injections start 3 seconds into the event, and they are sustained, i.e., they continue to inject power for the duration of the simulations. The red trace is for 1,000 MW of FFR, and the blue is for 250 MW. An injection of 1,000 MW is sufficient to completely arrest the frequency decline and reverse it. Consequently, the frequency nadir occurs at the time of the FFR injection. From the perspective of understanding the efficacy of the FFR with time, this is too much power – that is, once the frequency decline is stopped by injection of the FFR, the time of the injection defines the nadir. Thus, the FFR has, in a sense, saturated. We look further at the amplitude later. But for 250 MW of FFR, the impact on the downward frequency trajectory is apparent, and the FFR clearly has a beneficial impact on the nadir.

Light Load (LL) Case with FFR  
Event: Event: Trip 2 Palo Verde units

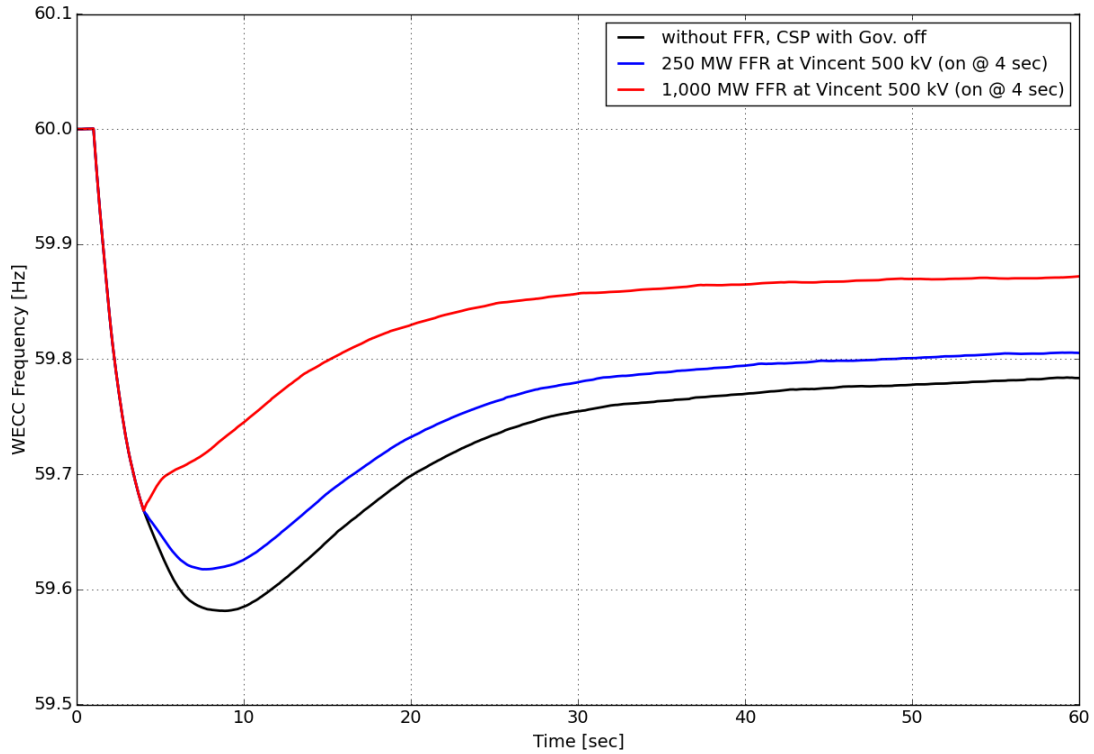


**Figure 65. Sustained fast frequency response: two different amplitudes**

Figure 66 shows the 250-MW FFR with a sweep similar to the impulse FFR in Figure 63. The sustained FFRs for each case are turned on 0.5-second intervals after the event begins.

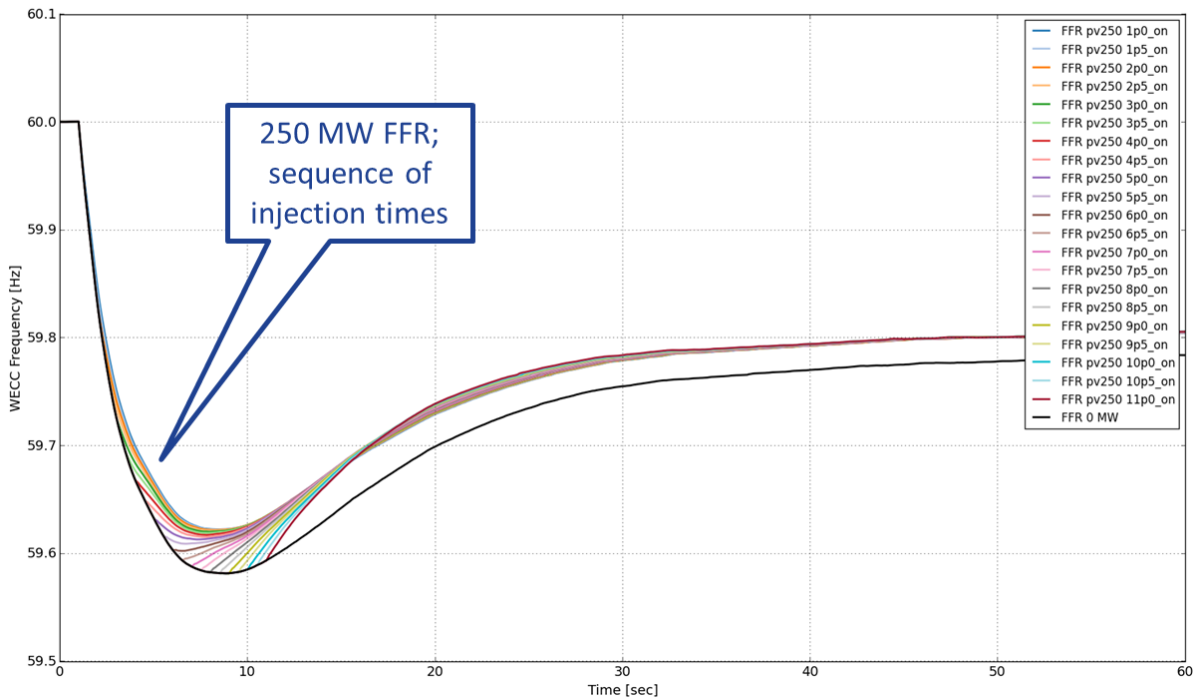


**Figure 66. A 250-MW fast frequency response at Vincent 500 kV: varied trigger timing**

Figure 67 shows the total results of this sweep (in blue), giving the impact on the nadir as a function of timing. This is an important result: the efficacy of the FFR is almost the same for deployments during the first 3 seconds of the event. That means that there is little systemic benefit in applying the FFR with undue haste. Waiting for good information with which to make the decision to “trigger” the FFR has a small performance penalty and might produce significant robustness benefits.

The second trace, in green, presents the same results except for the system where the CSP governors have been enabled. Note that the performance is similar. The overall curve is better (higher) because of the CSP governor contribution, but otherwise the impact is very similar. This is another significant result in that for a given operating condition, the beneficial contributions of multiple mitigations (in this case CSP governors plus FFR) are complementary and quite linear (they add up). This is not to say that the impacts are linear or uniform across very different operating conditions.

Light Load Case with FFR of 250 MW distributed at PVTERM (turn on)  
Event: Trip 2PV and FFR

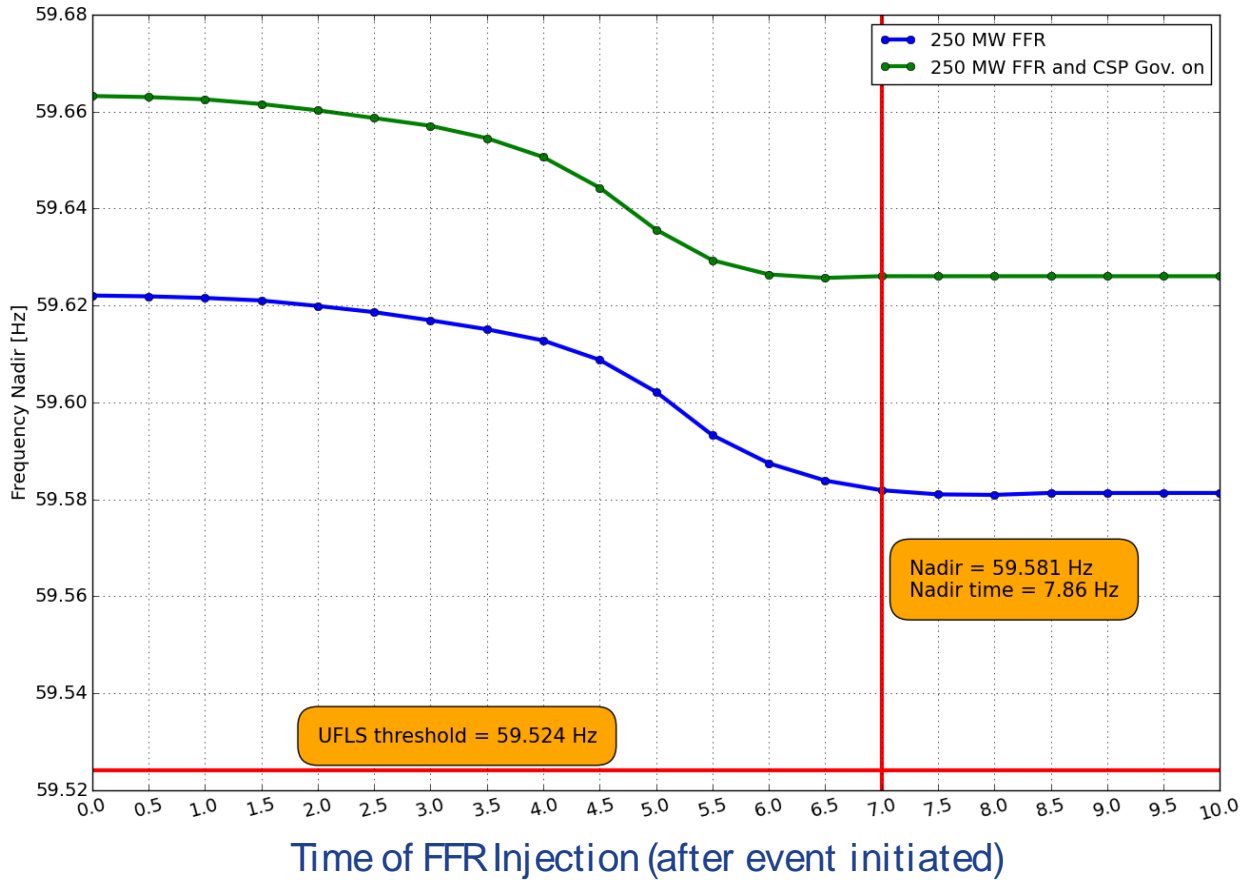


Figure 67. Timing and efficacy of 250-MW sustained fast frequency response

#### 7.4.1 Linearity of Fast Frequency Response Impacts

In this section, we present a deeper look at the behavior observed between the two cases in Figure 65. In that figure, the large (1,000-MW) FFR reversed the frequency decline, and the 250-MW significantly changed the trajectory and the nadir. In Figure 68, a sweep of FFR amplitudes is shown. Some caution is needed to read the figure. First, the amplitude of the FFR is decreasing from 1,000 MW from left to right, and, second, the spacing of the frequency steps is in two blocks, with steps of 250 MW down to 250 MW, then in steps of 50 MW down to -200 MW. For illumination, we have continued the exercise into the negative range. This would mean that extra power was withdrawn. Obviously, that is not something that would be intentional, but the exercise is interesting in that even down to zero and below the impact is relatively linear in the range from 250 MW to -200 MW. The “gain” of the system for the FFR injection now is given in the callout at 120  $\mu\text{Hz}/\text{MW}$  of FFR—i.e., 0.00012 Hz/MW, or, conversely, 830 MW, is required to improve the nadir by 0.1 Hz. This has similar units to that of FRO, but it is a measure of the efficacy of the FFR, not the PFR being measured for compliance with the FRO.

But as the FFR increases even further, the efficacy on improving the nadir declines. Between 250 and 500 MW, the “gain” is approximately 15  $\mu\text{Hz}/\text{MW}$  of FFR. Further, the curve is flat down to 500 MW. That means that any FFR greater than 500 MW immediately reverses the frequency

decline, and the nadir is at the time of the injection. In the narrow context of arresting frequency and improving nadir, anything greater than 500 MW is wasted here. This gives an interesting perspective: the event is approximately 2,750 MW, but more than 500 MW of FFR produces no additional benefit for this specific operating condition. The FFR works *as always* with the PFR from the committed generation that has active governors and headroom to act. The FFR does not impact the system in isolation, and the combination of the FFR and the amount and speed of PFR dictates the MW level of this inflection point.

Note that as (1) system inertia drops, (2) PFR becomes slower or scarcer, and the (3) ROCOF increases, this inflection point becomes a larger fraction of the size (in MW) of the event. The authors have observed this in smaller, lighter systems. In the limit—for example, as a system approaches no inertia—the breakpoint becomes equal to the size of the disturbance. That is, the FFR must fully, exactly, and quickly match the size of the disturbance to meet the frequency performance objective. The system under consideration in this study is far from that point.

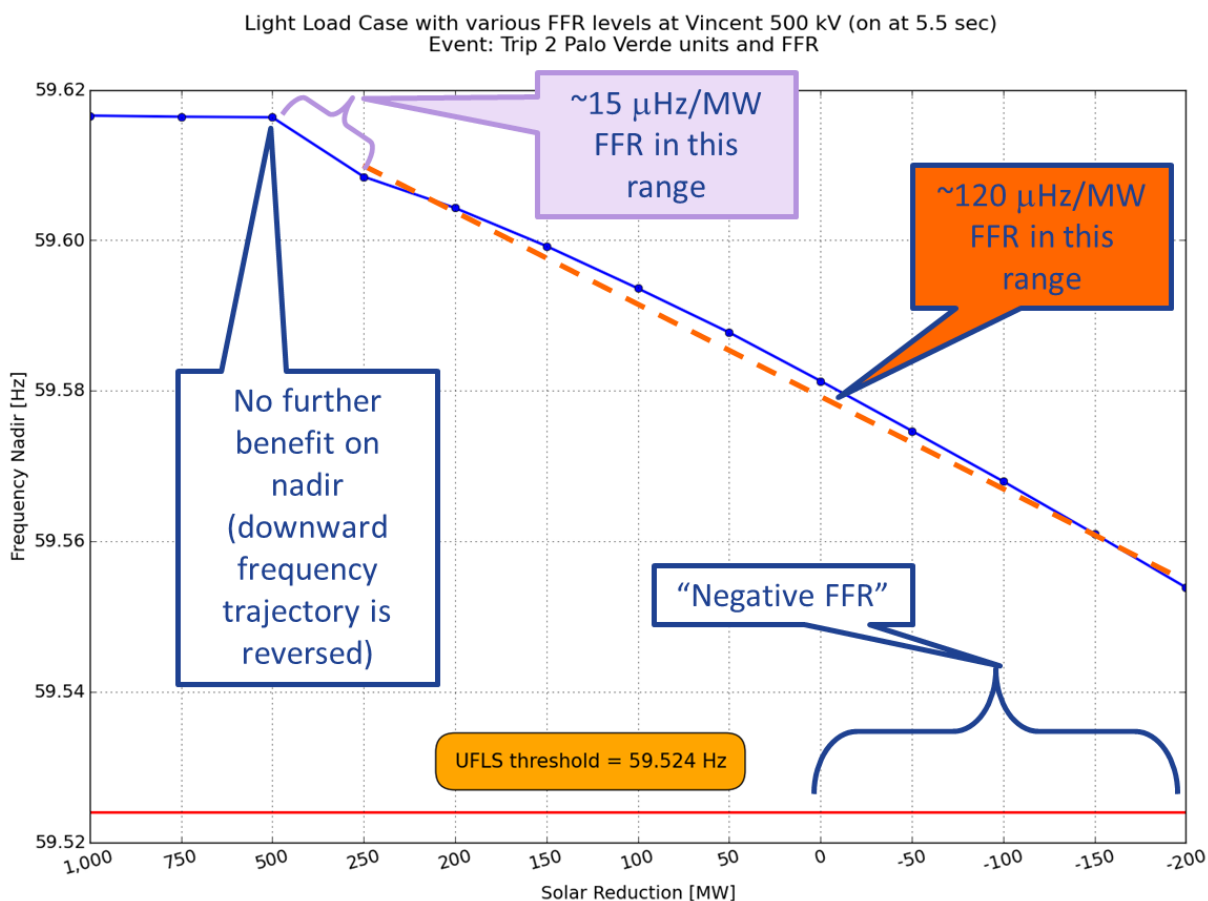


**Figure 68. Impact of sustained fast frequency response magnitude**

### 7.4.2 Locational Aspects of Fast Frequency Response

The results presented in Section 6.4 showed that the location of the disturbance on the system makes a difference in the system response, particularly during the first 1 to 2 seconds. Here we look at the locational aspect of the FFR.

In Figure 69, there are five cases shown. They compare the performance for a single large FFR device, injecting arresting power at a single node (Vincent 500 kV) with the behavior of the system when FFR is provided by *all* the utility-scale PV throughout the West. The incremental MW from each utility-scale PV plant is made in proportion to its output for a total across the entire system equal to the amount from the single FFR device. In the figure, the red and blue traces represent the response to 250 MW of FFR, and the green and yellow traces represent 1,000 MW. The results for the pairs are essentially identical. That means that the primary benefits of the arresting power injection in terms of influencing the common-mode “system” frequency are not particularly location dependent. Although the location of the FFR injection might impact swing modes, having the injection spread geographically *can* result in the same overall performance benefit.

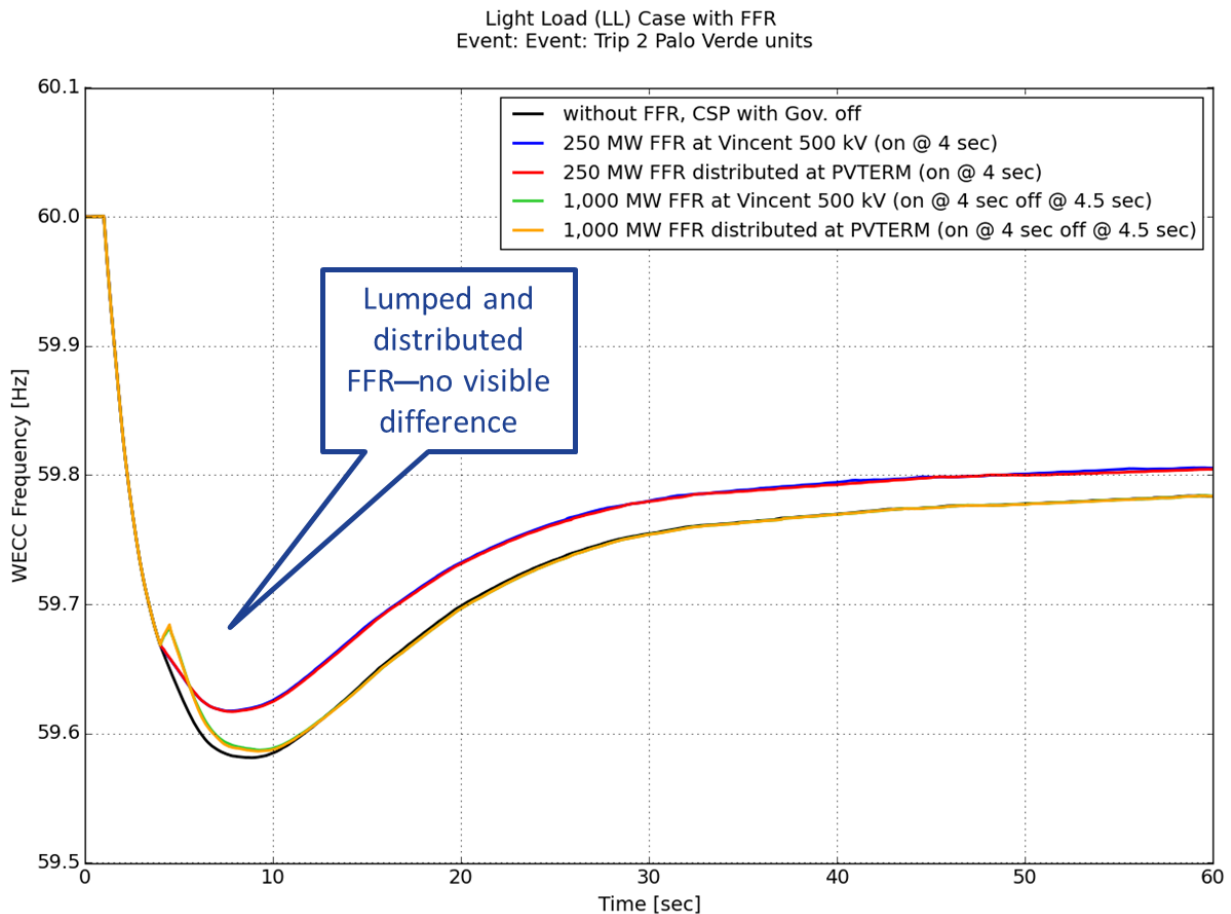


**Figure 69. Distributed (at utility-scale PV plants) compared to single node fast frequency response**

The FFR from utility-scale PV in these examples is assumed to be available by one of the techniques outlined in Section 7.2. But like the “generic” FFR at the central location (Vincent 500 kV), these findings are not specific to FFR from PV. Rather, they apply equally to other resources than can provide FFR. That includes essentially any energy storage medium that uses inverter grid interface, such as:

- Battery systems
- Flywheel systems
- Variable-speed pumped hydro
- Ultracapacitors
- Advanced load controls.

### 7.4.3 Temporal Relationship Between Fast Frequency Response and Rate of Change of Frequency

In this section, we examine the question: Is there meaningful insight to be gained by looking at the temporal relationship between FFR and ROCOF? Starting with the sustained FFR analysis results presented earlier, we look at the impact of FFR on ROCOF.

Figure 70 shows the ROCOF corresponding to the frequency traces of Figure 66. (The plot is for a narrower window of time to allow clearer inspection of the period before the nadir.) This is an unusual plot because the ROCOF discussion is typically restricted to the *initial* ROCOF, i.e., how quickly the frequency starts to drop when the event initiates. That corresponds to the left end of these traces, which is approximately 0.18 Hz/s, as shown in Table 10. As the frequency drop is arrested, the ROCOF improves. Here the ROCOF calculation is for a 500-ms sliding window: i.e.,  $\text{ROCOF} = -\Delta F/\Delta t$  where  $\Delta t$  is 500 ms. (We opted to use a sign convention of positive meaning that the frequency is *dropping*.) The step in ROCOF corresponds to the effect of the FFR at that time on the frequency trajectory. The nadir is defined as  $\text{ROCOF} = 0.0$ , so all the frequency derivatives less than zero are after the nadir (single blue arrow at around 8 seconds) and the frequency is recovering (as can be observed in Figure 66). A locus of points, each of which shows the ROCOF after FFR is injected at that time is sketched onto the figure (orange dotted line). The distance between the black trace and the orange trace is a metric of the efficacy of the FFR on improving ROCOF (i.e., moving in the positive direction). For example, the space between the two arrows is the change in ROCOF for 250 MW of FFR occurring at 6 seconds. For FFR at 6 seconds, the ROCOF immediately following the injection improves about 0.02Hz/sec. Overall, the efficacy in altering the ROCOF is similar to the change in frequency nadir shown in Figure 67.

Light Load (LL) Case  
 Event: Event: Trip 2 Palo Verde units

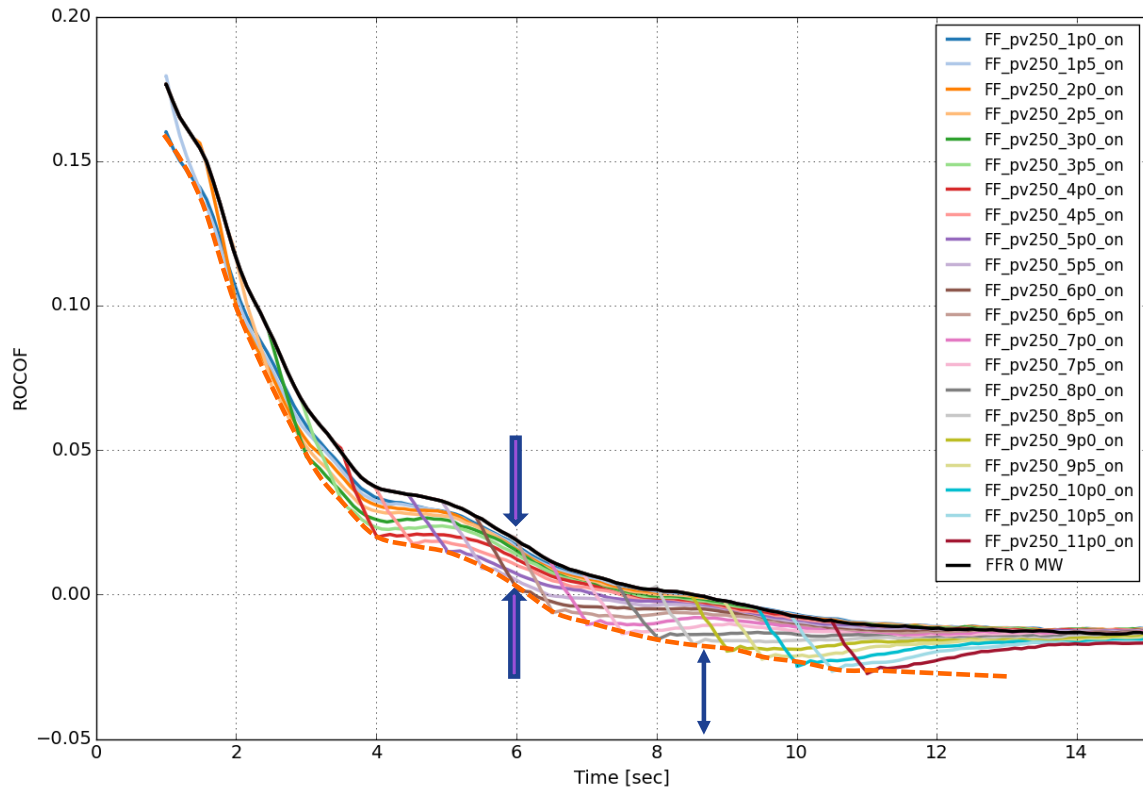


**Figure 70. Fast frequency response impact on rate of change of frequency**

In summary, the introduction of impulse and sustained FFR produces significant benefits on the nadir. Sustained FFR also improves the frequency response. For this system, initiating FFR a few seconds into the frequency event produces most of the benefit. Because there are significant locational issues associated with measuring frequency and ROCOF, delaying FFR avoids locational issues that might result in unnecessary triggering. These findings are consistent with other work in the industry (Wilches-Bernal 2017).

## 8 Enhanced Frequency Response from CSP

The cases presented throughout, especially those in Section 6.3, show a significant improvement in frequency response when CSP governors are enabled. Those cases were all using the governor models from the field validation (Section 3.2) on all the new CSP plants.

In this section, we explore the possibility of extracting even better frequency response from new CSP.

### 8.1 Concepts for Enhanced Frequency Response from CSP

The project team interviewed and obtained some documentation from a commercial supplier of CSP. In this section, we present some thoughts on how CSP steam systems might be created or modified to provide even better frequency response. The observations here should be taken as representative (of CSP steam turbines and boilers), not specific to a particular brand or in any way exclusive or exhaustive.

CSP developers on the project review committee emphasized two points regarding provision of frequency response from CSP:

1. The fast dynamics (e.g., frequency response) of steam turbines is not significantly impacted by the source of heat (solar vs. fossil). The steam turbine does not care much whether the heat is from a solar field, a thermal storage mass, or a fossil boiler.
2. The market has not demanded and not placed a significant value on *any* level of dynamic response from CSP. Suppliers have not been motivated to improve dynamic performance and development has been limited.

Some control basics for commercial power generation steam turbines:

- Primary frequency control is normally offered with a typical dynamic response of approximately 3%–5% of the turbine rating in 20–30 seconds. This response requires the valves to be active.
- Valves active is typically provided when the turbine is operating in the range from a low of 40%–60% to a high of 90% loading.
- Outside of this loading range, turbine operation is with valves wide open. In this case, the response is too slow to be of use in the stability time frame.
- Boiler-follow means that the turbine output is determined by the boiler. Steam flow is constant, unless the heat supply is changed (e.g., additional waste heat going into heat recovery steam generator).
- Load-following is similar to boiler-follow, except the boiler set point is being adjusted to change the fuel delivered to the boiler. The steam supply changes much later. This is too slow to have any contribution to PFR.
- Units *can* be designed to allow PFR throughout a wider power range.

The relationship between the steam and load dispatch is shown in a greatly simplified fashion in Figure 71. When the valves open to admit more steam—for example, in response to the governor

asking for more power—the main steam pressure drops. Coincident with this, the boiler control increases the fuel or heat supply to help raise the steam pressure back to, and beyond, the initial point. The time constants of this boiler step are much slower, on the order of several tens of seconds, and standard stability models, including those used here, do not capture any impact on the main steam pressure. The differences between the boiler and heat-recovery steam generator designs can be substantial, with some systems having much more steam inventory than others. Consequently, controls that might improve the steam behavior cannot be captured in standard stability models for steam turbine governors.

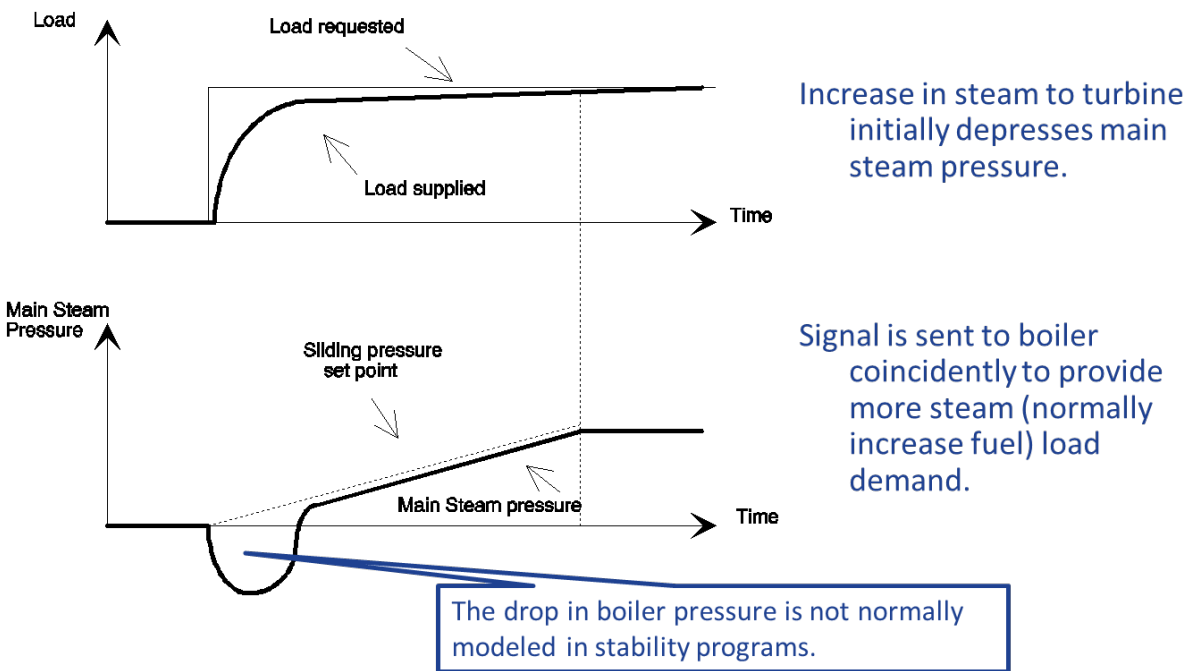


**Figure 71. CSP frequency control and steam balance**

Some options are available to increase steam turbine dynamic performance. They involve dynamic control of the steam of the entire turbine system. One option, in addition to the high-pressure steam valve opening, is that the unit master load control will close the steam bleedings connected to the low-pressure heaters and feed water tank. This diverts steam to intermediate-pressure and low-pressure turbines. This also requires control of condensate to the feed water tanks and other steps.

The point is that the turbine can sustain higher output for a period of time (minutes) at the expense of efficiency. This arrangement also presents the theoretical possibility to use thermal storage to give the steam pressure a transient “bump” for increased power during a frequency event.

In the case of thermal storage that might be provided with a CSP system, the storage will make it possible to *sustain the increased output*. The speed with which the storage might augment the heat supply to the boiler is unknown. It is possible that the physical location of the thermal storage could substantively affect how quickly the storage can help.

## 8.2 CSP Governor Response Compared to Inverter-Based Fast Frequency Response

In earlier results, we showed that the CSP governor response produces significant frequency response benefits. In this section, we compare the CSP to the inverter-based FFR.

For these discussions, we consider the response of the steam turbine to be PFR. To date, the industry has considered FFR to be from “other” resources, e.g., inverter-based generation and fast load control.

In Figure 72, we show an “equivalence” between the CSP governor and FFR. The reference case (black trace) is without FFR or CSP governor contribution. The blue trace is for the CSP governors enabled with no FFR. The green trace is for 250 MW of FFR without CSP governors. The CSP governors produce a somewhat better frequency nadir (in line with the arrow and dotted line) than the 250 MW of FFR. The red trace is for both, showing that the impacts are additive.

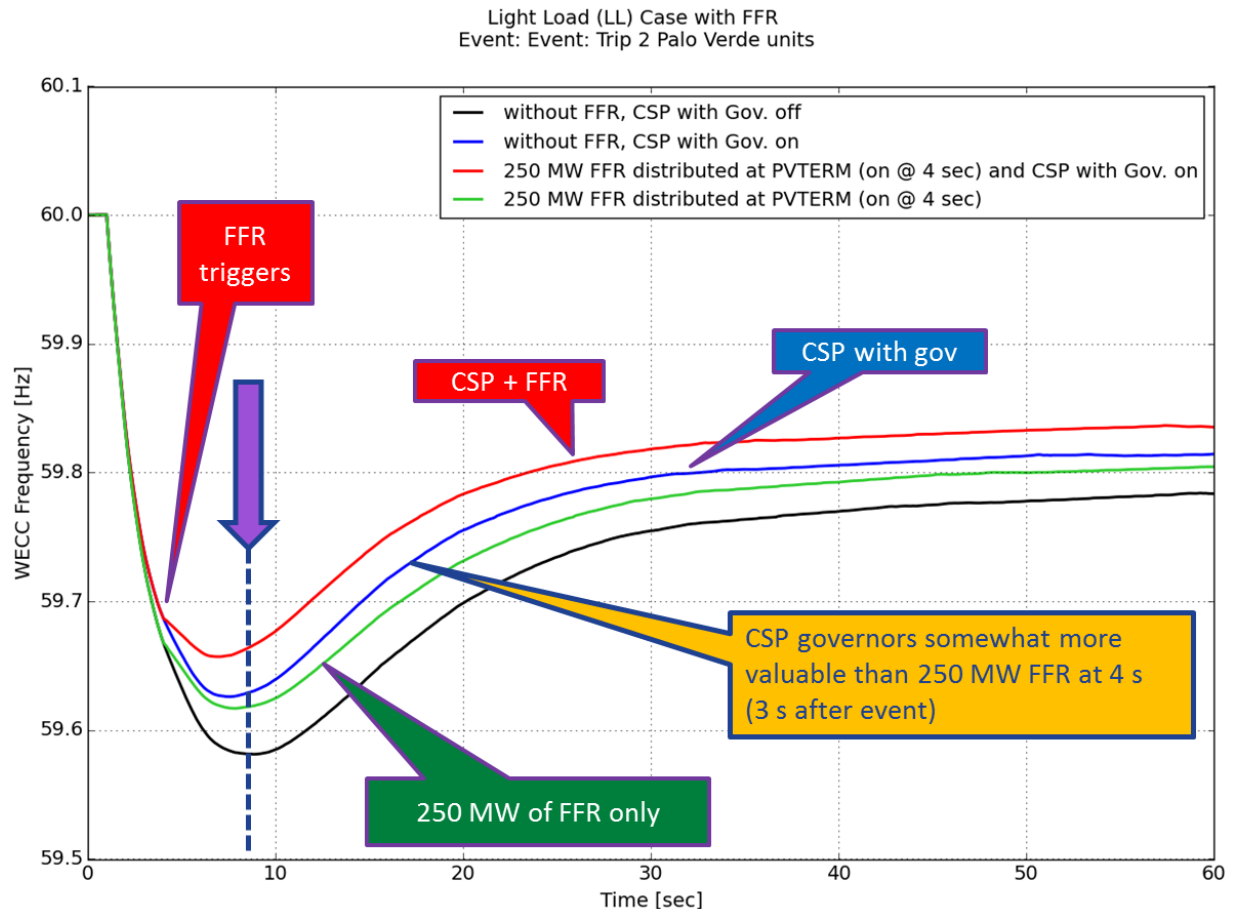


**Figure 72. CSP governor compared to fast frequency response: impact on frequency**

The response of the CSP units is shown in Figure 73, with the FFR associated with the green trace in Figure 72 superimposed. The CSP units collectively start to respond before this FFR, and they have reached approximately 325 MW of output by the time of the frequency nadir. When

viewed this way, the CSP has delivered somewhat more arresting energy (the area under the curves) by the time of the nadir. The better frequency nadir is consistent with the increased amount of energy delivered, and the CSP can be regarded as “worth” approximately 300 MW of FFR.

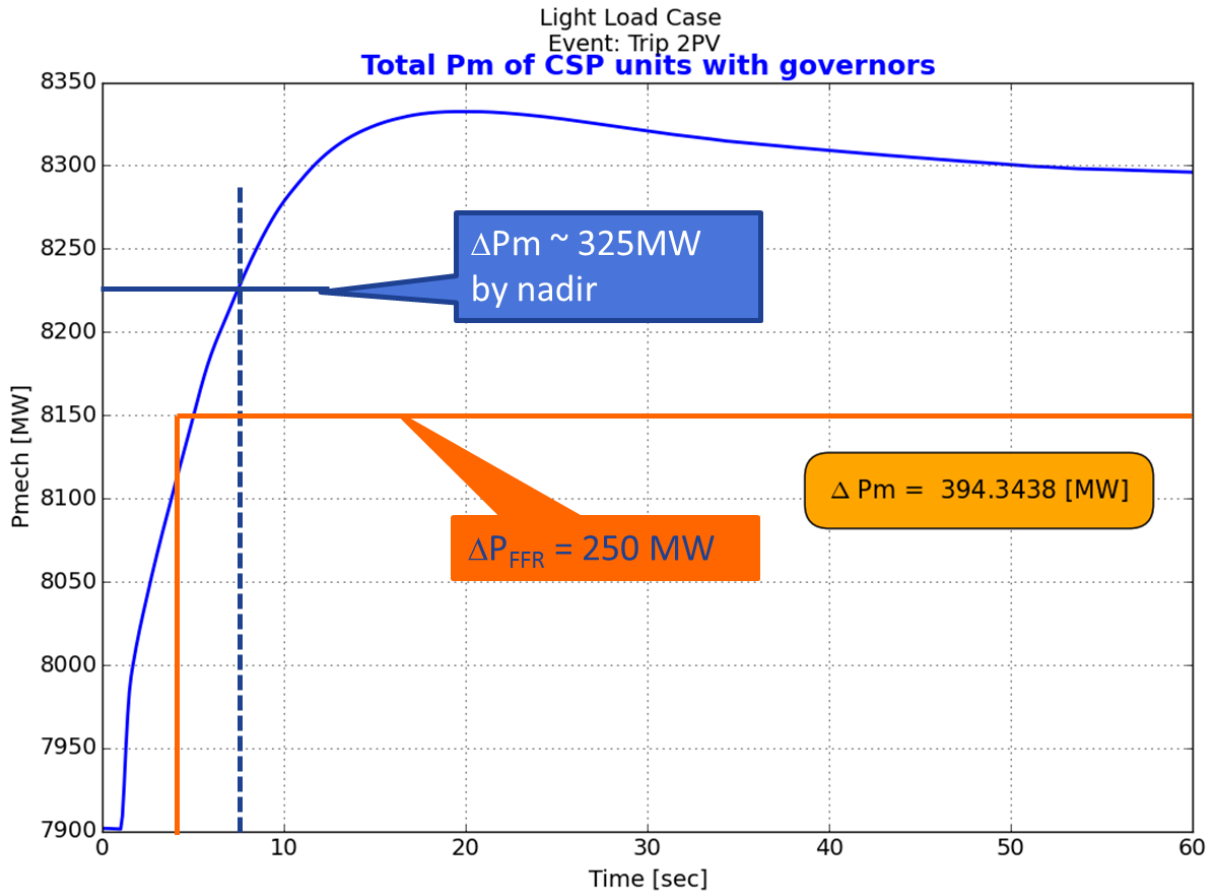


**Figure 73. CSP governor compared to fast frequency response: power response**

The addition of CSP governors contributes to the overall frequency response of the system. Because all the existing governors providing PFR have fixed, linear droops, the other units contribute less because of the smaller frequency excursion. A geographic representation of the governor responses is shown in Figure 74. The dots are plants with active governors. The warmer the color, the bigger the frequency response contribution of that unit. Comparing the results with (left) and without (right) CSP governors shows that other units work less when the CSP contributed. Figure 75 shows the difference between the plots and the incremental duty reduction on the other responsive generation caused by the contribution of the CSP. One unit in California has a very responsive governor, which is shown in red in the figure by the an approximate 5-MW change.

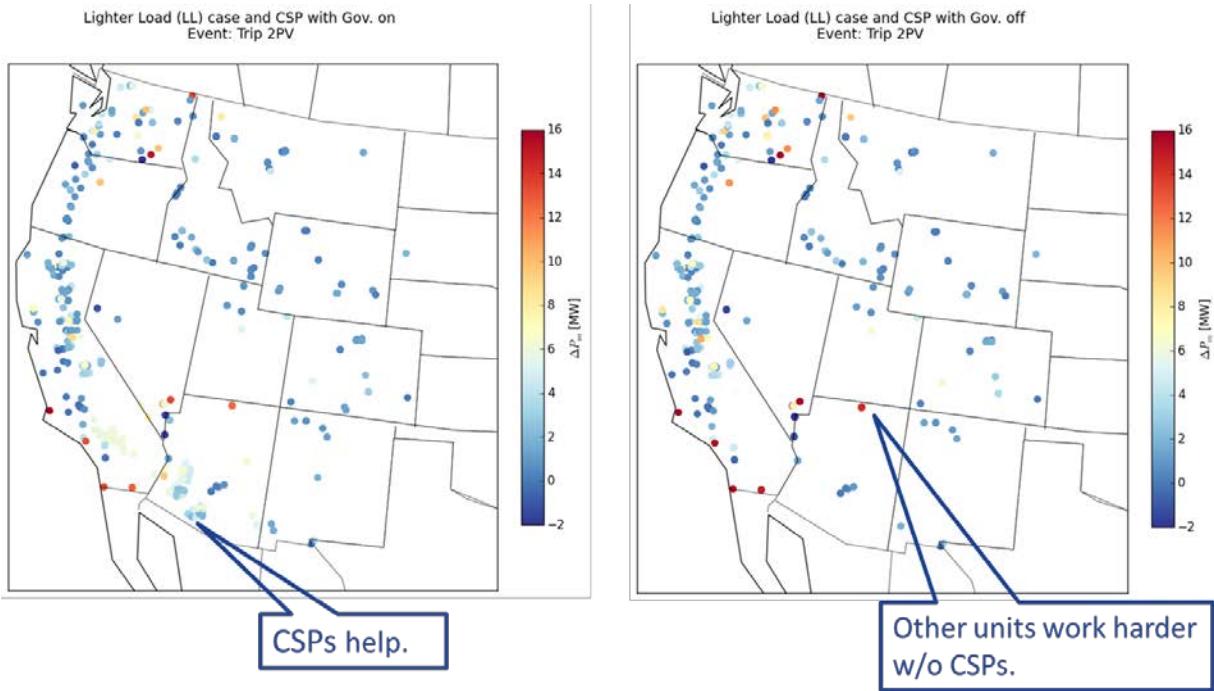


**Figure 74. Synchronous units with governor**

Lighter Load (LL) case, impact of CSP with Governors  
Event: Trip 2 Palo Verde units

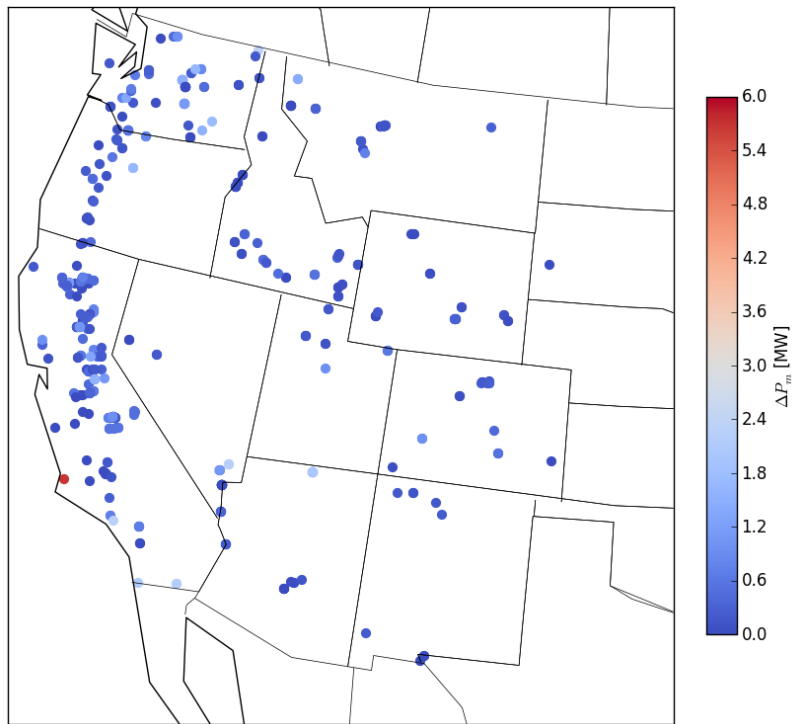


**Figure 75. Delta of governor response**

### 8.3 Fast Valving and Enhanced CSP Response Results

To date, industry consideration of FFR has been for controllable, usually inverter-based, resources (PV, batteries, etc.). So far in this study we have used an open-loop triggering mechanism with inverter-based FFR. In earlier work (WWSIS-3 and 3A), we also showed performance of closed-loop FFR (e.g., synthetic inertia for wind turbine generators).

But triggering mechanical valving in steam turbines by similar open-loop logic is possible. There is precedent for the use of fast-valving controls to combat synchronous overspeeds—it has been used selectively in thermal plants in the United States to manage transient stability problems (Pasternak and Bhatt 1988).

Here we assume a frequency or special protection scheme based on triggering fast valving of the new CSP plants. In these cases, we trigger a fast-valving event to *open* the turbine valves. A 5% increase in power reference is injected to the control immediately (100 ms) after the event. We have made no other changes to the dynamic model. This is a relatively crude proxy for a triggered control that does not depend solely on machine speed to actuate. The triggering is very fast (100 ms) because the experiment was intended to give an upper bound on the benefits (for this model).

Figure 76 shows the incremental improvement of the fast valving on all the new CSP (green trace). The mechanical power from the CSP units is shown in Figure 77. An extra 132 MW of response is enabled by the fast valving. In this figure, note that the initial PGEN = 7,589 MW on a MWCAP = 10,211 MW for new CSP. This extra power is less than the 5% requested; that is, 132 MW/10,211 MW is 1.3% rather than 510 MW.

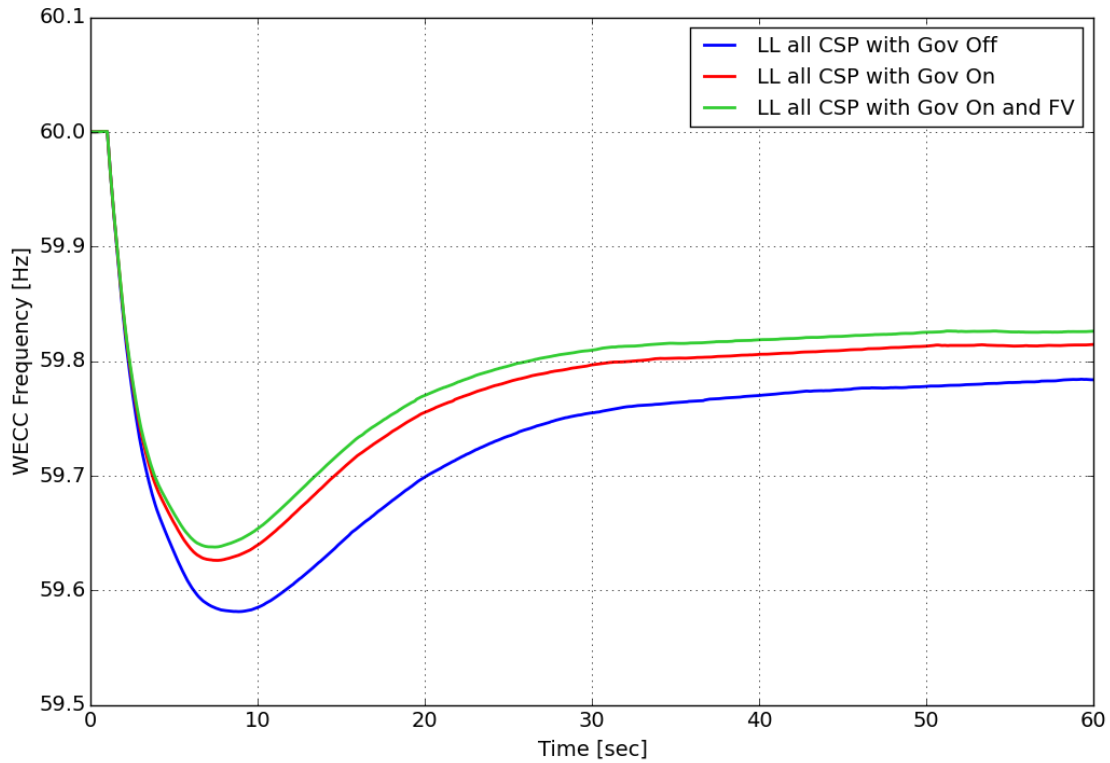


Figure 76. Frequency with CSP fast valving

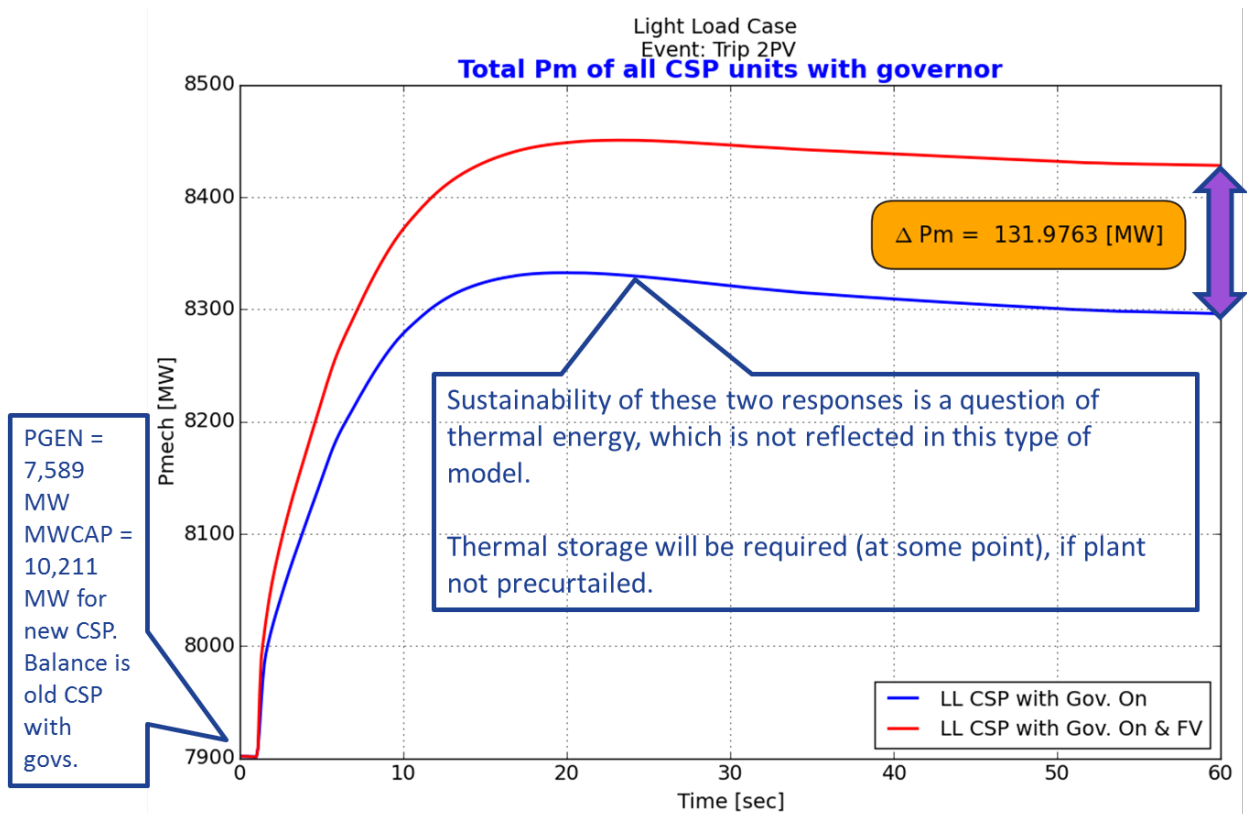


Figure 77. All CSP response with fast valving

To look closer, the performance of a single unit is shown in Figure 78. For this unit, the dispatch is 64 MW on a unit with capability of 94 MW. A 5% response on this base is 4.7 MW, so this unit exhibits the expected behavior. Closer inspection of other units shows that many of the CSP units are dispatched at or above 95% of rating, so a 5% step from fast valving cannot result in that increase in output. This lack of headroom is important, which is examined further in Section 9.3 and Section 9.4.

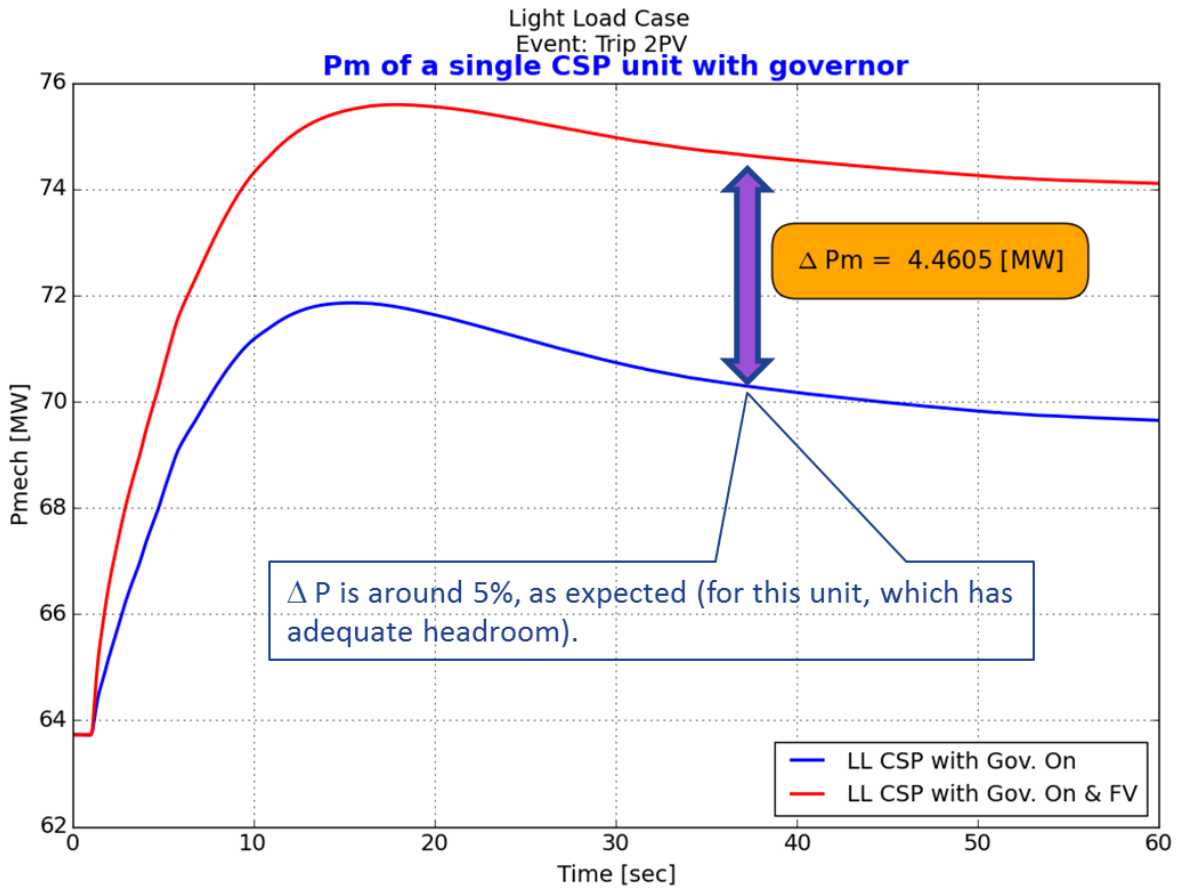


Figure 78. Fast valving on a single CSP unit

### 8.3.1 Frequency Response Comparison of CSP Fast Valving to Fast Frequency Response from PV

The total frequency response of the system for four cases is summarized in Table 11.

Table 11. Frequency Response: CSP Fast Valving Compared to Fast Frequency Response from PV

CASE	FR [MW/0.1 HZ]
LL all CSP with Gov Off	966
LL all CSP with Gov On	1192
LL all CSP with Gov On and FV	1287
115 MW FFR distributed at PVTERM (on @ 4 s) and CSP with Gov on	1261

From this table, and the result presented above, the overall benefit of CSP governors on nadir is similar to approximately 300 MW of FFR. This benefit increases to approximately 415 MW with fast valving. This is approximately 3%–4% (3 MW–4 MW FFR equivalency per 100 MW of CSP rating).

In summary, we find that enhanced steam turbine response is judged possible by designers of steam turbines interviewed for this project. The improvements are not unique to solar steam. Sustained (or better) steam pressure by control is possible. There is some possibility that the use of thermal storage might be advantageous. Although the faster valving produces significant improvements, the ability to trigger very fast is debatable and at odds with the locational results. Practical benefits are probably less than we have shown in these illustrations. These results are, in our opinion, purely illustrative. A detailed and fully validated dynamic model is needed to do quantitative analysis and benefits comparison.

## 9 Sunset Net Load Ramp and Frequency Response

So far in this study we have focused on conditions of relatively high instantaneous penetrations of solar and wind power. We have looked for a variety of stability concerns that might arise under those conditions and opportunities to use solar generation to mitigate those concerns and improve overall system performance.

One challenge that has surfaced for systems with high levels of solar is managing the system as the sun sets and there is a common-mode drop in the solar generation. As the solar power drops, there are potential issues with exhausting other resources. Thus, this class of concern is not about high instantaneous penetration but rather what might happen shortly afterward, when the sun sets.

We will look closely at California for insight, but the issues are more general, and the findings apply to other parts of the West and to other systems around the world that have or might have high levels of solar generation.

### 9.1 Discussion: California Duck Curve

One version of the California “duck curve” (CAISO 2016a) is shown in Figure 79. The net load curve, in red, represents the demand that needs to be served by resources controlled by CAISO—that is, it is the system load net of nominally non-dispatchable wind and solar generation. “Nominally” because CAISO generally has the ability to dispatch utility-scale wind and solar downward but has essentially no capability to dispatch (or even “see”) distributed generation, mainly distributed PV. There are two aspects of this net load curve that are important. First, there is low net load through midday, when there is heavy insolation, and high production from the solar generation. Second, when the sun sets, the net load grows rapidly, from the combination of lost solar generation and natural evening load rise. Together, these represent an operating challenge, because backing down and decommitting enough synchronous resources to allow the system to absorb the full output of the wind and solar is challenging because resources that can ramp up quickly later as the sunsets are needed. To keep resources available for the evening load rise, some must be kept operating at low or minimum power during the middle of the day when there is substantial solar generation. This presents a risk of over-generation. It is this evening net load ramp that is the motivation for CAISO’s pursuit of new ramping products.

The two main study cases, lighter load and heavy summer, have characteristics that allow us to investigate the sunset operating condition. The lighter load case is a reasonable proxy for operation during the low net load condition that precedes the start of sunset. This is noted in the left callout on the figure, which we added to CAISO’s drawing.

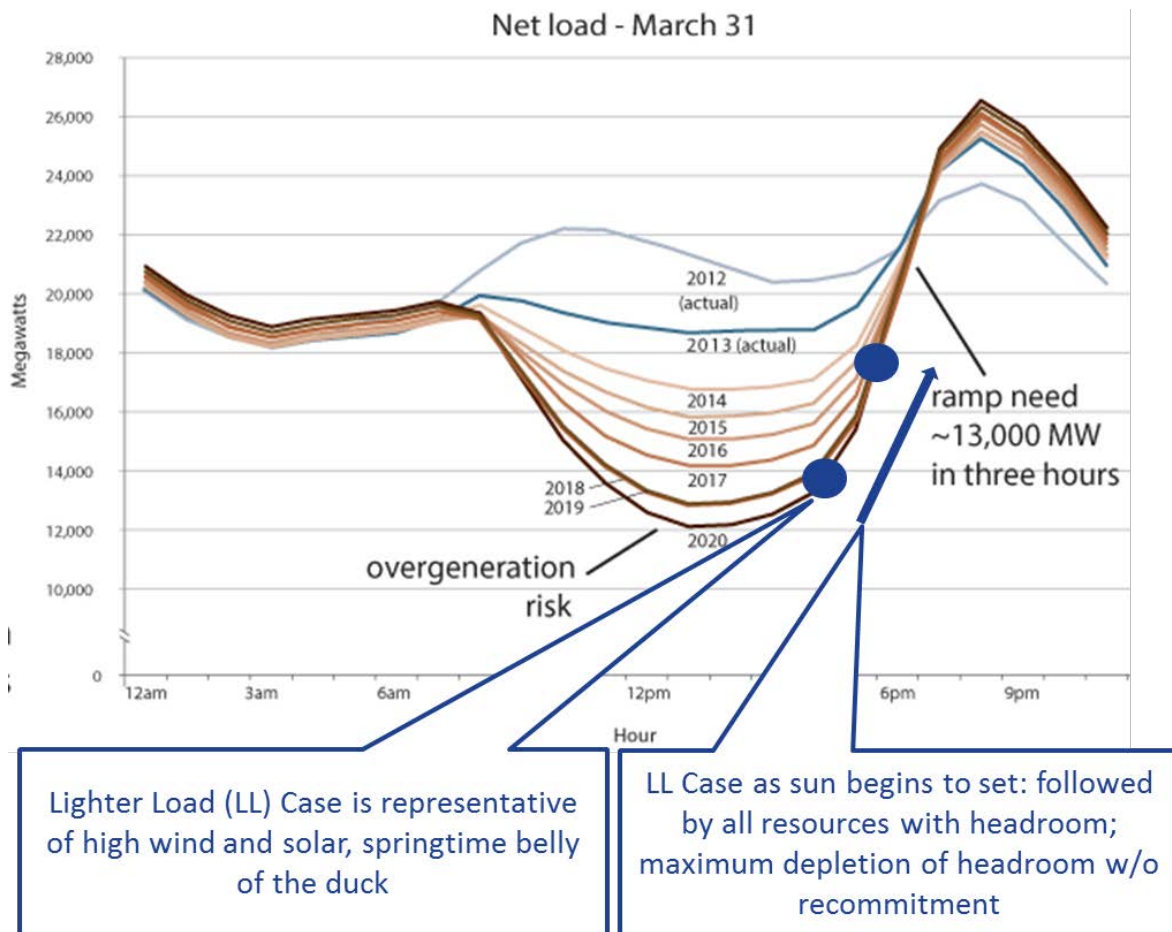


Figure 79. CAISO duck curve

## 9.2 Depletion of Headroom

In the time frames that are the focus of this study, one of the most pressing concerns that accompany sunset from high solar, light load conditions is frequency response. During sunset, the system needs to fill in the rise of net load by (1) dispatching up committed generation that has headroom and (2) committing or starting additional resources.

In this section, we present an exercise aimed at improving understanding of the relationship between this net load following and the depletion of generation headroom that accompanies the upward dispatch. To that end, we take the extreme case of looking at what happens if all the decrease in solar generation is followed by resources that are already committed in California.

The case starts with the lighter load condition, which is a reasonable proxy for the high solar, light load condition before the sun starts to set. The utility solar generation across the Western Interconnection, both PV and CSP, is ramped down uniformly (in proportion to the plant loading) to approximate the effect of dropping insolation that accompanies sunset. The committed gas-fired thermal generation, including combined-cycle steam, in California only is dispatched upward, with the dispatch on generation outside of California left fixed. Non-combined-cycle steam in California is also left unchanged. This continues until these units are effectively out of headroom and cannot increase output farther. At that point, the California

hydro with headroom is dispatched upward. The distinction might be important because when modeling hydro we assume that there is sufficient water (and headroom) to allow this upward dispatch. A much closer look at the hydrology would be needed to confirm this. As noted earlier in this work, and in earlier WWSIS work, the contribution of California hydro to meeting the CAISO FRO is significant under these study conditions. Closer inspection of the actual capability and performance of these hydro plants is warranted.

In Figure 80, a profile of the California dispatch/production(orange) and commitment (blue, i.e., unit MW rating) for the initial lighter load condition is shown on the left. On the right, the dispatch and commitment for this test is shown at the end of a 4,000-MW reduction in utility solar across the system. Notice that the gas headroom is completely depleted and that the hydro headroom is greatly reduced. PV and CSP have dropped. (Note that it has dropped outside of California as well, so the differences in this figure do not add up: solar drop is not equal to gas and hydro increase.)

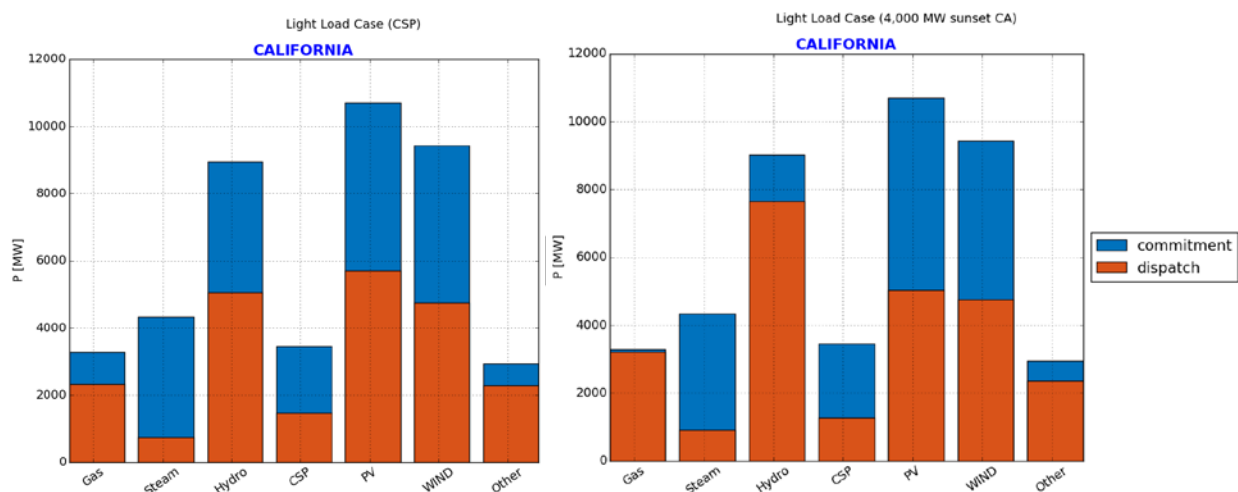


**Figure 80. California headroom - before and after reduction of 4,000 MW of utility-scale solar generation due to sunset**

The steady depletion of headroom from the responsive generation in California results in progressively worse frequency performance. In Figure 81, the system frequency is shown for 16 successive cases, each with 250 MW less solar production than the preceding case. Each trace includes the amount of reduced utility-scale solar generation due to the sun setting. After 1,250 MW of reduced utility-scale solar generation due to the sun setting, the gas-fired generation headroom is exhausted (the first 5 cases, as highlighted by the upper purple arrow in the figure), as the notation in the figure points out. From then on, the hydro follows, with progressive depletion of headroom (the remaining cases, as indicated by the lower purple arrow in the figure). As expected, the overall frequency performance degrades. By the end of the sequence, the margin above the underfrequency load-shedding at 59.5Hz is small, and the case is marginally compliant with the WECC stability criteria.

As the sequence of cases progresses, California contributes less toward arresting and restoring the system frequency. This is reflected as a drop in California frequency response (as defined by BAL-003-1). The declining California frequency response is shown in Figure 82. After

approximately 1,000 MW in reduced utility-scale solar generation due to the sun setting, the contribution of in-state generation to the California FRO drops below the target amount that was calculated for this study. (Per the discussion in Section 6.1.2, note that the actual figure is changed yearly and will likely be somewhat different.) The drop in frequency response with headroom is relatively linear. The orange trend line shows a loss of approximately 4.5 MW/0.1 Hz of frequency response for each 100 MW of headroom depletion.

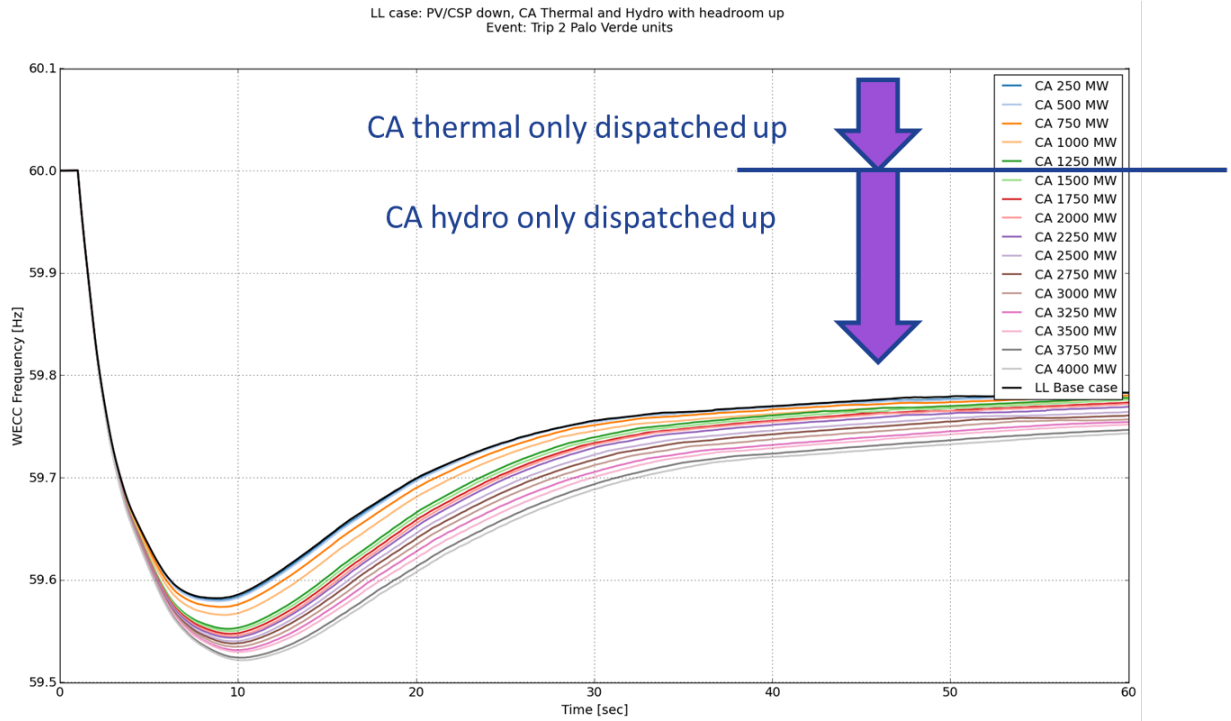


**Figure 81. Frequency response to Palo Verde event during sunset**

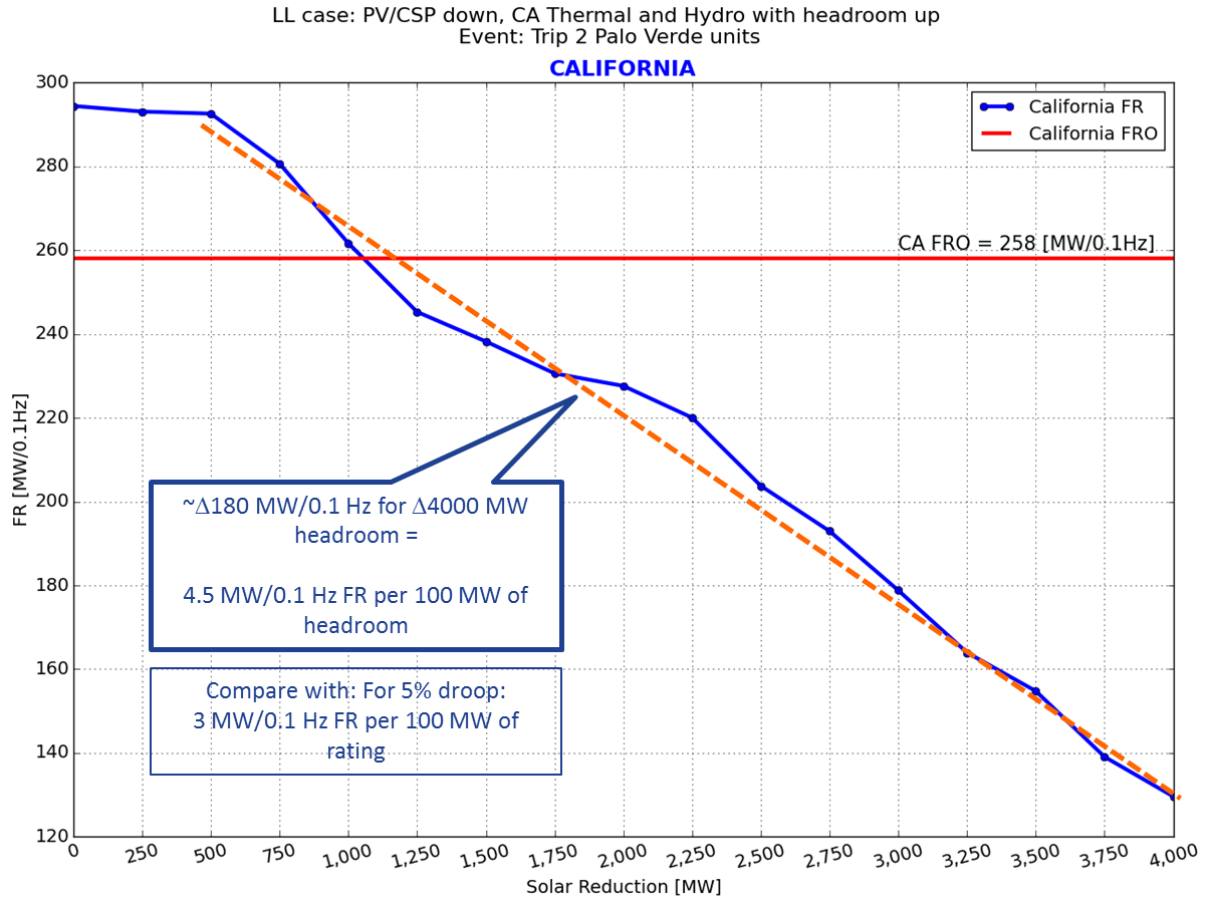


**Figure 82. California frequency response during sunset**

The impact on the overall system is similar but less dramatic. In Figure 83, the decline of frequency response for all the Western Interconnection is shown. At the systemic level, the interconnection drops below the target FRO after a 3,000-MW reduction in utility-scale solar generation due to the sun setting. This provides something of an upper bound for the system. Because CAISO (and all balancing authorities) have the option to procure frequency response services from outside, the fact that California stopped meeting its FRO with *in-state* generation is not necessarily a failure. CAISO already has mechanisms in place to procure frequency response from outside the state. So, from a practical perspective, the point in the sunset sequence at which violations of FRO occur is likely between 1,000 MW and 3,000 MW of reduced utility-scale solar generation due to the sun setting.

LL case: PV/CSP down, CA Thermal and Hydro with headroom up  
Event: Trip 2 Palo Verde units

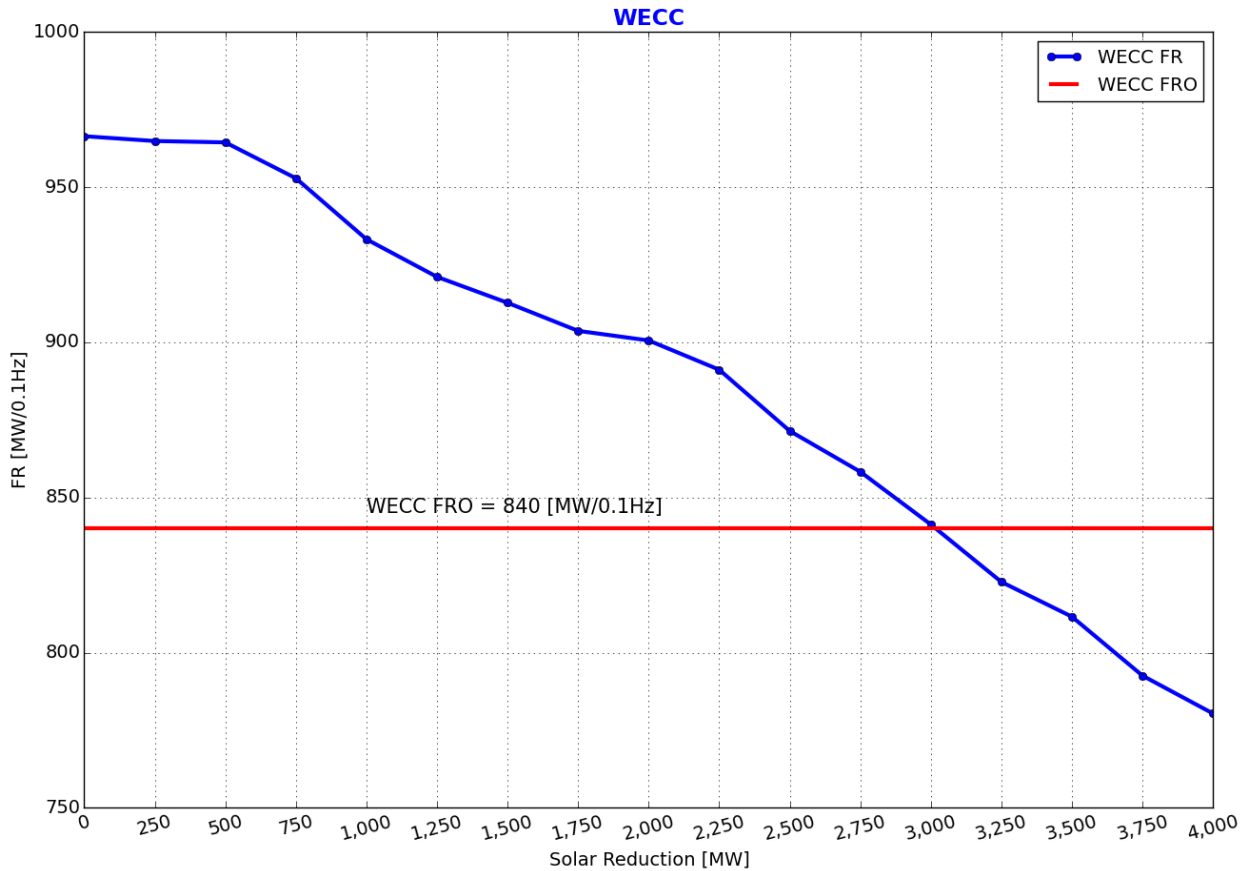


Figure 83. System-wide frequency response during sunset

### 9.3 Lighter Load Low Frequency Response Sunset Sensitivity Investigation

The results presented in the previous section are directionally and qualitatively consistent with operating experience, but CAISO expressed concern that the results are overly optimistic relative to current and near-term future performance.

Based on discussions with CAISO, a sensitivity case was developed that reflects a condition that is more stressful. The commitment and dispatch of the system has the potential to have considerably less headroom and frequency response than the lighter load case. CAISO suggested that a case with less wind, lower hydro, and more PV at higher production be examined. This moves closer to the situation faced by CAISO now or in the near future. This is not an effort to replicate all the upgrades to the dynamic data set that have been instituted since this project was started; rather, it is a sensitivity case aimed at gaining additional insight. The changes to the load flow in California from the lighter load to the case with lighter load and low frequency response were:

- Convert new wind to PV plants (with capacity of approximately 910 MW and dispatch at 340 MW).

- Decommit some wind, with an approximate target of 6 GW in California (per current American Wind Energy Association figures) (American Wind Energy Association 2017).
- Hydro units that were dispatched at < 20 MW were decommitted, and PV units are dispatched up (total of 144 units; capacity of approximately 3,200 MW and dispatch of approximately 1,030 MW).
- Wind is dispatched down by approximately 1,650 MW, reflecting a lower wind condition that could occur under these system conditions
- PV is dispatched up, reflecting a higher insolation condition that could occur under these system conditions

The before and after California dispatch and commitment are shown in Figure 84. A comparison of the case details is given in Table 12.

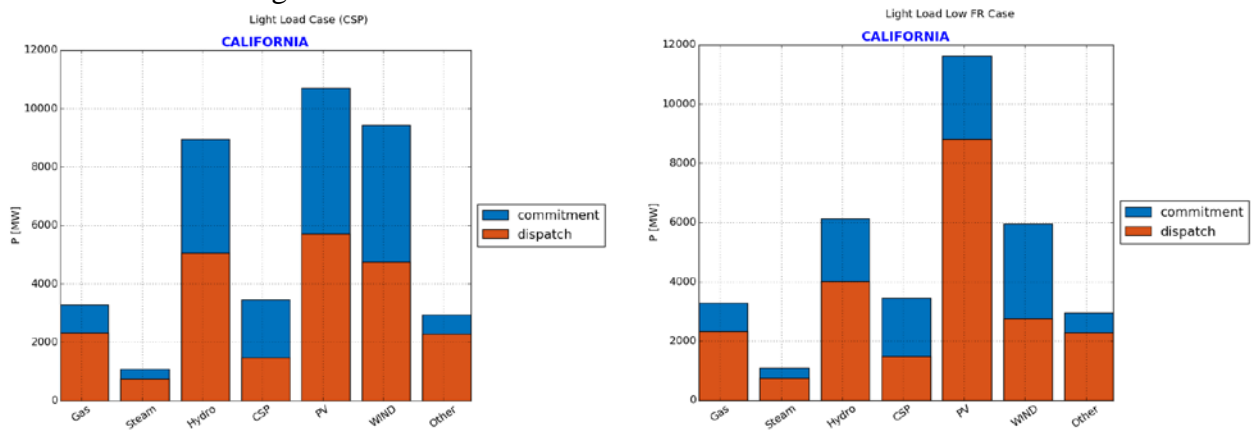


**Figure 84. Lighter load compared to California low frequency response case: commitment and dispatch**

**Table 12. Lighter Load Low Frequency Response CSP Scenario**

	<b>LIGHTER LOAD (LL) CSP CASE</b>	<b>LIGHTER LOAD LOW FR</b>
<b>Load [GW]</b>	78	78
<b>Wind [GW]</b>	25.5	24.01
<b>Utility PV [GW]</b>	10.2	12.8
<b>CSP [GW]</b>	8.5	8.5
<b>DG [GW]</b>	5.65	5.65
<b>Hydro [GW]</b>	14.7	13.7
<b>CSP to PV conversion</b>	No	No
<b>CSP governors</b>	On/off	On/off
<b>Instantaneous wind and solar Penetration (% of WECC)</b>	60.1	62.3
<b>SNSP commitment (%)</b>	66	67
<b>Retirement</b>	Yes	Yes
<b>New transmission</b>	Yes	Yes
<b>Headroom [GW]</b>	13	11.4
<b>Inertia metric (MVA*H)</b>	394,176	384,381
<b>Inertia (H)</b>	3.8	3.82
<b>Inertia (MVA*H/LOAD)</b>	5.03	4.91
<b>PDCI [MW]</b>	-2735	-2735
<b>Path 66 (COI) [MW]</b>	418	513
<b>Path 49 (EOR) [MW]</b>	5500	5475
<b>Parh 46 (WOR) [MW]</b>	9622	10233
<b>Path 26 (Northern-Southern California) [MW]</b>	-2558	-2444

As with the previous sequence, the gas-fired generation is dispatched up first, followed by the California hydro. The hydro runs out of headroom after approximately a 3,200-MW reduction in utility-scale solar generation due to the sun setting, so the sweep is halted there. The right-hand side of Figure 85 shows the final dispatch at this point. A similar sweep of system frequency is shown in Figure 86. Notations in this figure are the same as in Figure 81. The frequency excursions are more severe, and the final case barely avoids underfrequency load-shedding. The changes in the system operating profile for this case makes California’s frequency response substantially worse. The frequency response for this new case is shown in Figure 87 (green trace) along with the results shown from Figure 82 (blue trace). Even before the sunset starts, in this new sensitivity case California is not meeting its estimated FRO. The decline with depleted headroom is similar, although the rate at which the frequency response degrades with lost headroom is a little greater. This reflects the reduced number of units providing frequency response in the case. Nevertheless, it is interesting to see how linear the behavior is. This means that a variety of mitigation measures might be deployed, with a reasonable expectation that they would be additive in their benefits.

The impact on all the interconnection’s frequency response is shown in Figure 88. The whole West drops below its Western Interconnection FRO after about a 1,000-MW reduction in utility-scale solar generation due to the sun setting.

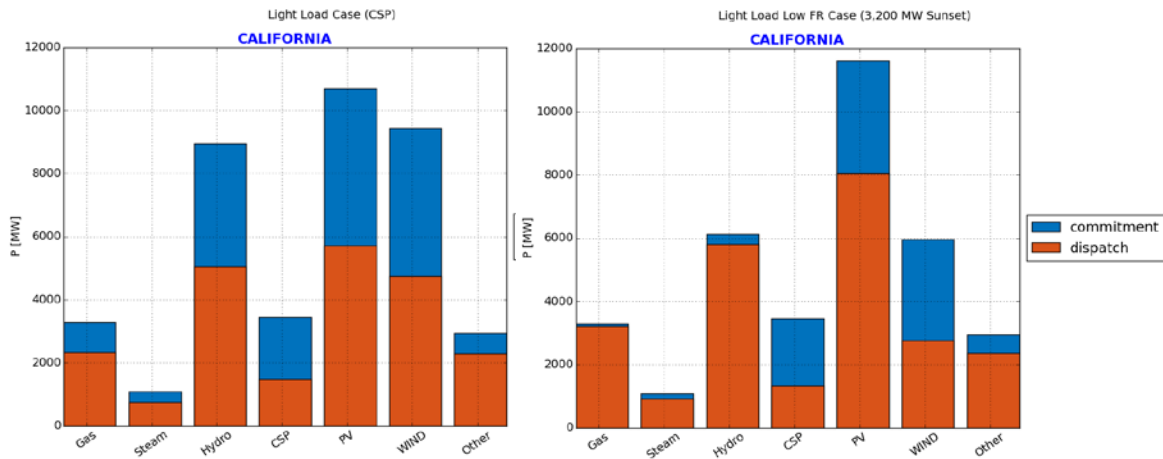


Figure 85. Lighter load low frequency response: dispatch at beginning and “end” of sunset

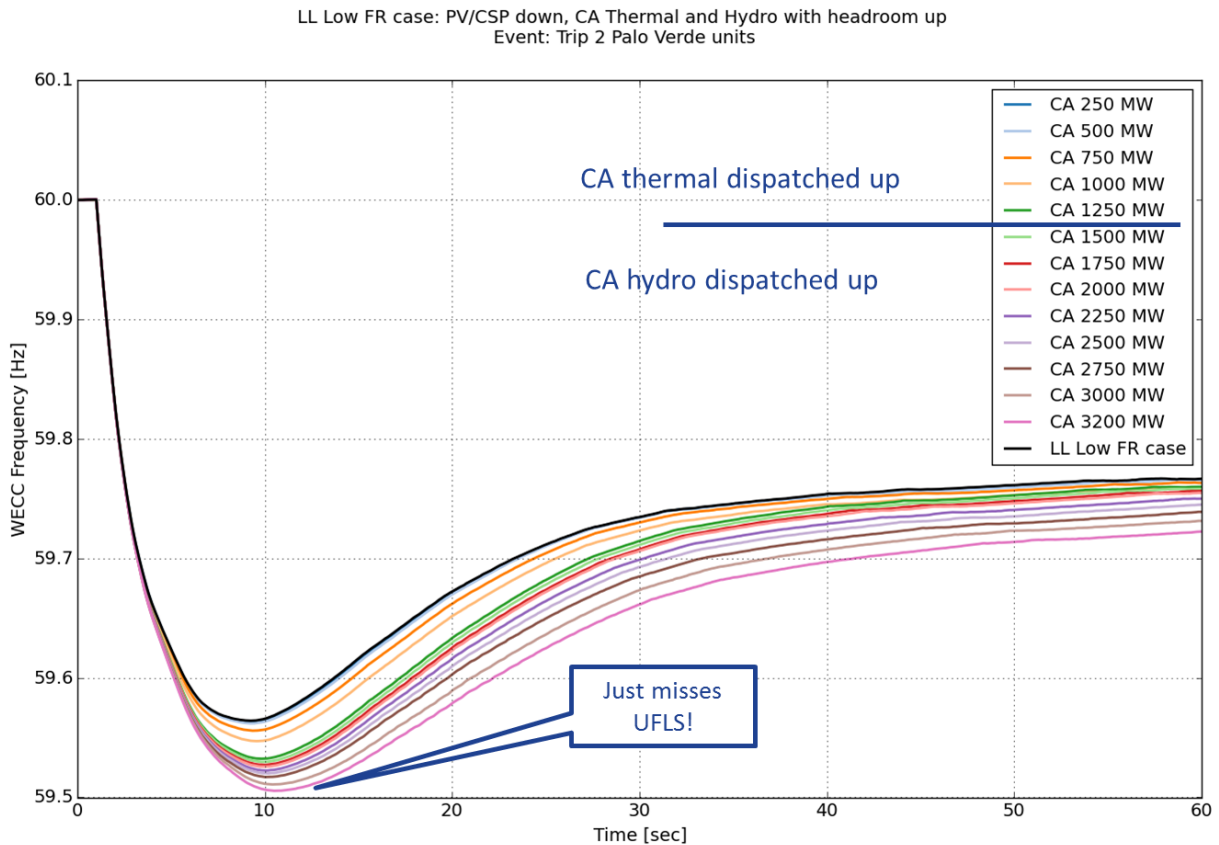
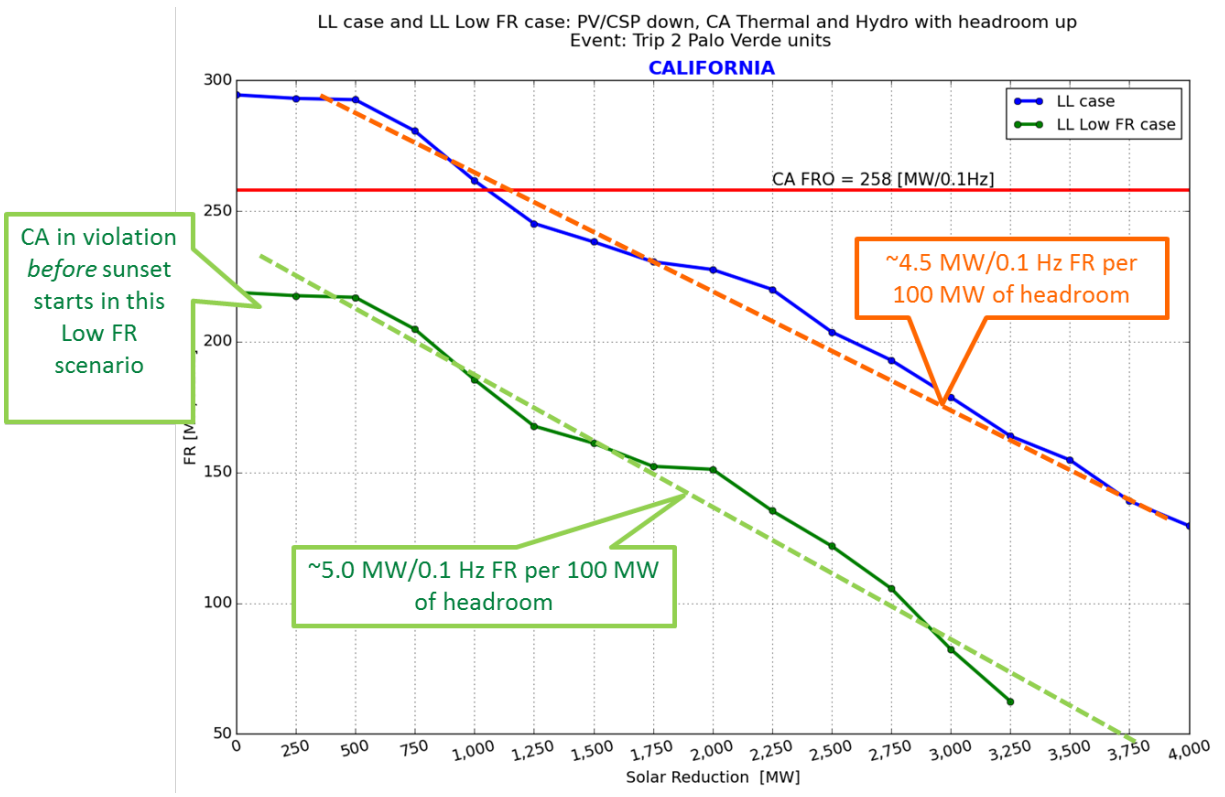
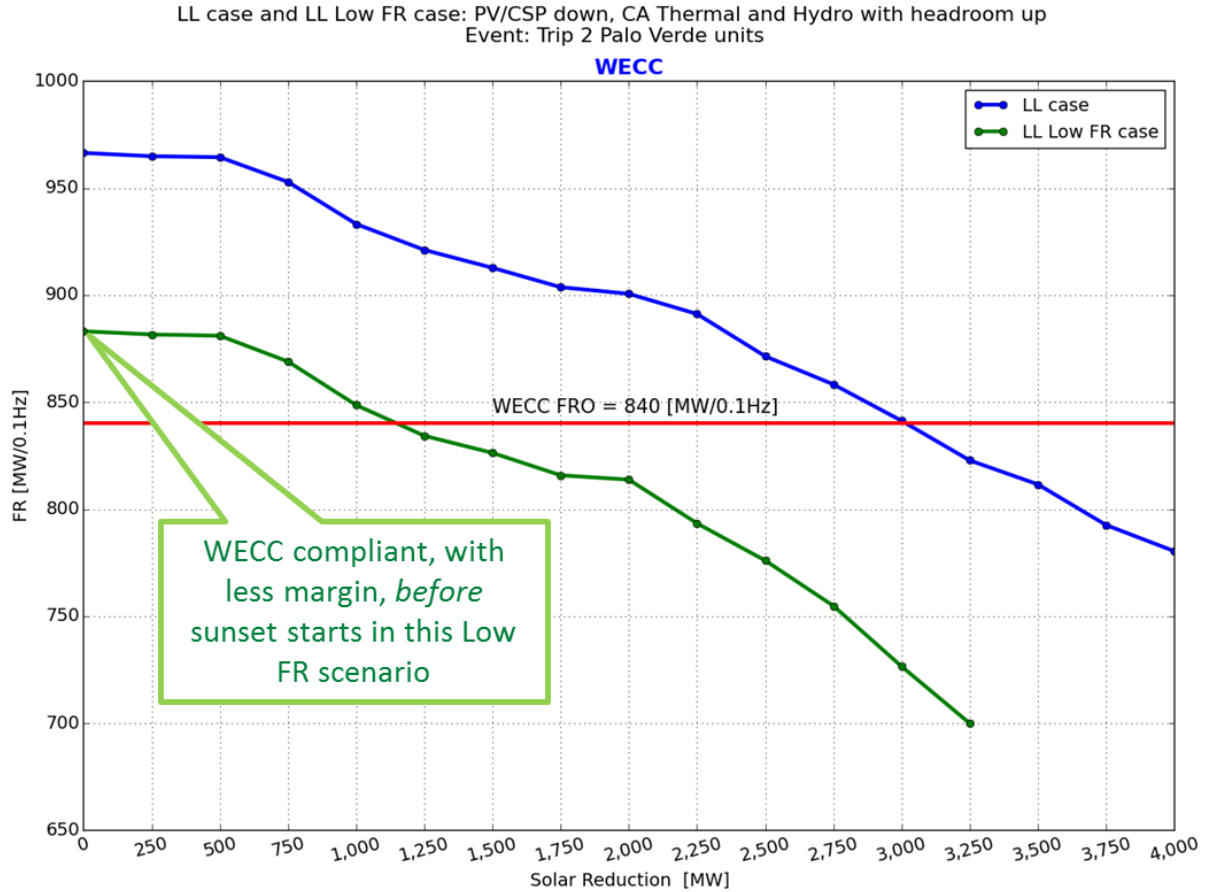


Figure 86. Lighter load low frequency response CSP sunset scenario



**Figure 87. Sunset impact on California frequency response: low frequency response case**



**Figure 88. Sunset impact on WECC frequency response: low frequency response case**

Frequency response is a key metric of system performance, but it is not the only one. The magnitude of the frequency nadir is also important. They are, of course, closely related. In Figure 89, the system frequency nadir is plotted for both cases. The more rapid drop in nadir with depletion of the thermal headroom (i.e., to the left of the vertical blue line) is indicative of the faster response of the gas turbines (and corresponding penalty with depletion of their capabilities to regulate frequency as they are dispatched upward). The fact that the frequency nadir is a about 59.53Hz, or 30mHz above UFLS, at the point in the sequence when the interconnection FR is at the interconnection FRO of 840 MW/0.1Hz, shows NERC’s intended relationship between FRO and avoiding UFLS. The standard (NERC 2012b) includes adjustments for real-life complexities such as initially low frequency, that aren’t captured in traditional stability simulations.

LL and LL Low FR case with sunset sequence  
Event: Trip 2 Palo Verde units

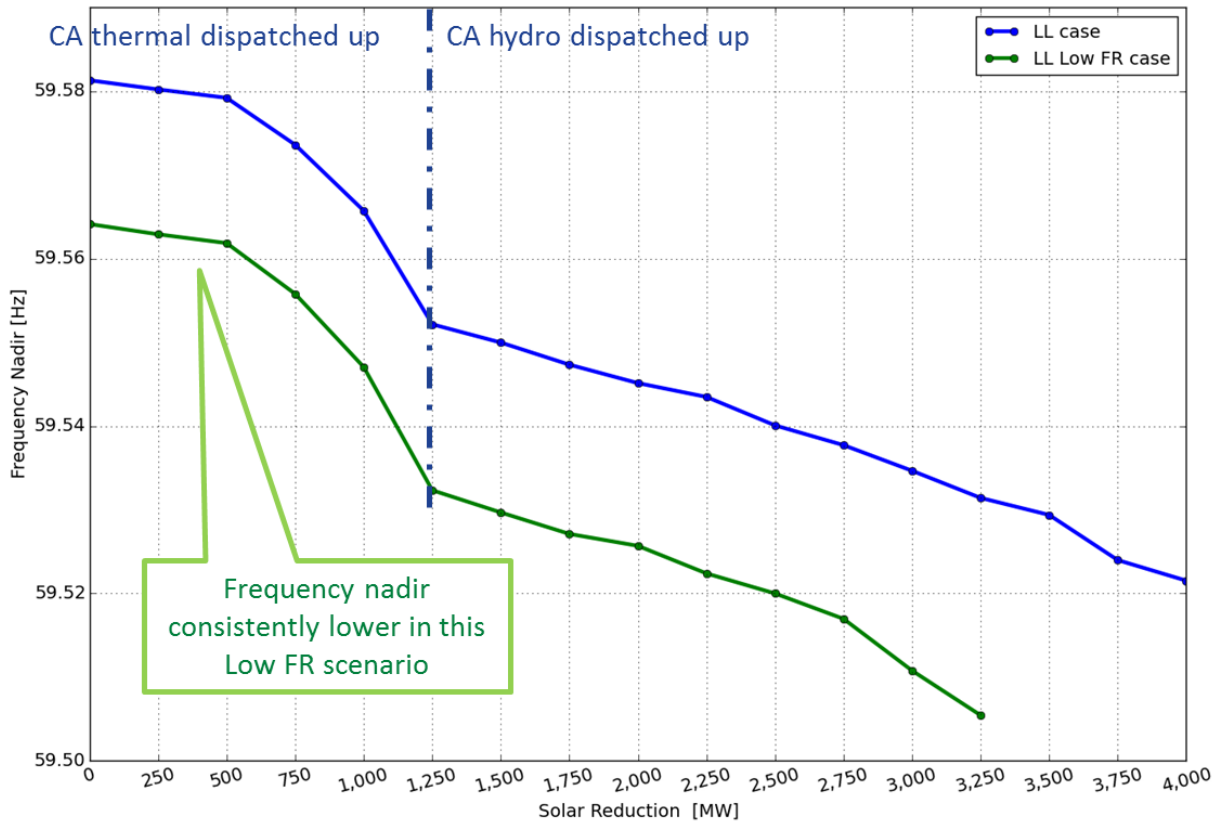
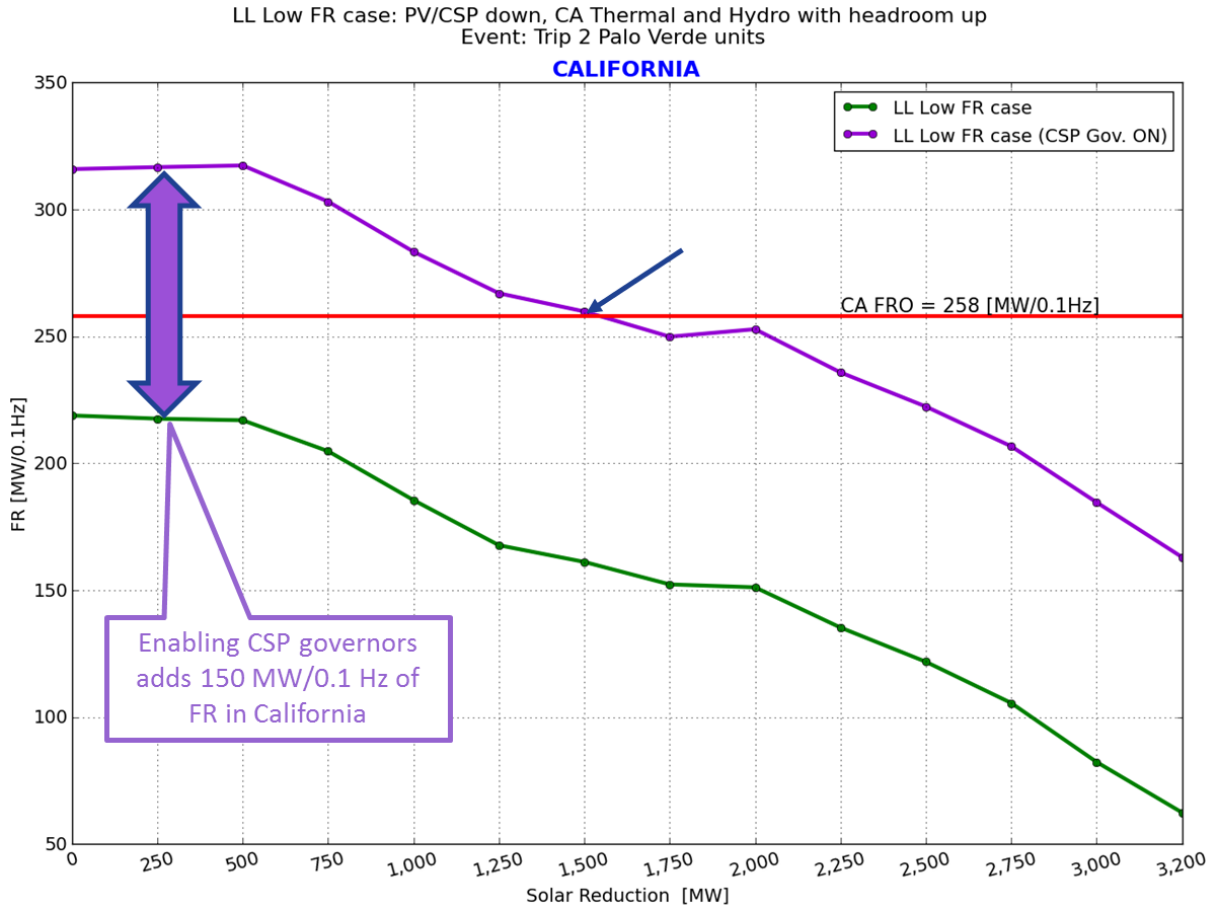


Figure 89. Sunset impact on frequency nadir: low frequency response case

### 9.3.1 Effect of Enabling CSP Governors During Sunset

Figure 87 shows that California was initially out of compliance for the lighter load with low frequency response case. This means that the motivation for adding CSP governors is high. A comparison set of cases for the low frequency response sensitivity was run with all CSP governors enabled. The benefit to California is substantial, initially adding 150 MW/0.1 Hz of frequency response to California, as shown in Figure 90. California can meet its frequency response for up to 1,500-MW reduction in utility-scale solar generation due to the sun setting.

As this new sweep starts, the frequency response (purple trace) initially increases, which is counter to expectations. Closer inspection of the frequency nadirs, shown in Figure 91, shows that the nadirs improve (red arrow) as the sun sets and the other generation loses headroom.



**Figure 90. Lighter load low frequency response during sunset with CSP governors on**

This result can be understood by looking at the response of the CSP plants with the governors on. In Figure 92, governor response (P mechanical) of the CSP plants for selected cases in the sunset sweep are shown. As the sun sets, the CSP dispatch drops. This frees up headroom on the plant. The action of enabling the governors means that *this model* expects there to be sufficient steam (per the discussion above in Section 8) to increase plant output, at least temporarily. A closer look at a single plant, in Figure 93, makes the trade-off between headroom and frequency response clearer. For this 200-MW plant, an increase in headroom results in a better response from the plant. In the traces, increasing the headroom from about 6 MW (blue trace) to about 17 MW (red trace) increases the frequency response from about 6 MW to about 13 MW. This figure also makes it clear that having more than about 10% headroom (green trace) produces no incremental frequency response for the system, although the transient swing, peaking at about 15 seconds, is a bit higher and helps the frequency dynamics. As has been observed in our earlier work: too much headroom on an individual unit (of any type or fuel) produces no frequency response benefit (for systems above underfrequency load-shedding frequency thresholds) when standard proportional (i.e., 5% droop) controls are used.

LL Low FR vs LL Low FR case and CSP Gov. On with sunset sequence  
Event: Trip 2 Palo Verde units

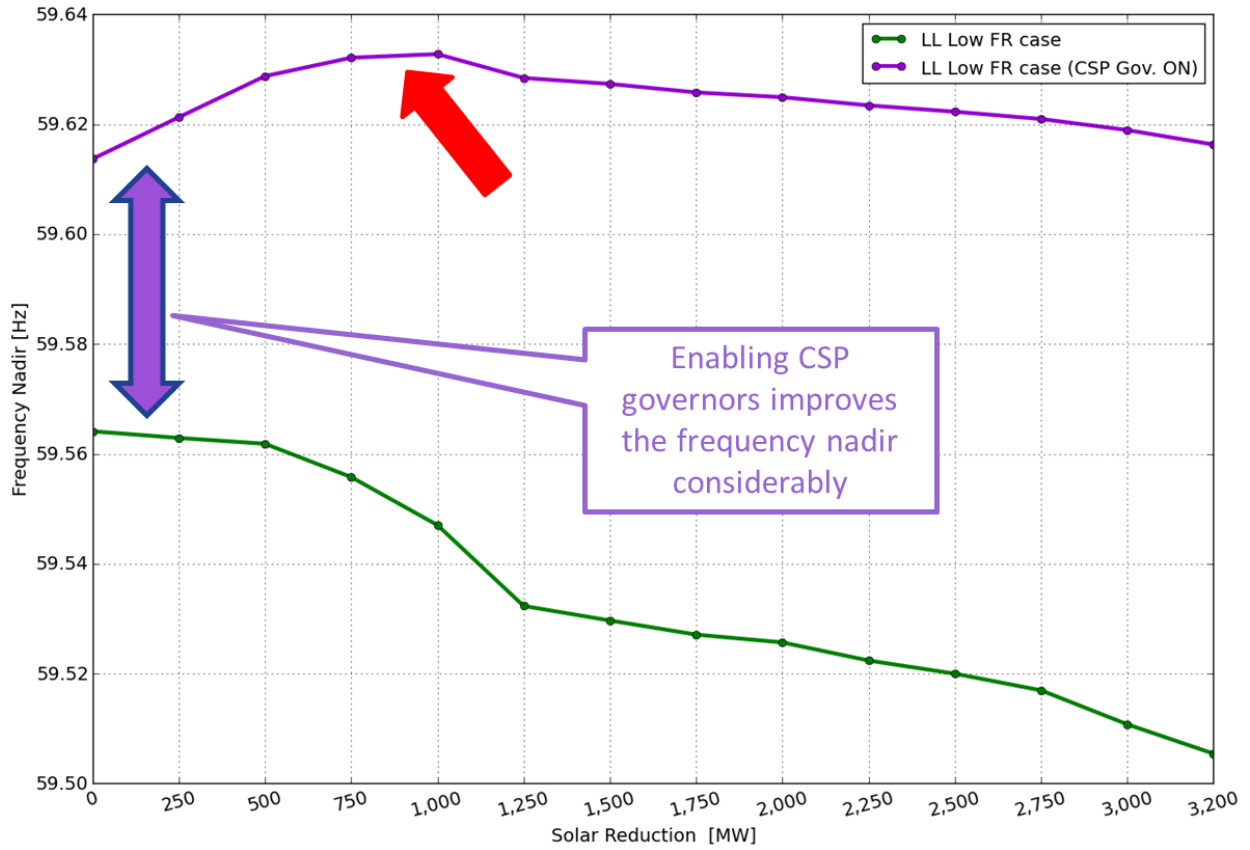
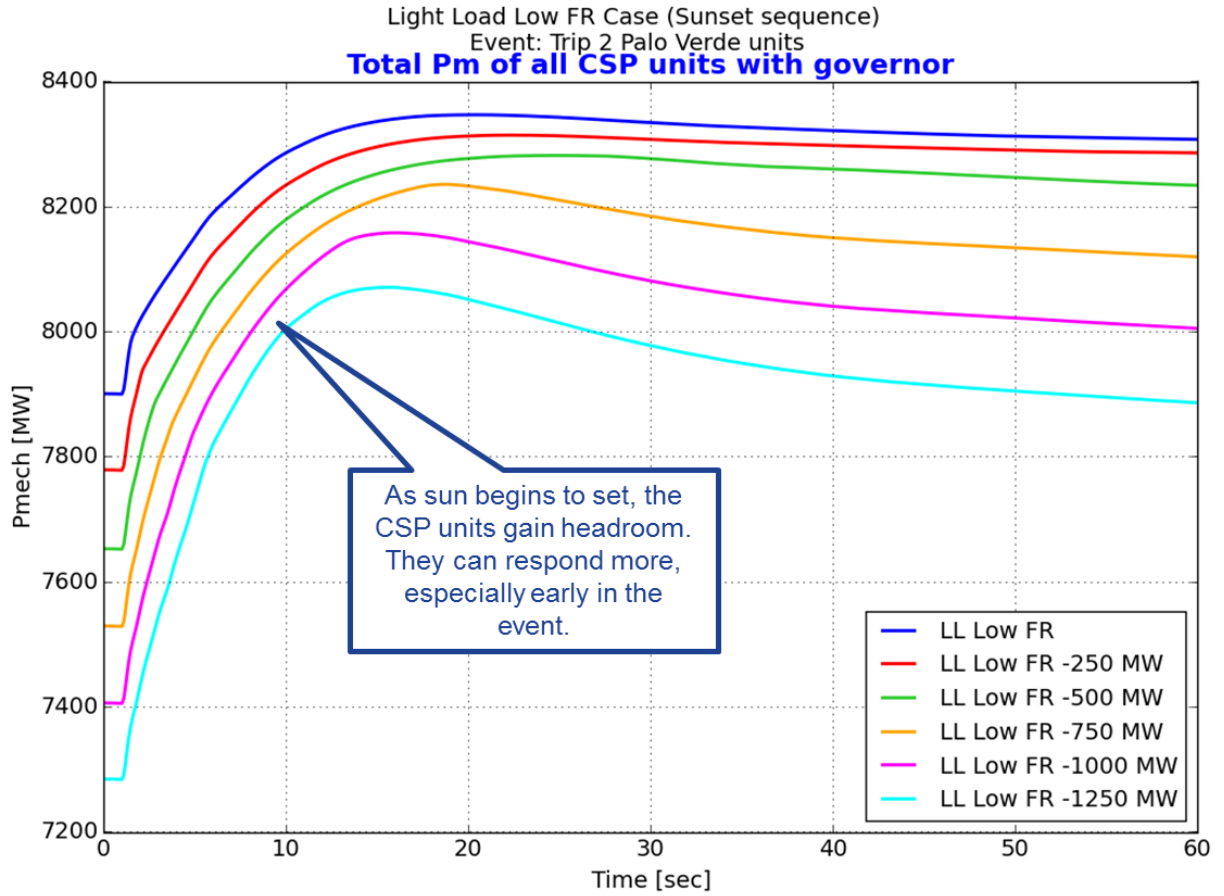
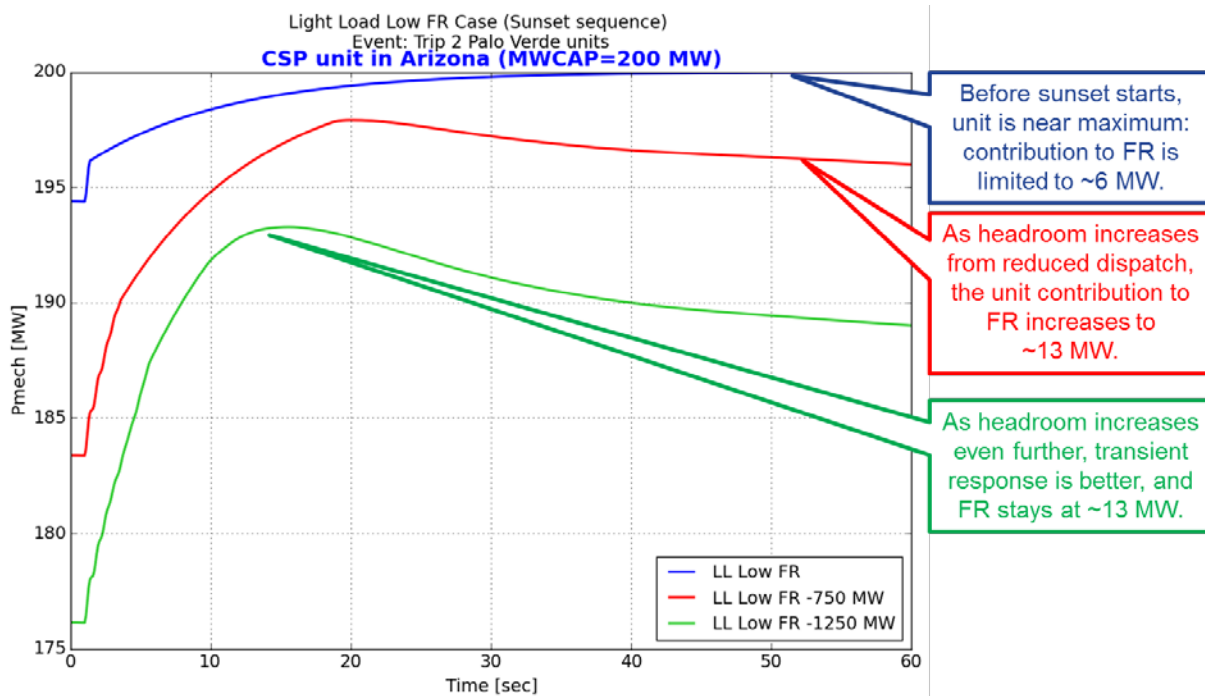


Figure 91. Nadirs with enabled CSP governors



**Figure 92. CSP governor response with headroom increase**



**Figure 93. Details of one CSP governor response as sun sets**

However, if other controls are added to take advantage of the additional headroom, the system can benefit. In Figure 94, a pair of cases run at a 1,500-MW reduction in utility-scale solar generation due to the sun setting is shown, along with the initial, presunset case (blue trace). The red trace (like the blue trace) is for the response of only the governors. It is substantially better because the incremental power delivered in the red case, with more headroom, is about 600 MW. By adding fast valving (as discussed above in Section 8.3), the performance (green trace) is further improved, by another 350 MW. The callout added to the legend on the right-hand side of the figure shows the California and system frequency response for the three cases. The benefits of the CSP headroom are substantial. Remember that much of the CSP is outside of California, so the benefits accrue to all of the West (and to the Southwest).

The actual frequency that goes with these three cases is shown in Figure 95. This figure shows that, from the perspective of improving the frequency nadir, the fast valving during sunset, when there is more headroom, is “worth” about a 1,500-MW reduction in utility-scale solar generation due to the sun setting.

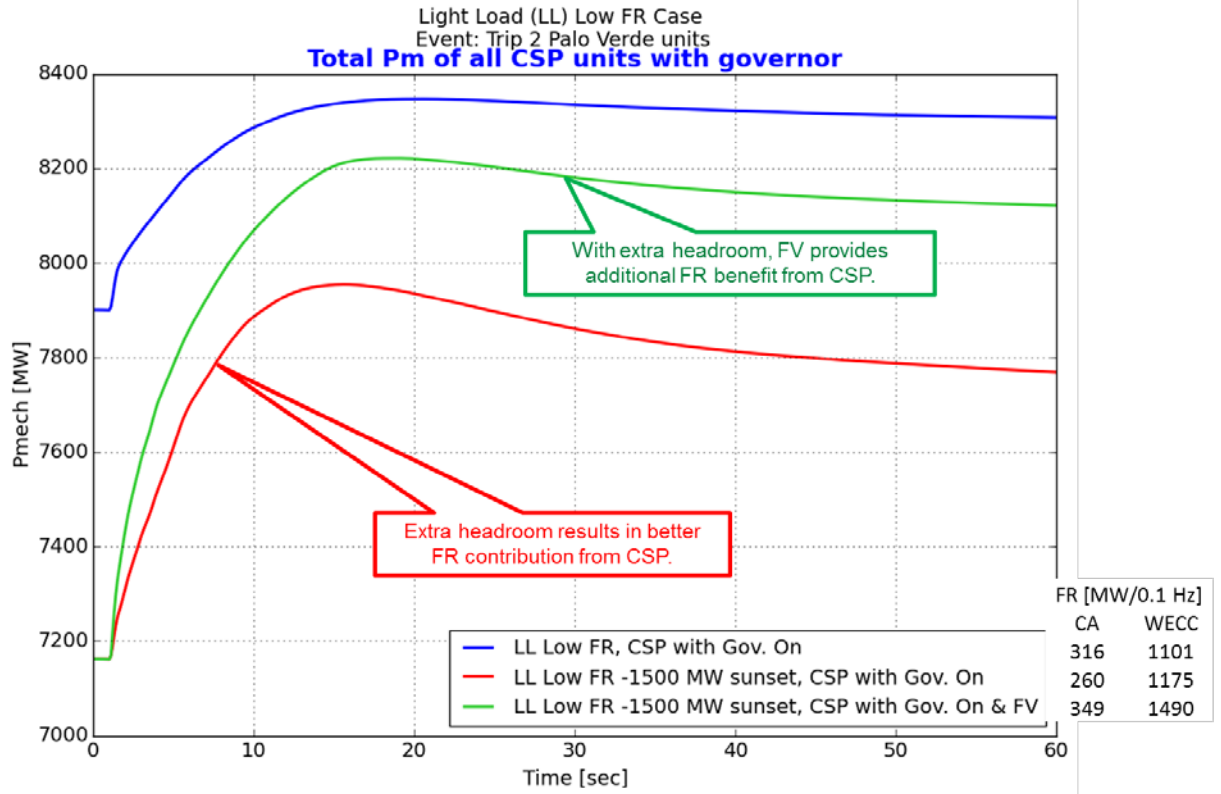


**Figure 94. Sunset with CSP governors plus fast valving**

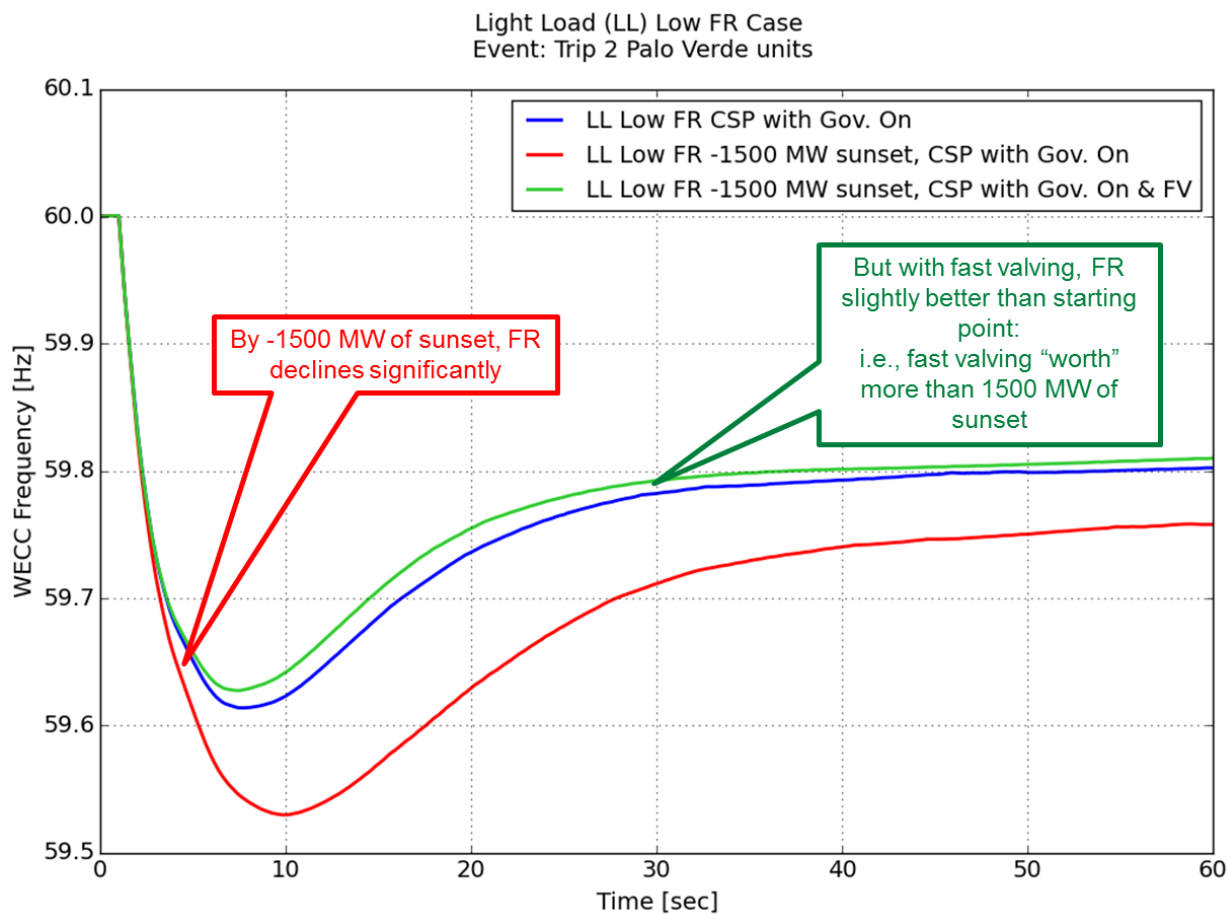


**Figure 95. Fast valving during sunset**

Better dynamic response is effectively a postponement of sunset in the sense that it provides a frequency response benefit like retaining headroom. The benefits of fast valving are shown with the red annotations in Figure 96. The red dot represents the improvement for this single fast-valving case. The red dotted line has the same slope as the frequency response trend of the purple and green lines. Those lines give the approximate relationship between sunset (declining headroom) and frequency response. We have shown that the relationship is quite linear, so the red dotted line is an extrapolation of the benefit with fast valving. In this construct, the fast valving is “worth” about a 1,700-MW reduction in utility-scale solar generation due to the sun setting. This is a nontrivial contribution to California’s duck curve. But whether such capability is possible returns us to question of whether control and/or thermal storage can be used to extract better—i.e., faster and more sustained—frequency response from CSP.

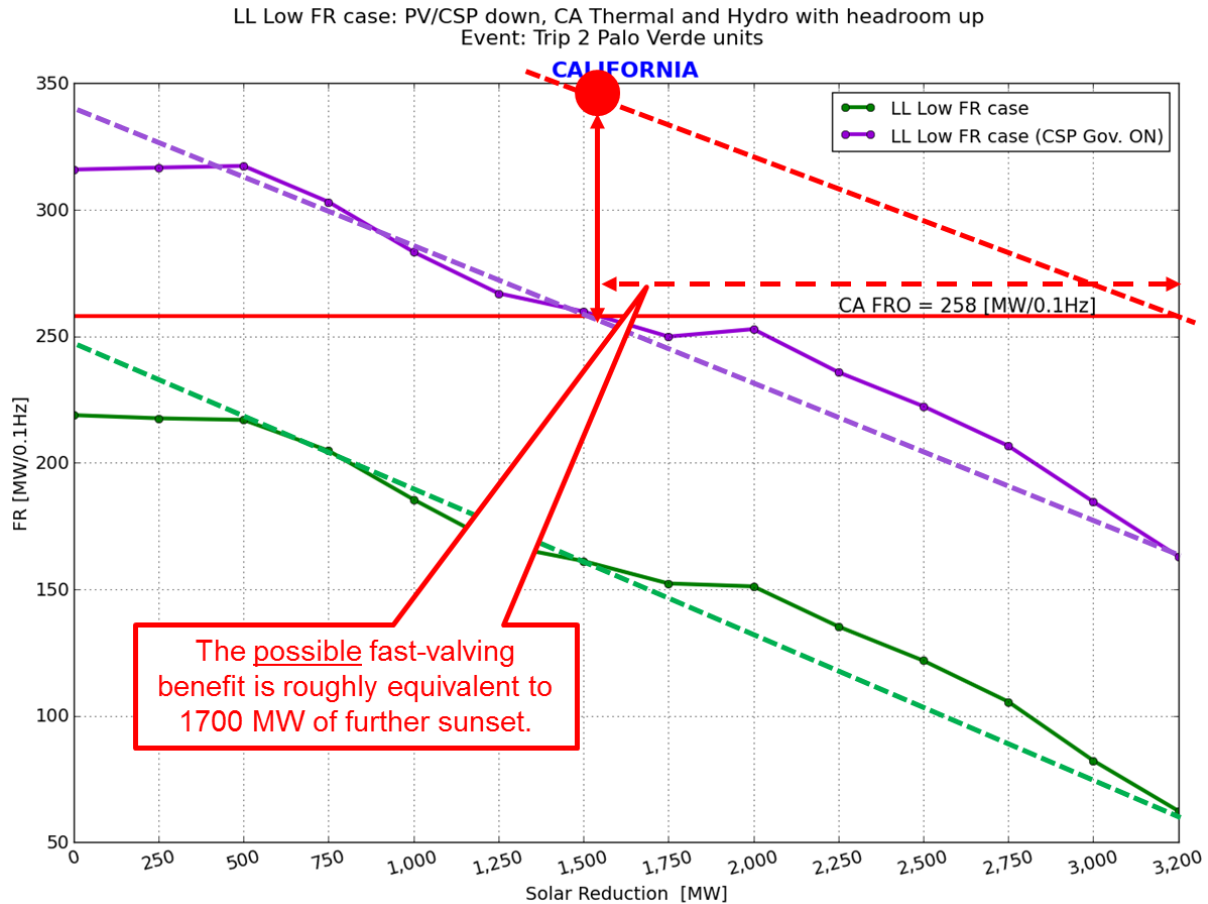


**Figure 96. CSP fast-valving benefit during sunset**

### 9.3.2 Governor: Headroom, Frequency Response, and Storage

This sequence of results raises some interesting economic and technical questions. The results show significant frequency response benefit from CSP if dispatched with some (approximately 5%–10%) headroom. In simple terms, this is consistent with other variable renewable work done earlier. That is, for wind and PV there are benefits to holding back some power (i.e., curtailing) to provide frequency response.

But unlike wind and PV, there are options for storing, rather than spilling, the curtailed power (i.e., thermal storage) (Mehos et al. 2016). Although out of scope, some questions arise:

- Does it make economic sense to do so?
- Does it make economic sense to consider an optimization of power island ( $MW_e$ ) rating compared to solar field ( $MW_t$ ) rating compared to thermal storage ( $MWh_{rt}$ ) rating?

These economic questions cannot be answered with stability tools, but it is possible to provide some stability limit guidance, which would be essential to framing and evaluating the economic benefit that might be realized by using thermal storage to improve frequency performance.

## 9.4 Implications for CSP Thermal Storage

Figure 97 illustrates the trade-off in dispatch as the sun sets. On the left, the figure shows the dispatch of the PV and CSP dropping across the system in a relatively uniform fashion. The orange boxes suggest the loss in production. On the right, the first block of bars shows the dispatch and commitment of the committed, dispatchable generation in California going into sunset. The second block shows the dispatch, with the change required to follow the sunset highlighted with the dotted lines and the up arrows. The point of the illustration is to show that if the dispatch of CSP could be sustained by drawing on thermal storage, it would effectively be a postponement of sunset. By continuing to dispatch, headroom on other frequency response resources is maintained, plus CSP continues to run and provide frequency response. The concept is illustrated by the orange locus sketched in Figure 98. In short, the thermal storage would offer an additional mechanism to ensure that the system has adequate dynamic range to meet its FRO.

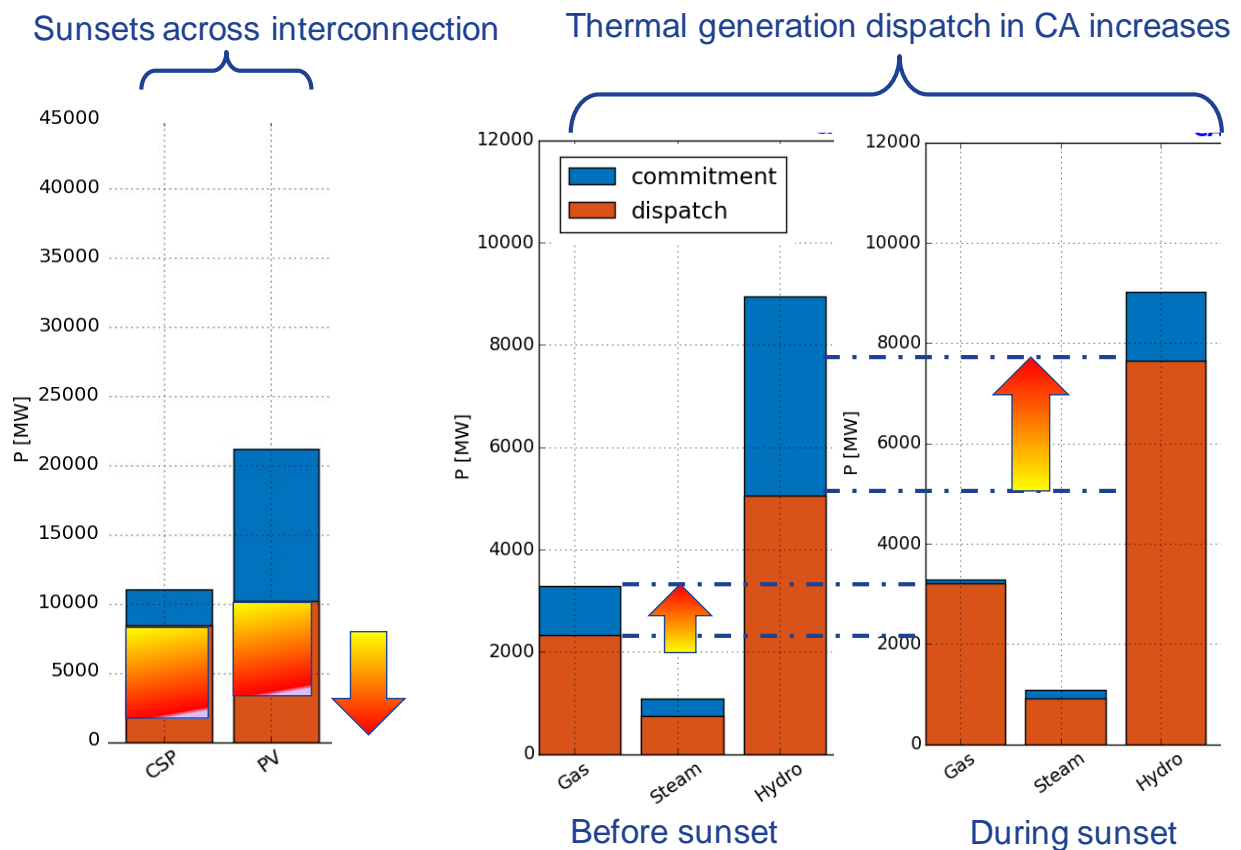
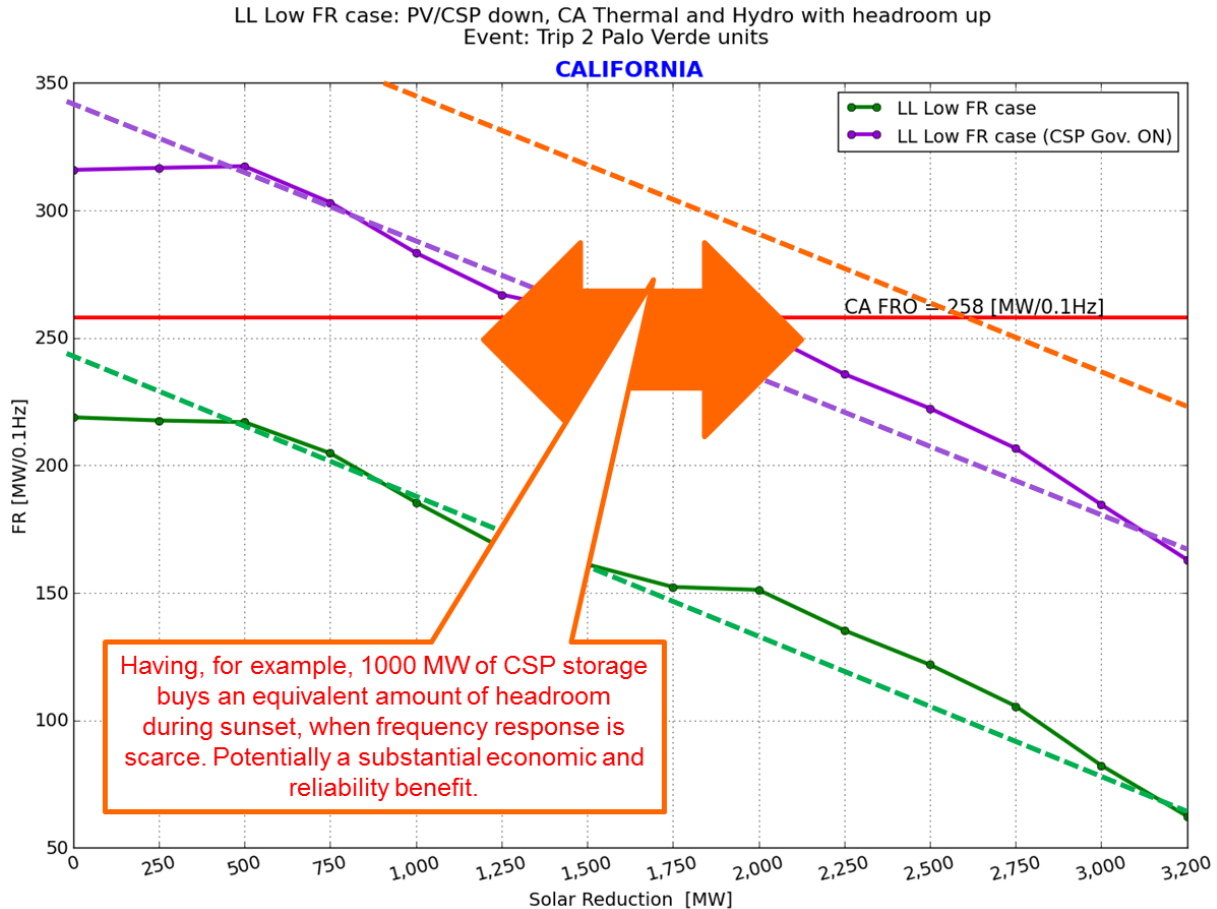


Figure 97. Thermal dispatch during sunset



**Figure 98. Fast frequency response and storage impact on frequency response during sunset**

## 9.5 Synopsis of Sunset Investigation

Several key summary points can be made based on the relatively complex discussion of this chapter:

- Sunset from the high solar condition can deplete headroom, causing problems in meeting FRO.
- This frequency response concern is during sunset, so it is not necessarily the high penetration condition but the condition that follows that is most concerning.
- Too much load following (by dispatch) without committing (starting) new resources (or obtaining frequency response from outside) will result in FRO violations.
- These cases show that it is possible for California to be short of frequency response; the new case showed the California short even before sunset starts.
- Thermal storage is effectively a postponement of sunset. Continuing to dispatch by drawing on the stored energy maintains the headroom on other frequency response resources and allows CSP to continue to run and provide frequency response.

- Better dynamic response, such as that provided by fast valving, is also effectively a postponement of sunset in the sense that it provides a frequency response benefit such as retaining headroom.

Some caution is needed in reviewing these results:

- WECC and the western utilities and operators are continuing to upgrade the WECC model. Increased fidelity modeling might show that these results are optimistic and that the available frequency response, especially in California, is more limited than these results indicate.
- The cases presented here are illustrative and are not a substitute for detailed planning studies.

# 10 Local Weak Grid and Regional High Simultaneous Nonsynchronous Penetration

## 10.1 Introduction

### 10.1.1 Weak Grid Visualization

One of the most challenging operating conditions for inverter-based generation is in a so-called weak grid. But what is a weak grid? Analytical descriptions have long been available (Tande and Olav 2000), but the question is one of relative size: Is the inverter-based generation relatively small or relatively large compared to the host grid? Here we present, again, a simple visualization intended to illustrate the concept (from WWSIS-3A) (Miller, Leonardi, and D'Aquila 2015).

Historically, wind power plants were relatively small compared to the grid. A 1-MW wind turbine connected to a 20-GW system has no more ability to move that system than a lap dog, even a badly behaved one, can bend a palm tree (Figure 99); however, as wind power plants became larger and are connected to smaller and more remote portions of the grid, they exert more influence. A 200-MW wind power plant connected to a 300-MW subsystem can now impact system response to a disturbance similar to the way in which an elephant can bend or break a palm tree unless it is trained not to (Figure 100).

It is this latter condition of high local concentration of solar, and the possible difference between supply by synchronous generation (i.e., CSP) or inverter-based generation (i.e., utility-scale PV) that is the focus of this section of the report.

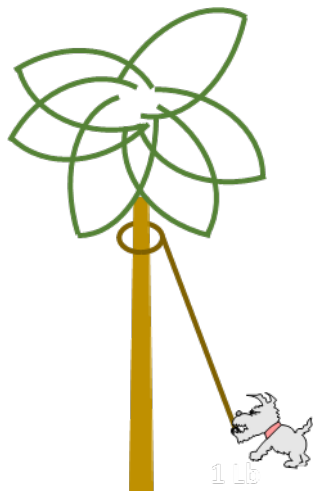


Figure 99. Small wind power plant relative to the electric grid

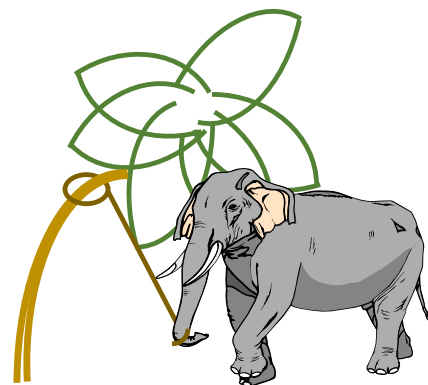


Figure 100. Large wind power plant relative to the electric grid

### 10.1.2 Investigation of Short-Circuit Strength on Weak and High-Change Buses

Section 4.2 showed the characterization and sorting of nodes in the system by short-circuit level and change in short-circuit strength caused by switching from CSP to utility-scale PV. In Figure

20, buses with large changes were shown. From among these three locations, we selected additional scenarios for more detailed analyses. The two buses with the largest short-circuit MVA change are:

- Gila Bend 230 kV (Arizona):
  - A reduction of 48% in short-circuit MVA occurs when CSP is converted to PV.
  - Eight CSP units are connected.
  - The total MVA from CSP/PV is 1,128 MVA.
  - The short-circuit ratio (SCR) is 3.7.
- Eagle Eye 230 kV (Arizona):
  - A reduction of 56% in short-circuit MVA occurs when CSP is converted to PV.
  - Eight CSP units and 1 PV are connected.
  - The total MVA from CSP/PV is 1,584 MVA.
  - The SCR is 2.44.

And a third, E-W-WILD 230 kV (SCE), has similarly low system strength.

With the addition of inverter-based generation, SCR is a well-established measure of system strength relative to the rating of HVDC or other individual inverter-based resources, such as a single wind or PV site. Inverter-based generation operating with a low SCR can have control stability issues.

## **10.2 Investigation of Low Short-Circuit Strength at Solar Power Plants**

The large-scale system disturbances examined in Section 5.2 show modest impacts of the added solar and transmission. Most of the big changes to the system are in Southern California and Arizona, and they have the potential to alter the system dynamics considerably on a local basis. The short-circuit screening and SNSP characterization presented in Section 4 gives a foundation for more detailed inspection of specific locations in the system. In this section, two locations are examined.

### **10.2.1 Gila Bend**

The simulated solar development at Gila Bend is extensive, with a cluster of projects in this study totaling more than 1 GW. The development has a largely radial 230-kV connection to the 500-kV backbone that runs across the southern edge of California. The 500-kV corridor is a key element in supply to Southern California, and generation connected to it has the potential to impact system security.

As noted, the Gila Bend 230-kV bus experiences a nearly 50% reduction in short-circuit strength when PV is substituted for CSP. Further, the radial double-circuit 230-kV path up to Gila River is very heavily loaded in this case.

When the system is subjected to a fault, cleared in primary time by the removal of one of the two Gila Bend 230/500-kV transformers, the cluster of generation at Gila Bend needs to maintain

synchronism through the remaining transformer. A plot of the voltage and the power flowing through the remaining circuit is shown in Figure 101. The behaviors are characteristic of radially connected synchronous and inverter-based generation. The synchronous CSP machines accelerate substantially during the fault, and they exert substantial incremental power into the grid as the synchronising torque of the grid pulls the machines back. The higher power flow and accompanying reactive stress results in some delay in the recovery of the voltage, as can be observed in the blue voltage trace. Subsequent oscillations are also characteristic of synchronous machines. Normally, power system stabilizers, which are mandatory in WECC, would be tuned to give better damping than this case exhibits. The behavior of the PV is, in comparison, relatively simple. There is no acceleration and no energy accumulated in the PV system during the load rejection. Consequently, the inverter controls act quickly to return the system to its predisturbance condition. The voltage immediately following clearing of the fault is relatively high. This is partly because of the model and partly a real consequence of the reactive power balance during recovery of the inverter. The stability model is a bit pessimistic in regard to post-switching overvoltages because the numerical stability constraints of the model result in understating the speed with which the control suppresses reactive current injection on fault clearing. Overall, the performance of both systems is acceptable and meets WECC and NERC stability criteria.

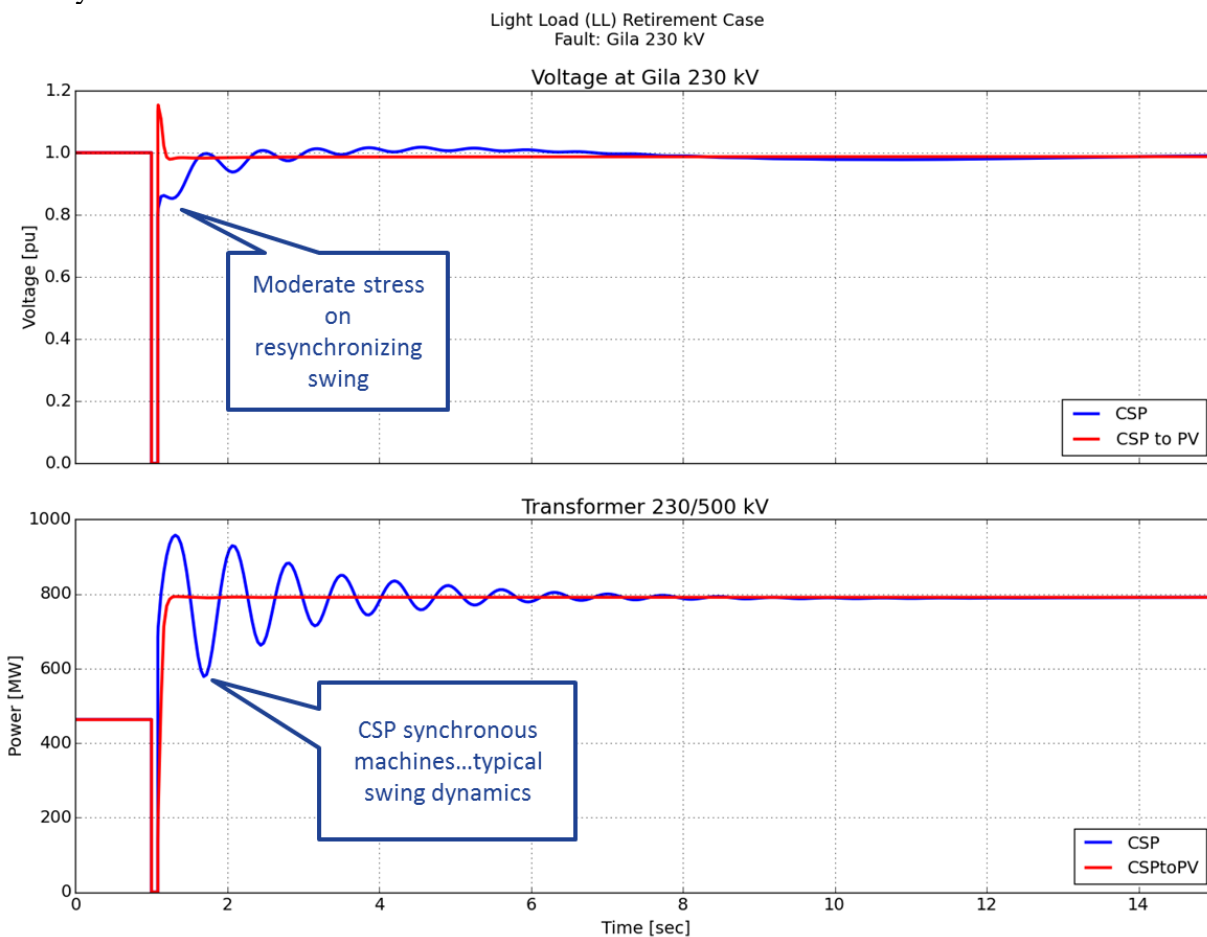


**Figure 101. Gila Bend disturbance: CSP compared to PV dynamics**

To further stress this system, we tried a more severe fault with a three-phase fault and with a stuck breaker at the Gila 230-kV bus. Again, we tripped the 230/500-kV transformer. The case is more severe, and we expected to have a stability failure. The CSP plant swings are more acute, and although the case is stable, the voltage recovery swing does not meet WECC criteria for a stuck breaker (Class C) event (WECC 2003). Had the power export been higher, or the disturbance longer, the CSP machine would have lost synchronism after the fault was cleared.

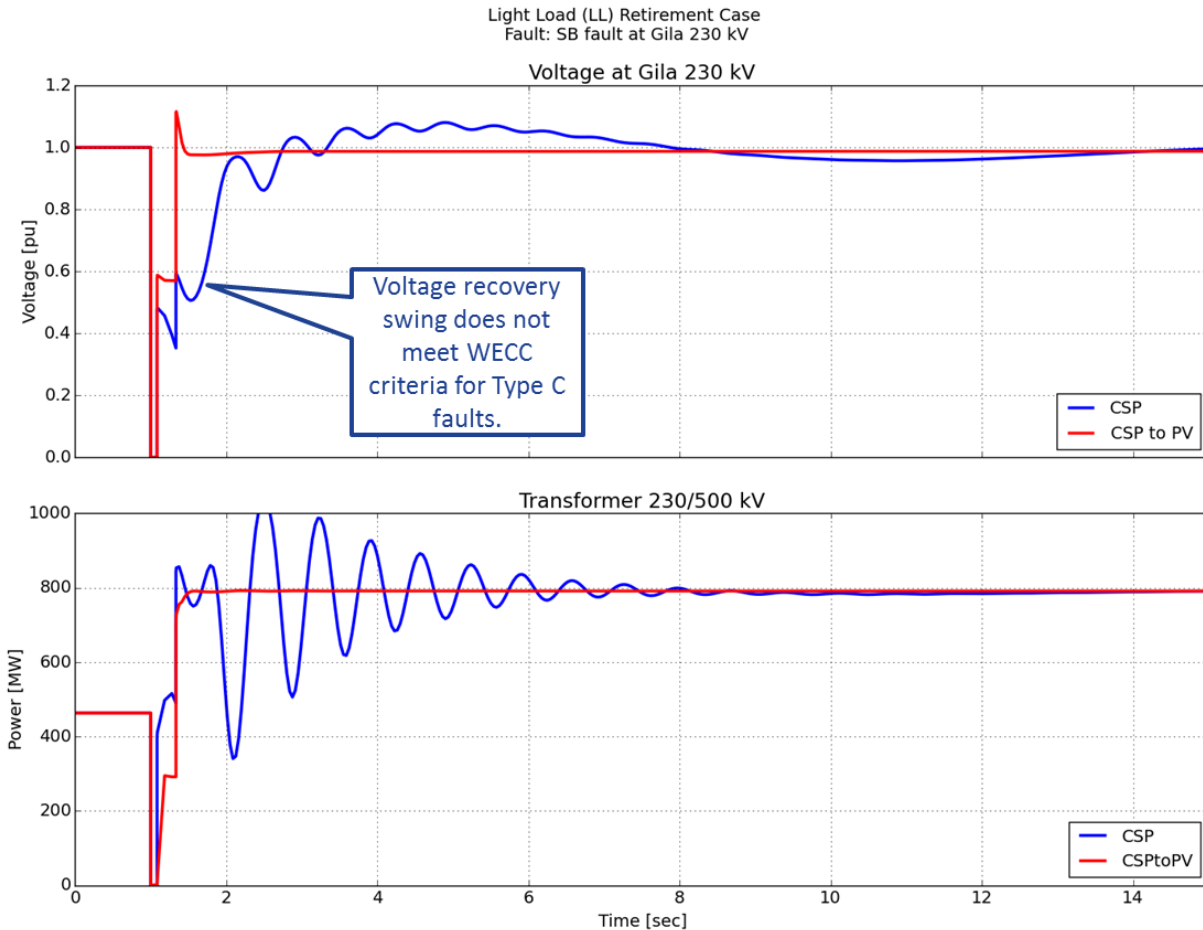


**Figure 102. Gila Bend disturbance: CSP compared to PV stuck breaker case**

### 10.2.2 Eagle Eye

The Eagle Eye 230-kV bus in the Mohave Desert has the lowest short-circuit level of the high solar buses screened. The solar PV at that node results in an SCR before the fault of 2.44. This is near the lower end of short-circuit strengths generally considered acceptable without detailed consideration of control stability and potential mitigation measures (discussed more later).

A test with fault and clearing of one of the lines out of Eagle Eye was run. The results were quite like the tests shown in the previous subsection for the Gila Bend event, even though the SCR is considerably lower (2.44 here compared to 3.7 for Gila Bend).

Because SCR is one of the key metrics for concern about inverter-based generation instability, a further test was devised in which the grid was degraded by removal of one of the 230-kV lines providing egress for the power from the solar power plants. In this case, the SCR before the fault

is 2. In Figure 103, a comparison of these two cases, with the system degraded, is shown. The voltages in the upper set of axes show the CSP in blue and the utility-scale PV in red. The power swings of the local solar power plants are shown in the next two sets, with the CSP synchronous machines swings in the middle and the PV power on the bottom. The swing of the synchronous CSP machines is somewhat greater. Both cases meet WECC criteria.

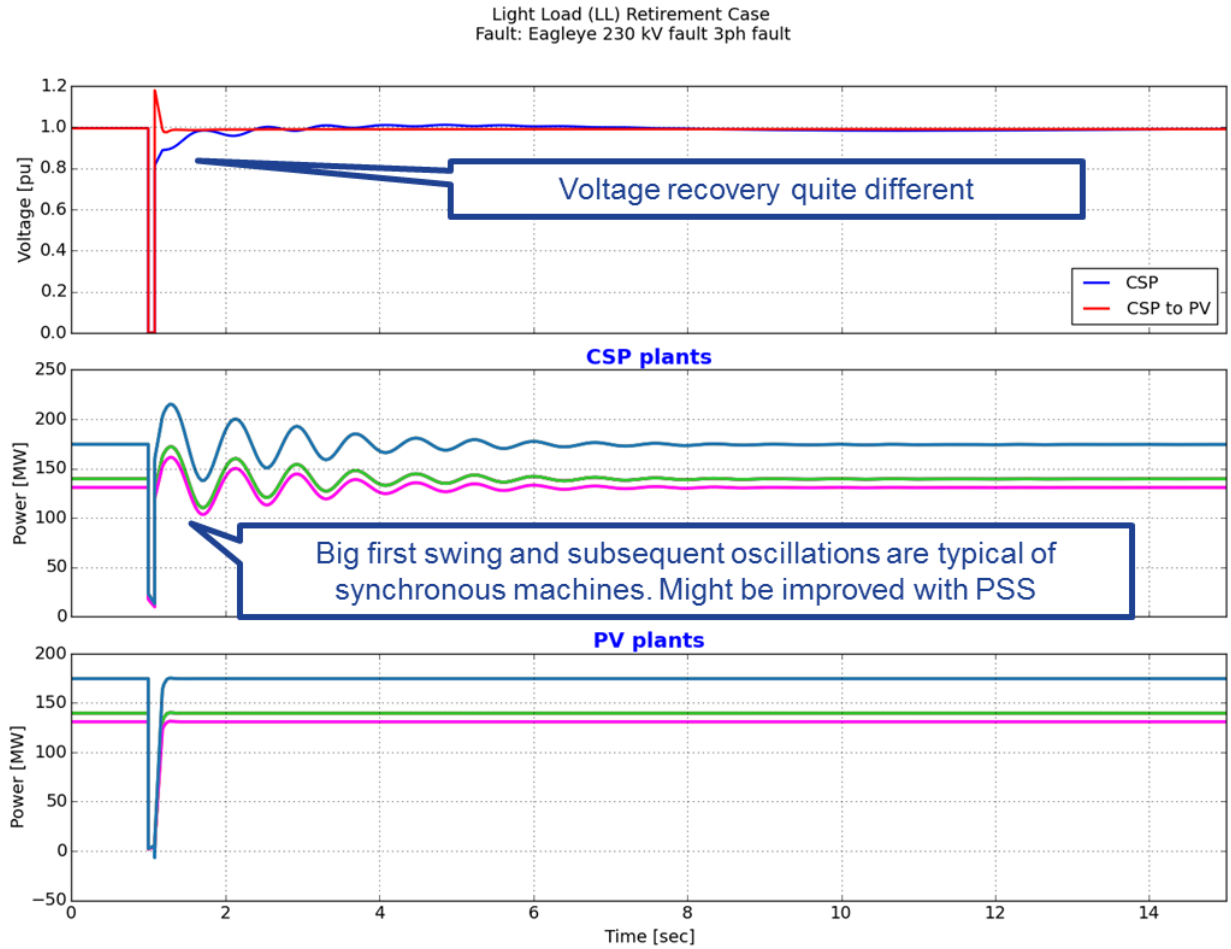


**Figure 103. Eagle Eye fault: CSP compared to utility-scale PV**

Light Load (LL) Retirement Case  
 Fault: Eagleye 230 kV 3ph fault (line-out case)

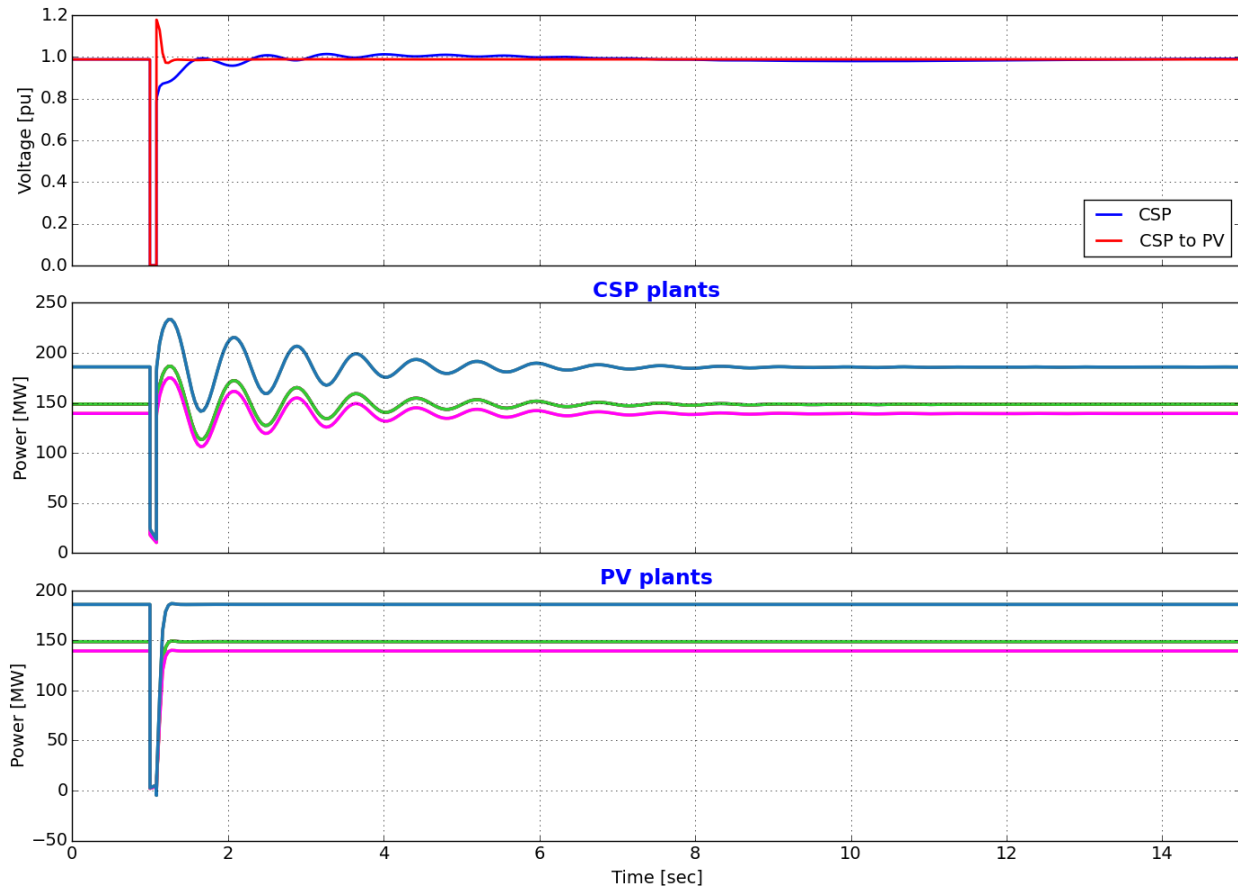


Figure 104. Eagle Eye fault: with initially lower short-circuit ratio

### 10.2.3 Discussion of Mechanisms of Weak Grid Inverter Instability

The cases involving Eagle Eye had the lowest SCR found by the screening for this study system. These SCR levels are not extremely low, and the authors have encountered systems in which inverter-based generation has been proposed for much lower system strengths. Nevertheless, for the solar-rich region of Southern California and Arizona, the necessity to provide adequate thermal capability with new transmission seems to have resulted in avoiding unduly low system strength.

It is worth examining the physical mechanisms by which inverter-based generation can become unstable. Here we provide a synopsis of three distinct (*in*)stability mechanisms:

1. Fast voltage collapse. Analysis of this phenomenon requires adequate modeling of the inverter (and plant) voltage regulator and accompanying active and reactive power controls. This problem is suitable for phasor analysis. (Taylor 1994) Great care is needed with generic models, and it is possible that some aspects of the generic models might not be adequate.
2. Fast regulator stability. Analysis of this phenomenon requires adequate representation of phase-locked loops and other synchronizing mechanisms employed by individual original

equipment manufacturers. These are not in standard PV models. Getting the details right in the models is tricky, and they vary by original equipment manufacturer. The problem is generally tractable using the phasor analysis structure present in transient stability programs, but it requires care and usually cooperation with the equipment supplier. Generic stability models might give optimistic results, showing good performance when the application behaves poorly in low SCR situations. The minimum system strength specified by the converter supplier can provide guidance for when different models and tools are required.

3. Very fast firing instability. This phenomenon is not detectable or possible to model with phasor analysis (i.e., positive sequence/stability program). Like many other nonfundamental frequency phenomena (e.g., subsynchronous resonance), this risk needs to be addressed as a system specification issue. Composite SCR and other methods are suitable for risk screening. For applications that are flagged, equipment-specific electromagnetic transient, three phase point-on-wave (EMT) modeling is required. Generic EMT models are mostly useless for analysis of this behavior because controls and equipment structures employed by individual original equipment manufacturers vary and are generally proprietary.

For the low short-circuit conditions being approached in the Eagle Eye (and Gila Bend) examination, it is possible for solar PV regulators that have not been tuned for low short-circuit levels to misbehave. In Figure 105, an approximately 9-Hz weak grid instability is shown. This event is a simulation replicating a measurement from an actual field event (the device trips at approximately 0.6 second). This behavior (of the second type in the listing above) can occur when regulator gains are too high for the strength of the system. This can occur from improper application and is mainly a risk when the system is degraded (as we tried in the recent case presented).

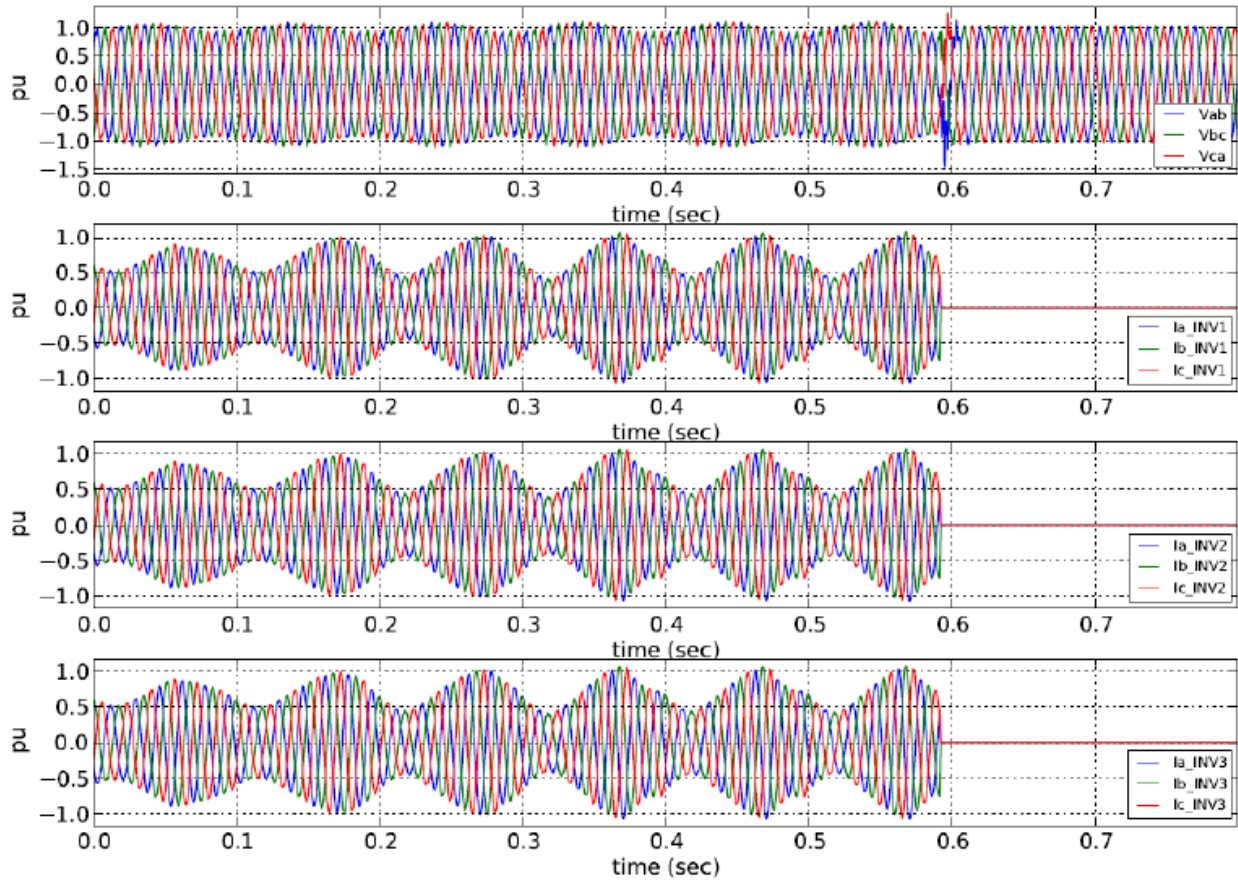


**Figure 105. Measured utility-scale PV inverter instability**

### 10.2.4 Experiments with Deliberately Induced PV Regulator Instability

For this investigation, we further experimented with the PV plant model at Eagle Eye based on the behavior shown above. Specifically, we pushed the PV model toward control settings that:

1. Might be found in a very stiff system
2. We know can cause regulator stability problems in weak systems.

Again, for the Eagle Eye three-phase fault on the SCR degraded case (with a line-out), the SCR before the fault is 2. The results are shown in Figure 106. Notice that voltage after the fault clears has a rapid oscillation. This 13-Hz instability is representative of the behavior shown in Figure 105. The slower oscillations observable before the event are also characteristic of a weak grid and voltage regulator instability.

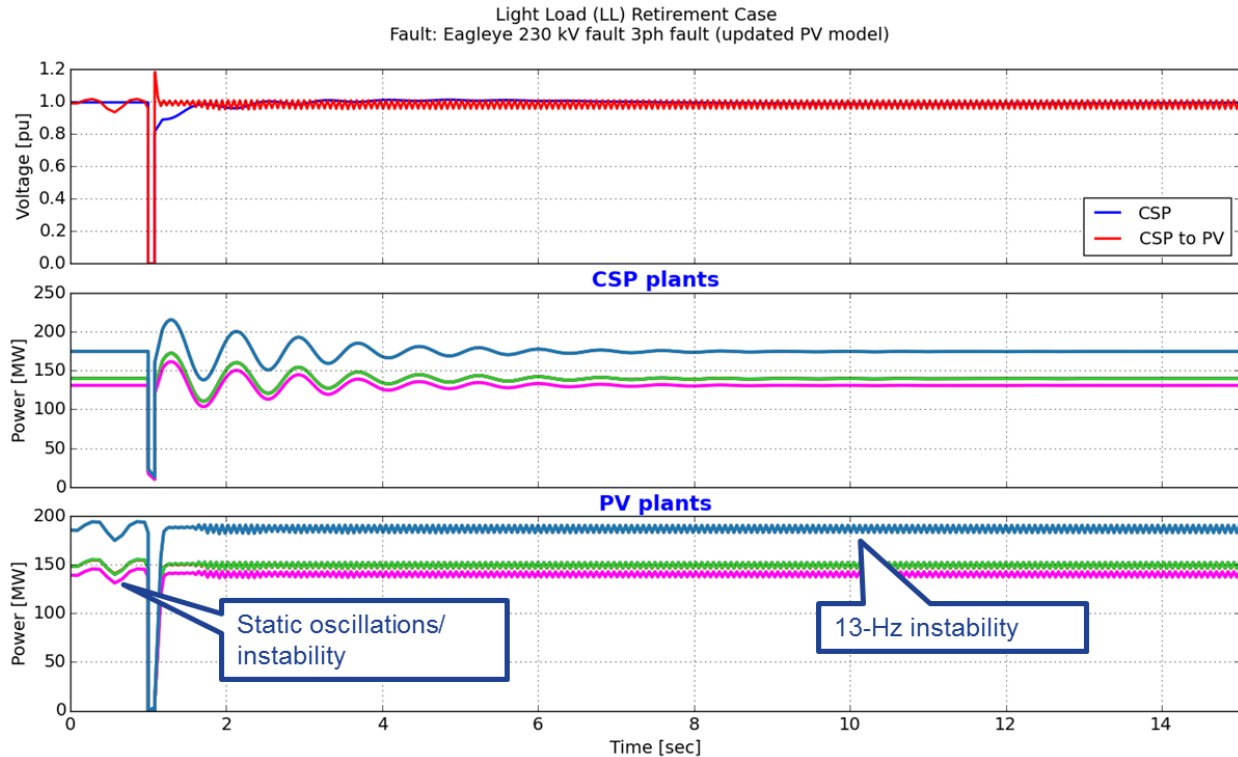


**Figure 106. PV voltage regulator induced instability**

### 10.3 Key Observations on Low Levels of Synchronous Generation

Some summary comments on the weak grid instability investigation follow.

Overall, the stability of the solar power plants that were flagged by our short-circuit level screening to be the most vulnerable to weak grid instabilities demonstrated satisfactory performance. For the cases tests, both CSP and utility-scale PV plants meet WECC criteria for primary cleared faults.

It is possible for either type of plant to have stability problems. The backup clearing faults of longer duration caused a voltage swing violation for the CSP plant in one case. Even longer faults would cause the synchronous generators of the CSP plants to trip on loss of synchronism. We were able to roughly capture voltage regulator instability in the PV plant by using settings that should be applied only in a much stronger grid. On this later point, the simulations are illustrative only. In practice, the modeling of PV and all positive sequence analysis are highly suspect at these frequencies (9 Hz, 13 Hz). Definitive analysis is impossible with these tools. Further, default generic stability models are not particularly well suited to capturing this risk. They tend to be optimistic in that voltage support and current control can appear more stable. This is a concern that requires attention to equipment specifications provided by the manufacturers and that might require other analytical tools to fully evaluate. However, we have not seen practical cases where weak grid instability cannot be fixed by control tuning. This does not mean this is always true, but it also means do not panic and do not assume that minimum synchronous generation levels will necessarily be limiting. Emerging good practice will dictate

that applications of inverter-based resources that can feed into very weak systems must be analyzed with tools and models that are more sophisticated than generic stability models allow.

# 11 Key Findings and Conclusions

This investigation shows that the integration of large amounts of solar power in the western system, for the conditions studied, does not present any obviously intractable challenges. We find that frequency response can be aided significantly by frequency sensitive controls on CSP and PV solar. Anticipated weak grid stability problems were not substantial.

This is relatively new ground for the industry, and this investigation is not a substitute for detailed planning, but the risks illustrated can be analyzed and mitigated. Tools, data, and the current state-of-the-art interconnection and bulk power system stability studies, if used following good system engineering practice as the system is built out, will ensure continued reliability of the power system.

## 11.1 Key Findings

### 11.1.1 *Changes in Frequency and Transient Stability Resulting from Solar and Wind Build-Out*

Transmission added in solar-rich areas to avoid thermal and voltage violations, plus changes in dispatch and commitment, have some effect on transient stability. The impacts are mixed, with some improvements and decreases. No stability violations (noncompliance with WECC criteria) were found for the primary clearing cases tested. Voltage swing violations were observed for a backup cleared fault with a large cluster of CSP plants. As noted, good planning practices need to be observed. Path ratings and remedial actions schemes might need to be revisited.

System-wide inertia dropped up to 27%–32% from earlier light load planning cases with less wind and solar generation. The lower system inertia did not present any significant stability or frequency response challenges.

We did not observe systemic issues related to frequency and transient stability as a result of the solar and wind build-out. That is, the overall behavior was similar in character to the present system. The system seems to tolerate nondesign basis north-south separation better.

So, for example, for the conditions tested, moving to SNSP on the order of 70% on a system-wide or regional level was not a clear indicator of degraded transient stability. Transient stability issues seemed to be rather localized.

### 11.1.2 *Primary Frequency Response from CSP*

PFR from CSP benefits frequency response, improves the system nadir, and helps the system (and regions thereof, such as California) meet the FRO.

For comparison with FFR from PV, in these cases, the benefit of frequency response from CSP is approximately equivalent to 3% of FFR from inverter/switched resources. That means, for example, that for each 100MW of CSP providing PFR, the equivalent of 3 MW of FFR is provided at that time. In this system, with approximately 10 GW of CSP, PFR on all the units would provide the same benefit for FRO as 300 MW of inverter-based FFR. Batteries or utility-scale PV, as discussed in Section 7.2, have potential to provide FFR. Obtaining FFR from these inverter-based resources will have accompanying costs, which might include costs of curtailment. The timing of available PFR or FFR will vary by resource. Both the amount (i.e., the

number of hours per year that the service is available) and the timing (i.e., what hours the service is available) will be different by resource. Consequently, the overall (or annualized) economic value of the various alternatives derive from overall operational impact (i.e., over the full 8,760 hours of a year).

Fast-valving-type open-loop controls on CSP might increase this benefit to approximately 4.5%. Concepts were presented in the work for such controls, which would need further engineering design to ensure feasibility.

Thermal storage should help the sustainability of PFR and might help the speed of response. Again, more detailed design is required.

### **11.1.3 Fast Frequency Response**

Provision of FFR by utility-scale PV or other inverter-based resources, such as energy storage devices, can improve the system frequency nadir and add margin against underfrequency load-shedding.

Responding quickly after the disturbance produces improved performance (in terms of improved nadir). But a response of 1–2 seconds produces most of the benefit. Faster response produces only marginally better performance, and it introduces robustness concerns. Specifically, local differences in frequency during disturbances suggest that triggering FFR should be no faster than 0.5 sec.

For energy-limited FFR (e.g., synthetic inertia from wind), the best efficacy is for FFR a few seconds into the event.

For systemic events, the location of the FFR resources is not very important. The impact of the amount of FFR is quite linear for moderate amplitude actions, but it declines in efficacy with large power levels.

FFR from PV, as modeled, is sustainable and therefore also improves frequency response.

Transient overload of inverters, and/or possible reversion to active power preference might provide free FFR. Otherwise FFR from PV requires advanced curtailment.

Simulations here show mechanisms by which the relative efficacy of FFR compared to PFR can be determined. Market mechanisms for FFR will need to recognize that it is possible to compare the two and that the relative benefit depends on the system operating condition.

### **11.1.4 Dynamic Models**

CSP thermal plant models have good correlation to field tests.

CSP models lack the modeling detail needed for dynamic testing of thermal energy storage dynamic impacts. Approximations showed significant promise, but more detailed modeling efforts are required for definitive quantitative results.

Utility-scale PV models might be optimistic for weak grid conditions. In particular, generic models might not accurately capture fast voltage and fast regulator stability concerns under

short-circuit conditions below equipment specifications. Generic models might show good performance when the application behaves poorly in low SCR situations. The minimum system strength specified by the converter supplier can provide guidance for when different models and tools are required.

Displacing fossil-fueled generation by renewables increases dependence on hydro and makes modeling fidelity more important.

### **11.1.5 Stability Implications of CSP Compared to PV**

Short-circuit levels in solar-rich areas tended to increase because of added transmission, which offsets effects of decommitting synchronous generation. The SCR levels from this work are not extremely low, and the authors have encountered systems in which inverter-based generation has been proposed for much lower system strengths. For the solar-rich regions of Southern California and Arizona, the necessity to provide adequate *thermal* capability with new transmission seems to have resulted in avoiding unduly low system strength.

System strength declines as PV is substituted for CSP.

The lowest grid strength here (i.e., SCR of slightly more than 2.0) is where inverters for stiffer grids might misbehave. Stress tests in simulations showed instability like that observed in the field; however, instabilities are outside the accuracy of these positive sequence tools. More sophisticated analysis is required for evaluation and mitigation. The behavior of inverter-based generation is specific to individual equipment designs. In low-grid-strength applications, guidance from the manufactures, by specification or direct inquiry, is needed. Analysis with more detailed, proprietary simulation tools, including nonfundamental frequency screening tools and EMT time simulations, might be needed.

Transient stability of solar exporting areas generally showed better transient stability with PV compared to CSP. No transient stability issues that resulted in violation of WECC criteria were observed for primary fault clearing regardless of the type of solar generation.

The range of tests performed here did not show evidence of any widespread concerns about weak grid, high SNSP, or low short-circuit levels for the predominantly utility-scale PV case. These cases do not provide observable motivation to prefer synchronous CSP over inverter PV regarding system transient and voltage stability.

### **11.1.6 Economic Implications of CSP Compared to PV**

This investigation was limited to system stability, and it is not an economic study. Nevertheless, the stability constraints of the Western Interconnection must be respected, and they have a substantive impact on the variable cost of operation. The various options presented in this study, including especially mechanisms to meet the FROs and changes in transfer limits, can be included in production cost simulations as boundary conditions. For example, use of thermal energy storage in CSP plants to maintain headroom and add frequency response would provide an additional operations option that will reduce the variable cost of operation. This savings could be quantified in a properly configured production study.

## **11.2 Future Work**

This work illuminates a few areas for which further study, analysis using different tools, and the development of new tools would move forward the industry's understanding of grid operations with low levels of synchronous generation. Such understanding might alter the planning landscape for CSP.

### **11.2.1 Western Interconnection Analysis**

Further investigations of different network topologies with even lower levels of synchronous generation (e.g., Southern California) would be of interest. Both the system assumptions and economic operation of a very high variable renewables scenario in the West (and particularly California) need more investigation. Combined production simulation and transient stability work (i.e., so-called round-trip analysis) is needed more than ever.

### **11.2.2 Protection and Relaying Investigation**

Analyses of system stability using fundamental frequency, positive sequence analysis, including those presented in this report, generally assume that protective relaying and protection (e.g., circuit breakers) will continue to perform as presently modeled. For example, the faults used in this study were assumed to be of a “standard” four-cycle duration. The fault clearing times used in stability studies are usually conservative approximations of actual protection system behavior. This behavior is based on the level and character of short-circuit currents, which are substantially different and less well known from inverter-based generation. Whether these assumptions are still valid in systems with predominantly inverter-based generation warrants further investigation.

### **11.2.3 Load Modeling**

Load behavior continues to have a substantive impact on system frequency performance and transient stability. Although significant effort has been devoted in recent years, including the introduction of the composite load model, there is still much to be done. The industry would benefit from (1) better loads models, with good field validation and (2) better methods to meaningfully address the planning and operations uncertainty that accompanies the inevitable inaccuracies of load modeling.

## 12References

- Aggarwal, R.; R. Daschmans, R. Schellberg, V. Venkatasubramanian, and S. Yirga, 1997 “Validation studies of the July 2, 1996 WSCC system disturbance event”, Operating Capability Study Group, Western Systems Coordinating Council, July 1997.
- American Wind Energy Association. 2017. “U.S. Wind Energy State Facts.” <https://www.awea.org/state-fact-sheets>.
- California Independent System Operator. 2016a. “What the Duck Curve Tells Us About Managing a Green Grid.” [https://www.caiso.com/Documents/FlexibleResourcesHelpRenewables\\_FastFacts.pdf](https://www.caiso.com/Documents/FlexibleResourcesHelpRenewables_FastFacts.pdf)
- California Independent System Operator. 2016b. *2016-2017 Transmission Planning Process Unified Planning Assumptions and Study Plan*. Folsom, CA.
- CIGRE. 2016. “Connection of Wind Farms to Weak AC Networks.” Paris, France: Working Group B4.62.
- Eirgrid 2015/ “The DS3 Programme” <http://www.eirgridgroup.com/site-files/library/EirGrid/DS3-Programme-Brochure.pdf>
- Electric Reliability Council of Texas. 2010. *Primary Frequency Response Requirement from Existing WGRs (PRR833)*. Austin, TX.
- Elgerd, O.I. 1971. *Electric Energy Systems Theory: An Introduction*, p. 478. Chicago: McGraw-Hill.
- FERC 2005. Order 661-A Interconnection for Wind Energy.
- GE Energy. 2010a. *Western Wind and Solar Integration Study* (Technical Report NREL/SR-550-47434). Golden, CO: National Renewable Energy Laboratory.
- GE Energy. 2010b. *Western Wind and Solar Integration Study: Executive Summary*. (Technical Report NREL/SR-550-47781). Golden, CO: National Renewable Energy Laboratory.
- Jorgenson, J., P. Denholm, and M. Mehos. (2014). Estimating the Value of Utility-Scale Solar Technologies in California under a 40% Renewable Portfolio Standard. NREL Report No. TP-6A20-61685.
- Kroposki, B.; B. Johnson, Y. Zhang, V. Gevorgian, P. Denholm, B. Hodge, B. Hannegan (2017) “Achieving 100% Renewable Grids—Operating Electric Power Systems with Extremely High Levels of Variable Renewable Energy” *IEEE Power and Energy* 15:2, 61-73.
- Lew, D., and G. Brinkman. 2013. *Western Wind and Solar Integration Study: Phase 2—Executive Summary* (Technical Report NREL/TP-5500-58798). Golden, CO: National Renewable Energy Laboratory.

Lew, D., G. Brinkman, E. Ibanez, A. Florita, M. Heaney, B.-M. Hodge, M. Hummon, G. Stark, J. King, S.A. Lefton, N. Kumar, D. Agan, G. Jordan, and S. Venkataraman. 2013. *Western Wind and Solar Integration Study: Phase 2* (Technical Report NREL/TP-5500-55588). Golden, CO: National Renewable Energy Laboratory.

Matevosyan, J., S. Sharma, S.-H. Huang, D. Woodfin, K. Ragsdale, S. Moorthy, P. Wattles, and W. Li. 2015. "Proposed Future Ancillary Services in Electric Reliability Council of Texas." *Proceedings of IEEE PowerTech*.

Mehos, M.; C. Turchi; J. Jorgenson; P. Denholm; C. Ho; K. Armijo (2016) On the Path to SunShot: Advancing Concentrating Solar Power Technology, Performance, and Dispatchability NREL/TP-6A20-65800

Miller, N.W., B. Leonardi, and R. D'Aquila. 2015. *Western Wind and Solar Integration Study: Phase 3A—Low Levels of Synchronous Generation* (Technical Report NREL/TP-5D00-64822). Golden, CO: National Renewable Energy Laboratory.

Miller, N.W., et.al. 2017. *Technology Capabilities for Fast Frequency Response: Report on Fast Frequency Response Specification to Australian Energy Market Operator*. Melbourne,, Australia: Australian Energy Market Operator.

Miller, N.W., M. Shao, S. Pajic, and R. D'Aquila. 2014a. *Western Wind and Solar Integration Study: Phase 3—Frequency Response and Transient Stability* (Technical Report NREL/SR-5D00-62906). Golden, CO: National Renewable Energy Laboratory.

Miller, N.W., M. Shao, S. Pajic, and R. D'Aquila. 2014b. *Western Wind and Solar Integration Study: Phase 3—Frequency Response and Transient Stability: Executive Summary* (Technical Report NREL/SR-5D00-62906-ES). Golden, CO: National Renewable Energy Laboratory.

Milligan, M.; Frew, B.; Kirby, B.; Schuerger, M.; Clark, K.; Lew, D.; Denholm, P.; Zavadil, B.; O'Malley, M.; Tsuchida, B. (2015) "Alternatives No More: Wind and Solar Power Are Mainstays of a Clean, Reliable, Affordable Grid," *IEEE Power and Energy Magazine*, 13:6 78-87

North American Electric Reliability Corporation. 2012a. *Frequency Response Initiative Report: Draft*. Washington, D.C. <http://www.nerc.com/docs/pc/FRI%20Report%209-30-12%20Clean.pdf>

North American Electric Reliability Corporation. 2012b. *Standard BAL-003-1, Frequency Response and Frequency Bias Setting*. Washington, D.C

O'Sullivan, J., A. Rogers, and A. Kennedy. 2011. "Determining and Implementing an Approach to System Frequency and Inertial Response in the Ireland and Northern Ireland Power System." *Proceedings of the IEEE Power and Energy Society General Meeting*.

Pasternak, B.K, and N.B. Bhatt. 1988. "The Rockport Plant-Analysis of Temporary Fast Turbine Valving Tests." *IEEE Transactions on Power Systems*.

Tande, J., and G. Olav. 2000. “Exploitation of Wind-Energy Resources in Proximity to Weak Electric Grids. *Applied Energy* 65 April: 395–401.

Taylor, C.W. 1994. *Power System Voltage Stability*. New York: McGraw-Hill.

Western Electricity Coordinating Council. 2003. *WECC Reliability Criteria*. Salt Lake City, UT: April.

Western Electricity Coordinating Council. 2011. *System Performance: TPL-001-WECC-CRT-2.1: Regional Criterion*. Salt Lake City, UT. <https://www.wecc.biz/Reliability/TPL-001-WECC-CRT-2.1.pdf>.

Western Electricity Coordinating Council. 2012. *Composite Load Model for Dynamic Simulations: Report 1.0*. (Technical Report) Salt Lake City, UT: Western Electricity Coordinating Council Modeling and Validation Work Group. <https://www.wecc.biz/Reliability/WECC%20MVWG%20Load%20Model%20Report%20ver%201%200.pdf>.

Wilches-Bernal, F., R. Concepcion, J. Neely, R. Byrne, and A. Ellis. 2017. “Communications-Enabled Fast-Acting Imbalance Reserve (CE-FAIR).” Submitted to *IEEE Engineering Letters*.